

©Copyright 2017
Jens von der Linden



This work is licensed under a Creative Commons Attribution
4.0 International License.
<http://creativecommons.org/licenses/by/4.0>

Investigating the Dynamics of Canonical Flux Tubes

Jens von der Linden

A dissertation
submitted in partial fulfillment of the
requirements for the degree of

Doctor of Philosophy

University of Washington

2017

Reading Committee:

Setthivoine You, Chair

Brian Nelson

Uri Shumlak

Program Authorized to Offer Degree:
Aeronautics & Astronautics

University of Washington

Abstract

Investigating the Dynamics of Canonical Flux Tubes

Jens von der Linden

Chair of the Supervisory Committee:

Assistant Professor Setthivoine You

William E. Boeing Department of Aeronautics & Astronautics

Observations indicate that the dynamics of plasmas in our cosmos, the heliosphere, and terrestrial experiments can involve conversions between magnetic and kinetic energies over a wide range of plasma scales, such as in reconnection and dynamos. Canonical flux tubes present the distinct advantage of reconciling all plasma regimes, e.g. single particle, kinetic, two-fluid, and magnetohydrodynamics (MHD), with the topological concept of helicity: twists, writhes, and linkages. This thesis presents the first application of the theory of canonical helicity transport to design a laboratory canonical flux tube experiment, develop methods to measure a large volumetric dataset of magnetic field and ion flow, reconstruct the 3D dynamics of canonical flux tubes, and determine the canonical helicity evolution. Newcomb's variational ideal MHD stability analysis is used to identify the possibility of a lengthening current-carrying magnetic flux tube undergoing a sausage-kink instability cascade. The instability cascade may couple to smaller scales at which conversions between species helicities are expected to occur. Experiment control and high-throughput field-programmable gate array (FPGA) based digitizers provide the means to measure the large datasets. Ion and electron canonical flux tubes are visualized from a dataset of Mach, triple, and \dot{B} probe measurements at over 10,000 spatial locations of a gyrating kinked plasma column. The flux tubes co-gyrate with the peak density and electron temperature in and out of a measurement subvolume. The electron and ion flux tubes twist with opposite handedness and the ion canonical flux tube writhes around the electron

canonical flux tube. Videos of the canonical flux tube reconstructions are available as supplemental material in ProQuest Dissertations & Theses Global. The cross helicity between the magnetic and ion flow vorticity flux tubes dominates the ion canonical helicity and is anticorrelated with the magnetic helicity. The methods developed in this thesis can be applied to other laboratory experiments to improve the understanding of canonical helicity transport; which could help identify how destabilizing magnetic twist is converted to stabilizing shear flows in astrophysical jets and could aid in developing methods for driving shear flow transport barriers in fusion devices.

TABLE OF CONTENTS

	Page
List of Figures	vi
List of Tables	xiii
Chapter 1: Introduction	1
1.1 Plasma physics: a multiscale problem	1
1.1.1 Hierarchy of plasma scales	1
1.2 Context: astrophysical, heliospheric, and laboratory plasmas	4
1.2.1 Astrophysical jets	4
1.2.2 Coronal loops in the heliosphere	6
1.2.3 Topological change in fusion energy concepts	7
1.3 Generalized fluxes and their helicity provide insight across scales	8
Chapter 2: Canonical flux tubes and their helicity	9
2.1 Introduction	9
2.2 Canonical flux tubes	9
2.2.1 Definitions	9
2.2.2 Frozen-in canonical flux condition	11
2.2.3 Theoretical and experimental studies	13
2.3 Canonical helicity	20
2.3.1 Relative canonical helicity	21
2.3.2 Canonical helicity transport	23
2.4 Conclusion	25
Chapter 3: Sausage instabilities on top of kinking lengthening current-carrying mag- netic flux tubes	27
3.1 Background	28

3.2	Theory	30
3.3	Numerics	40
3.4	Discussion	45
3.5	Conclusion	48
Chapter 4:	Experiment control and high-throughput FPGA based digitizers for canonical helicity measurements	50
4.1	Challenge of measuring canonical helicity	50
4.2	Mochi.Labjet: Canonical flux tubes with boundary conditions relevant to astrophysical jets	51
4.3	Mochi Control: Experiment control & data storage	53
4.3.1	Mochi Control user interface	56
4.3.2	Mochi Control architecture	58
4.4	High-throughput FPGA based digitizers	62
4.5	Conclusion	64
Chapter 5:	Measurements of canonical flux tubes and their helicity	65
5.1	Overview of RSX experiment	66
5.1.1	A gyrating kinked canonical flux tube	66
5.2	Diagnostics	67
5.2.1	\dot{B} probes	69
5.2.2	Triple probes	69
5.2.3	Mach probes	70
5.3	Step 1: Prepare data	71
5.3.1	Identifying a coherent shot subset	71
5.3.2	Conditional sampling of measurements across shots	73
5.3.3	Interpolating the measurements to a common rectilinear grid	73
5.3.4	Constraining the under determined velocity	74
5.4	Step 2: Reconstruct and interpret canonical flux tubes	77
5.4.1	Gyration path	77
5.4.2	Canonical Flux Tubes	81
5.5	Step 3: Determine vector potential and reference fields	88
5.5.1	Comparing vector fields	89
5.5.2	Reference fields: Solving Laplace equation with fast Fourier methods	90

5.5.3	Two-component vector potential	92
5.6	Step 4: Reconstruct and interpret canonical helicity	94
5.7	Conclusion	98
Chapter 6:	Conclusion and outlook	99
Bibliography	102
Appendix A:	Fluxtube stability code	116
A.1	Dependencies	116
A.2	Setup	117
A.3	Important files	117
A.4	Run	117
A.5	newcomb.py description	118
A.6	Source code	118
A.6.1	init_database.py	118
A.6.2	skin_core_scanner.py	119
A.6.3	paper_figures.py	124
A.6.4	call_provenance.py	139
A.6.5	equil_solver.py	139
A.6.6	newcomb.py	173
A.6.7	newcomb_init.py	183
A.6.8	newcomb_f.py	186
A.6.9	newcomb_g.py	189
A.6.10	find_singularities	195
A.6.11	singularity_frobenius.py	198
A.6.12	external_stability.py	203
A.6.13	lambda_k_plotting.py	206
A.6.14	analytic_condition.py	217
A.6.15	diagnostic_plots.py	223
A.6.16	test_equil_solver.py	226
A.6.17	test_newcomb.py	227

Appendix B: MochiControl & MochiFPGAControl code	231
B.1 MochiControl	231
B.1.1 Requirements	232
B.1.2 Important Files	233
B.1.3 Setup	233
B.1.4 Adapting the code to new hardware	234
B.1.5 Reference	234
B.1.6 Acknowledgments	235
B.1.7 Contact	235
B.2 MochiFPGAControl	235
B.2.1 Requirements	235
B.2.2 Important Files	236
B.2.3 Setup	237
B.2.4 Reference	237
B.2.5 Improvements	237
B.2.6 Acknowledgments	238
B.2.7 Contact	238
Appendix C: Mochi.PSU1	239
C.1 Overview figures	240
C.2 Drawings	242
C.2.1 Capacitor Bank Assembly	242
C.2.2 Plates	244
C.2.3 Ignitron cover parts	251
C.2.4 Panels	258
Appendix D: Canonical flux tube and helicity reconstruction code	270
D.1 Dependencies	270
D.2 RSX data and analysis scripts	271
D.3 Directory structure	271
D.4 Important files	271
D.5 Reference	272
D.6 Contact	272

D.7	Main Scripts	272
D.7.1	write_measurements_to_unstructured_grid.py	272
D.7.2	fit_field_null.py	275
D.7.3	interpolate_measurements.py	280
D.7.4	calculate_dependent_quantities.py	284
D.7.5	calculate_helicity.py	292
D.7.6	vis_canonical_fluxtubes.py	298

LIST OF FIGURES

Figure Number	Page
<p>1.1 Characteristic plasma length scales in a protostellar jet (purple), coronal loop (red), and the Mochi.Labjet laboratory experiment (black). All lengths are normalized to the respective scale length L. For the protostellar jet $T_e = T_i = 1 \text{ eV}$ [7], $n_0 = 10^{12} \text{ m}^{-3}$ [7], $m_i = m_p$, $B = 10^{-5} \text{ T}$ [8], $Z = 1$, $L = 10^{14} \text{ m}$ [7] were chosen. For the coronal $T_e = T_i = 100 \text{ eV}$ [9], $n_0 = 10^{15} \text{ m}^{-3}$ [9], $m_i = m_p$, $B = 10^{-3} \text{ T}$ [4], $Z = 1$, $L = 10^8 \text{ m}$ [9] were chosen. For Mochi.Labjet $T_i = 1 \text{ eV}$, $T_e = 5 \text{ eV}$, $n_0 = 10^{22} \text{ m}^{-3}$, $m_i = m_p$, $B = 0.1 \text{ T}$, $Z = 1$, $L = 1 \text{ m}$ were chosen based on the initial experiment design parameters. Z is the ionization number ($q_i = Ze$) and $m_p = 1.7 \cdot 10^{-27} \text{ kg}$ is the mass of a proton.</p>	5
<p>2.1 Artist's interpretation of canonical flux tube. When density is uniform, a canonical flux tube (grey) is the weighted sum of a magnetic flux tube (red) and a flow vorticity flux tube (blue).</p>	10
<p>2.2 Five distinct flux tubes of quantities constrained by a choice of dipole vacuum magnetic field \bar{B}, uniform current \bar{j}, and electron velocity \bar{u}_e parallel to \bar{B} of magnitude \bar{u}_e. a) Current-carrying magnetic flux tube ψ_{jet}. b) Electron and ion flow flux tubes ψ_e and ψ_i. c) Electron and ion flow vorticity flux tubes \mathcal{F}_e and \mathcal{F}_i. d) Electron and ion canonical momentum flux tubes \mathcal{P}_e and \mathcal{P}_i. e) Electron and ion canonical flux tubes Ψ_e and Ψ_i. Bar denotes dimensionless quantities. Reproduced from [16] by permission of the AAS.</p>	13
<p>2.3 Left) Bulged ion canonical vorticity flux tube Ψ_i (dark gray) for a diffuse core current jet with low current ($\bar{\lambda} = 0.175$) and a large electron velocity ($\bar{u}_e = 40$). Bar denotes dimensionless quantities. Reproduced from [16] by permission of the AAS. Right) M2-9 Butterfly nebula (NASA HST STIS/CCD – MIRVIS), a bipolar planetary nebula with distinctive bulging that resembles the ion canonical flux tube on the left. By ESA/Hubble, CC BY 4.0 [27].</p>	14

2.4	Two counter-helicity spheromaks merge. The initial magnetic helicities are experimentally varied and characterized by the eigenvalue λ_0 . During the merging process magnetic reconnection converts magnetic energy into ion heating, ion flows, and magnetic activity. When the ion skin depth λ_i over the system length L is large the magnitude of the shear flows becomes large. The ion heating and ion flows form an enthalpy difference across the flux tubes. If the initial magnetic helicity is below a threshold, the helicity is annihilated and the final configuration is an FRC with negligible magnetic helicity and $\lambda \approx 0$. If the initial magnetic helicity is above a threshold, low mode number magnetic activity restores magnetic helicity and the final configuration is a spheromak with finite magnetic helicity and $\lambda \neq 0$. Image credit: Setthivoine You	15
2.5	Threshold of initial eigenvalue $\lambda_0/\lambda_{Taylor}$ as a function of the size parameter S^* for forming a spheromak or a FRC from counter-helicity merging. Reprinted from [28]. Copyright 2005 IOP Publishing.	16
2.6	Gauge-dependence of helicity. An integral over the gray volume cannot count the number of linkages of the two flux tubes external to the grey volume. Adapted from [24]. Image credit: Jaclyn Lake.	22
3.1	a) Sausage $m = 0$ instability. Increased B_{θ_2} exerts an increased pinch force. Magnetic pressure and tension from compressed and bent magnetic field resist the perturbation. b) Kink $m = 1$ instability. The magnetic pressure gradient in B_θ from the inboard side to the outboard side of the perturbation accelerates the perturbation. Magnetic tension from bent axial magnetic field resists the perturbation.	28
3.2	Three idealized flux tubes. 2D plots show axial current density and pressure profiles. Axial magnetic field is uniform for all cases. 3D figures show magnetic field (red) in the core, skin of the flux tube and in vacuum. a) The skin current case used by Tayler and Kruskal-Shafranov. b) Diffuse current case used by Newcomb. c) Core-skin current case used in this derivation.	31
3.3	Analytical $\bar{k} - \bar{\lambda}$ stability spaces parameterized with core current fraction ϵ and rigidness δ . a) Stability spaces for $\epsilon = 0.1$ and $\delta = 0.1$. White region is stable, gray is unstable, hatched region is kink ($m = 1$) unstable, and crosshatched region is unstable to both kink and sausage ($m = 0$) modes. b) Kink stability space dependence on ϵ with $\delta = 0$. Dark red region is unstable. c) Sausage stability space dependence on ϵ with $\delta = 0.7$. Dark green region is unstable. d) Sausage stability boundary dependence on δ with $\epsilon = 0.2$. Dark green region is unstable.	38

3.4	Radial profiles of \bar{j}_z , \bar{B}_θ , and \bar{p} for a) $\epsilon_{eff} = 0.7$, b) $\epsilon_{eff} = 0.5$, and c) $\epsilon_{eff} = 0.1$ used for the calculations shown in fig. 3.5. Dashed vertical lines demarcate (from left to right): core, transition, skin, and transition regions.	39
3.5	Numerical $\bar{k} - \bar{\lambda}$ stability spaces with relative growth rates. Normalized kink $\delta W_{m=1}$ contours for (a) $\epsilon_{eff} = 0.7$, (b) $\epsilon_{eff} = 0.5$, and (c) $\epsilon_{eff} = 0.1$; Normalized sausage $\delta W_{m=0}$ contours for (d) $\epsilon_{eff} = 0.7$, (e) $\epsilon_{eff} = 0.5$, and (f) $\epsilon_{eff} = 0.1$. The cross hatched regions indicate Suydam unstable regions in the $m = 1$ plots and regions with internal instabilities in the $m = 0$ plots. [Associated dataset available at http://dx.doi.org/10.5281/zenodo.230611]. [43] . . .	43
3.6	The ratio of $\delta W_{m=0}/\delta W_{m=1}$ for (a) $\epsilon_{eff} = 0.7$, (b) $\epsilon_{eff} = 0.5$, and (c) $\epsilon_{eff} = 0.1$. In the white space either at least one of the potential energies is positive or undetermined. [Associated dataset available at http://dx.doi.org/10.5281/zenodo.230611]. [43]	44
3.7	Critical $\bar{\lambda}$ value for a given size parameter S^* above which the instability will couple to microscopic scales. The hatched region starts at the minimum sausage unstable $\bar{\lambda}$ for an $\epsilon_{eff} = 0.7$ current profile. The dashed line denotes the Taylor criterion $\bar{\lambda} = 2\sqrt{2}$	48
4.1	Three-electrode planar plasma gun configuration: showing magnetic field (red), electric field (black), gas valves (grey), outer electrode (orange), middle electrode (gold), inner electrode (gray), current (green), and flows (blue). The gas injection slits in the electrode are azimuthally symmetric. a) Vacuum \vec{B} and \vec{E} fields are imposed by a solenoid and the applied electrode potentials, respectively. b) Initial breakdown occurs along arched magnetic field. c) MHD pumping has collimated the magnetic field. Core and skin currents are driven by the applied electrode potentials. d) MHD pumping drives axial flows. The azimuthally symmetric gas injection slits allow the plasma to freely rotate in response to the radial electric field.	52
4.2	Experiment control: Operators control the experiment with a PC application using LabVIEW DAQmx and LabVIEW FPGA module to program the PXI Cards. The pulse generators / counters and digital outputs generate fast pulses and DC signals. These signals are converted to optical outputs, travel through optical isolation fibers, and are converted back to electrical signals at the experiment. 120 analog inputs digitize diagnostic signals. Control of the 6 pulse generators in the PXI-6133 is not yet implemented.	55
4.3	GUI of experiment control software: a) Timing sequence panel, b) PSU/DIO control panel, c) Global settings panel, d) slow digitizer panel, e) fast digitizer panel, and f) storage control panel.	56

4.4	Experiment control software: The initialize block loads default settings and creates a queue. The queue is passed to two loops running in parallel. The producer loop handles GUI events by creating jobs and enqueueing them. The consumer dequeues jobs. Jobs are processed in the corresponding state of the state machine with calls to DAQmx and NISync Vis. If the state is part of a multi-state sequence, the state may enqueue further jobs. The shutdown event closes the queue and both loops and calls the shutdown block.	58
4.5	Shot sequence in the state machine: Operators pressing the <i>FIRE</i> button trigger the shot sequence. Each state is processed in order. DIO are digital output tasks controlling the DC receivers. After <i>Clean Up</i> the state machine returns to the <i>Idle</i> state.	59
4.6	FPGA block diagram: The FPGA code consists of four single-cycle-timed loops (SCTL): 1) Initialize and register manipulation loop (40 MHz), 2) Acquire loop (50 MHz), 3) Write to DRAM (100 MHz), and 4) Readout DRAM (100 MHz).	61
5.1	Left) CCD image of emission from kinked canonical flux tube. Right) Artist's interpretation of gyrating canonical flux tube. Axial flow and vacuum magnetic field are directed towards the anode. The current flows in the opposite direction. Measurement planes and interpolation volume are shown in purple.	66
5.2	Coherent gyration. a) Gun current (dashed green) and azimuthal magnetic field (red) measured 5 cm from gyration center by the stationary fiducial probe during a typical shot (#15253). After the current exceeds the Kruskal-Shafranov limit, the magnetic field develops a modulation corresponding to the magnetic flux tube gyration. b) Frequency distribution across all shots of the modulation in the fiducial probe signal. Frequencies are determined by the peak of a Fourier transform. A Gaussian with a constant offset is fit to the distribution. c) Distribution of modulation amplitude in the fiducial probe signal just before the crowbar across all shots.	67
5.3	Plasma length and time scales, and maximum achieved spatial and temporal resolution of internal probes (cross-hatched). The resolution is set by the Nyquist frequency of the digitizers 10 MHz and the Nyquist length of the smallest achieved spatial resolution (0.006 m). Plasma scales are calculated with magnetic field $B = 0.02 T$, number density $n = 3 \cdot 10^{19} m^{-3}$, electron temperature $T_e = 10 eV$, ion temperature $T_i = 1 eV$, and flux tube length $L = 0.5 m$ [65].	68

5.4	Left) Normalized power spectrum density of azimuthal magnetic field measured 5 cm from gyration axis by fiducial probe before the crowbar, averaged across 10 shots with significant gyration (#15256–15262 and #15267–15269), and 10 shots without gyration (#15305, #15306, #15336, #15352, #15408, #15408, #15410, #15412, #15414, #15416, and #15418). Right) Normalized spectral power distribution for all 2,369 shots obtained by integrating the red area in the left plot.	72
5.5	Points at which measurements were taken in the coherent shot set with \vec{B} , triple, and Mach probes. The (purple hatched) region is the union of measurement spaces which is used to reconstruct canonical flux tubes and their helicity. . . .	75
5.6	Linear barycentric interpolation: for interpolation on a 2D grid the vertices of a triangle are weighted by the z values. Each triangle has a uniform slope in the x and y directions ($\Delta z/\Delta x$ and $\Delta z/\Delta y$). The RSX data is on a 3D grid, so tetrahedrons are used.	76
5.7	Left) Field null iteration scheme. \vec{B} and $ \vec{B} $ at time $t = 8.5 \mu s$ in the $z = 25$ cm plane. A field line (successive steps from light gray to black) is integrated in both directions starting from the peak of $ \vec{B} $, a circle is least squares fitted to the field line, and a new integration starting point is determined by moving 10% of the radius towards the circle center (successive steps from light gray to black). Right) Field nulls over one gyration period of $17 \mu s$ (white to black). Error bars (light gray) are determined by repeating the field null iteration scheme with successively stronger filtered data, averaging across shots. The field null gyration lies on a circle (dashed red). Circles with 2 cm radius are plotted around every 25 th field null. 2 cm is the radius at which current and density drop of by $1/e$ [65]. Light gray region is the space in which both measurements of B_x and B_y were made. Dark gray region is the joint measurement space of all diagnostics used for flux tube reconstruction and helicity integrals.	78
5.8	Gyrating electron canonical flux tubes. $n\vec{B}$ ($\vec{\Omega}_e$) field lines trace two electron canonical flux tubes over one gyration period of $17 \mu s$ in the joint measurement volume. The field lines are launched from circles of 1 mm (orange) and 5 mm (red) radii centered at the null of B_x and B_y in the $z = 25$ cm plane. A single field line (dark red) on the outer flux tube helps visualize the twist. Contours of j_z are plotted in the $z = 25$ cm plane, the colorbar units are $\frac{A}{m^2}$. The field null is inside the joint measurement from $t = 4.1 \mu s$ to $t = 12 \mu s$	81

5.9	Stationary electron canonical flux tubes. $n\vec{B}$ ($\vec{\Omega}_e$) field lines tracing out two electron canonical flux tubes over one gyration period of $17 \mu s$. The field lines are launched from circles of 1 mm (orange) and 5 mm (red) radii centered at $x = 0$ and $y = 0$. A single field line (dark red) on the outer flux tube helps to visualize the twist. Contours of j_z are plotted in the $z = 25 \text{ cm}$ plane, the colorbar units are $\frac{A}{m^2}$	82
5.10	Isosurfaces of n normalized by the peak value in each of the x-y measurement plane over one gyration period of $17 \mu s$. The last isosurface encloses the top 10% of n . For comparison, electron canonical flux tubes and j_z from fig. 5.8 are plotted.	83
5.11	Isosurfaces of T_e normalized by the peak value in each x-y measurement plane over one gyration period of $17 \mu s$. The last isosurface encloses the top 10% of T_e . For comparison, electron canonical flux tubes and j_z from fig. 5.8 are plotted.	84
5.12	Gyrating ion canonical flux tubes. $\vec{\Omega}_i$ field lines trace out two ion canonical flux tubes over one gyration period of $17 \mu s$. The field lines are launched from circles of 1 mm (black) and 5 mm (grey) radii centered at the null of B_x and B_y in the $z = 25 \text{ cm}$ plane. For comparison \vec{B} flux tubes and j_z from fig. 5.8 are plotted.	85
5.13	Schematics of twists and writhe. The positive axial direction is from left to right. Left) A right-handed twist (black) and a left-handed twist (red). Right) The black tube writhes with right-handed sense around the red tube.	86
5.14	Taylor plot comparing known vacuum magnetic field (black star) with gradient of scalar potential (red triangles) obtained for 4 grid resolutions with the discrete cosine transform method for solving the Laplace problem. The known vacuum field is in the upper right quadrant of a x-y coordinate system with the conductor at its center. The known magnetic field is used as Neumann boundary condition for the Laplace solver.	91
5.15	Left) Test problem setup for the two-component vector potential solver. The known test fields are the magnetic fields from a gyrating current-carrying cylindrical conductor at several angles. Right) Taylor plot comparing known magnetic fields from gyrating current-carrying conductor at various angles with curl of vector potential solutions obtained with the two-component vector potential method (squares).	93

5.16	Magnetic (red), cross (green), flow (blue), and total ion canonical (black) helicity in the joint measurement volume identified in figs. 5.7 and 5.5. a) Gauge-dependent helicities with real units. b) Relative helicities with real units. c) Boxcar (1.02 μs width) filtered relative helicities, normalized to the maximum relative cross helicity. Dark gray shading marks the time the field null is inside the joint measurement volume. Light gray shading marks the time at which the field null is inside the region with both B_x and B_y measurements shown in fig. 5.7. Dashed orange shows the magnetic helicity of a simplified model problem. The model problem consists of a cylindrical conductor with 0.02 m radius and uniform current density $j = 140 \text{ kA/m}^2$ with an exponential density cloud, $n(r) = 1.3 \cdot 10^{19} e^{r/(0.02m)} \text{ m}^{-3}$, where r is the radius. The conductor is gyrating along the red dashed circle fitted to the field null path in fig. 5.7. All helicities are the mean determined from running the analysis nine times with successively increasing the standard deviation of the Gaussian kernel filtering of the interpolated measurements. The standard deviation of the runs is plotted as an envelope around the helicity curves, however, the helicity calculations are insensitive to this filtering and the envelope is only partially visible.	95
C.1	Mochi.PSU1: Two capacitor banks in an 80-20 frame enclosed with ABS plastic panels.	240
C.2	One bank of PSU1: ABS panels have been removed. The acrylic tube around the ignitron coaxial housing is visible.	241
C.3	Exploded view of capacitor bank assembly.	242

LIST OF TABLES

Table Number	Page
1.1 Select plasma length and time scales. B is the magnetic field, T_σ is the species temperature, n_0 is, assuming quasi-neutrality, the particle number density, q_σ is the species charge, ϵ_0 is the vacuum permittivity, k_B is Boltzmann's constant, c is the speed of light, k_D is the drift wave number, and Λ is the plasma parameter which is the number of particles in a Debye sphere.	2

ACKNOWLEDGMENTS

This thesis describes the methods and results of my work as a graduate student; however, it does not capture the human nature of this endeavor. I am indebted to Professor Setthivoine You for his patience and insight throughout this work. He invited me to participate in the great opportunity of building a new plasma physics laboratory. It is amazing to consider how far we have come from an empty room to regularly generating plasma jets traveling at a hundred thousand miles per hour, with temperatures of a hundred thousand degrees, and hundreds of kiloamps of current. I will always cherish the discussions on engineering, physics, and the totally absurd I had with my fellow graduate students while we were building the experiment: Alexander Card, Evan Carroll, Eric Sander Lavine, Iman Datta, Manuel Azuara-Rosales, Morgan Quinley, Keon Vereen, and Yu Kamikawa. I thank the Department of Energy SCGSR program for funding my stay at Lawrence Livermore National Laboratory (LLNL) where I reconstructed canonical flux tubes from the RSX dataset. I am grateful to Dr. Jason Sears for mentoring me during my year at LLNL. I thank Dr. Alan Glasser for introducing me to his DCON code and discussions on MHD stability analysis. The faculty of the Aeronautics & Astronautics department, especially: Prof. Antonio Ferrante, Prof. Brian Nelson, Prof. Tom Jarboe, Prof. Raymond Golingo, and Prof. Uri Shumlak taught me how to think, design, and question like a plasma physicist. The machinists at the Physics, Mechanical Engineering, and Aeronautics & Astronautics machine shops, especially Ron Musgrave taught me how to work safely and helped me design and build components for our experiment. I also would like to thank my graduate student friends, the Pacific Science Center, and Software Carpentry for much fun and time away from research. I have immense respect for my father, Walter, for how he cared for me after the loss of his wife, my mother, Barbara. I thank him for his continuing support and

encouragement to this day. And most of all I thank my best friend and wife, Taralyn. Thanks for supporting me, for your artistic eye and input on my figures, for reading over this thesis, and for your patience! I look forward to our next adventures with your growing family of four siblings and their spouses. Thanks to them too for their patience and support. I promise to make up for all the birthdays and holidays missed.

DEDICATION

In loving memory of my mother, Barbara Sue von der Linden, and in deep gratitude to my father, Walter von der Linden.

Chapter 1

INTRODUCTION

1.1 Plasma physics: a multiscale problem

A plasma is a quasi-neutral gas of electrically charged and neutral particles that exhibits collective behavior [1]. Each kind of charged particle in the gas of a specific charge and mass is designated a plasma species σ , e.g., electrons e and ions i . It has been estimated that 99% of the visible matter in the universe is plasma [2]. The study of plasma physics provides the basis for the dynamics of space and astrophysical systems from the solar corona to accretion disks surrounding black holes. On earth, plasmas are used in many applications ranging from fluorescent lights to industrial material processing. Fusion energy research endeavors to harness energy resulting from the fusion of low atomic number ions such as deuterium and tritium. A crucial difference between plasma and conventional fluids, solids, and gases is the importance of collective effects. Plasma particles interact simultaneously with a large number of particles over long distances through electromagnetic forces. In principle, one could determine the behavior of a plasma by integrating the equations of motions of individual particles and evolving electromagnetic fields according to Maxwell's equations. However, the sheer number of particles ($10^{19} - 10^{22} m^{-3}$ for the experiments discussed in chapters 4 and 5) combined with the wide range of spatial and temporal scales at which the particles interact make this approach practically impossible [3]. Particle collisions and long range electromagnetic fields influence plasma behavior on a hierarchy of temporal and spatial scales [4, 5].

1.1.1 Hierarchy of plasma scales

Table 1.1 shows select characteristic plasma lengths and frequencies in their approximate hierarchical ordering. The exact ordering depends on the parameters of the plasma of interest. Ref.

Debye length	λ_D	$\sqrt{\frac{\epsilon_0 k_B T_e}{n_0 q_e^2}}$	electron plasma frequency	ω_{pe}	$\sqrt{\frac{n_0 q_e^2}{\epsilon_0 m_e}}$
electron skin depth	λ_e	$\frac{c}{\omega_{pe}} = c \sqrt{\frac{\epsilon_0 m_e}{n_0 q_e^2}}$	ion cyclotron frequency	ω_{ci}	$\frac{q_i B}{m_i}$
thermal ion Larmor radius	r_{Li}	$\frac{v_{th}}{\omega_{ci}} = \frac{\sqrt{m_i k_B T_i}}{q_i B}$	ion plasma frequency	ω_{pi}	$\sqrt{\frac{n_0 q_i^2}{\epsilon_0 m_i}}$
ion skin depth	λ_i	$\frac{c}{\omega_{pi}} = c \sqrt{\frac{\epsilon_0 m_i}{n_0 q_i^2}}$	Alfvén transit frequency	ω_A	$\frac{B}{\pi L \sqrt{\mu_0 n_0 m_i}}$
electron mean free path	λ_{mfp}	$\frac{v_{th}}{\nu_{ei}} = \frac{12\pi^{3/2} \epsilon_0^2 (k_B T_e)^2}{\sqrt{2} n_0 q_i^2 q_e^2 \ln \Lambda}$	drift wave frequency	ω_D	$\frac{k_y d n_0 / dx k_B T_e}{n_0 q_e B_z}$
system scale length	L	-	electron-ion collision frequency	ν_{ei}	$\frac{\sqrt{2} n_0 q_i^2 q_e^2 \ln \Lambda}{12\pi^{3/2} \sqrt{m_e} \epsilon_0^2 (k_B T_e)^{3/2}}$
			electron-ion energy equilibration frequency	ν_{Eei}	$\approx \frac{m_e}{m_i} \nu_{ei}$

Table 1.1: Select plasma length and time scales. B is the magnetic field, T_σ is the species temperature, n_0 is, assuming quasi-neutrality, the particle number density, q_σ is the species charge, ϵ_0 is the vacuum permittivity, k_B is Boltzmann’s constant, c is the speed of light, k_D is the drift wave number, and Λ is the plasma parameter which is the number of particles in a Debye sphere.

[5] surveys the hierarchy of time scales. Here, an overview of the hierarchy of length scales in a plasma will be given. In the absence of external forces, plasmas are microscopically neutral. The Debye length λ_D is the scale at which charge is shielded. At the Debye length λ_D , the thermal particle energy, which causes charge separation, and the opposing electrostatic energy balance [1]. The stability of the macroscopic neutrality of a plasma is described by the electron skin depth λ_e . When an external perturbation displaces a charge from its equilibrium position, resulting electric fields will give rise to electron motion which restores charge neutrality [1]. The characteristic frequency of oscillation for the electrons in a plasma is the electron plasma frequency ω_{pe} . The electron skin depth λ_e is the wavelength of electromagnetic waves of this frequency $c = \lambda_e \omega_{pe}$, where c is the speed of light. λ_e depends only on the particle density n_0 . In plasmas with magnetic fields the thermal ion cyclotron frequency ω_{ci} is the frequency associated with electrostatic (Bernstein) and electromagnetic cyclotron waves, which can be used to heat a plasma [5]. The thermal ion Larmor radius r_{Li} is the cyclotron radius for thermal ions. Magnetic fields constrain perpendicular motion of charged particles. When the Larmor radius is much shorter than the mean free path of a particle species, it acts as an effective

mean free path in fluid closure schemes, which allow the plasma species to be treated as fluids on scales larger than the Larmor radius. This separates kinetic models which track the evolution of velocity distribution functions for each species from fluid models where the distribution function is assumed to be Maxwellian, and only the evolution of the moments describing the Maxwellian need to be tracked. A magnetic field may also restrict the motion of electrons, allowing heavier ions to respond to a displacement. The characteristic oscillation frequency of ions is the ion plasma frequency ω_{pi} . The ion skin depth or ion inertial length λ_i is the wavelength of electromagnetic waves of this frequency. Beyond this length scale the difference in ion and electron inertia becomes negligible, allowing the ions to move together with the electrons and for models to treat the species as a single conducting fluid (magnetohydrodynamics, MHD). λ_i is a factor of the charge ratio times the square root of the ion-to-electron mass ratio ($q_e/q_i \sqrt{m_i/m_e}$) larger than λ_e . Collisions between particles of a like and unlike species lead to transfer of momentum (directed velocity) and energy (thermal velocity) [6]. The collision frequencies for momentum and energy transfer in and between species have their own hierarchical ordering in terms of powers of the electron-to-ion mass ratio m_e/m_i . The electron mean free path λ_{mfp} is the length scale at which momentum is transferred between electrons and ions and is of the same order of magnitude as the length scale at which momentum is equilibrated among electrons. The transfer of directed velocity between electrons and ions inhibits the flow of current and is responsible for resistivity. When the resistivity is small the plasma can be treated as perfectly conducting (ideal MHD). In ideal MHD plasmas, the magnetic field and plasma density oscillate together and waves propagate at the Alfvén velocity v_a . The characteristic time of the ideal MHD model is given by the transit time of an Alfvénic wave through the system scale length L .

In typical plasmas, several orders of magnitude separate the Debye length from the electron mean free path. One challenge for a plasma physicist is to identify the relevant scales of the problem of interest and build an appropriate model involving kinetic, two-fluid, or MHD approximations. This task is complicated by the tendency of phenomena on one scale to couple to disparate scales. Drift waves in plasmas with density gradients provide a prominent exam-

ple. Although the characteristic frequency of the drift wave instability is usually several orders of magnitude larger than the ion cyclotron frequency, the it can couple kinetic effects to slow MHD timescales [5, 6].

1.2 Context: astrophysical, heliospheric, and laboratory plasmas

Fig. 1.1 provides examples of characteristic length scales in three distinct plasmas: an astrophysical jet from a star forming region, a coronal loop, and the Mochi.Labjet laboratory experiment.

1.2.1 Astrophysical jets

Astrophysical jets are collimated, high-speed outflows from rotating accretion disks surrounding massive objects. Jet lengths range from less than a light year ($10^{16} m$) in young stellar objects (YSO) to megaparsecs ($10^{22} m$) in active galactic nuclei (AGN) [7]. Jets are collimated and very straight; their aspect ratio can be in the order of 10:1 to 1000:1. Outflow velocities vary from $\sim 100 km s^{-1}$ in protostellar jets to relativistic speeds in AGN jets. Observations of signatures of helical magnetic fields [10, 11] with plasma parameters listed in fig. 1.1 indicate that the jets can be described with MHD models. This raises several questions: Why are jets so long and thin, often without apparent signs of large scale instabilities that are common in laboratory plasma experiments? When jets do form irregularities such as bulges, knots, and wiggles, what causes them and can they provide insights into activities in the source of the jets? Observations of azimuthal rotation [12, 13] and axial shear flow [14] suggest that shear flows may stabilize MHD instabilities as has been observed in laboratory experiments [15]. It has been hypothesized that destabilizing helical magnetic twist may be converted to stabilizing helical shear flows at length scales of ion inertial lengths or ion Larmor radii [16]. In fig. 1.1 the characteristic plasma scales in a protostellar jet vary from the Debye length λ_D to the electron mean free path λ_{mfp} by six orders of magnitude; the jet length is 16 orders of magnitude longer than λ_D . A mechanism must therefore be identified that could couple the MHD scales

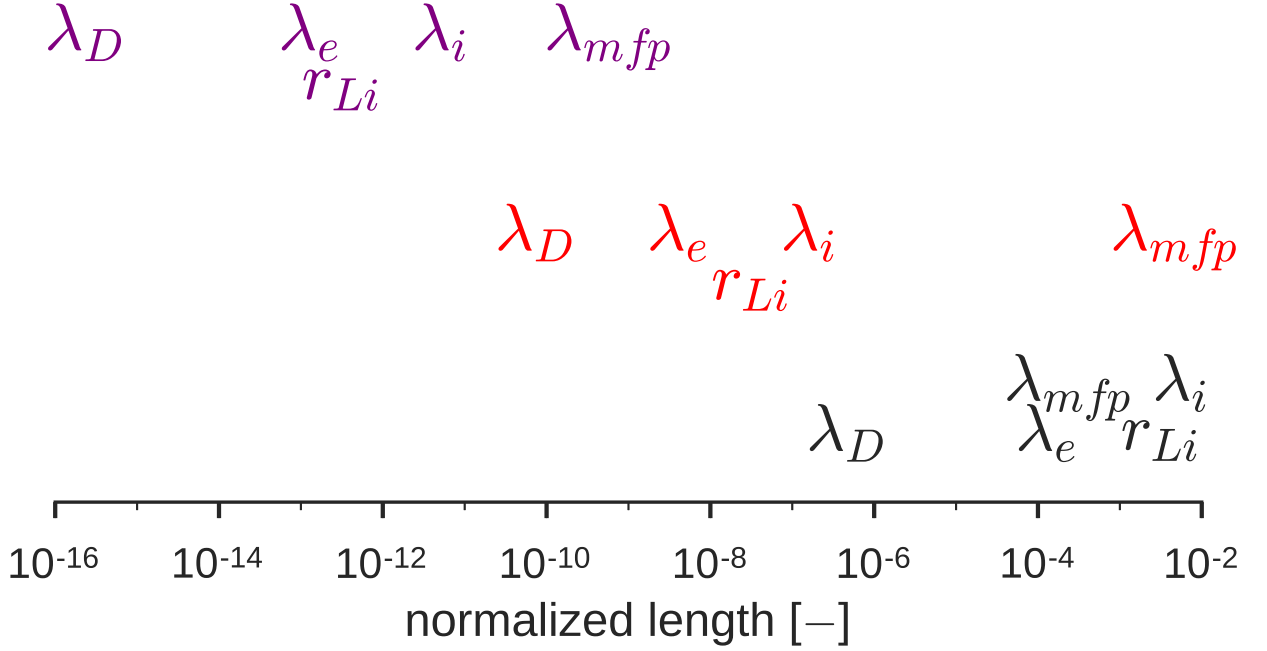


Figure 1.1: Characteristic plasma length scales in a protostellar jet (purple), coronal loop (red), and the Mochi.Labjet laboratory experiment (black). All lengths are normalized to the respective scale length L . For the protostellar jet $T_e = T_i = 1 \text{ eV}$ [7], $n_0 = 10^{12} \text{ m}^{-3}$ [7], $m_i = m_p$, $B = 10^{-5} \text{ T}$ [8], $Z = 1$, $L = 10^{14} \text{ m}$ [7] were chosen. For the coronal $T_e = T_i = 100 \text{ eV}$ [9], $n_0 = 10^{15} \text{ m}^{-3}$ [9], $m_i = m_p$, $B = 10^{-3} \text{ T}$ [4], $Z = 1$, $L = 10^8 \text{ m}$ [9] were chosen. For Mochi.Labjet $T_i = 1 \text{ eV}$, $T_e = 5 \text{ eV}$, $n_0 = 10^{22} \text{ m}^{-3}$, $m_i = m_p$, $B = 0.1 \text{ T}$, $Z = 1$, $L = 1 \text{ m}$ were chosen based on the initial experiment design parameters. Z is the ionization number ($q_i = Ze$) and $m_p = 1.7 \cdot 10^{-27} \text{ kg}$ is the mass of a proton.

to the two-fluid λ_i and kinetic r_{Li} scales.

1.2.2 Coronal loops in the heliosphere

Coronal loops are arched structures formed when twisted magnetic flux rises above the photosphere with their footpoints anchored to the photosphere. The loops may become further twisted due to footpoint motion. Coronal loops vary in length from $10^6 m$ to $10^9 m$. Plasma flows along the coronal loops with velocities between $5 km s^{-1}$ and $30 km s^{-1}$, with densities ranging from $10^{15} m^{-3}$ to $10^{17} m^{-3}$ [17]. Solar flares and coronal mass ejections may be associated with coronal loop interactions. A solar flare is a rapid, local release of electromagnetic energy in form of x-ray and gamma ray radiation. Coronal mass ejections (CME) are often associated with flares and are large releases of plasma matter threaded with magnetic fields. Coronal loops can produce collimated jets with lengths of 7,000–40,000 km, lifetimes of minutes and velocities of $10 - 1000 km s^{-1}$. The coronal plasma with temperatures over a million Kelvin is much hotter than the photosphere plasma below the corona with temperatures of only 6000 Kelvin [18]. Magnetic reconnection may release magnetic energy injected by coronal foot point motion into heat, electromagnetic waves, and plasma particle kinetic energy. Models of reconnection that rely on resistive reconnection on MHD scales (Sweet-Parker, Petschek) do not predict reconnection fast enough to reconcile with observations of solar flares [19]. Thus, solar magnetic reconnection is a prominent example of interactions between different plasma scales. A large global region is thought to feed magnetic flux to small localized regions where two-fluid and kinetic effects allow fast breaking of field lines and conversion of magnetic energy to thermal and kinetic energy [20]. Fig. 1.1 illustrates the wide separation of scales. The ion Larmor radius r_{Li} and the ion inertial length λ_i are eight and seven orders of magnitude smaller than the length of the coronal loop, respectively.

1.2.3 Topological change in fusion energy concepts

Plasma jets and loops can be created in the laboratory; one approach to do this uses planar plasma guns. In these experiments, breakdown occurs along a magnetic dipole field linking concentric electrodes. Gas puffed in through discrete holes in the electrodes forms dense plasma arches with a low density background. The dense plasma arches merge, because they carry parallel currents, forming a central current-carrying jet. The magnetic dipole field is flared and current is driven by an electrode potential difference along the flux tube fulfilling the conditions for MHD pumping and collimation of the flux tube [21]. A pressure gradient and $\vec{J} \times \vec{B}$ forces accelerate plasma axially to Alfvénic velocities. The flow carries magnetic flux and stagnates at the end of the jet where the increased magnetic flux collimates the jet [22]. The dense part of flux tube lengthens continuously and collimates throughout the shot ($\sim 10 - 100 \mu\text{s}$ duration), while the current of the power supply ramps up. If the aspect ratio times the ratio of current of axial magnetic field exceeds a certain value, the Kruskal-Shafranov limit, the plasma jet may kink. Ref. [23] observed Rayleigh-Taylor instabilities forming on top of the kinking jet plasmas. The acceleration of the kink acts as an effective gravity for Rayleigh-Taylor instabilities to develop. The Rayleigh-Taylor instabilities may create small enough spatial scales to generate regions where two-fluid or kinetic physics might allow faster reconnection and topological change to occur which result in the formation of toroidal configurations of interest for fusion energy concepts. Toroidal plasma configurations, called spheromaks, have been observed to form from linear pinches and jets ejected from plasma guns [24]. Another toroidal configuration, called spherical torus, has been formed from flux tubes with current driven by washer guns [25]. Laboratory experiments are diverse; in fig. 1.1 the Mochi.Labjet experiment at the University of Washington serves as an example to illustrate the characteristic plasma scales. Seven orders of magnitude separate the jet length from the Debye length λ_D . The ion Larmor radius r_{Li} and ion inertial length λ_i are both within three orders of magnitude of the jet length. The low temperature and high densities shift the electron mean free path λ_{mfp} below the thermal ion Larmor radius r_{Li} .

1.3 Generalized fluxes and their helicity provide insight across scales

The above examples show that there are a wide range of length scales in typical plasmas and several indications for coupling between different scales. These phenomena can be modeled by subdividing plasmas into regions where different physics apply. Some models of reconnection treat the global scale with MHD, while microscopic reconnection points are treated with two-fluid or kinetic models [19]. Difficulties arise at the boundaries of these regions, where two-fluid physics or the non-Maxwellian nature of kinetic velocity distributions have to be reconciled with MHD. This thesis will focus on a complementary approach by studying the evolution of generalized fluxes and their helicity. For example, in ideal MHD the plasma density is frozen-in to the magnetic flux, i.e. particle excursions off flux surfaces can be neglected. This means it is sufficient to track the evolution of magnetic flux tubes. The magnetic flux tubes evolve subject to the topological constraint of helicity conservation, their twist, writhe, and interlinking is conserved. At scales where non-ideal effects, such as ion inertia, kinetic distribution functions, and finite Larmor radius effects become important the frozen-in magnetic flux condition is generalized to the frozen-in canonical flux condition [16]. Each plasma species is frozen-in to a canonical flux related to its canonical momentum. Canonical momentum includes both fluid flow and magnetic terms, so canonical helicity can be expressed as the sum of helicity of fluid flow and helicity of magnetic fields. Conversions between magnetic and kinetic energy can be viewed topologically as conversions between magnetic and fluid flow twist while conserving the overall twistedness of canonical flux tubes of all species. Chapter 2 will define canonical flux tubes and their helicity and review recent theoretical and experimental studies, with a focus on the spatial scales at which the different helicities are conserved and when conversions can occur. Chapter 3 will identify an instability cascade during which conversions between the fluid, cross, and magnetic terms of helicity can occur. Chapter 4 will describe the development of experimental control schemes and diagnostics to aid in measuring the 3D evolution of canonical flux and helicity. Chapter 5 will reconstruct canonical flux tubes and their helicity from measurements of a laboratory experiment.

Chapter 2

CANONICAL FLUX TUBES AND THEIR HELICITY

2.1 Introduction

This chapter first defines canonical flux tubes and reviews the canonical Ohm's equation which shows that there is a one-to-one relationship between a plasma species and its canonical flux tubes. Next, a review of experimental observations focuses on the dynamics of canonical flux tubes and relaxation subject to the constraint of canonical helicity: the twist, writhe, and interlinking of canonical flux tubes. The observations are interpreted with the recent theory of canonical helicity transport and dimensional analysis of helicity injection and decay. The overview of canonical helicity includes a new discussion of the effect of density gradients on helicity volume integrals.

2.2 Canonical flux tubes

2.2.1 Definitions

Each species in a plasma has a canonical momentum

$$\vec{P}_\sigma = \rho_\sigma \vec{u}_\sigma + \rho_{c\sigma} \vec{A}, \quad (2.1)$$

which is the weighted sum of the species velocity \vec{u}_σ and the magnetic vector potential \vec{A} . The weights are the mass function ρ_σ and the charge function $\rho_{c\sigma}$. The choice of the functions depends on the plasma model [26]. For single particles, the functions reduce to the particle species mass and charge $\rho_\sigma \rightarrow m_\sigma$ and $\rho_{c\sigma} \rightarrow q_\sigma$. In kinetic models which track the velocity distribution function f_σ for the particles of each species, the appropriate choice is $\rho_\sigma \rightarrow f_\sigma m_\sigma$ and $\rho_{c\sigma} \rightarrow f_\sigma q_\sigma$. In fluid models which track the number density n_σ , velocity \vec{u}_σ and energy / temperature T_σ of a fluid species, the functions reduce to $\rho_\sigma \rightarrow n_\sigma m_\sigma$ and $\rho_{c\sigma} \rightarrow n_\sigma q_\sigma$. This

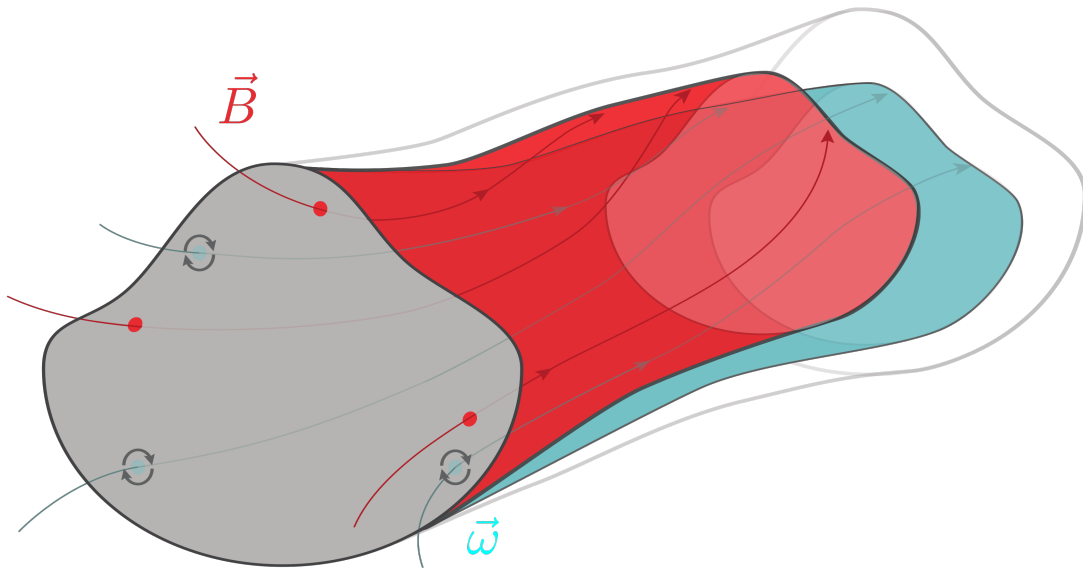


Figure 2.1: Artist's interpretation of canonical flux tube. When density is uniform, a canonical flux tube (grey) is the weighted sum of a magnetic flux tube (red) and a flow vorticity flux tube (blue).

thesis will focus on two-fluid systems with an ion ($\sigma \rightarrow i$) and electron ($\sigma \rightarrow e$) species. The curl of canonical momentum is called canonical circulation $\vec{\Omega}_\sigma = \nabla \times \vec{P}_\sigma$,

$$\vec{\Omega}_\sigma = n_\sigma m_\sigma \vec{\omega}_\sigma + n_\sigma q_\sigma \vec{B} + \frac{\nabla n_\sigma}{n_\sigma} \times \vec{P}_\sigma, \quad (2.2)$$

where $\vec{\omega}_\sigma$ is the flow vorticity, $\nabla \times \vec{u}_\sigma = \vec{\omega}_\sigma$, and \vec{B} is the magnetic field. Canonical circulation is divergence-free, meaning a cross-sectional area traced out by field lines integrated from an initial closed arbitrary area will enclose a constant amount of canonical flux. The canonical flux Ψ_σ is the surface integral of canonical circulation

$$\Psi_\sigma = \int_S \vec{\Omega}_\sigma \cdot d\vec{S}, \quad (2.3)$$

where S is the surface and \vec{S} the elementary surface normal. For the barotropic case of no density variation, canonical flux tubes can be written as a weighted sum of a magnetic flux tube $\psi = \int B \cdot d\vec{S}$ and a flow vorticity flux tube $\mathcal{F} = \int \omega_\sigma \cdot d\vec{S}$ (fig. 2.1),

$$\Psi_\sigma = n_\sigma m_\sigma \mathcal{F}_\sigma + n_\sigma q_\sigma \psi. \quad (2.4)$$

In the limit of negligible electron mass (inertia) the electron canonical flux tube becomes a magnetic flux tube ($\Psi_e \rightarrow \psi$).

2.2.2 Frozen-in canonical flux condition

Ref. [26] shows that the same set of canonical field equations in terms of canonical momentum and circulation can be derived from a Lagrangian-Hamiltonian formulation of relativistic single particle equations, the kinetic Vlasov equation, and the two-fluid evolution equations. This means that for all plasma scales the canonical fields evolve according to Maxwell's equations. The equation of motion for each model can be re-expressed as the canonical Ohm's law

$$\vec{\Sigma}_\sigma + \vec{u}_\sigma \times \vec{\Omega}_\sigma = -\vec{R}_\sigma. \quad (2.5)$$

The canonical force-field $\vec{\Sigma}_\sigma$ represents the conservative and inductive forces, $\vec{u}_\sigma \times \vec{\Omega}_\sigma$ represents the forces that do no work, e.g. Coriolis and Lorentz forces, and \vec{R}_σ represents the

dissipative forces. Analogous to the electric field the canonical force field is the sum of a potential gradient and an inductive term $\vec{\Sigma}_\sigma = -\nabla h_\sigma - \partial \vec{P} / \partial t$. For the two-fluid case the enthalpy h_σ ,

$$h_\sigma = n_\sigma q_\sigma \phi + \frac{1}{2} n_\sigma m_\sigma \vec{u}_\sigma^2 + \mathcal{P}, \quad (2.6)$$

combines the conservative electrostatic potential ϕ and scalar pressure \mathcal{P} , and the kinetic energy. Taking the curl of Ohm's law (2.5), in the absence of friction, results in the canonical induction equation [16], a generalization of the ideal MHD induction equation to include non-negligible inertia,

$$\frac{\partial \vec{\Omega}_\sigma}{\partial t} - \nabla \times (\vec{u}_\sigma \times \vec{\Omega}_\sigma) = 0. \quad (2.7)$$

This shows that in the absence of friction the canonical circulation is frozen-in to the species motion at all scales. There is a one-to-one relationship between the canonical flux tubes and the species. A consequence of the frozen-in condition appears under equilibrium conditions. Setting the time-varying and frictional terms in eq. (2.5) to zero, dotting with $\vec{\Omega}$, and assuming a steady-state equilibrium, yields

$$\nabla h_\sigma \cdot \vec{\Omega}_\sigma = 0. \quad (2.8)$$

For an equilibrium, gradients of enthalpy are always perpendicular to canonical circulation. When no potentials are applied, the pressure gradient is perpendicular to $\vec{\Omega}$. In the barotropic case where the pressure is purely density dependent, the condition reduces to

$$\nabla n_\sigma \cdot \vec{\Omega}_\sigma = 0. \quad (2.9)$$

Gradients of a species density are perpendicular to a species canonical circulation. For a single fluid MHD plasma without vorticity this condition reduces to the familiar flux surface condition

$$\nabla n_\sigma \cdot \left(n_\sigma q_\sigma \vec{B} + \frac{\nabla n_\sigma}{n_\sigma} \times \vec{P}_\sigma \right) = \nabla n_\sigma \cdot \vec{B} = 0. \quad (2.10)$$

Optical emission visible in images of a uniform temperature plasma is roughly proportional to the square of the density. The intensity profiles visible in these emission images are signatures of the magnetic, or more generally, the canonical flux [16].

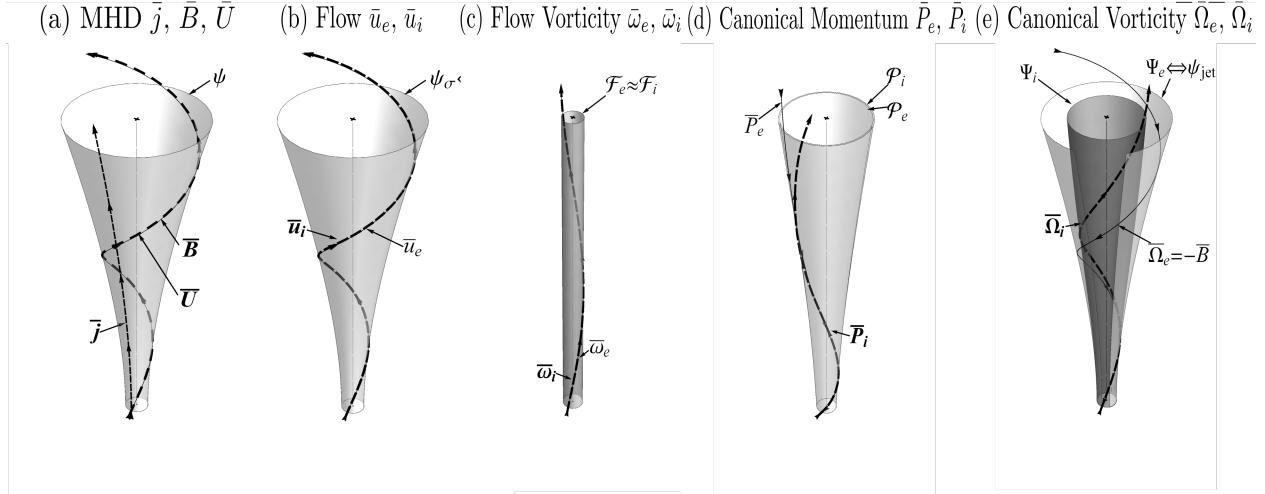


Figure 2.2: Five distinct flux tubes of quantities constrained by a choice of dipole vacuum magnetic field \bar{B} , uniform current \bar{j} , and electron velocity \bar{u}_e parallel to \bar{B} of magnitude $|\bar{u}_e|$. a) Current-carrying magnetic flux tube ψ_{jet} . b) Electron and ion flow flux tubes ψ_e and ψ_i . c) Electron and ion flow vorticity flux tubes \mathcal{F}_e and \mathcal{F}_i . d) Electron and ion canonical momentum flux tubes \mathcal{P}_e and \mathcal{P}_i . e) Electron and ion canonical flux tubes Ψ_e and Ψ_i . Bar denotes dimensionless quantities. Reproduced from [16] by permission of the AAS.

2.2.3 Theoretical and experimental studies

Several laboratory experiments generate linear canonical flux tubes and study their dynamics with a focus on magnetic flux tubes. Plasma discharges along arched magnetic field lines connecting two electrodes create current-carrying arched magnetic flux tubes with geometries similar to coronal loops [29, 30]. Other experiments have a flared magnetic field, e.g. a dipole field connects a circular electrode with an outer annular electrode. A flared field is a field with radial and axial components, the radial component varies along the central axis. MHD

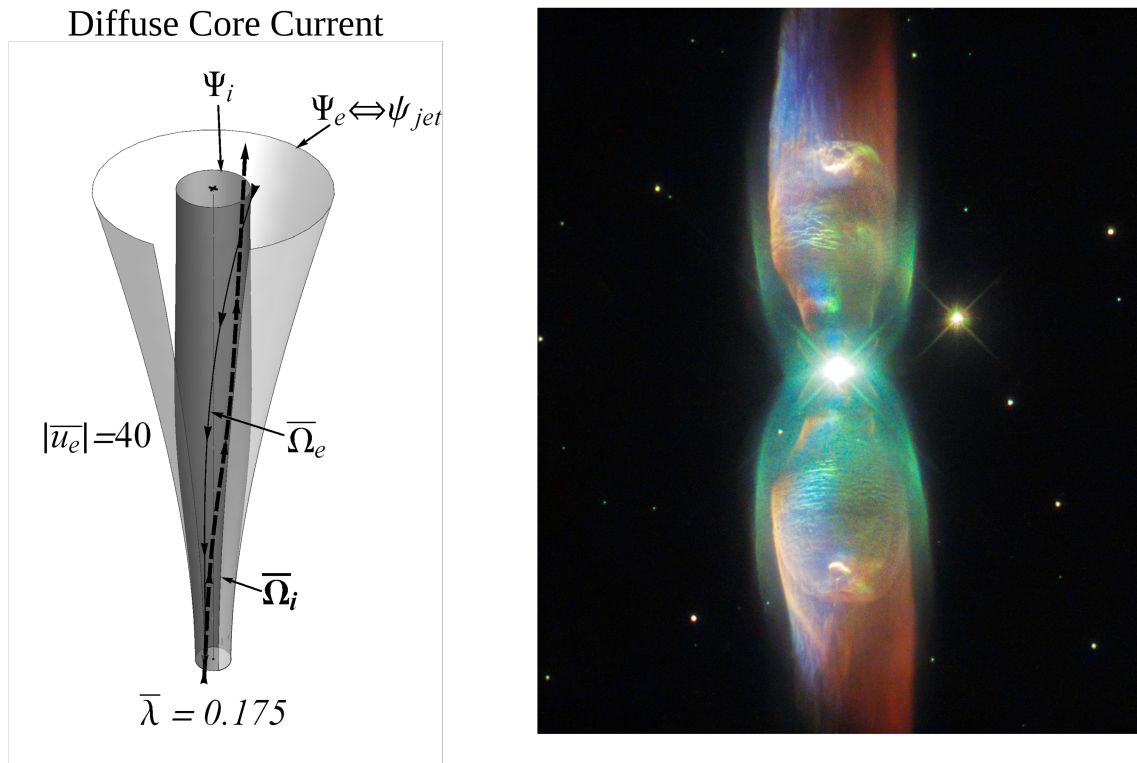


Figure 2.3: Left) Bulged ion canonical vorticity flux tube Ψ_i (dark gray) for a diffuse core current jet with low current ($\bar{\lambda} = 0.175$) and a large electron velocity ($\bar{u}_e = 40$). Bar denotes dimensionless quantities. Reproduced from [16] by permission of the AAS. Right) M2-9 Butterfly nebula (NASA HST STIS/CCD – MIRVIS), a bipolar planetary nebula with distinctive bulging that resembles the ion canonical flux tube on the left. By ESA/Hubble, CC BY 4.0 [27].

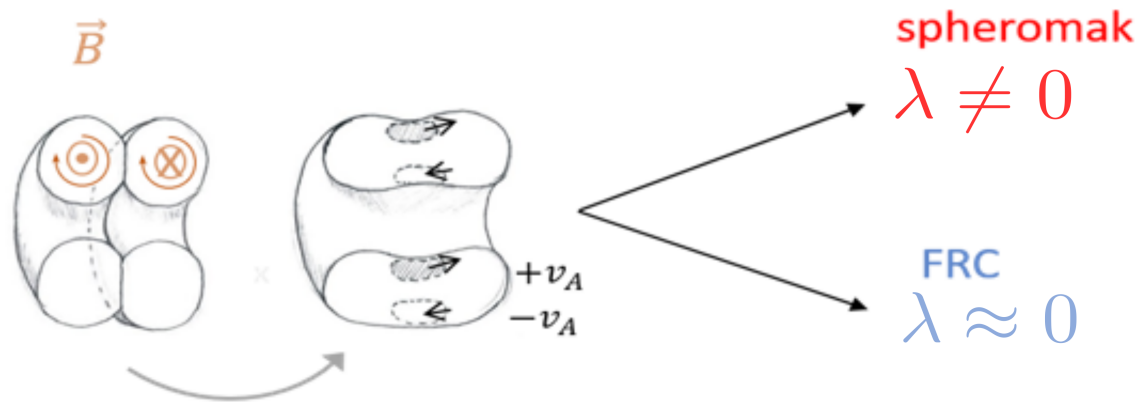


Figure 2.4: Two counter-helicity spheromaks merge. The initial magnetic helicities are experimentally varied and characterized by the eigenvalue λ_0 . During the merging process magnetic reconnection converts magnetic energy into ion heating, ion flows, and magnetic activity. When the ion skin depth λ_i over the system length L is large the magnitude of the shear flows becomes large. The ion heating and ion flows form an enthalpy difference across the flux tubes. If the initial magnetic helicity is below a threshold, the helicity is annihilated and the final configuration is an FRC with negligible magnetic helicity and $\lambda \approx 0$. If the initial magnetic helicity is above a threshold, low mode number magnetic activity restores magnetic helicity and the final configuration is a spheromak with finite magnetic helicity and $\lambda \neq 0$. Image credit: Setthivoine You

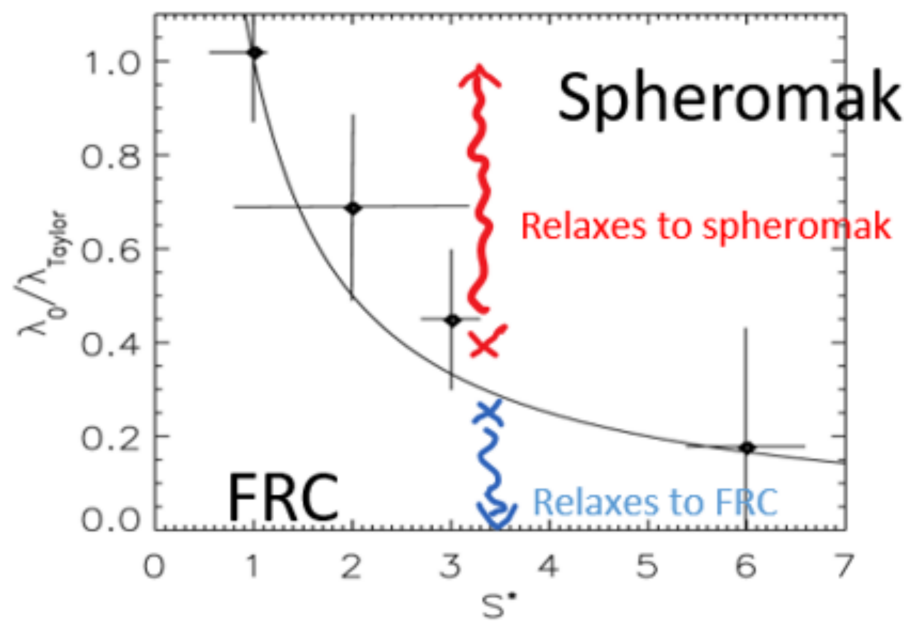


Figure 2.5: Threshold of initial eigenvalue $\lambda_0/\lambda_{Taylor}$ as a function of the size parameter S^* for forming a spheromak or a FRC from counter-helicity merging. Reprinted from [28]. Copyright 2005 IOP Publishing.

pumping will pump density and magnetic flux along the arched flux tubes, collimating them into lengthening current-carrying magnetic flux tubes [21, 22]. Recently, an analytical study visualized the topology of current-carrying canonical flux tubes in a flared magnetic field [16]. The study assumes a barotropic two-fluid with massless electrons. Fig. 2.2 shows equivalent flux tubes of a system with an imposed flared vacuum magnetic field in the axial and radial directions and a uniform current parallel to the vacuum magnetic field. Fig. 2.2 (a) shows the current-carrying flared magnetic flux tube $\psi = \int \vec{B} \cdot d\vec{S}$ with twisted magnetic field lines due to the superposition of the flared dipole field and the dynamic magnetic field generated by the uniform current j . The center-of-mass flow \vec{u} is frozen into the magnetic flux surface. The center-of-mas flow \vec{u} is equivalent to the ion flow \vec{u}_i if the electron mass is assumed to be negligible. Fig. 2.2 (b) shows the ion and electron flow tubes $\psi_\sigma = \int \vec{u}_\sigma \cdot d\vec{S}$. The electron flow is parallel to the magnetic field since the electrons are assumed to be massless. The ion flow is fully constrained by the imposed current \vec{j} and the electron speed ($\vec{j} = n_0 (q_i \vec{u}_i - q_e \vec{u}_e)$). Both species flow tubes overlap and the species flows remain on the flow flux tube. Fig. 2.2 (c) shows the species flow vorticity flux tubes $\mathcal{F} = \int \vec{\omega}_\sigma \cdot d\vec{S}$. Since there is no azimuthal current the azimuthal species velocities and axial flow vorticity are identical. The axial flow vorticity dominates the radial flow vorticity at moderate to large currents, collimating the vorticity flux tubes. Fig. 2.2 (d) shows the canonical momentum tubes $\mathcal{P}_\sigma = \int \vec{P}_\sigma \cdot d\vec{S}$. These flux surfaces are distinct for each species; while the electron canonical momentum is identical to the magnetic vector potential surface, the ion flow momentum pulls the ion canonical momentum surface towards the ion velocity surfaces. Fig. 2.2 (e) shows flux tubes of canonical circulation: the canonical flux tubes. The electron canonical flux tube overlaps with the magnetic flux tube. The ion canonical flux tube collimates due to the contribution of the axial flow vorticity. When a diffuse current profile with a low ratio of current to vacuum magnetic flux and high electron velocity is imposed the canonical flux tube can bulge as shown in fig. 2.3. This resembles the bulging of emission observed in astrophysical jets launched from planetary nebula. It is important to remember that these visualizations were based on a kinematic model. The canonical quantities were determined directly by the imposed current, vacuum magnetic

field, electron flow velocity, and ignoring the self-consistent dynamics of canonical equations of motion (which would require a full simulation). This explains why the ion flows seem to violate the canonical frozen-in condition by following the magnetic flux surface instead of the ion canonical circulation flux surface. Nevertheless, canonical flux tubes offer a topological view of, in this case, two-fluid physics and indicate that two-fluid effects may contribute to collimation and bulge formation. The detailed dynamics and the reason the two-fluid terms of the equation of motion should be significant at the long scales of an astrophysical jet (see fig. 1.1) remain to be identified.

As is illustrated in the canonical flux tube visualization, driving a current along a canonical flux tube twists up the magnetic field and flows, twisting the canonical flux tube. A current is generated by applying a potential difference across the ends of the canonical flux tube. More generally applying an enthalpy difference will lead to canonical flux tubes twisting, writhing, and interlinking. This twist, writhe, and interlinking of canonical flux tubes is called canonical helicity. In many systems, it has been observed that the helicity is well conserved compared to the system energy leading to a constrained relaxation towards a minimum energy state for a given helicity [31]. The minimum energy states for plasmas with a finite magnetic helicity (twisted magnetic flux tubes) have been widely studied. In a simply connected vacuum chamber the minimum energy state is called a spheromak, in a toroidal vacuum chamber it is called a reversed-field configuration (RFP) [24]. Spheromaks and RFPs have been observed in many experiments, see [32, 33]. In RFPs relaxation occurs in sawtooth events which are discrete in time. The internal magnetic field profile evolution in RFPs during these sawtooth crashes has been reconstructed from equilibrium models using measured pressure and edge magnetic fields. The decay rate of magnetic energy is 2-4 times as large as the decay rate of magnetic helicity [34].

However, there are also experimental observations that indicate a fast conversion of twisted magnetic flux tubes into twisted flow vorticity flux tubes. Attempts to generalize relaxation theory to plasmas with canonical helicity [35] have identified the field-reverse configuration as a possible minimum energy state for plasmas with finite fluid helicity (twisted flow vorticity flux

tubes) but no (negligible) magnetic helicity. Both spheromaks and FRCs are compact toroids (see fig. 2.4). It is useful to define a coordinate system consisting of toroidal and poloidal directions. A spheromak has both toroidal and poloidal magnetic fields, while an FRC only has poloidal magnetic field with no (or a weak) toroidal field. At the TS-4 experiment [36] two spheromaks with opposite magnetic helicity but no flows merge and may form either a single spheromak with finite magnetic helicity or a field-reversed configuration (FRC) with negligible magnetic helicity and finite fluid helicity (fig. 2.4). The formation of either a spheromak or FRC is a bifurcation characterized by a sharp threshold depending on the initial helicity in the two merging spheromaks [28]. The initial helicity of the spheromaks can be characterized by the eigenvalue λ which quantifies the amount of current parallel to the magnetic field. If the magnetic helicity in the spheromaks is exactly equal and opposite $\lambda = 0$, otherwise λ will be a finite value. The minimum λ eigenvalue necessary to form a spheromak is called λ_{Taylor} . Fig. 2.5 shows the threshold λ/λ_{Taylor} to be exceeded by the merging spheromaks for a spheromak to form, against the size parameter S^* , which is the ratio of the ion Larmor radius r_{Li} over the system length L . S^* is varied by using different gases, i.e. varying the ion mass to change r_{Li} while keeping L constant. If the initial λ/λ_{Taylor} eigenvalue is below (above) the threshold a FRC (a spheromak) is formed. Ref. [28] observed that initially the magnetic helicity (λ) decreases in all merging experiments through magnetic reconnection. The outflows from the magnetic reconnection cause a ‘slingshot’ effect which generates magnetic activity, ion shear flows, and ion heating [37, 38, 39]. The magnetic activity cascades from high (Fourier) mode numbers down to low mode numbers. Magnetic activity at low mode numbers has been observed at other experiments to amplify poloidal magnetic flux and may cause the increase in magnetic helicity for spheromak end states. However, for low values of the size parameter the shear flows become large and their ratio with the Alfvén velocity exceeds a value that has been shown to stabilize low mode number instabilities in current-carrying plasma columns with no axial magnetic fields (Z-pinches) [15, 40]. This shear flow stabilization may prevent the restoration of magnetic helicity and lead to the formation of an FRC.

Ref. [28] explains in a qualitative matter the mechanisms responsible for the bifurcation;

however, to understand the observed threshold quantitative models are needed of: 1) the partitioning of the magnetic energy into magnetic activity, ion heating, and ion flows, 2) the strength of the flux amplification through low mode magnetic activity, 3) the threshold of azimuthal shear flow stabilization (in a toroidal geometry), and 4) possible nonlinear feedback between these three mechanisms. The theory of canonical helicity can provide a complementary explanation, sidestepping the detailed mechanisms and instead focusing on the transfer of electron to ion canonical helicity. The shear flow and ion heating occurring during the spheromak merging at the TS-4 experiment represent an enthalpy difference being applied to a canonical flux tube. To understand under what conditions the enthalpy leads to injection of electron (magnetic) helicity and the formation of a spheromak or the injection of ion (fluid flow) helicity the canonical helicity transport equations must be derived and analyzed.

2.3 Canonical helicity

Helicity is the volume integral of vector potential of a flux quantity dotted with the flux quantity. For canonical flux tubes the canonical helicity is defined as

$$K_\sigma = \int \vec{P}_\sigma \cdot \vec{\Omega}_\sigma dV. \quad (2.11)$$

Substituting the two-fluid limits of expressions (2.1) and (2.2) yields

$$K_\sigma = \int n_\sigma^2 [m_\sigma^2 \vec{u}_\sigma \cdot \vec{\omega}_\sigma + q_\sigma^2 \vec{A} \cdot \vec{B} + m_\sigma q_\sigma (\vec{u}_\sigma \cdot \vec{B} + \vec{A} \cdot \vec{\omega}_\sigma)] + \vec{P}_\sigma \cdot \left(\frac{\nabla n_\sigma}{n_\sigma} \times \vec{P}_\sigma \right) dV. \quad (2.12)$$

Since a cross product dotted with one of its factors is always zero the last term can be dropped. While canonical flux tubes depend on density gradients, their canonical helicity is independent of any density gradients but is locally weighted by the square of the number density n_σ^2 . Applying vector identities and Gauss's theorem a surface integral can be extracted from the volume integral

$$K_\sigma = \int n_\sigma^2 [m_\sigma^2 \vec{u}_\sigma \cdot \vec{\omega}_\sigma + q_\sigma^2 \vec{A} \cdot \vec{B} + 2m_\sigma q_\sigma \vec{u}_\sigma \cdot \vec{B}] dV + \int n_\sigma^2 \vec{A} \times \vec{u}_\sigma \cdot d\vec{S}. \quad (2.13)$$

For an isolated system where neither the flow vorticity nor the magnetic field penetrate the integration volume, the three vectors \vec{A} , \vec{u}_σ , and $d\vec{S}$ are coplanar so the last term of the equation

above is zero. The canonical helicity can be expressed as the sum of three helicities

$$K_\sigma = \mathcal{H}_\sigma + \mathcal{X}_\sigma + \mathcal{K}_\sigma. \quad (2.14)$$

The three helicities are the fluid helicity

$$\mathcal{H}_\sigma = m_\sigma^2 \int n_\sigma^2 \vec{u}_\sigma \cdot \vec{\omega}_\sigma dV, \quad (2.15)$$

the cross helicity

$$\mathcal{X}_\sigma = 2m_\sigma q_\sigma \int n_\sigma^2 \vec{u}_\sigma \cdot \vec{B} dV, \quad (2.16)$$

and the magnetic helicity

$$\mathcal{K}_\sigma = q_\sigma^2 \int n_\sigma^2 \vec{A} \cdot \vec{B} dV. \quad (2.17)$$

Canonical helicity can thus be understood as the sum of helicity between flux tubes of flow vorticity $\int \vec{\omega}_\sigma \cdot \vec{S}$, helicity between flux tubes of magnetic field $\int \vec{B} \cdot \vec{S}$, and helicity due to interlinking between the flow vorticity and magnetic flux tubes. While many references define the fluid, cross, and magnetic helicities without the mass and charge factors, this thesis will include them to make the units uniform for all helicities. In the limit of negligible electron mass, electron canonical flux tubes reduce to magnetic flux tubes. The ion canonical flux tubes are a weighted sum of flow vorticity and magnetic flux tubes. The spheromak discussed previously has only magnetic helicity and no fluid helicity, so its electron and ion helicities are equal if the ions are singly ionized. The FRC has no (negligible) magnetic helicity and significant fluid helicity, so its electron helicity is negligible but its ion helicity is significant.

2.3.1 Relative canonical helicity

The expressions for canonical helicity presented so far are only unambiguous for isolated systems where neither the flow vorticity $\vec{\omega}_\sigma$ nor the magnetic field \vec{B} penetrate the integration boundary. When current is driven along magnetic flux tubes by a static potential difference applied to electrodes, the magnetic flux tubes necessarily intersect the electrode. If flux tubes penetrate the integration volume there is an ambiguity in their helicity since the linkages outside the volume cannot be measured [24] (fig. 2.6). Moreover, ref. [39] notes that each time



Figure 2.6: Gauge-dependence of helicity. An integral over the gray volume cannot count the number of linkages of the two flux tubes external to the grey volume. Adapted from [24].
Image credit: Jaclyn Lake.

species flux tubes intercept, as would be the case in the spheromak merging experiments there is a gauge dependent ambiguity since species integration volumes are intersecting. To alleviate this problem, ref. [39] introduces a gauge-invariant relative canonical helicity

$$K_{\sigma rel} = \int \vec{P}_{\sigma-} \cdot \vec{\Omega}_{\sigma+} dV, \quad (2.18)$$

where the plus and minus subscripts offset a vector \vec{X} by a reference field $\vec{X}_{pm} = \vec{X} \pm \vec{X}_{ref}$. The canonical reference field must satisfy the conditions [16]

$$\begin{aligned} \nabla \times \vec{\Omega}_{\sigma ref} \Big|_V &= 0, \\ \vec{\Omega}_{\sigma ref} \cdot d\vec{S} &= -\vec{\Omega}_{\sigma} \cdot d\vec{S}, \text{ and} \\ \nabla \times \vec{P}_{\sigma ref} &= \vec{\Omega}_{\sigma ref}. \end{aligned} \quad (2.19)$$

This means that the normal component of the reference canonical circulation must be equal and opposite to the canonical circulation at the integration boundary. The three helicity expression eq. (2.14) of canonical helicity can be written in relative form

$$K_{\sigma rel} = \mathcal{H}_{\sigma rel} + \mathcal{X}_{\sigma rel} + \mathcal{K}_{\sigma rel}. \quad (2.20)$$

The three helicities are the relative fluid helicity

$$\mathcal{H}_{\sigma rel} = m_{\sigma}^2 \int n_{\sigma}^2 \vec{u}_{\sigma-} \cdot \vec{\omega}_{\sigma+} dV, \quad (2.21)$$

the relative cross helicity

$$\mathcal{X}_{\sigma rel} = m_{\sigma} q_{\sigma} \int n_{\sigma}^2 (\vec{u}_{\sigma-} \cdot \vec{B}_{+} + \vec{u}_{\sigma+} \cdot \vec{B}_{-}) dV, \quad (2.22)$$

and the relative magnetic helicity

$$\mathcal{K}_{\sigma rel} = q_{\sigma}^2 \int n_{\sigma}^2 \vec{A}_{-} \cdot \vec{B}_{+} dV. \quad (2.23)$$

2.3.2 Canonical helicity transport

The canonical helicity evolution equation can be obtained by combining the derivative of eq. (2.18) with the canonical Ohm's law eq. (2.5) and induction equation eq. (2.7)

$$\frac{dK_{\sigma rel}}{dt} = - \int (\vec{\Sigma}_{\sigma+} \cdot \vec{\Omega}_{\sigma-} + \vec{\Sigma}_{\sigma-} \cdot \vec{\Omega}_{\sigma+}) dV - \int h_{\sigma-} \vec{\Omega}_{\sigma+} \cdot d\vec{S} - \int \vec{P}_{\sigma-} \times \frac{\partial \vec{P}_{\sigma+}}{\partial t} \cdot d\vec{S} + \int (\vec{P}_{\sigma-} \cdot \vec{\Omega}_{\sigma+}) \vec{v}_{\sigma} \cdot d\vec{S}. \quad (2.24)$$

The integral terms represent a dissipative term, a battery term, an inductive term, and a Leibniz term due to the boundary motion \vec{v}_σ of the system, respectively. The battery term injects helicity when an enthalpy difference is applied to a canonical flux tube, e.g. when a potential is applied at the ends of a canonical flux tube or, in the case of spheromak merging, when kinetic energy and pressure differences are created by reconnecting canonical flux tubes. To understand when helicity is preferentially injected as magnetic or fluid helicity it is helpful to look at the battery term in isolation. In the limit of constant density, the ion battery term can be rewritten to differentiate between injection into the flow vorticity flux tube and the magnetic flux tube

$$\dot{K}_{rel} = m_i \Delta h_{i-} \int \vec{\omega}_{i+} \cdot d\vec{S} + q_i \Delta h_{i-} \int \vec{B}_+ \cdot d\vec{S} \quad (2.25)$$

where Δh_{i-} is the relative enthalpy difference across the ion canonical flux tube. The ratio of helicity injection into the magnetic and flow vorticity flux tubes can be defined as the helicity injection threshold [39]

$$\bar{K}_{thr} \equiv \frac{|m_i \Delta h_i \int \vec{\omega}_i \cdot d\vec{S}|}{|q_i \Delta h_i \int \vec{B} \cdot d\vec{S}|} \sim \frac{m_i u_{ith}}{q_i L B} \sim \frac{r_{Li}}{L} \sim \frac{1}{S^*}. \quad (2.26)$$

Applying dimensional analysis to the helicity injection threshold recovers the same size parameter S^* dependence as was observed in the TS-4 experiment ¹.

To understand when a species helicity dissipates slower than the system energy, i.e. is a suitable relaxation constraint, the species helicity evolution has to be compared to the energy evolution. Ref. [26] derives an energy H evolution equation from the same Lagrangian-Hamiltonian formation that was used to derive the canonical evolution equations, with a dissipative term $dH/dt = -\int \vec{\Sigma}_\sigma \cdot \vec{u}_\sigma dV$. In a fixed, isolated system, with no intersecting species flux tubes, all terms except for frictional dissipation can be ignored and no reference fields are needed

$$\frac{\Delta K_\sigma}{\Delta H_\sigma} = 2 \frac{\int \vec{R}_\sigma \cdot \vec{\Omega}_\sigma dV}{\int \vec{R}_\sigma \cdot \vec{u}_\sigma dV} \frac{H_{\sigma 0}}{K_{\sigma 0}} \sim 2 \frac{\vec{\Omega}_\sigma}{\vec{u}_\sigma}. \quad (2.27)$$

¹Strictly the dimensional analysis can not specifically identify the ion Larmor radius r_{Li} . The analysis identifies a dependence on the square root of the ion mass $\sqrt{m_i}$, since $u_{ith} \sim 1/\sqrt{m_i}$. The ion skin depth also has a dependence on $\sqrt{m_i}$.

Applying dimensional analysis to the factor yields

$$\frac{\Delta K_\sigma}{\Delta H_\sigma} = 2 \frac{\vec{\Omega}_\sigma}{\vec{u}_{\sigma 0}} \sim 2 \frac{\frac{n_0 m_\sigma u_{\sigma 0}}{L} + q_\sigma B_0}{u_0} \quad (2.28)$$

where $u_{\sigma 0}$ and B_0 are the characteristic species flow and magnetic field, respectively. A characteristic Larmor radius r_L can be identified by pulling out the mass density and then a factor of $q_\sigma B$

$$\frac{\Delta K_\sigma}{\Delta H_\sigma} \sim \frac{n_0 m_\sigma}{\frac{L m_\sigma u_{\sigma 0}}{2(u_{\sigma 0} m_\sigma + q_\sigma B_0 L)}} \sim \frac{n_0 m_\sigma}{\frac{\frac{L m_\sigma u_{\sigma 0}}{q_\sigma B_0}}{2\left(\frac{u_{\sigma 0} m_\sigma}{q_\sigma B_0} + L\right)}} \sim \frac{\rho_0}{\frac{L r_L}{2(r_L + L)}} \sim \frac{\rho_0}{2\left(\frac{1}{L} + \frac{1}{r_L}\right)}. \quad (2.29)$$

The ratio of the rate of change in species helicity over energy scales with a mass density gradient. Identifying L as a characteristic scale of circulation L_c , the scale length $L_H = 1/(1/L_c + 1/r_L)$ is a hybrid length of a characteristic length of flow circulation L_c and a characteristic Larmor radius r_L . When the mass density gradient scale is below the hybrid length L_H then the species helicity will decay faster than energy. Ref. [39] shows that while one species helicity may decay the other will increase so that the sum of the ion and electron helicities will be conserved.

2.4 Conclusion

Recent theoretical work and experimental observations suggest that canonical flux tubes and their helicity may provide a complimentary point of view, valid across all scales of plasma physics. The theory of canonical helicity transport recovers the plasma size parameter S^* scaling dependence which is observed as the bifurcation threshold in compact toroid merging experiments. Density gradients on the scale of the species Larmor radius r_L for magnetically dominated plasmas have been identified as the condition under which species helicity decay and conversion to the other species may occur. Analytical models have explored the kinematic evolution of canonical flux tubes. This thesis aims to connect these previous results with experimental physics by 1) identifying dynamics in current-carrying magnetic flux tubes that may create small-scale structures at which the density gradients could meet conditions for species

helicity decay and conversion, 2) developing experimental and numerical techniques to facilitate the measurement of large scale datasets needed to reconstruct canonical flux tubes and their helicity from measurements, and 3) reconstructing canonical flux tubes and their helicity from measurements of a linear plasma column.

Chapter 3

SAUSAGE INSTABILITIES ON TOP OF KINKING LENGTHENING CURRENT-CARRYING MAGNETIC FLUX TUBES

This chapter will theoretically explore the possibility of sausage instabilities developing on top of a kink instability in lengthening current-carrying magnetic flux tubes. Recent laboratory experiments suggest that hierarchies of instabilities, such as kink and Rayleigh-Taylor, could create small scale structure and density gradients at which conversions of electron (magnetic) and ion (fluid) canonical helicity may occur. Sausage instabilities can also provide this coupling mechanism between disparate scales. Flux tube experiments can be classified by the flux tube's evolution in a configuration space described by a normalized inverse aspect-ratio \bar{k} and current-to-magnetic flux ratio $\bar{\lambda}$. A lengthening current-carrying magnetic flux tube traverses this $\bar{k} - \bar{\lambda}$ space and crosses stability boundaries. We derive a single general criterion for the onset of the sausage and kink instabilities in idealized magnetic flux tubes with core and skin currents. The criterion indicates a dependence of the stability boundaries on current profiles and shows overlapping kink and sausage unstable regions in the $\bar{k} - \bar{\lambda}$ space with two free parameters. Numerical investigation of the stability criterion reduces the number of free parameters to a single one that describes the current profile, and confirms the overlapping sausage and kink unstable regions in $\bar{k} - \bar{\lambda}$ space. A lengthening, ideal current-carrying magnetic flux tube can therefore become sausage unstable after it becomes kink unstable.

The primary part of this chapter is reproduced from von der Linden, J., & You, S. (2017). Sausage instabilities on top of kinking lengthening current-carrying magnetic flux tubes. *Physics of Plasmas*, 24(5), 052105 [41], with the permission of AIP Publishing.

The code used for the analysis and to generate figs. 3.3, 3.4, 3.5, and 3.6 in this chapter has been published on Zenodo at

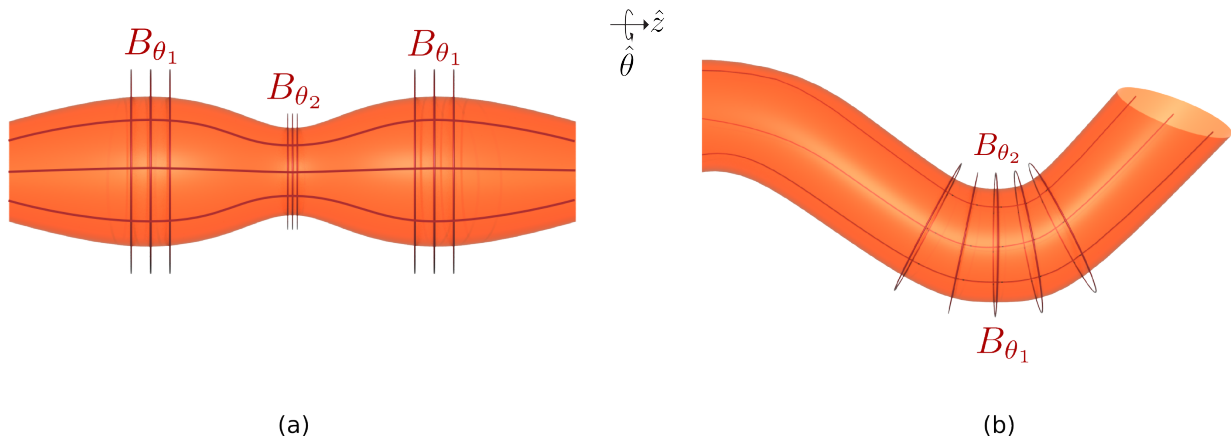


Figure 3.1: a) Sausage $m = 0$ instability. Increased B_{θ_2} exerts an increased pinch force. Magnetic pressure and tension from compressed and bent magnetic field resist the perturbation. b) Kink $m = 1$ instability. The magnetic pressure gradient in B_{θ} from the inboard side to the outboard side of the perturbation accelerates the perturbation. Magnetic tension from bent axial magnetic field resists the perturbation.

<https://doi.org/10.5281/zenodo.230489> and is included in appendix A [42].

The dataset underlying fig. 3.5 and fig. 3.6 has been published on Zenodo at <https://doi.org/10.5281/zenodo.230611> [43].

3.1 Background

Magnetic flux tubes are defined as a bundle of magnetic field lines that run through a closed contour [44]. When current flows along a magnetic flux tube, several current-driven instabilities may develop (fig. 3.1), which are generally well understood with the ideal magnetohydrodynamic (MHD) behavior of current-carrying flux tubes [45], where for mathematical convenience, the column is modeled by an infinitely long cylinder and classified into one of two ideal analytical models: a skin screw pinch (with an axial magnetic field and an electrical

current flowing only on an infinitely thin boundary layer separating the plasma from vacuum) [46], or a diffuse pinch (with an axial magnetic field, no skin current, but some distribution of current inside the plasma) [47]. In all cases, classical instability onset conditions are retrieved from the Energy Principle [48] on Fourier perturbed states of the idealized current-carrying magnetic flux tube: i.e. starting from a static equilibrium like a ball at rest on a hill or valley, if the perturbed potential energy is negative, the system would be unstable to that particular mode. Indications that the coupling of different types of instabilities may play a role in astrophysical, heliospheric, and laboratory phenomena have motivated a renewed interest in revisiting and extending classical instability criteria. MHD instabilities may be responsible for structure formation in astrophysical jets [49] and understanding these structures may provide insight into activity at the source of the jets. Kink and sausage instabilities have been observed in coronal loops and could trigger large energy releases and heating of the solar corona [18]. Instabilities appear to be necessary for the formation of toroidal plasma configurations from initially open flux tubes, such as spheromaks [50, 51] and spherical tori [25]. Recent experiments have identified an instability cascade, where a macroscopic instability triggers a microscopic instability, creating small scale structures which directly couple the disparate plasma scales [52]: the acceleration of a growing kink on the scale length of the flux tube acts as an effective gravity, leading into a Rayleigh-Taylor instability. The Rayleigh-Taylor instability forms structures on the scale of ion inertial lengths, enabling fast reconnection [23]. Two neighboring current-carrying magnetic flux tubes may kink on system scale lengths, attract each other, merge, reconnect on ion inertial lengths, and launch ion-cyclotron waves [18]. Spheromak merging experiments observe annihilation of magnetic helicity followed by the formation of a Field-Reversed Configuration (FRC) with ion flows, when the scale lengths approach ion Larmor radii [28, 39]. Partially-toroidal flux tubes in a solar loop laboratory experiment erupt when they are unstable to both the torus and kink instabilities, but fail to erupt when they are unstable to only one of the instabilities [29]. In toroidal fusion devices the merging of discrete temperature flux tubes has been associated with global sawtooth events [53]. To identify possible couplings between MHD instabilities, it is necessary to examine current-carrying magnetic

flux tube stability beyond the conditions used to derive classical stability criteria. Finite-length screw pinches with one or both ends tied down have kink instability criteria modified from classical Kruskal-Shafranov values [54], explaining some experimental results [55]. Sheared axial plasma flow stabilizes the Z-pinch to kink and sausage instabilities [15], an effect subsequently observed in the laboratory [40]. In many flux tube experiments the flux tube is bound between two electrodes and remains at a fixed length while the current ramps up. In contrast, a flared current-carrying magnetic flux tube generated from one boundary, gives rise to strong axial plasma flows before collimating into a filamentary cylinder. This collimation occurs continuously as the flows convect magnetic flux into the flared end of the flux tube, resulting in a lengthening of the collimated flux tube while the current ramps up. This behavior was described theoretically [21] and observed experimentally [22]. The same flux tube has then been observed to become kink unstable, detach from the source electrodes and form a spheromak [50]. The detachment of the flux tube may be initiated by a sausage-like instability, but comparisons between measurements and theory currently rely on stability criteria derived for skin screw-pinch models of infinite length, even though the experiment's flux tube has a distributed current and lengthens during the shot duration. This paper presents a single general stability criterion for the onset of ideal MHD instabilities in a lengthening current-carrying magnetic flux tube with both a diffuse internal and sharp skin current and comparisons to numerical calculations.

3.2 Theory

Here, the general, minimized form of the perturbed potential energy of the system is subdivided into 3 terms: the first (internal) term is simplified with Newcomb's analysis [47] of internal stability; the second (skin) term is further simplified by considering Bellan's analysis [21] of a self-collimating flared flux tube; the third (vacuum) term is simplified by assuming the wall is at infinity. Differing from standard treatments, none of the terms are subsequently set to zero in the analytical treatment (fig. 3.2).

The starting point is the general, minimized, 1D perturbed potential energy of the current-

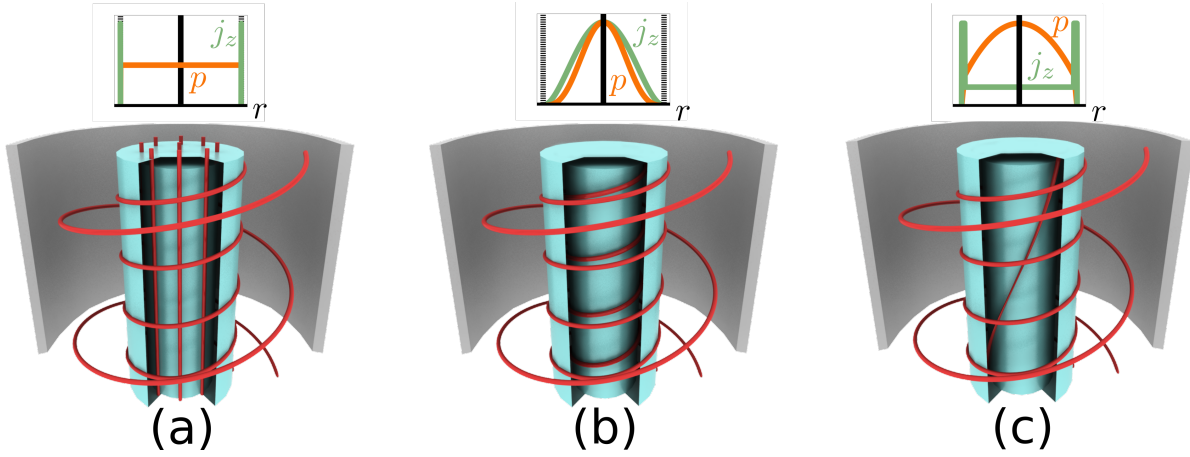


Figure 3.2: Three idealized flux tubes. 2D plots show axial current density and pressure profiles. Axial magnetic field is uniform for all cases. 3D figures show magnetic field (red) in the core, skin of the flux tube and in vacuum. a) The skin current case used by Tayler and Kruskal-Shafranov. b) Diffuse current case used by Newcomb. c) Core-skin current case used in this derivation.

carrying magnetic flux tube $\delta W(\xi)$ which depends only on the radial displacement $\xi(r)$ of the flux surface at radial position r . This real 1D scalar expression is reduced from $\delta W(\vec{\xi})$, a complex expression of the infinitesimal 3D displacement $\vec{\xi} = \xi(r)\hat{r} + \eta(\phi)\hat{\phi} + \zeta(z)\hat{z}$, with classical assumptions: the idealized cylindrically-symmetric flux tube with periodicity length L , radius a , is surrounded by vacuum, no walls (wall at radius $r = b \rightarrow \infty$), and subdivided into the internal (plasma) volume between $0 \leq r \leq p$ and a thin shell (interface or skin) between $p \leq r \leq v$, where p is the ‘plasma’ side of a and v is the ‘vacuum’ side of a . The plasma pressure is isotropic and inviscid. The plasma is incompressible, $\nabla \cdot \vec{\xi} = 0$, which is the most unstable worst case scenario and allows reduction of the 3D $\vec{\xi}$ to a 1D ξ . This assumption also removes pressure-driven instabilities from consideration, leaving only the current-driven contributions. The fundamental instabilities are the sausage ($m = 0, n \geq 1$) and kink ($|m| \geq 1, n \geq 1$) modes, where m is the azimuthal mode number and n the longitudinal mode number of the Fourier perturbation on the cylinder. The perturbations are small and linear, to ignore

higher order terms, and adiabatic, so the perturbed plasma pressure can be simply expressed in terms of the equilibrium pressure and the displacement ξ . The longest (worst-case, $n = 1$) perturbation wave length is assumed so that $k = 2\pi/L$. The system is described by ideal MHD so the perturbed magnetic field can be expressed simply in terms of the plasma displacement and the equilibrium magnetic field. The system is assumed initially to be in static equilibrium, so equilibrium quantities are not time dependent and integration constants can be put to zero.

The linearly perturbed potential energy δW is thus integrated by parts into contributions δW_{pl} from the plasma, δW_i from the interface and δW_v from the vacuum [45]. The δW_{pl} term represents the available free energy of the plasma, with contributions from the internal vacuum magnetic field, the plasma pressure and internal currents (δW_{B_1} , δW_{p_1} , δW_{J_0} respectively). The δW_i term represents the work required to move the boundary between the plasma and the vacuum. The δW_v represents the energy transferred to the external vacuum magnetic fields. From the Energy Principle, the flux tube is stable if the total perturbed potential energy $\delta W = \delta W_{pl} + \delta W_i + \delta W_v \geq 0$ and unstable otherwise. The general, minimized form of the perturbed potential energy of the system is thus subdivided into three terms and, differing from standard treatments, none of the terms are subsequently set to zero in our analytical treatment. We simplify the first (internal) term with Newcomb's analysis [47] of internal stability, the second (skin) term with Bellan's analysis [21] of a self-collimating flared flux tube, and the third (vacuum) term with the assumption the wall is at infinity. We now look at each term individually. The incompressible plasma's perturbed potential energy δW_{pl} is given by [47]

$$\delta W_{pl} = \frac{\pi L}{2\mu_0} \left(\int_0^p \left[f \left(\frac{\partial \xi}{\partial r} \right)^2 + g \xi^2 \right] dr + [h \xi^2]_0^p \right) \quad (3.1)$$

where $f = r(krB_z + mB_\phi)/(k^2r^2 + m^2)$, $h = (k^2r^2B_z^2 - m^2B_\phi^2)/(k^2r^2 + m^2)$ and g is also a function of k , r , B_z , B_ϕ that will soon be eliminated, and m is the azimuthal mode number. The first term of eq. (3.1) can be minimized if ξ is the solution to the associated Euler-Lagrangian equation

$$\frac{\partial}{\partial r} \left[f \frac{\partial \xi}{\partial r} \right] - g \xi = 0. \quad (3.2)$$

Eq. (3.2) has a singular point in the flux tube whenever $f = 0$, i.e. wherever $q = m$, having defined $q = 2\pi r B_z / (L B_\phi)$, corresponding to rational mode surfaces $q = m/n$ with $n = 1$. Solutions ξ thus only exist in regions between two singular points (called an ‘interval’). It is sufficient to only consider stability to the $m = 0, \pm 1$ modes because if a column is stable to both, it is also stable to higher order modes [47]. So the ‘no singular point’ condition becomes $q \neq 0, \pm 1$. Newcomb [47] proves extensively the conditions for the existence of solutions and the conditions for internal stability ($\delta W_{pl} \geq 0$) of a collimated magnetic flux tube: a collimated magnetic flux tube is stable if and only if (a) the Suydam criterion [56] is satisfied for $r > 0$ (but doesn’t have to be at $r = 0$); (b) the Euler-Lagrangian solutions satisfy the ‘small’ conditions on the left-hand side of an interval, namely

$$\xi(0) = 0 \quad \text{if } m \neq \pm 1 \quad \text{and} \quad \frac{\partial \xi}{\partial r} = 0 \quad \text{if } m = \pm 1 \quad (3.3)$$

and (c) the Euler-Lagrangian solution doesn’t vanish twice in any interval. The existence of singularities and solutions are dependent on the experimental conditions, so numerical codes are generally employed to solve eq. (3.2). But we proceed analytically for now.

The lengthening flux tube is initially stable, therefore the three conditions (a), (b), and (c) are fulfilled. Early in the discharge, the collimated flux tube is short (L small) and stable (small B_ϕ), so $q \approx r B_z / (L B_\phi) \gg 1$. As the collimated flux tube lengthens and current increases, q approaches one from above and is always non-zero. Hence, just before the onset of instability, there are no singular points inside the flux tube and we can consider the whole plasma cross-section as a unique ‘interval’ where the three Newcomb stability conditions are fulfilled, in particular, conditions (b) and (c). So, except at $r = 0$, the solution $\xi(r) \neq 0$ and the Euler-Lagrangian eq. (3.2) is satisfied, giving $g = \partial / \partial r [f \partial \xi / \partial r] / \xi$, which can be substituted into eq. (3.1) to give

$$\delta W_{pl} = \frac{\pi L}{2\mu_0} \left(\left[f \xi \frac{\partial \xi}{\partial r} \right]_0^p + [h \xi^2]_0^p \right). \quad (3.4)$$

Strictly, the lower bound is at $r_c < a$ with $r_c \rightarrow 0$, but those terms vanish since, at the flux

tube center, the solutions all satisfy the Newcomb small-value conditions $\xi(0) = 0$ or $\xi'(0) = 0$ where $'$ denotes $\partial/\partial r$. At the plasma edge $r = p$, we take $\xi(p) = \xi(a) \equiv \xi_a$, $\xi'(p) \approx \xi_a \delta/a$ where δ represents a 'rigidness' of the displacement of the boundary and $f(p) = f(a)$. The plasma term eq. (3.4), thus becomes

$$\delta W_{pl} = \frac{\pi L}{2\mu_0} \delta \frac{f(a)}{a} \xi_a^2 + \frac{\pi L}{2\mu_0} h(a) \xi_a^2. \quad (3.5)$$

For the interface term δW_i , the standard derivation [57] of the perturbed potential energy gives

$$\delta W_i = \frac{\pi a L}{2} \xi_a^2 \left(\left[\frac{\partial}{\partial r} \frac{B^2}{2\mu_0} \right]_v - \left[\frac{\partial}{\partial r} \left(P + \frac{B^2}{2\mu_0} \right) \right]_p \right) \quad (3.6)$$

where $B^2 = B_\phi^2 + B_z^2$ and the plasma pressure P are the equilibrium values. This term only exists if a surface skin current exists and represents the work required to move the plasma boundary. Since we assumed the starting point to be a static, axisymmetric equilibrium, then the pinch force $-B_\phi/(\mu_0 r)$ balances the total pressure gradient $\partial/\partial r [P + B^2/(2\mu_0)]$. The 'jump' in the current profile from the core plasma current to the skin current value is represented by $B_\phi(p)$ being different to $B_\phi(v)$ giving

$$\delta W_i = \frac{\pi L}{2\mu_0} \xi_a^2 (B_{\phi p}^2 - B_{\phi v}^2). \quad (3.7)$$

The classical skin current model assumes no plasma current inside the flux tube, i.e. $B_{\phi p} = 0$, but we keep both terms here. The vacuum contribution δW_v is given by the usual expression [57] (with wall radius $b \rightarrow \infty$)

$$\delta W_v = -\frac{\pi L}{2\mu_0} (kaB_{zv} + mB_{\phi v})^2 \frac{\xi_a^2 K_m(|ka|)}{ka K'_m(|ka|)} \quad (3.8)$$

where K_m is the modified Bessel function of the second kind of order m . Reassembling eqs. (3.5), (3.7), and (3.8) gives the total perturbed potential energy as

$$\begin{aligned}
\delta W = & \frac{\pi L}{2\mu_0} \delta \frac{f(a)}{a} \xi_a^2 + \frac{\pi L}{2\mu_0} h(a) \xi_a^2 \\
& + \frac{\pi L}{2\mu_0} \xi_a^2 (B_{\phi p}^2 - B_{\phi v}^2) \\
& - \frac{\pi L}{2\mu_0} (kaB_{zv} + mB_{\phi v})^2 \frac{\xi_a^2}{ka} \frac{K_m(|ka|)}{K'_m(|ka|)},
\end{aligned} \tag{3.9}$$

which is compared to zero to determine the onset of stability. After dividing by $\pi L/(2\mu_0)\xi_a^2$ and defining $\bar{k} \equiv ka$ and $m \rightarrow -m$, for convenience since for the kink the most unstable modes will be perpendicular to the magnetic field ($kB_\theta + mB_z = 0$), the flux tube is stable if

$$\begin{aligned}
& \frac{(\delta + 1)\bar{k}^2 B_{zp}^2 + (\delta - 1)m^2 B_\phi^2 + 2\delta m \bar{k} B_{\phi p} B_{zp}}{\bar{k}^2 + m^2} + B_{\phi p}^2 - B_{\phi a}^2 \\
& - \frac{(mB_{\phi v} - \bar{k}B_{zv})^2}{\bar{k}} \frac{K_m(|\bar{k}|)}{K'_m(|\bar{k}|)} > 0.
\end{aligned} \tag{3.10}$$

This is normally as far as we can go since B_{zp} , B_{za} , B_{zv} and $B_{\phi p}$, $B_{\phi a}$, $B_{\phi v}$ are generally independent parameters that have to be determined experimentally. To continue, we remember $\lambda = \frac{\mu_0 I}{\psi}$ with $\psi = B_z \pi r^2$, so Ampere's law $B_\phi = \mu_0 I / (2\pi r)$ can be rewritten as

$$\lambda_p = \frac{2B_{\phi p}}{aB_{zp}} \quad \text{and} \quad \lambda_v = \frac{2B_{\phi v}}{aB_{zv}} \tag{3.11}$$

for the plasma side and the vacuum side respectively. Previous experimental results [22] showed our starting point (collimated magnetic flux tube) results from MHD pumping in a flared flux tube [21]. The MHD pumping theory points out that once collimated, the magnetic flux tube must have uniform axial magnetic field across the interface, i.e. $B_{zp} = B_{za} = B_{zv}$, where the plasma current is entirely axial. Therefore, if the flux tube is fully collimated at the onset of instability, after defining dimensionless $\bar{\lambda} \equiv \lambda_p a$ and $\lambda_p a \equiv \epsilon \bar{\lambda}$, the stability condition eq. (3.10) reduces to

$$\frac{[2\bar{k} - m\epsilon\bar{\lambda}][(\delta + 1)2\bar{k} - (\delta - 1)m\epsilon\bar{\lambda}]}{\bar{k}^2 + m^2} + (\epsilon^2 - 1)\bar{\lambda}^2 - \frac{(m\bar{\lambda} - 2\bar{k})^2 K_m(|\bar{k}|)}{\bar{k} K'_m(|\bar{k}|)} > 0 \quad (3.12)$$

with the conditions $B_{\phi_v} = B_{\phi_a} \neq 0$ and $\bar{\lambda} \neq 0$. If the left-hand side of (3.12) is negative for $m = 0$ then the flux tube is sausage unstable and if it is negative for $m = 1$ it is kink unstable. The Kruskal-Shafranov $m = 1$ kink condition can be retrieved from (3.12) by bearing in mind it is usually derived for a long, thin column ($k \rightarrow 0$) with a skin current and no internal currents ($\epsilon = 0$). For small argument, $K_1(x) \rightarrow x^{-1}$ and $K'_1(x) \rightarrow -x^{-2}$, which simplifies (3.12) to the Kruskal-Shafranov condition $\bar{k} > \bar{\lambda}/2$ for $\delta \rightarrow 0$. Remembering that $\bar{k} = 2\pi a/L$ and $\bar{\lambda} = \mu_0 I a / \psi$ where $\psi = B_z \pi a^2$ and $\mu_0 I = B_\phi / (2\pi a)$ gives the well-known $2\pi a B_z / (L B_\phi)$ in cylindrical geometry. The Tayler criterion [58] for sausage $m = 0$ stability in a skin screw-pinch can also be retrieved from (3.12) by taking the same limits. One obtains $\bar{\lambda} > 2\sqrt{2}$ for $\delta \rightarrow 1$, equivalent to the more familiar $B_z^2 > B_\phi^2/2$.

The stability condition (3.12) thus maps out a stability space (fig. 3.3). The kink instability region is hatched, to the right of the curve that approaches the classical Kruskal-Shafranov condition (dotted line $\bar{k} = \bar{\lambda}/2$). The region that is both sausage and kink unstable is cross-hatched, to the right of the curve that falls on the $\bar{k} = 0$ axis away from the origin. A short, low current magnetic flux tube ($\bar{k} \rightarrow \text{large}$, $\bar{\lambda} \rightarrow 0$) thus starts out stable at the top left of the space (white region). As the column lengthens and current increases ($\bar{k} \rightarrow 0$, $\bar{\lambda} \rightarrow \text{large}$), the column's (\bar{k} ; $\bar{\lambda}$) point travels to the bottom-right of the space, crossing the $m = 1$ threshold to be kink unstable (hatched region). Eventually, the column may cross the $m = 0$ threshold and becomes sausage unstable (cross hatched). The parameter $\epsilon = \lambda_p a / \bar{\lambda}$ represents the ratio of the internal current to the skin current, and characterizes the ‘hollowness’ of the current profile across the flux tube, e.g., if $\epsilon = 0$ the plasma column has no internal current, only a skin current. The parameter $\delta = a \xi'(a) / \xi(a)$, represents the ‘abruptness’ or ‘rigidness’ of the displacement of the plasma boundary with respect to the internal plasma. If $\delta = 0$, the plasma cross-section moves rigidly radially without compressing, as in a kink instability. If $\delta = 1$ then

the boundary layer displacement is greater than the internal layers' displacement, as in the compressing sausage instability. Eq. (3.12) thus demonstrates three things: 1) a dependence of both the kink and sausage instability boundaries on the current profile ϵ ; 2) a significant region that is *both* kink and sausage unstable; and 3) a dependence of the instability boundaries on the value of the rigidness parameter δ .

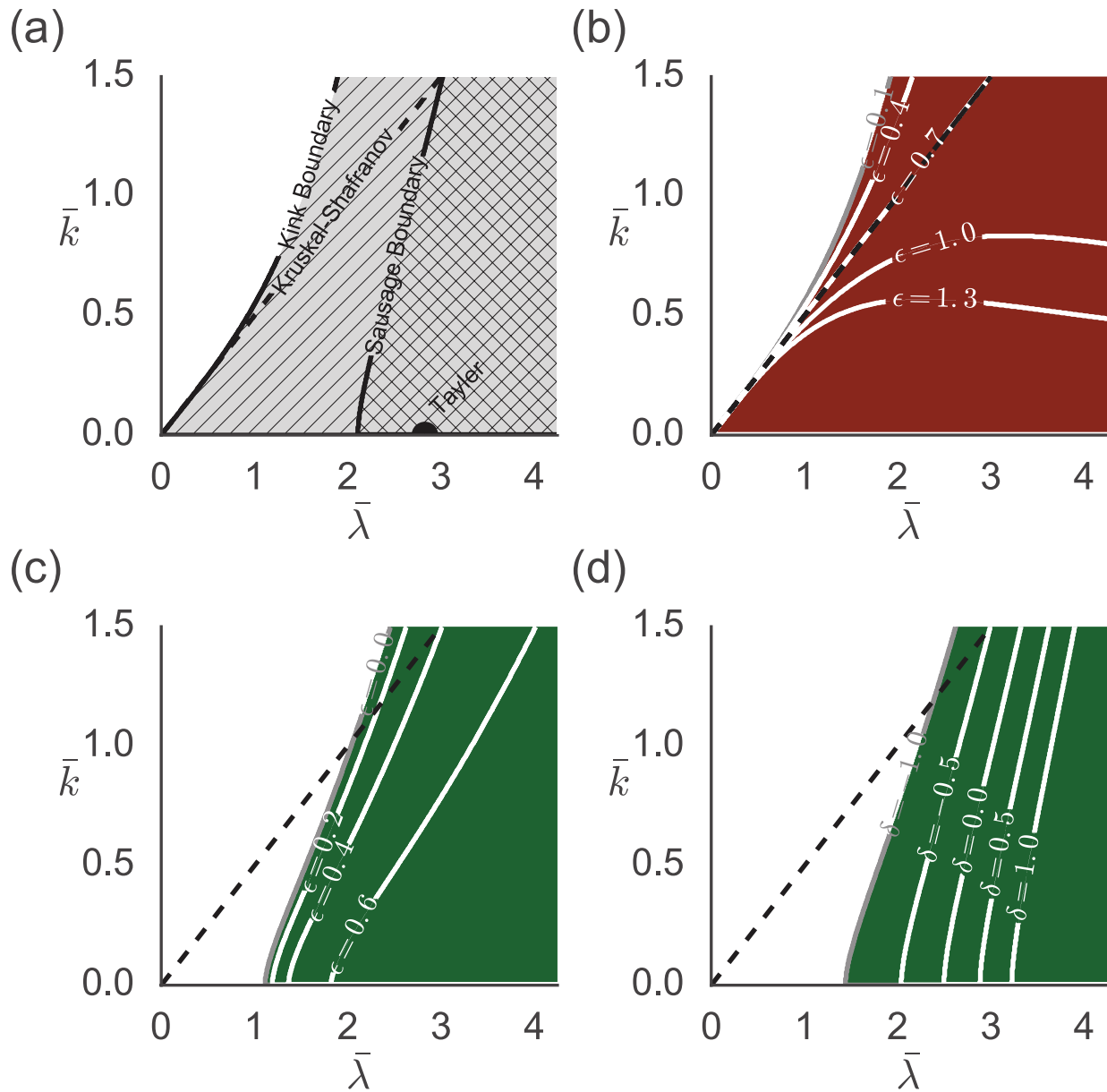


Figure 3.3: Analytical \bar{k} - $\bar{\lambda}$ stability spaces parameterized with core current fraction ϵ and rigidity δ . a) Stability spaces for $\epsilon = 0.1$ and $\delta = 0.1$. White region is stable, gray is unstable, hatched region is kink ($m = 1$) unstable, and crosshatched region is unstable to both kink and sausage ($m = 0$) modes. b) Kink stability space dependence on ϵ with $\delta = 0$. Dark red region is unstable. c) Sausage stability space dependence on ϵ with $\delta = 0.7$. Dark green region is unstable. d) Sausage stability boundary dependence on δ with $\epsilon = 0.2$. Dark green region is unstable.

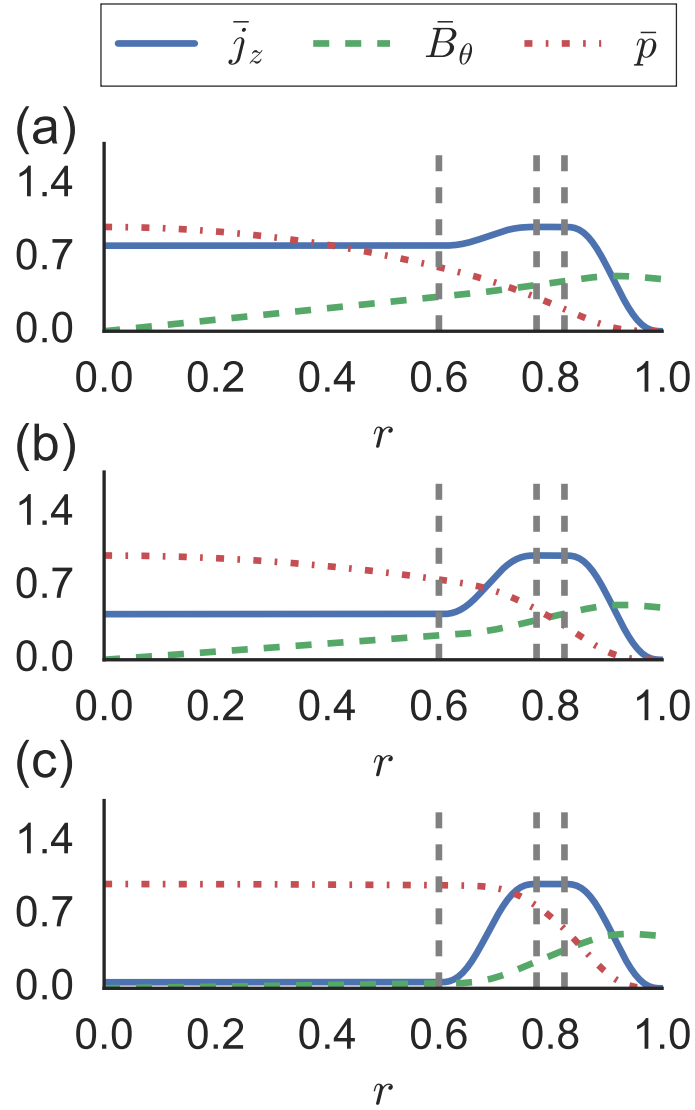


Figure 3.4: Radial profiles of \bar{j}_z , \bar{B}_θ , and \bar{p} for a) $\epsilon_{eff} = 0.7$, b) $\epsilon_{eff} = 0.5$, and c) $\epsilon_{eff} = 0.1$ used for the calculations shown in fig. 3.5. Dashed vertical lines demarcate (from left to right): core, transition, skin, and transition regions.

3.3 Numerics

Although we cannot solve analytically for δ , its value is uniquely determined for given periodicity numbers (m and \bar{k}), axial magnetic field ($\bar{\lambda}$), and current profile (ϵ) by the Euler-Lagrange equation (eq. 3.2). Numerical integration of eq. (3.2) will thus constrain our value of δ . Eq. (3.2) is a second order ordinary differential equation that can have several singularities. For numerical integration, the skin current region can no longer be assumed to be infinitesimal, so we construct profiles with a skin region of finite thickness. To continue, the equilibrium quantities will be expressed as dimensionless quantities (denoted by an over bar). The dimensionless axial current density \bar{j}_z is described by a step function (fig. 3.4); in the core, the current density is constant, rises smoothly to the skin current and drops off smoothly to zero at the plasma edge. The smoothly varying transition regions are described by fourth order polynomials, continuous with the core and skin regions up to the second derivative. Since \bar{j}_z smoothly varies to zero, the parameter $\epsilon = 0$. The current profile is described by the fraction of core-to-total current $\epsilon_{eff} = I_{core}/I_{total}$, where I_{core} is the current in the constant current core region and I_{total} is the total current driven along the flux tube. The azimuthal magnetic field \bar{B}_θ is determined by Ampere's law. The axial magnetic field \bar{B}_z is taken to be constant across the flux tube. The pressure gradient \bar{p}' is balanced by $\bar{j}_z \bar{B}_\theta$. Given the above assumptions, all profiles are uniquely determined by the dimensionless numbers ϵ_{eff} , \bar{k} , and $\bar{\lambda}$. A fourth dependent dimensionless number is the ratio of plasma pressure to magnetic pressure at the axis β_0 .

Since the Euler-Lagrange equation may have several singularities the adaptive solver LSODA from ODEPACK is used. The solver is accessed through wrappers in the Python `scipy.integrate` library [59]. The Euler-Lagrange equation is re-expressed as a system of two first order ODEs:

$$\frac{d\bar{\xi}}{d\bar{r}} = \bar{\xi}' \quad \text{and} \quad \frac{d}{d\bar{r}}(\bar{f}\bar{\xi}') = \bar{g}\bar{\xi} \quad (3.13)$$

LSODA is an adaptive solver, where the stepsize is modified to achieve the desired accuracy. So a request for the value of the derivatives can be made at any given r . To accommodate these requests, the profiles are stored as cubic splines created with FITPACK routines accessed through Python wrappers in `scipy.interpolate`. Each interval, bounded by the singularities, can

be integrated separately using the small solution eq. (3.3) as initial value to the right of the singularity. Since this study is only concerned with external stability, it will suffice to test the equilibrium for Suydam stability at the singularities and integrate only the last interval.

To determine the initial value to the left of the singularity, we use the Frobenius power series method for regular singular points [60]. The Frobenius power series expansion gives the relationship between $\bar{\xi}$ and $\bar{\xi}'$ close to the singularity at $\bar{r} = 0$, for $m = 0$: ($\bar{\xi} \sim C\bar{r}^1$ and $\bar{\xi}' \sim C\bar{r}^0$), and for $m \neq 0$: ($\bar{\xi} \sim C\bar{r}^{|m-1|}$ and $\bar{\xi}' \sim C|m-1|\bar{r}^{|m-2|}$). Since the constant C can not be determined, the magnitude of $\bar{\xi}$ is arbitrary and only the ratio $\bar{\xi}'/\bar{\xi}$ has meaning. At the non-geometric ($\bar{r} \neq 0$) singularities, the Frobenius method gives a quadratic indicial equation

$$n_{\pm} = -\frac{1}{2} \pm \sqrt{\frac{1}{4} + \frac{\beta}{\alpha}} \quad (3.14)$$

with

$$\alpha = \frac{\bar{r}_s \bar{B}_{\theta}^2 \bar{B}_z^2}{\bar{B}^2} \left(\frac{\bar{q}'}{\bar{q}} \right)^2 \quad \text{and} \quad \beta = \frac{2\bar{B}_{\theta}^2 \beta_0}{\bar{B}^2} \frac{d\bar{p}}{d\bar{r}} \quad (3.15)$$

where \bar{r}_s is the radial position of the singularity. The initial values for $\bar{\xi}$ to the right of the singularity are given by $|\bar{r} - \bar{r}_s|^{n_{\pm}}$. The solution with the larger n is the ‘small’ solution [47]. The small solution may diverge at \bar{r}_s but will be well behaved away from the singularity. If $\frac{\beta}{\alpha} < -\frac{1}{4}$ the exponents n will be complex, resulting in rapid oscillations through $\bar{\xi} = 0$ around the singularity. The condition for complex exponents is equivalent to the Suydam instability [60]. These initial values are used to integrate $\bar{\xi}$ for the given magnetic field profiles in the last interval of the Euler-Lagrange equation. The values of δ and $\bar{\xi}_a$ are then substituted into eq. (3.12) with ϵ set to zero, to determine the δW of each mode.

The perturbed potential energy δW is calculated at 50×50 points in the $\bar{k} - \bar{\lambda}$ space, and then interpolated throughout the space [42]. The results of numerical calculations of the $\bar{k} - \bar{\lambda}$ stability space are shown in fig. 3.5 for three values of the current fraction ϵ_{eff} : 0.7, 0.5, and 0.1. In contrast to the analytical approach in fig. 3.3, the numerical integration shows that the rigidity parameter δ is not a constant but varies with \bar{k} and $\bar{\lambda}$ although the quantitative behavior is similar. The magnitude of δW is arbitrary in the variational approach, however we can compare relative magnitudes (all δW values plotted are normalized). The kink unstable

region matches the Kruskal-Shafranov condition for the long-thin regime, low \bar{k} (fig. 3.5 a, b, c). In regions of high $\bar{\lambda}$, β_0 becomes large and the β term in eq. (3.14) dominates. Since the pressure gradient for the chosen current profiles is always negative, any singularity due to the safety factor q crossing a rational mode will result in infinite oscillations of the displacement ξ , i.e. be Suydam unstable. Eq. (3.2) is the $\rho\omega^2 \rightarrow 0$ case of the general cylindrical eigenvalue problem, where ρ is the plasma density, ω is the mode frequency, and ω^2 the eigenvalue. The solutions to the eigenvalue problem are Sturmian, their zero-crossings decrease with decreasing values of the eigenvalue ω^2 [60]. This means that Suydam-unstable profiles are likely unstable to the external kinks, as decreasing zero-crossings allow the eigenfunction ξ to match the vacuum boundary conditions. To express this likely external kink instability, without solving the full eigenvalue problem, the Suydam-unstable regions are cross-hatched in fig. 3.5 a, b, c. The stability boundaries of both the sausage mode and kink modes depend on the core-to-total current fraction ϵ_{eff} (fig. 3.5 d, e, f). As in the analytical results, there is a significant region which is unstable to both the kink and sausage modes. For high ϵ and high $\bar{\lambda}$ the solution to the Euler-Lagrange equation indicates external stability, however, ξ does cross zero in these cases, suggesting internal instability. Again, taking the Sturmian property of the general eigenvalue problem into account, these zero crossings will likely allow the eigenfunction ξ to match vacuum boundary conditions at lower ω^2 . To express this likely sausage instability the internally unstable region is cross-hatched in fig. 3.5 d. While the variational approach can not determine the linear growth rates, the ratio of the potential energies $\delta W_{m=0}/\delta W_{m=-1}$, determines which mode will have the faster growth rate. In the region where both sausage and kink instabilities occur, the sausage instability has a larger linear growth rate for higher \bar{k} values (shorter, fatter tubes) and this boundary shifts downward as the ϵ_{eff} decreases (fig. 3.6 a, b, c). This suggests that a sausage could develop rapidly on top of a slowly growing kink.

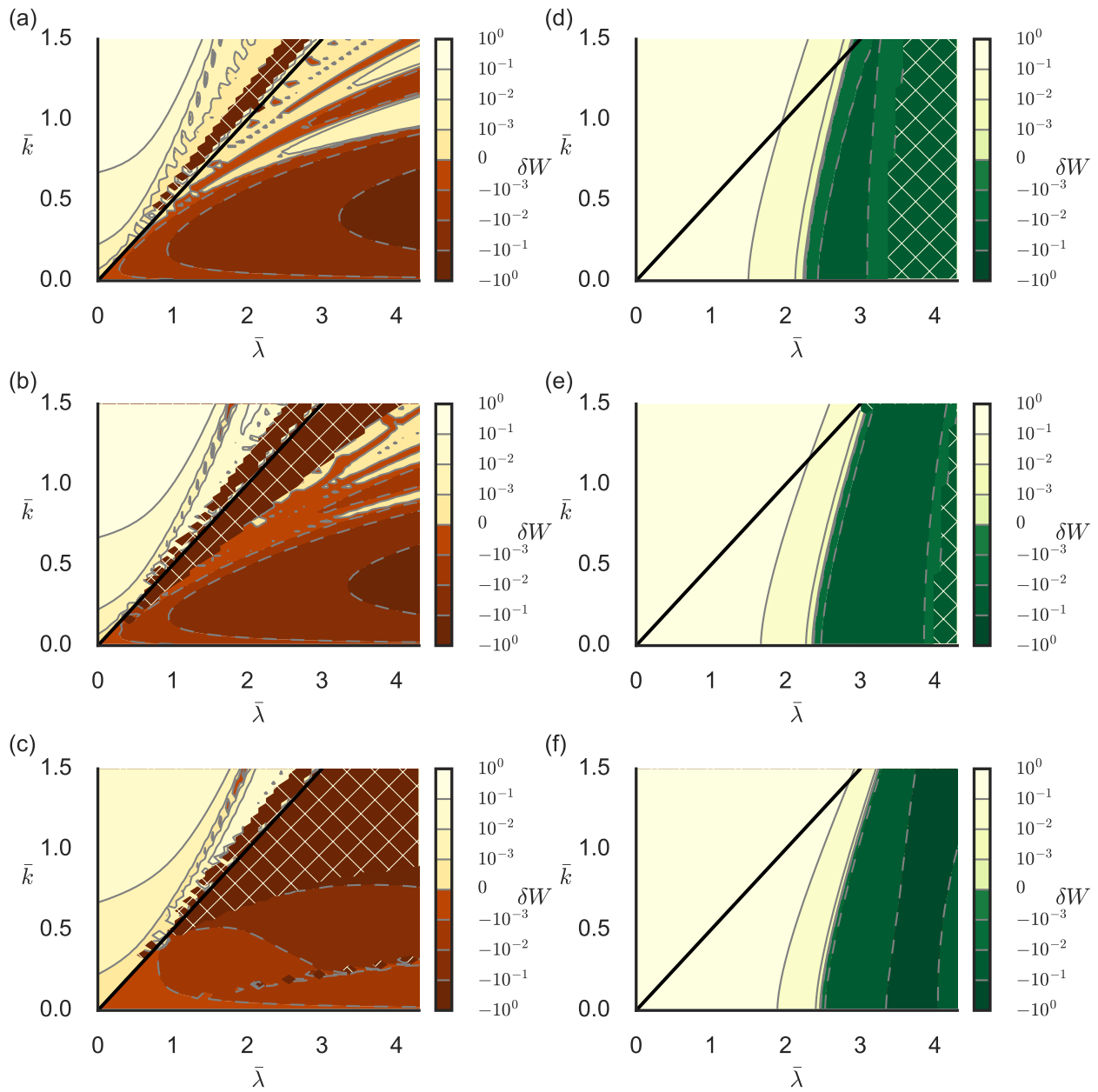


Figure 3.5: Numerical \bar{k} – $\bar{\lambda}$ stability spaces with relative growth rates. Normalized kink $\delta W_{m=1}$ contours for (a) $\epsilon_{eff} = 0.7$, (b) $\epsilon_{eff} = 0.5$, and (c) $\epsilon_{eff} = 0.1$; Normalized sausage $\delta W_{m=0}$ contours for (d) $\epsilon_{eff} = 0.7$, (e) $\epsilon_{eff} = 0.5$, and (f) $\epsilon_{eff} = 0.1$. The cross hatched regions indicate Suydam unstable regions in the $m = 1$ plots and regions with internal instabilities in the $m = 0$ plots. [Associated dataset available at <http://dx.doi.org/10.5281/zenodo.230611>.][43]

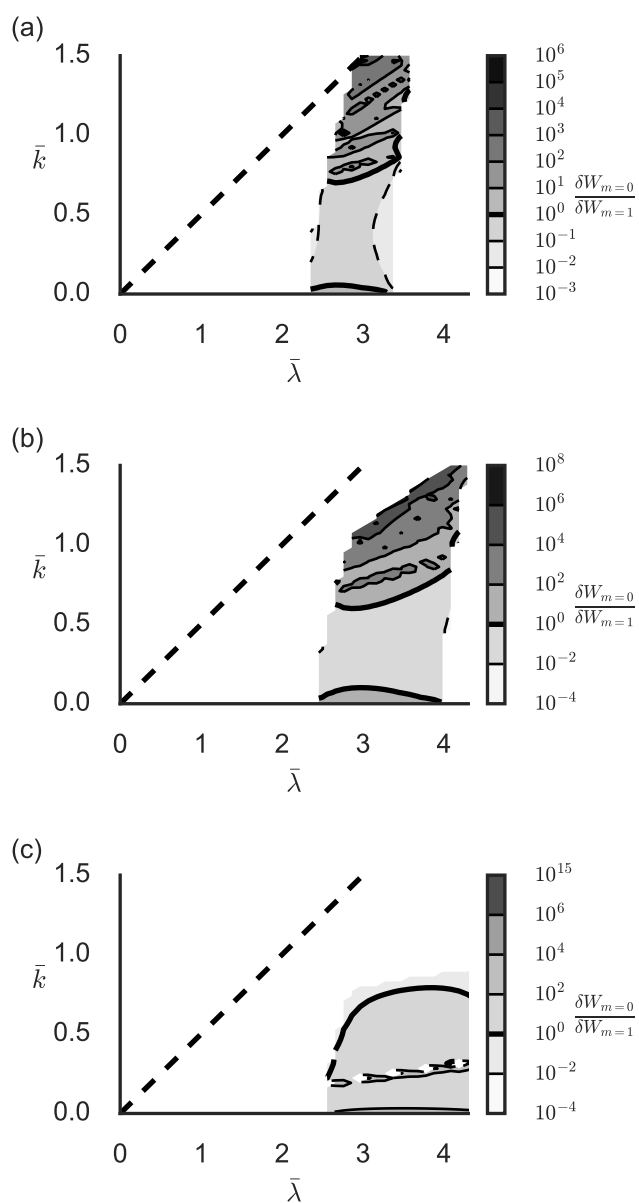


Figure 3.6: The ratio of $\delta W_{m=0}/\delta W_{m=1}$ for (a) $\epsilon_{eff} = 0.7$, (b) $\epsilon_{eff} = 0.5$, and (c) $\epsilon_{eff} = 0.1$. In the white space either at least one of the potential energies is positive or undetermined. [Associated dataset available at <http://dx.doi.org/10.5281/zenodo.230611>][43]

3.4 Discussion

The analytical and numerical stability conditions present evidence for the possibility of a sausage instability developing on top and after a kink instability in a lengthening current-carrying magnetic flux tube, particularly in the general case of a flux tube with internal *and* skin currents. A sausage instability in a screw pinch plasma may be unfamiliar because classical analyses consider diffuse or skin currents separately, however, evidence for sausage instabilities have been observed in coronal loops [61], and predicted in magnetospheric current sheets [62] and cylindrical liner compression experiments with axial fields [63]. We note that in ideal MHD a linear configuration without magnetic field reversal is never sausage unstable without also being unstable to the kink. Sausage instabilities are commonly observed in Z-pinchs [64], which are always unstable to the kink. Likewise, for current-carrying magnetic flux tubes the sausage unstable regions are inside the kink unstable regions of the $\bar{k} - \bar{\lambda}$ space. In magnetic flux tubes with helical fields, kinks have been observed to redistribute the current path, and amplify the axial field [50]. The increased axial field could stabilize both the kink and sausage mode. A sausage instability is thus most likely to occur if the magnetic flux tube can quickly evolve to the upper right quadrant of the $\bar{k} - \bar{\lambda}$ configuration space where the sausage mode growth rates dominate. The linear growth rates will be on the order of the Alfvén transit time, however, nonlinear effects may lead to saturation of the kink instability as is observed in other experiments [65]. A sausage instability has been observed forming on top of a kinking current-carrying liquid mercury column [66].

Another crucial feature of the $\bar{k} - \bar{\lambda}$ stability space is the dependence of both the kink and sausage instability on the current distribution ϵ . This effect is not observed in linear plasma experiments driven by washer guns [55, 67] since the current ramp-up occurs on a much longer time scale than the lengthening of the flux tube. Washer-gun driven flux tubes are confined to low \bar{k} when appreciable $\bar{\lambda}$ values are reached (bottom right of $\bar{k} - \bar{\lambda}$ space). In the long-thin (low \bar{k}) regime the kink instability boundary always matches the classical Kruskal-Shafranov condition (assuming ideal periodic boundaries). Plasma jets produced by planar plasma gun

experiments, however, evolve in \bar{k} and $\bar{\lambda}$ on the same time scale. In these plasma jets, rapid pinching of the plasma from the gun followed by detachment have been observed at high $\bar{\lambda}$, which may be an indication for a sausage instability [50]. Solar loop stability experiments have noted the effect of finite aspect ratios (large \bar{k}) [29].

In regard to experiments it is important to understand what implications a kink-sausage instability might have, and if there are any unique signatures. In Z-pinch discharges, sausage instabilities are associated with beams of high energy ions [64, 68]. The ions could be accelerated by a strong electric field generated from the increased resistivity in the pinched region of the sausage mode. While the magnetic field in a Z-pinch is purely azimuthal, in a current-carrying magnetic flux tube the field is helical with shear across the magnetic flux surfaces. The compression of these sheared magnetic flux surfaces would provide a favorable magnetic topology for reconnection. An interesting question is whether a kink sausage instability could couple the MHD system to microscopic scales of ion inertial lengths or ion Larmor radii where two-fluid and kinetic effects become important and can lead to fast reconnection [23]. The assumptions of MHD are invalid when the ratio of drift over Alfvén velocity is close to or exceeds unity. At high drift velocities kinetic effects such as wave-particle interactions and the decoupling of perpendicular ion and electron motion described by the Hall term could dominate. To understand when this may occur it is helpful to express the ratio of the average drift velocity $v_d = I_z/(\pi a^2 n_0 q)$ and the Alfvén velocity $v_A = B/\sqrt{\mu_0 n_0 m_i}$ in terms of the configuration space parameters, where n_0 is the number density, q is the charge, m_i the ion mass, and μ_0 the magnetic permeability. Starting with the velocity definitions

$$\frac{v_d}{v_A} = \frac{I_z}{\pi a^2 n_0 q} \frac{\sqrt{\mu_0 n_0 m_i}}{\sqrt{B_{\theta v}^2 + B_{zv}^2}} \quad (3.16)$$

we can cancel a power of the azimuthal magnetic field after replacing the current with Ampère's law $I_z = 2\pi a B_\theta / \mu_0$

$$\frac{v_d}{v_A} = \frac{\sqrt{m_i}}{\sqrt{\mu_0 n_0 q^2 a}} \frac{2}{\sqrt{1 + \frac{B_{zv}^2}{B_{\theta v}^2}}}. \quad (3.17)$$

Substituting the magnetic field ratio $\bar{\lambda}_v$, eq. (3.11) and the ratio of the characteristic length

over the ion skin depth λ_i , also called the size parameter $S^* = a/\lambda_i = a\sqrt{\mu_0 n_0 q_i^2/m_i}$, choosing the radius a as the characteristic length and assuming singly ionized plasmas, we obtain

$$\frac{v_d}{v_A} = \frac{1}{S^*} \frac{2}{\sqrt{1 + \frac{4}{\bar{\lambda}_v^2}}}. \quad (3.18)$$

The critical value of $\bar{\lambda}_v$ at which the velocity ratio becomes unity is given by

$$\bar{\lambda}_{vcrit} = \frac{2S^*}{\sqrt{4 - S^{*2}}}. \quad (3.19)$$

This condition has a singularity at $S^* = 2$ with a relative shallow slope before $S^* 1.5$, indicating that for low S^* a sausage instability could couple to microscopic scales (fig. 3.7). Low values of S^* can be achieved with plasmas with higher ion masses, lower densities and by reaching the top right corner of the $\bar{k} - \bar{\lambda}$ configurations space where the flux tube radius is still large. Sausage instabilities can still occur when MHD dominates, at high S^* , without coupling to kinetic and two-fluid scales.

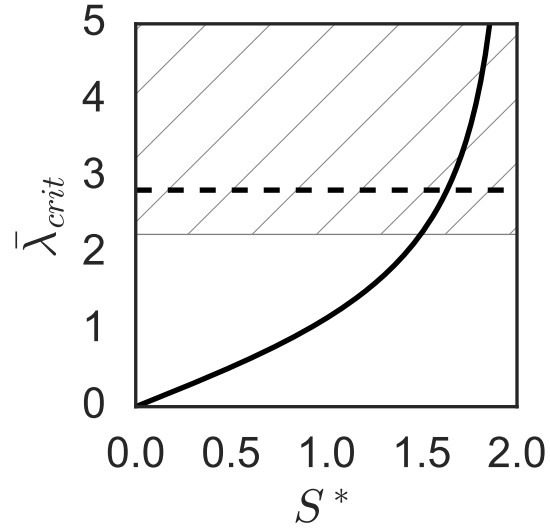


Figure 3.7: Critical $\bar{\lambda}$ value for a given size parameter S^* above which the instability will couple to microscopic scales. The hatched region starts at the minimum sausage unstable $\bar{\lambda}$ for an $\epsilon_{eff} = 0.7$ current profile. The dashed line denotes the Taylor criterion $\bar{\lambda} = 2\sqrt{2}$.

3.5 Conclusion

This work presents a general stability condition for current-carrying magnetic flux tubes with a wide range of aspect ratios, current-to-magnetic flux ratios, and current profiles. The analytical and numerical results point to sausage instabilities on top of kinking flux tubes as a possible cascade of instabilities. Further numerical and experimental studies are in progress to verify the $\bar{k} - \bar{\lambda}$ configuration space and determine growth rates of the kink and sausage instabilities. A new triple electrode planar plasma gun, Mochi.Labjet, is designed to generate magnetic flux tubes with discrete core and skin currents evolving over a wide range of the $\bar{k} - \bar{\lambda}$ stability space. Preliminary results indicate that the magnetic flux tube life time is several Alfvén transit times while the peak rate of increase of $\bar{\lambda}$ is at least an order of magnitude faster than the Alfvén transit time and four times faster than the rate of increase of \bar{k} . This indicates the

sausage unstable region of the $\bar{k} - \bar{\lambda}$ configuration space should be accessible. The kink-sausage instability cascade could couple to two-fluid and kinetic regimes when the size parameter S^* is small. This can be achieved with high ion masses, e.g. argon or krypton plasmas. High spatial resolution magnetic probe arrays will identify the cascade of MHD instabilities.

If the kink-sausage instability cascade couples to two-fluid or kinetic scales, species canonical helicity conversions could occur. Experimental techniques are needed to explore the $\bar{k} - \bar{\lambda}$ space, to reliably recreate the instability cascade, and to take large volumetric datasets needed to calculate helicity volume integrals.

Chapter 4

EXPERIMENT CONTROL AND HIGH-THROUGHPUT FPGA BASED DIGITIZERS FOR CANONICAL HELICITY MEASUREMENTS

4.1 *Challenge of measuring canonical helicity*

Several methods have been proposed to determine helicity of a vector field [69]. The most straightforward method is to measure the canonical quantities in a finite volume and integrate the volume integral eq. (2.18). An alternative method is to examine the topology of discrete flux tubes reconstructed from the measurements and determine their twist [70]. A third approach relies on determining the helicity flux on the surfaces of the volume of interest by measuring the injection terms in the helicity transport equation (2.24) [71]. The helicity flux approach does not require measurements inside the volume of interest but is only able to determine the total canonical helicity injected; species conversion occurring inside the volume cannot be captured. The finite volume and twist number methods require measurements of the canonical quantities throughout the finite volume. For a laboratory, linear canonical flux tube experiment evolving in a cube of 1 m length, ~10 cm width, and height with a 1 cm ion inertial length ~80,000 measurement points would be needed to resolve the ion inertial length over the whole volume (using Nyquist length of 0.5 cm). At each location, multiple measurements over multiple experiment shots are needed to sample the statistical distribution of the measured quantities. Hence, in order to gather the measurements necessary to determine canonical helicity, it is advantageous to develop 1) experiment control to create reproducible shots and 2) high-throughput digitization in order to take as many measurements as possible per shot.

This chapter will introduce the Mochi.Labjet experiment and its experiment control and high-throughput FPGA (field-programmable gate array) based digitizers.

The experiment control LabVIEW application, the MDSplus data storage model, and the high-throughput FPGA code has been published on Zenodo under <https://doi.org/10.5281/zenodo.495643>, <https://doi.org/10.5281/zenodo.495631>, and <https://doi.org/10.5281/zenodo.495787> [72, 73, 74]; appendix B provides additional information about setup and dependencies of this software.

4.2 *Mochi.Labjet: Canonical flux tubes with boundary conditions relevant to astrophysical jets*

Mochi.Labjet is a planar plasma gun experiment, designed to drive current profiles, and axial and azimuthal shear flows in a canonical flux tube. The Mochi.LabJet gun consists of three planar electrodes. The inner and middle electrodes can be biased with ignitron-triggered capacitor banks independently between 0 and -10 KV with respect to the grounded outer electrode. A dipole magnetic field (up to 1 T) connects the inner electrode with the outer electrode and the middle electrode with the outer electrode (fig. 4.1 a). Gas is injected through azimuthally symmetric slits in the electrodes (fig. 4.1 b). Breakdown occurs along the arched magnetic field lines connecting the electrodes. The arched plasma “Bundt cake” merges into a central collimated canonical flux tube. An axial $\vec{j} \times \vec{B}$ force drives an Alfvénic plasma flow. The flowing plasma convects frozen-in magnetic flux to the flared region, increasing magnetic flux in that region and collimating the flux tube [21, 22]. The differentially biased electrodes are intended to drive discrete core and skin currents in the canonical flux tube (fig. 4.1 c). Ref. [21] shows that the axial velocity of the plasmas depends on the flaring of the magnetic field and the current, thus the current profile imposes an axial shear flow. The radial electric field between electrodes combined with the bias field is equivalent to an azimuthal rotation in ideal MHD, $\vec{E} = -\vec{u} \times \vec{B}$, mimicking the azimuthal rotation in an astrophysical jet-accretion disk system (fig. 4.1 d). The plasma gun is mounted to a spherical vacuum chamber with 1.4 m diameter. Roughing pumps and a cryopump provide a vacuum of down to 10^{-7} Torr. The high vacuum enables a large density gradient between plasma and background which results in sharp boundaries in plasma emission in camera images. Ref. [75] describes the triple elec-

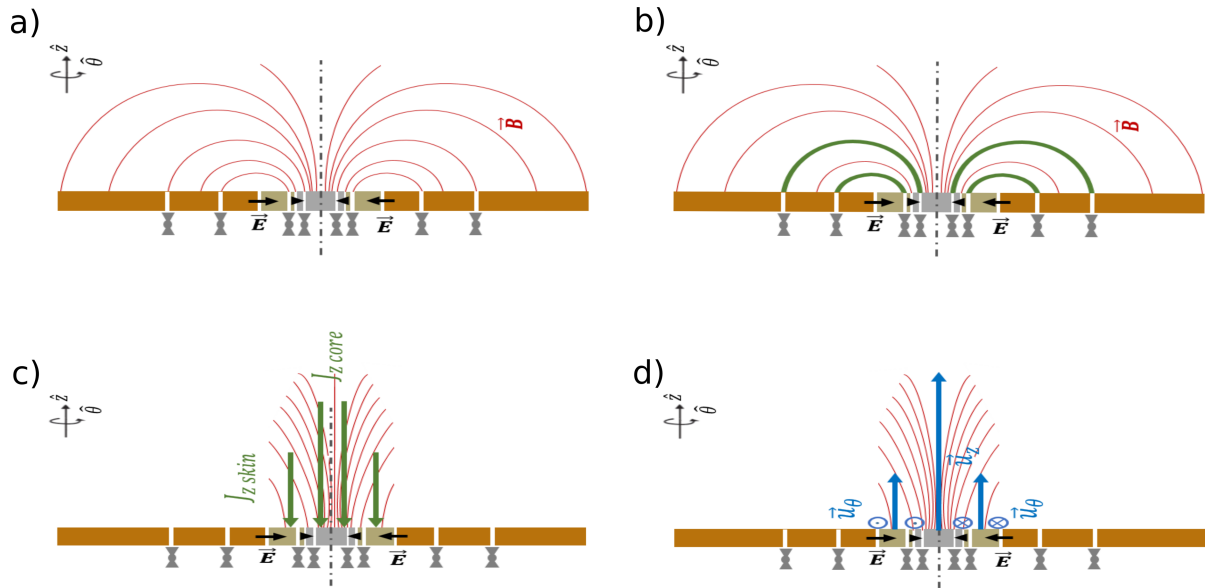


Figure 4.1: Three-electrode planar plasma gun configuration: showing magnetic field (red), electric field (black), gas valves (grey), outer electrode (orange), middle electrode (gold), inner electrode (gray), current (green), and flows (blue). The gas injection slits in the electrode are azimuthally symmetric. a) Vacuum \vec{B} and \vec{E} fields are imposed by a solenoid and the applied electrode potentials, respectively. b) Initial breakdown occurs along arched magnetic field. c) MHD pumping has collimated the magnetic field. Core and skin currents are driven by the applied electrode potentials. d) MHD pumping drives axial flows. The azimuthally symmetric gas injection slits allow the plasma to freely rotate in response to the radial electric field.

trode plasma gun design in detail. There are three gun power supplies (PSU). Mochi.PSU1 is described in appendix C. Mochi.PSU2 and Mochi.PSU3 are described in ref. [75].

4.3 Mochi Control: Experiment control & data storage

Pulsed power plasma experiments, such as Mochi.Labjet, share several features in common. These experiments achieve plasma breakdown by injecting neutral gas and applying large voltages from pulsed power supplies with short ns - ms discharge durations. Magnetized plasma experiments require pulsing current through external field coils several hundreds of milliseconds before breakdown. This time allows the magnetic field to soak in through the conducting electrodes and vacuum chamber. To achieve breakdown, the gas injection valves, magnetic field coil, and electrode power supplies need to be triggered with accurately timed electrical pulses. In contrast, other components such as high voltage relays for charging and dump circuits need to be energized for durations of up to several minutes, for which switching within human timescales is acceptable. Charging power supplies generally can be charged to a specified voltage by setting the charging time according to their RC time constant. In summary, to control a pulsed power experiment, two types of signals are required: 1) Fast input pulses with $100\ \mu s$ or shorter durations and starting times specified within $100\ ns$. 2) Non-varying DC input signals with durations of up to several minutes and with start times specified within seconds or manually operated on a graphical user interface.

Mochi Lab uses Mochi Control, a flexible National Instruments (NI) LabVIEW experiment control application¹, based on the producer-consumer design pattern, to allow operators real-time control over all experimental settings, including 16 timing channels with a dynamic timing map, 120 digitizer channels, and a MDSplus settings save and load interface. Fig. 4.2 gives an overview of the experiment control system. Operators control the experiment from a PC running Mochi Control connected through fiber optic cables to two NI chassis. The application programs NI cards housed in the chassis. The synchronizing, timing, and multi-function cards generate the control signals. Transmitter circuits convert the signals to optical pulses, carried by fiber optic cables. Custom built receiver circuits convert the signals back to electrical inputs for the respective experiment components. Ref. [75] describes the circuits in detail. The

¹Developed in collaboration with Woodruff Scientific Inc.

operators control the non-varying DC control signals by switching 88 digital outputs on the PXI-6602 and PXI-6133 cards. For the fast input pulses the operators pre-select the timings. The experiment control application transmits the desired experiment timings to the PXI-6602 cards which use 16 on-board clocks / pulse generators to generate optically isolated trigger pulses for the gas puff valves, oscilloscopes, and bias coil and plasma gun capacitor banks. Voltages from diagnostics are acquired by 24x 14 *bit*, 2.5 *MS/s* analog inputs on the PXI-6133 and 96x 12 *bit*, 50 *MS/s*, AC coupled analog inputs on the NI-5752 digitizers. Measurements from diagnostics electrically connected to the experiment such as high voltage probes are isolated with custom fiber optic transmitter-receiver circuits [76], whereas measurements from diagnostics without electrical contact to the experiment, such as \dot{B} probes and Rogowski coils, are directly digitized. The fiber optic cables between operator PC and chassis, and between chassis and experiment provide electrical isolation for operator safety, for protection of the NI equipment, and to avoid ground loops.

A hierarchical MDSplus tree [77] stores all experiment settings such as capacitor bank voltages and discharge times together with all data acquired through National Instruments PXI-6133 and NI-5752 digitizer cards, Tektronix TDS-2024B oscilloscopes, and a Princeton Instruments PI-MAX 3 fast framing camera. Operators can load previous shot settings from the MDSplus tree and manipulate the settings. The experiment control application accesses the storage through the MDSplus LabVIEW interface [78], which leverages object oriented and multi-threaded features of MDSplus, allowing the code to simultaneously translate LabVIEW data types and MDSplus data types, write and read to and from multiple MDSplus tree nodes. For each experimental shot MDSplus creates a new tree structure based on a model tree [73]. This tree can store numbers, strings, data arrays, and 2D data/time conglomerations called signals. Experimental data from diagnostics are stored together with experimental settings to facilitate interpretation and shot reproducibility. Using jScope, the stored data arrays from any previous shot can be accessed in graphical format.

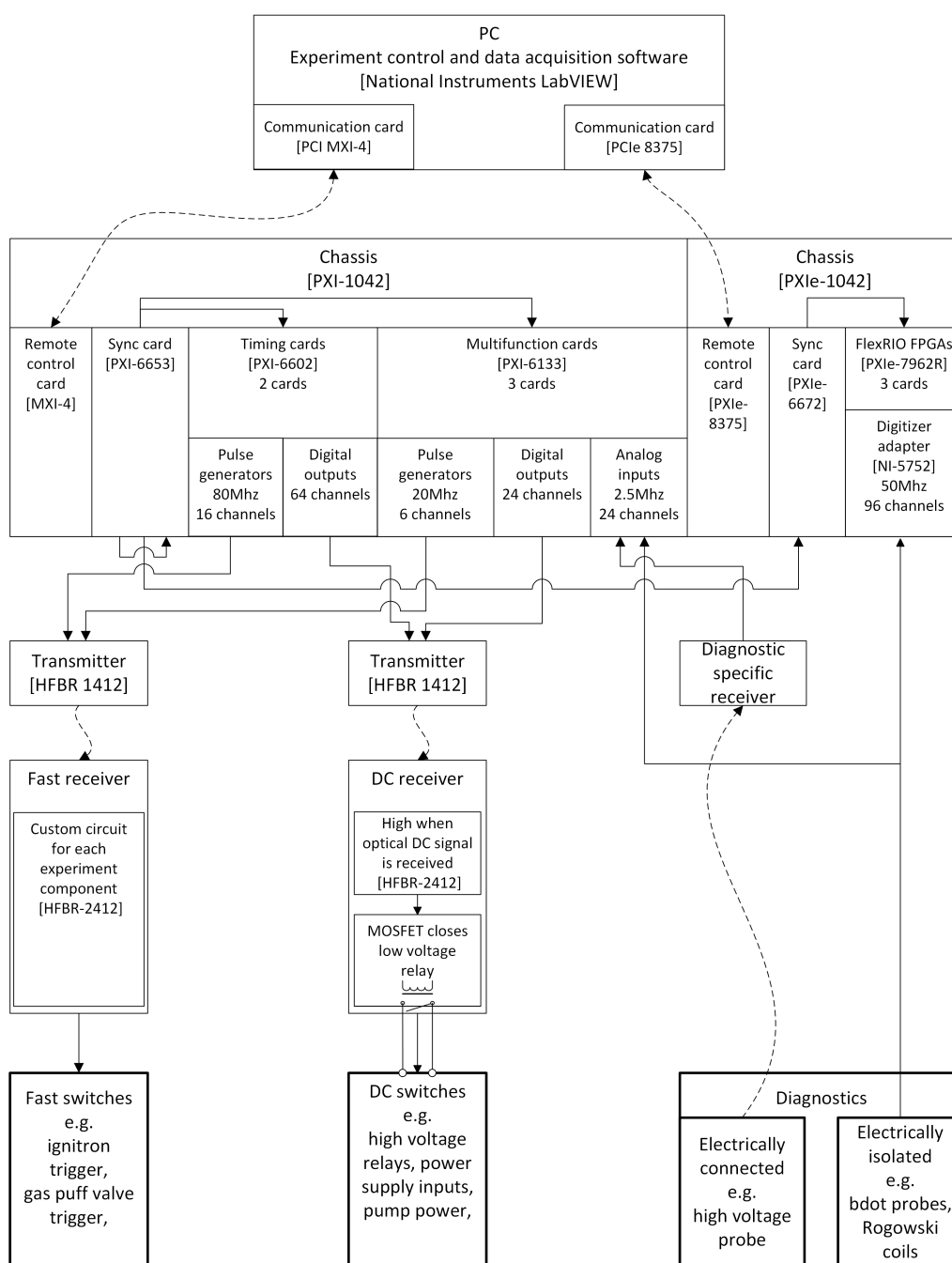


Figure 4.2: Experiment control: Operators DC control the experiment with a PC application using LabVIEW DAQmx and LabVIEW FPGA module to program the PXI Cards. The pulse generators / counters and digital outputs generate fast pulses and DC signals. These signals are converted to optical outputs, travel through optical isolation fibers, and are converted back to electrical signals at the experiment. 120 analog inputs digitize diagnostic signals. Control of the 6 pulse generators in the PXI-6133 is not yet implemented.

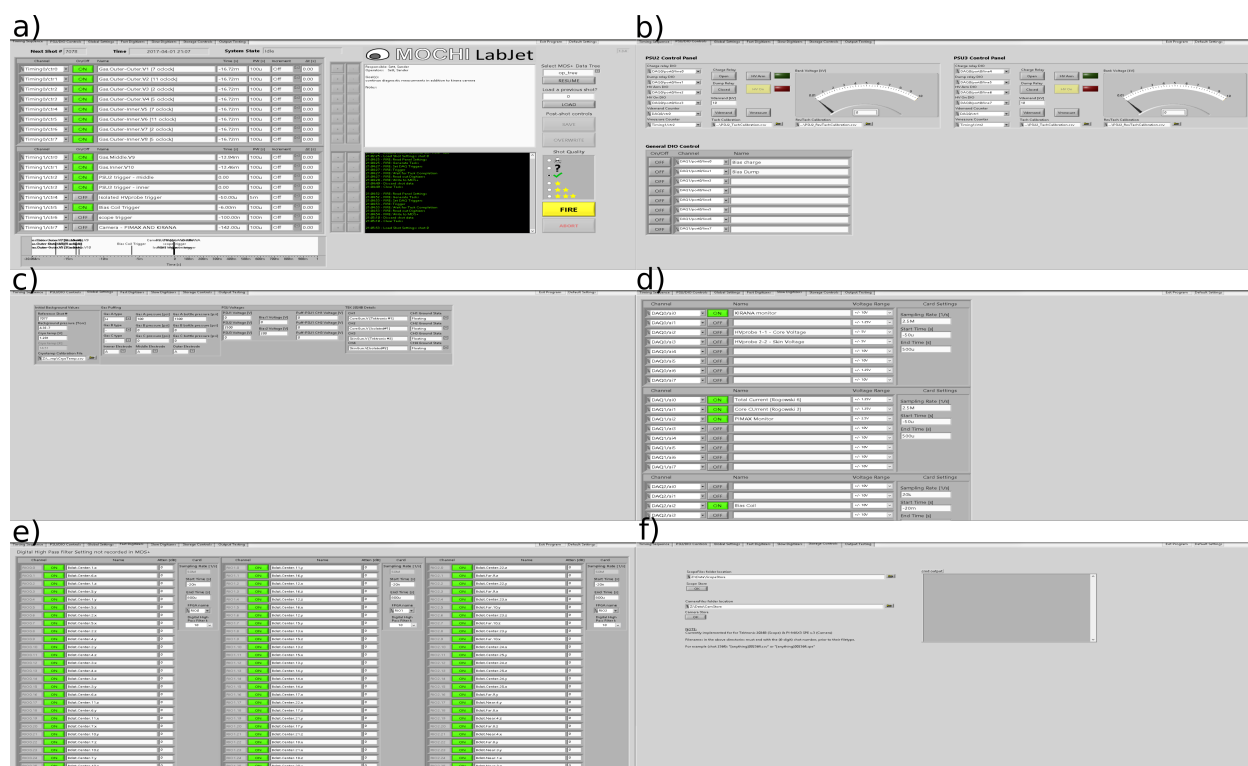


Figure 4.3: GUI of experiment control software: a) Timing sequence panel, b) PSU/DIO control panel, c) Global settings panel, d) slow digitizer panel, e) fast digitizer panel, and f) storage control panel.

4.3.1 Mochi Control user interface

Using the front-panel interface shown in fig. 4.3, operators can adjust experimental settings such as component trigger timings, data acquisition start times, durations, and sampling rates, charge the capacitor banks, and store data acquired on oscilloscopes and fast framing cameras. The *timing sequence* panel (fig. 4.3 a) serves as the main control panel. Operators can use the *resume* and *load* buttons to load all settings from a previous shot stored in MDSplus. In addition, operators can set the trigger time for each pulse generator / counter and specify a name that will be stored in MDSplus. The *FIRE* button initiates a shot sequence during which status updates are displayed in the black terminal. After a shot has been completed, operators

can rate the quality of the shot and record additional notes in the white *shot notes* window. The shot can either be saved to MDSplus with the *save* button or discarded with the *overwrite* button. With the *PSU/DIO control* panel (fig. 4.3 b) operators can control the charging of capacitor banks, specifying and switching the digital outputs. In the *global settings* panel (fig. 4.3 c) operators can store experiment settings not directly controlled by the application, such as the type of gas injected, the background reference shot, the chamber pressure, the charging voltage of the power supplies and to which diagnostics the oscilloscope channels are connected. Under the *slow digitizers* panel (fig. 4.3 d) operators can select which of the 2.5 *MS/s* analog inputs should record data, name the inputs, set input range, and acquisition times. The FPGA digitizers read the settings from the *fast digitizers* panel (fig. 4.3 e) the channels can be named, the acquisition time, and an internal digital high pass filter can be set. The digital high pass filter removes a resonance that occurs around 50 *kHz* in the ADC chips of the NI-5752. Ref. [79] shows the frequency response curves for each filter setting. A good default value is K10. The oscilloscope and the PI-MAX3 fast framing camera are not controlled by the experiment control application but through software provided by their respective vendors. At the end of the day the operators can use the *storage controls* panel (fig. 4.3 f) to load the data files of the Oscilloscope and fast framing camera to the MDSplus tree.

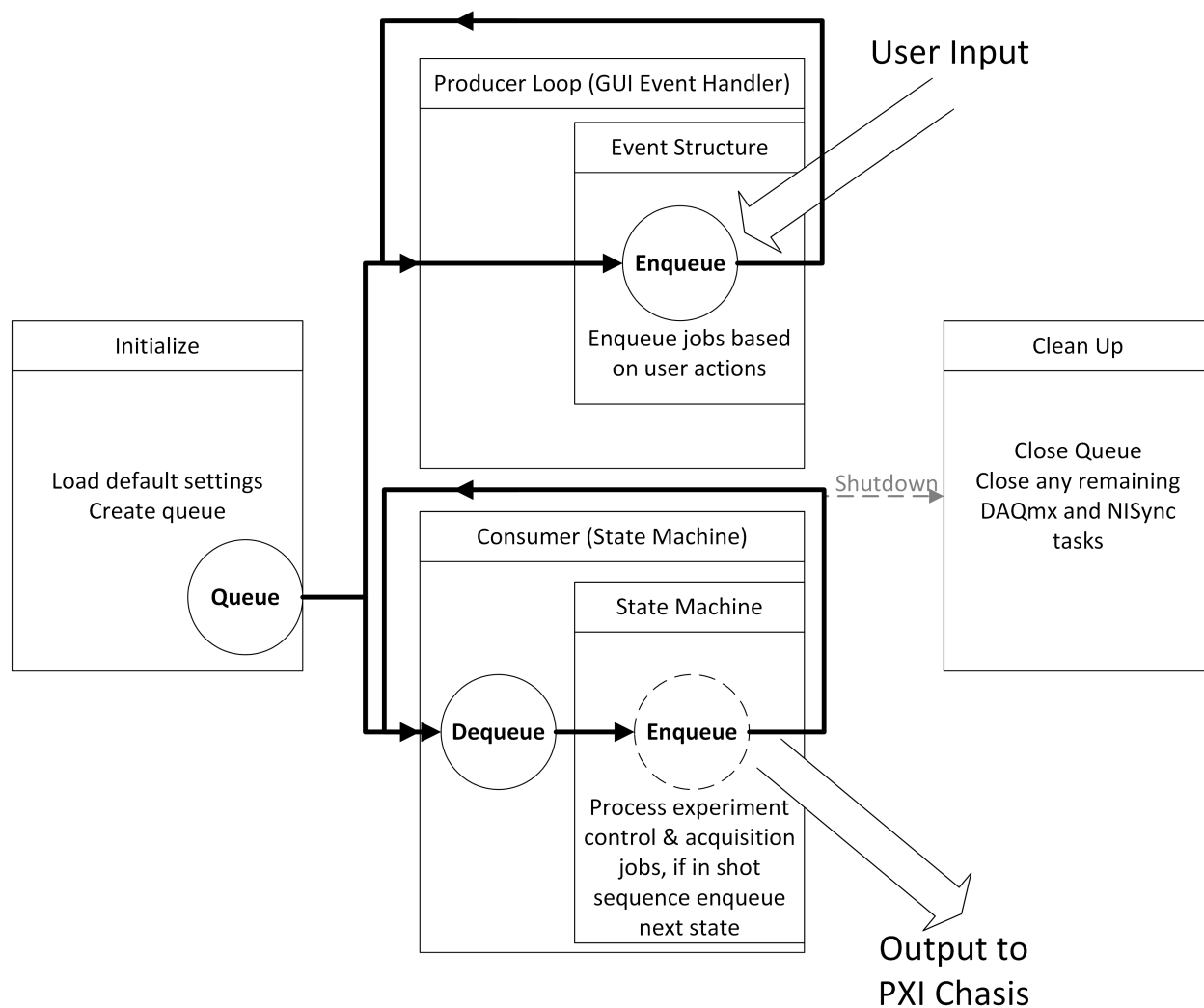


Figure 4.4: Experiment control software: The initialize block loads default settings and creates a queue. The queue is passed to two loops running in parallel. The producer loop handles GUI events by creating jobs and enqueueing them. The consumer dequeues jobs. Jobs are processed in the corresponding state of the state machine with calls to DAQmx and NISync Vis. If the state is part of a multi-state sequence, the state may enqueue further jobs. The shutdown event closes the queue and both loops and calls the shutdown block.

4.3.2 Mochi Control architecture

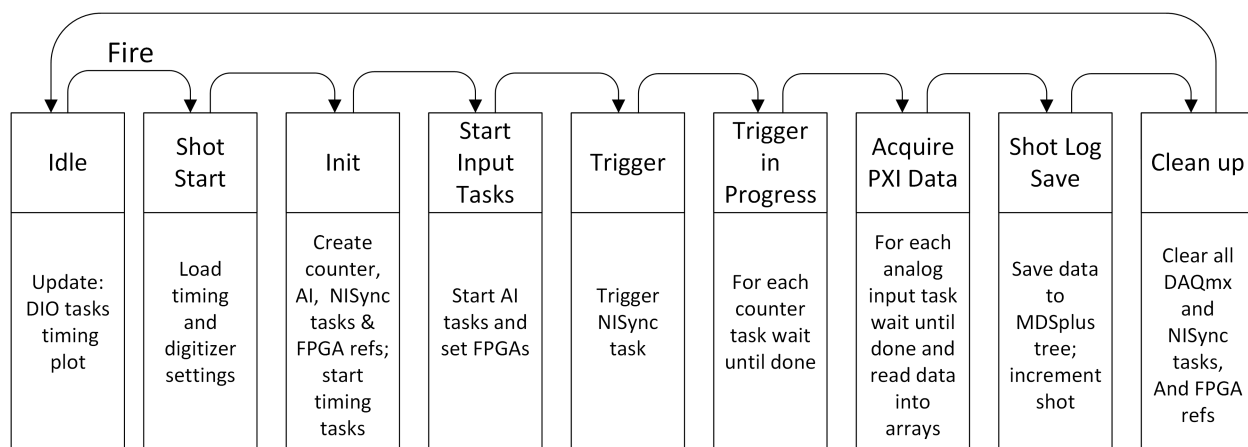


Figure 4.5: Shot sequence in the state machine: Operators pressing the *FIRE* button trigger the shot sequence. Each state is processed in order. DIO are digital output tasks controlling the DC receivers. After *Clean Up* the state machine returns to the *Idle* state.

The Mochi Control LabVIEW virtual instrument (VI) consists of 4 blocks. At startup, the initialize block loads the default settings into the front panel, and clears any existing NI tasks on the computer. A message queue is created that facilitates communication between the parallel threads of the application. The producer and consumer loops separate user interface interactions and experiment control in two parallel threads preventing user input from being lost and the application from becoming unresponsive. The producer loop is designed to listen with an event structure for user generated events, interpret the events as jobs, and place the jobs into the queue. The consumer loop dequeues these jobs and processes them in the order they were received (fig. 4.4). The consumer loop uses the DAQmx library and a custom built FPGA host library to communicate with the digital outputs, analog inputs, and counters / pulse generators. The DAQmx library abstracts the interactions with the NI hardware to tasks. DC signals and can be switched on and off on demand with “DIO write” tasks while fast pulses and data acquisitions are only initialized during a shot, once the *FIRE* button is pressed (Fig. 4.5). At that instant, all fast timing and digitizer settings are loaded from the front panel GUI. These

settings are used to create the appropriate DAQmx pulse generation tasks for the fast timing, and DAQmx analog input tasks and FPGA references for the data acquisition. Next all pulse generation, FPGA references and analog input tasks are set to be triggered, by a NI Sync task. NI-Sync is a library of VIs for setting up the synchronization cards. For each synchronization card one NI-Sync task is created. To synchronize the two chassis, one synchronization card acts as a leader and the other as a follower. The leader and follower synchronization modules need to start sending trigger signals to the cards in each chassis at the same time. The leader synchronization module sends out a trigger pulse to the follower synchronization module through a 1 m coaxial cable, to account for any cable propagation delay the leader module also sends out a trigger pulse along a 1 m coaxial cable that reconnects to the leader module. Once the respective pulse arrives, the synchronization cards send out the trigger pulses to other cards. The fire sequence waits for all tasks to complete and reads in the data from the analog input tasks, then proceeds to store the data arrays and experimental settings as discussed in the following section. After storing, the code runs its cleaning task, preparing for another shot. When the consumer loop receives input from the storage control panel to store the oscilloscope and camera data into the MDSplus tree, the producer loop calls Python scripts to read in the oscilloscope files (csv) and camera image files (spe). The csv files are read with io functions in the numerical Python (numpy) package [80]. The spe files are read with the tsphot Python package [81]. When a shutdown event is received by the producer loop, a shutdown job is enqueued and the producer terminates. Upon dequeuing a shutdown event, the consumer loop terminates itself and the clean up block is initiated which closes the queue and all remaining DAQmx, NIsync, and FPGA references.

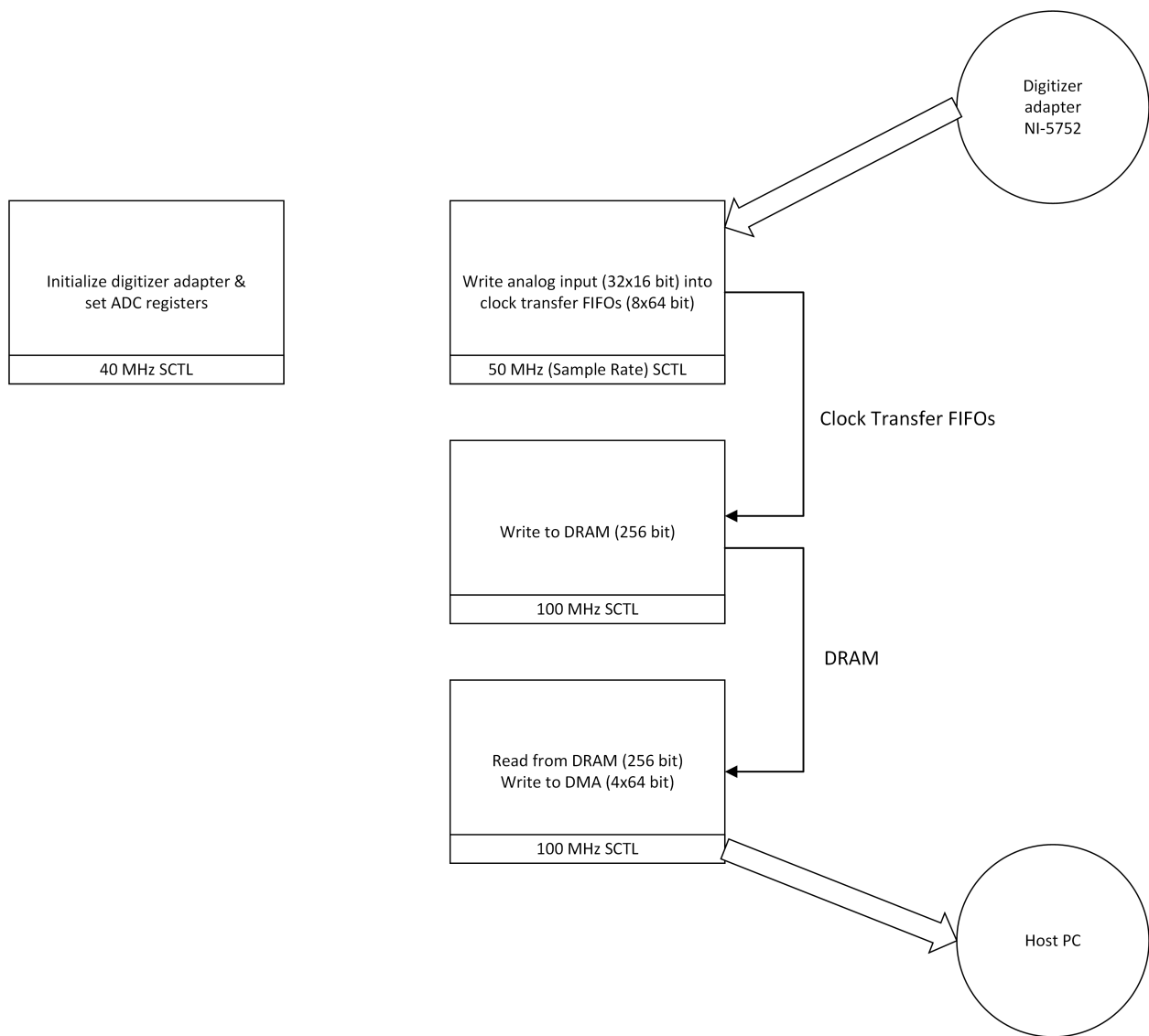


Figure 4.6: FPGA block diagram: The FPGA code consists of four single-cycle-timed loops (SCTL): 1) Initialize and register manipulation loop (40 MHz), 2) Acquire loop (50 MHz), 3) Write to DRAM (100 MHz), and 4) Readout DRAM (100 MHz).

4.4 High-throughput FPGA based digitizers

Data acquisition consists of high frequency analog to digital conversions of an input voltage and the rapid storage of these data samples. FPGAs are configurable integrated circuits consisting of logic and storage elements. The wires or interconnects between the elements can be programmed, rearranged to achieve different functionality. As circuits FPGAs are inherently suited for parallel transfer of digitization samples from many channels to storage. The PXI-6133 multi-function card is FPGA based, however the FPGA is not configurable by end users. The National Instruments FlexRIO product line separates the FPGA and the analog-to-digital conversion (ADC) into two separate modules which are purchased separately. The digitizer adapter modules can be swapped out to accommodate different digitization needs. Mochi Lab purchased three PXIe-7962 FPGAs and three NI-5752 digitizer adapters. Each NI-5752 adapter includes four Texas Instruments AFE5801 ADC chips which simultaneously sample 32 channels at 50 MS/s with 12 bit. The channels are AC coupled with a 3 dB point at 16 kHz. By default, an anti-alias filter internal to the ADC chips operates with a 3 dB frequency of 14 MHz. Custom breakout boards have been designed to breakout VHDCI inputs of the NI-5752 to double shielded twisted pair CAT-7 cables. The CAT-7 cables combine the inductive pickup rejection of twisted pair cables with capacitive pickup shielding. The breakout boards have load balanced switchable 0 – 76 dB attenuators. The load balancing enhances the capacitive and inductive pickup common mode rejection of differential digitization [82].

A clip provided by National Instruments for the PXIe-7962 FPGAs reads out the samples as 16 bit words, resulting in a data throughput of 3.2 GB/s. A custom FPGA code developed and optimized with the LabVIEW FPGA module achieves a throughput to the on-board DRAM of ~ 3 GB/s, limiting the acquisition time to 800 μ s when the overflow data fills the on-board block memory. After each experiment shot the experiment control application reads out and stores the data into the MDSplus tree.

The FPGA code is optimized for high-throughput [83]. As shown in fig. 4.6 the code consists of four single-cycle-timed loops running in parallel. Single-cycle-timed loops execute at every

tick of a specified clock. The loop running at 40 MHz initializes the NI-5752 adapter clip and then processes any input from the host PC to modify the ADC registers. The digital high pass filters mentioned in sec. 4.3.1 are set with these ADC registers. The acquire loop runs at the sampling rate of 50 MHz and transfers thirty-two 16 bit samples from the analog inputs to first-in first-out (FIFO) arrays implemented in block RAM. FIFOs are necessary to transfer data between loops with different clocks, from the data acquisition clock (50 MHz) to the DRAM read-write clock (100 MHz). In the DRAM write loop the samples are transferred from the FIFOs to the DRAM. Write operations to the DRAM can fail and take more than one cycle to complete, so it is necessary to use handshaking patterns. Each sample is stored in a feedback node, that will store the sample between loop cycles, and the next sample is only read from the FIFO if the write operation to the DRAM has succeeded. The maximum throughput to the DRAM is ~ 3 GB/s, which is below the 3.2 GB/s data throughput from the analog input. With the FIFOs acting as a buffer, more than 800 μ s of data can be stored before the FIFOs overflow. The last loop is the read DRAM loop where the data is read from the DRAM and written to a direct memory access (DMA) to the control PC. This readout process is only initiated after the acquisition to maximize the write throughput to the DRAM. A read from DRAM always takes at least two clock cycles to complete. In the first clock cycle an address is requested and in the second cycle the corresponding data is received. At least one cycle will pass before the data is available. As the DMA throughput to the control PC is slower than the DRAM throughput, handshaking is necessary to ensure that no data is lost. The size of the packets written to the FIFOs and DRAM, 8x 64 bit and 256 bit, respectively, have been carefully chosen to maximize throughput. The samples have to be leaved together to form these packet sizes which necessitates a deleaving step on the control PC before the data can be stored in the MDSplus tree.

With further work, it is possible to increase the sampling time. The samples could be bit-packed, removing the 4 bits that contain no data from each sample and placing parts of two samples into 16 bit words which would reduce the data inflow below the DRAM throughput limit. However, the number of channels that can be bitpacked may be limited by the logic

resources available on the PXIe-7962.

4.5 Conclusion

This chapter develops the experimental techniques to gather the large volumetric datasets needed to calculate canonical helicity integrals. The experiment control application Mochi Control provides operators with real-time control over all experimental settings, and a MDSplus settings save and load interface. Mochi Control facilitates creating reproducible shot conditions to gather measurements of coherent plasma phenomena over many shots. High-throughput FPGA digitizers have been developed to provide measurements on 96x 12 *bit* channels at 50 *MHz*. Data analysis techniques are needed to assemble measurements from many shots, identify coherent plasma behavior, and calculate the necessary reference fields to determine gauge-independent relative canonical helicity.

Chapter 5

MEASUREMENTS OF CANONICAL FLUX TUBES AND THEIR HELICITY

This chapter reconstructs canonical flux tubes and their helicity from measurements of magnetic field and ion flow of gyrating plasma columns. The Mochi.LabJet experiment is currently in a campaign to acquire these vector fields. To prepare for the Mochi.LabJet data, the analysis methods to reconstruct canonical flux tubes and their relative canonical helicity will be developed with a volumetric dataset of \dot{B} , triple probe, and Mach probe measurements from the Reconnection Scaling Experiment (RSX). The data analysis can be divided into four steps:

1. Prepare data: Since the measurements are taken over 2,369 shots a coherent shot subset with common canonical flux tube motion must be identified. The measurements are conditionally sampled using the common relative time base of the canonical flux tube gyration and then are interpolated to a rectilinear grid.
2. Reconstruct and interpret canonical flux tubes: Line integrals of the interpolated vector measurements trace out canonical flux tubes in RSX.
3. Determine vector potential and reference fields: Fast Fourier methods solve the Laplace equation for reference circulation fields and an appropriate gauge choice simplifies the calculation of vector potentials needed to determine relative canonical helicity.
4. Reconstruct and interpret canonical helicity: The time evolution of canonical helicity is determined inside a 3D subvolume of the RSX experiment.

The canonical flux tube and helicity reconstruction code [84] has been published on Zenodo under <https://doi.org/10.5281/zenodo.58119> and is described in appendix D.

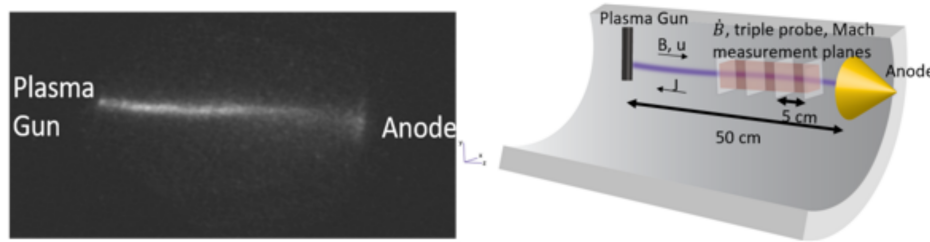


Figure 5.1: Left) CCD image of emission from kinked canonical flux tube. Right) Artist's interpretation of gyrating canonical flux tube. Axial flow and vacuum magnetic field are directed towards the anode. The current flows in the opposite direction. Measurement planes and interpolation volume are shown in purple.

5.1 Overview of RSX experiment

5.1.1 A gyrating kinked canonical flux tube

RSX could generate up to four current-carrying canonical flux tubes of radius $a = 2 - 3 \text{ cm}$ in a cylindrical vacuum chamber of 0.2 m radius between negatively biased plasma washer guns and a translatable conical anode [85] (fig. 5.1). This study analyses a dataset of shots with a single canonical flux tube and a 22° half-angle conical anode fixed at a distance of $L = 0.52 \text{ m}$ from the washer gun [65]. Current flowing through external coils provided, for the duration of the discharge, a constant axial guide field of $B_z = 0.02 \text{ T}$. The lifetime of a single plasma column in the RSX experiment comprises three distinct phases (fig. 5.2). 1) The flux rope current ramps up. 2) Once the current exceeds the Kruskal-Shafranov limit, the flux rope kinks, displaces helically, and gyrates. 3) At 2.1 ms the current supply circuit is crowbarred and the current decays. Ohmic heating through the current achieves electron temperatures of $10 - 15 \text{ eV}$ and ion temperatures of 1 eV . The washer plasma gun carefully controls the gas injection achieving an ion to neutral particle ratio of 10 with an ion particle density of $1 - 3 \cdot 10^{19} \text{ m}^{-3}$. All shots used hydrogen as gas. The plasma gun injects axial flow ($\leq 2.5 \cdot 10^4 \text{ m/s}$), directed

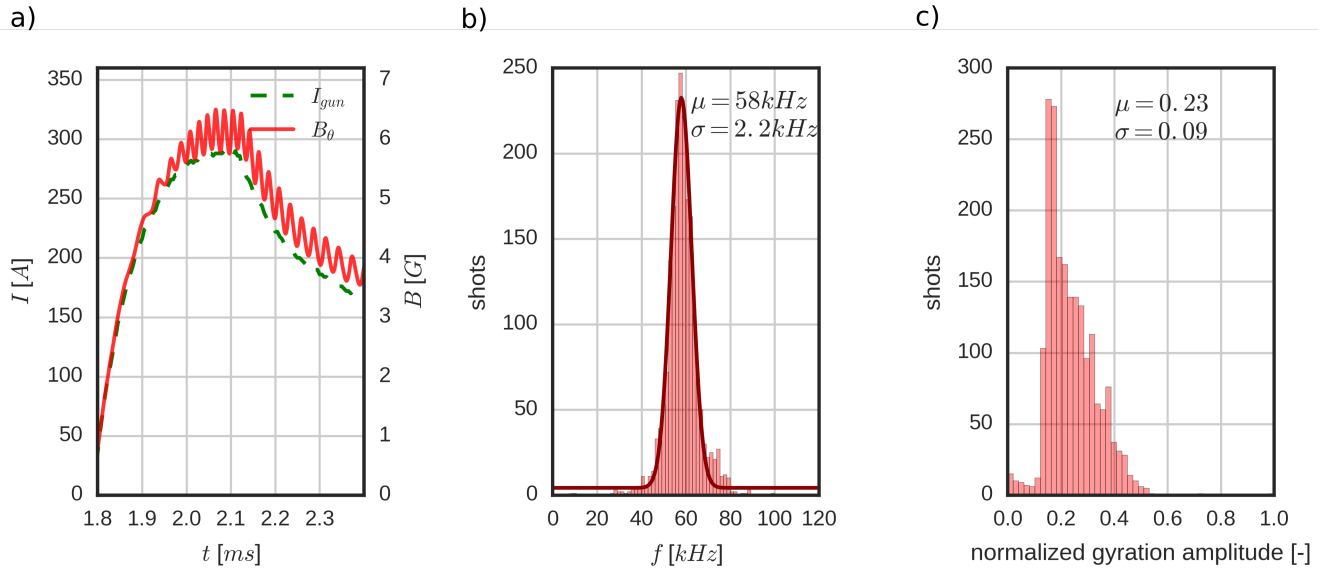


Figure 5.2: Coherent gyration. a) Gun current (dashed green) and azimuthal magnetic field (red) measured 5 cm from gyration center by the stationary fiducial probe during a typical shot (#15253). After the current exceeds the Kruskal-Shafranov limit, the magnetic field develops a modulation corresponding to the magnetic flux tube gyration. b) Frequency distribution across all shots of the modulation in the fiducial probe signal. Frequencies are determined by the peak of a Fourier transform. A Gaussian with a constant offset is fit to the distribution. c) Distribution of modulation amplitude in the fiducial probe signal just before the crowbar across all shots.

towards the anode, into the flux rope. This axial flow makes the helical displacement of the kink appear to be gyrating for stationary observers, such as internal probes.

5.2 Diagnostics

Internal Mach, magnetic, and triple probes measured ion velocity, change in magnetic field, density, temperature, and electric potential, respectively. During each shot, all probes measured the quantity of interest locally at one discrete point, except for the \dot{B} probes which have 6–20

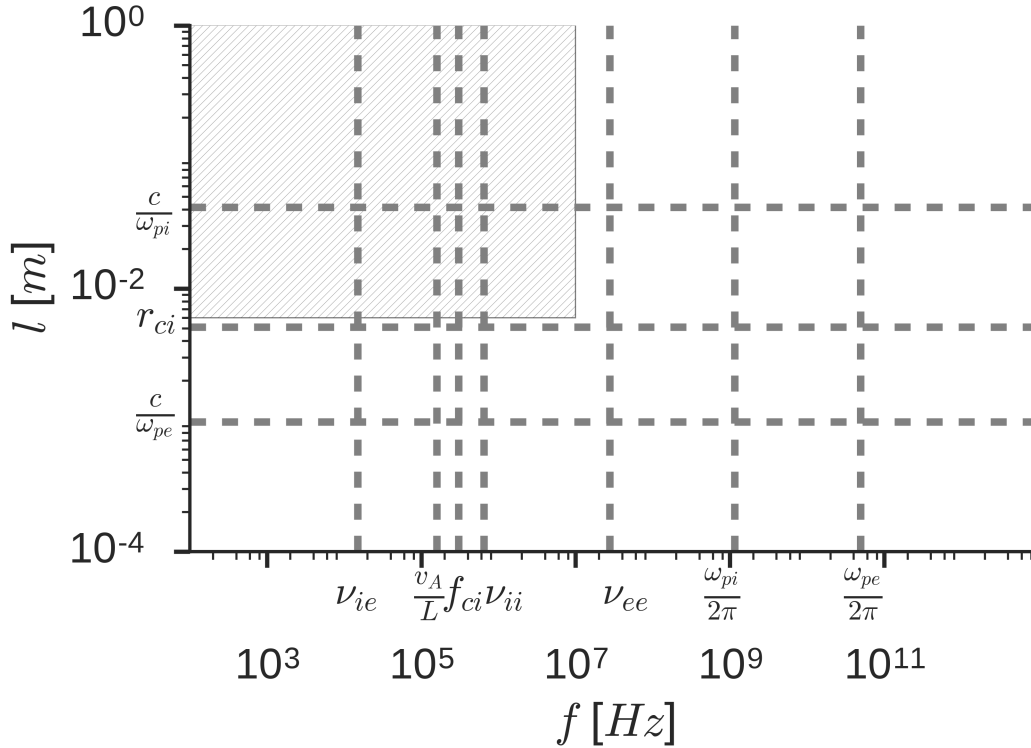


Figure 5.3: Plasma length and time scales, and maximum achieved spatial and temporal resolution of internal probes (cross-hatched). The resolution is set by the Nyquist frequency of the digitizers 10 MHz and the Nyquist length of the smallest achieved spatial resolution (0.006 m). Plasma scales are calculated with magnetic field $B = 0.02$ T, number density $n = 3 \cdot 10^{19} \text{ m}^{-3}$, electron temperature $T_e = 10$ eV, ion temperature $T_i = 1$ eV, and flux tube length $L = 0.5$ m [65].

sensors. The probes are positioned between shots through flat plane ports [86] to cover x-y cut planes at four axial locations: 24.9 cm, 30.2 cm, 35.7 cm, and 41.6 cm. In the remainder of this chapter the planes will be referred to by their first two significant digits. The spatial accuracy of the probe positioner in the x-y cut planes is 0.5 mm, in this data set a resolution of

3 mm was achieved. The digitization rate is 20 MHz. Fig. 5.3 shows the spatial and temporal resolution of internal probes together with plasma scales. The ion inertial length is resolved but not the ion plasma frequency. The ion gyrofrequency is resolved; the ion gyroradius is within the same order of magnitude as the spatial resolution.

This study uses the results of the data analysis conducted in ref. [65] as a starting point. The magnetic field, density, electron temperature, and ion Mach number are treated as the ‘raw’ data. Although the raw probe data was not analyzed for this study a brief description of the probes will be given to help understand sources of uncertainty originating from the instruments and the raw data analysis.

5.2.1 \dot{B} probes

The 3D magnetic field vectors are measured with \dot{B} probes. The \dot{B} probes contain multiple (6–20) inductor chips [87] aligned in three perpendicular directions and covered by an electrostatic shield inside a pyrex tube. Following Faraday’s law, the change in magnetic field perpendicular to the area A traced out by the inductor chip loops is proportional to the voltage V induced in each chip $dB/dt = -V/(NA)$, where N is the number of loops. The effective NA , taking into account misalignment, is determined through calibration with a known magnetic field applied in the x, y, and z directions of the lab frame [87, 88]. The response of the \dot{B} probes rolls off for MHz frequencies. dB/dt is integrated with the trapezoidal method. The instrument uncertainty is expected to be smaller than the shot-to-shot variation in the magnetic field.

5.2.2 Triple probes

In a plasma where the electron velocity distribution is Maxwellian, the current density (particle flux) impinging on a conducting probe inserted in the plasma will be $\propto e^{q_e V/T_e}$ between the ion saturation current density $j_{isat} = q_e n \sqrt{m_e/k_B T_e}$ and the electron saturation current density $j_{esat} = j_{isat} \sqrt{m_i/m_e}$ [89]. Triple probes determine three points on the I - V curve, so the

electron temperature and density can be determined. Triple probes have a probe head with three electrodes; two are floating with a constant bias potential ΔV between them and one is floating freely. The negative electrode of the pair will draw the ion saturation current $I_1 = I_{isat}$ at a voltage V_1 while the positive electrode will draw an equal and opposite current $I_2 = -I_{isat}$ at voltage $V_2 = V_1 + \Delta V$. The floating electrode will be at the plasma floating potential $V_3 = V_f$ and draw no current $I_3 = 0$. Subtracting the ion saturation current I_{isat} from the current of the positive electrode and the floating electrode current and taking their ratio, yields

$$\frac{I_2 - I_{isat}}{I_3 - I_{isat}} = 2 = e^{\frac{q_e \Delta V}{k_B T_e}}, \quad (5.1)$$

allowing the electron temperature to be determined. The electron density can be determined from the I_{isat} current.

Both the electron mean free path ($\lambda_{mfp} \approx 2 \mu m$) and the electron collision frequency ($\nu_{ee} \approx 30 \text{ MHz}$) are smaller than the probe and faster than the digitization frequency, respectively, making it a reasonable assumption that the electrons are Maxwellian. The electrode spacing of the triple probe has to be below the temperature and density gradient scale lengths for the three probes to sample the ‘same’ plasma. Instrument uncertainty stems from imperfections in the electrode surface area, both in the physical geometry of the surface area and from phenomena which increase the effective area such as secondary electron emission, photoemission of electrons, and negative ions [89].

5.2.3 Mach probes

Mach probes have two conducting faces on opposite sides of a probe head. The electrodes are biased to collect the ion saturation current. When there is no ion drift velocity, the ion saturation current on both electrode faces is identical. A non-zero ion drift increases the ion saturation current on the upstream side I_{up} and decreases the current on the downstream side I_{down} [90]. The ratio of currents through the electrode surface is proportional to the exponential raised to the power of the Mach number [91]. Taking the logarithm the Mach number M can

be expressed as

$$M = M_c \ln\left(\frac{I_{up}}{I_{down}}\right), \quad (5.2)$$

where M_c is a model dependent constant. The ion velocity is obtained by multiplying the Mach number with the acoustic speed $c_s = \gamma \sqrt{k_B T_e / m_i}$, where γ is the ratio of specific heats of the plasma and taken to be unity. Models for M_c depend on the magnetization of the ions characterized by the ratio of the ion Larmor radius over the size of the electrode r_{Li}/a [92]. In RSX the ratio is $0.5r_{Li}$, a weakly magnetized regime. The RSX team uses $M_c = 0.45$, however, no independent measurement exists to verify this value. Error bars of a factor of two should be assumed, based on the variation of M_c values reviewed in ref. [93]. It may be possible to constrain the range of M_c values by comparing with the $\vec{E} \times \vec{B}$ term of ideal Ohm's law [89], or time of flight measurements [91], however, this has not been attempted. Additional uncertainty comes from differences in the size of the electrodes on each side of the probe, resulting in differences in the upstream and downstream currents even in the case of no drift flow.

5.3 Step 1: Prepare data

This study aims to reconstruct the 3D plasma behavior from single point measurements taken from 2,369 experimental shots. Studies drawing on data across all shots require preparing and structuring the data, so that relevant shots can easily be assembled and coherent features across shots can be differentiated from shot variability.

5.3.1 Identifying a coherent shot subset

During RSX operation, raw digitizer traces were stored in a MDSplus database, and shot settings were recorded in several spreadsheets and handwritten lab books. For this study, an SQL database is created and populated with all shot settings and MDSplus shot numbers to facilitate selecting subsets of shots meeting specified conditions. To ensure that the analysis takes account of shot variability, several shot heuristics are stored in the database that quantify

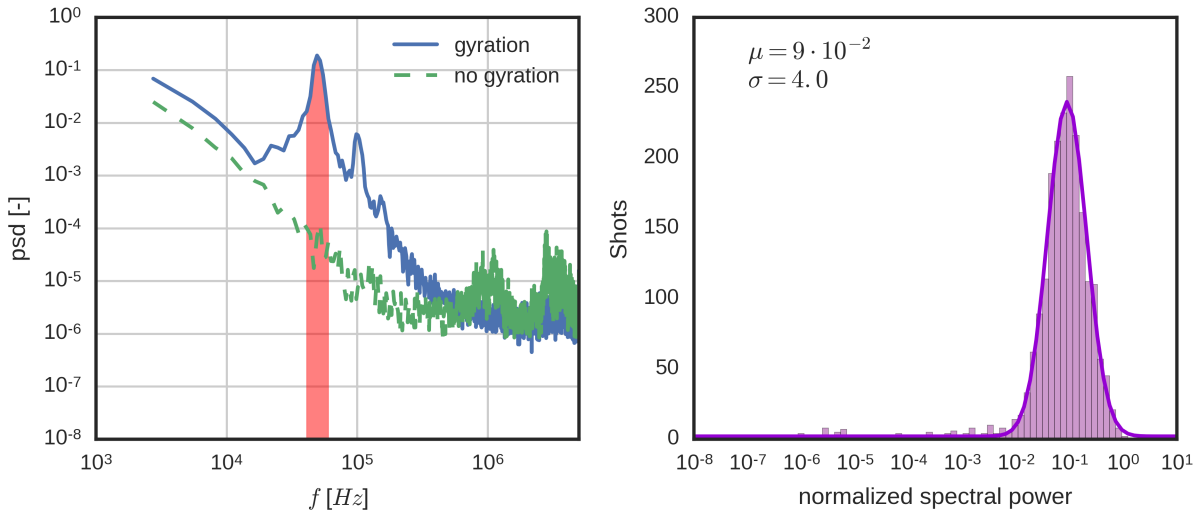


Figure 5.4: Left) Normalized power spectrum density of azimuthal magnetic field measured 5 cm from gyration axis by fiducial probe before the crowbar, averaged across 10 shots with significant gyration (#15256 – 15262 and #15267 – 15269), and 10 shots without gyration (#15305, #15306, #15336, #15352, #15408, #15408, #15410, #15412, #15414, #15416, and #15418). Right) Normalized spectral power distribution for all 2,369 shots obtained by integrating the red area in the left plot.

the coherence. The plasma behavior across shots can be differentiated into coherent behavior, dependent on applied currents and magnetic fields being consistent across shots, and into behavior with intermittent and chaotic effects that vary from shot-to-shot. The gyration appears as a modulation to the azimuthal magnetic field B_θ measured by a stationary fiducial probe 5 cm from the gyration axis (fig. 5.2). The standard deviation in the observed frequencies and amplitudes of the modulation are 8% and 40% of the mean values, respectively, which makes the gyration remarkably coherent across shots. The onset of gyration varies between shots and can occur after the crowbar. The power supply acts as a current source only before the crowbar. After the crowbar the current varies with the plasma impedance which has a large

shot-to-shot variation. Hence, only shots where significant gyration has developed before the crowbar are considered to be coherent. The spectral power density of the gyration frequency can be determined from the square of the discrete-time Fourier transform of the fiducial signal. Histograms of the spectral power density before the crowbar in all shots reveal a log Gaussian distribution with a non-Gaussian tail towards low densities (fig. 5.4). Only shots in which the spectral power density in a time window before crowbarring is within the Gaussian part of the distribution are considered for this study to eliminate shots that have no or too low gyration.

5.3.2 *Conditional sampling of measurements across shots*

Among the gyrating kink shots, there are variations of $100 \mu s$ in onset time. The variations in onset time can be taken into account by conditional sampling [94]: time shifting all probe traces so that the gyration oscillation in the fiducial traces are phase aligned. Start thresholds in the quadrature amplitude and slope in the sinusoidal modulation of the fiducial probe signal time align all shots in the relative time base of one gyration phase of $17 \mu s$ with 250 time steps of $68 ns$.

5.3.3 *Interpolating the measurements to a common rectilinear grid*

Fig. 5.5 shows the measurement locations for each diagnostic on all four planes. The union of the measurement locations for all diagnostics is cross-hatched and is used as the joint measurement volume for reconstructing canonical flux tubes and integrating canonical helicity. The triple probe measurements in the $z = 30 cm$ plane are dropped from further analysis, as they were qualitatively different from the measurements in the other planes; there are no localized peaks in temperature and density. The measurement locations follow a regular grid, but there are several gaps and irregularities. To simplify the data analysis, all measurement quantities are interpolated onto a common rectilinear grid with linear barycentric interpolation using a Delaunay triangulation of the measurement points of each quantity (fig. 5.6). The Delaunay triangulation is performed with the scientific Python (scipy) wrapper around the Qhull code

[95, 96]. Most locations only have a single measurement. To quantify the uncertainty in the helicity integrations the analysis is repeated several times; each time applying a Gaussian filter with successively larger standard deviations to the interpolated measurements. This averages the measurements over different shots at the cost of a coarser grid.

5.3.4 *Constraining the under determined velocity*

Mach probe measurements were only taken in the y direction on the $z = 0.42 \text{ m}$ plane and in the z direction on the $z = 0.36 \text{ m}$ and $z = 0.42 \text{ m}$ planes. The assumption of rigid rotation constrains the Mach numbers in the x direction. The Mach numbers in the x direction are determined by shifting the Mach numbers in the y direction by a quarter gyration period. For this study only the Mach measurements in the $z = 0.42 \text{ m}$ plane are used, which means that the axial variation of the ion velocity stems from the axial variation of the electron temperature.

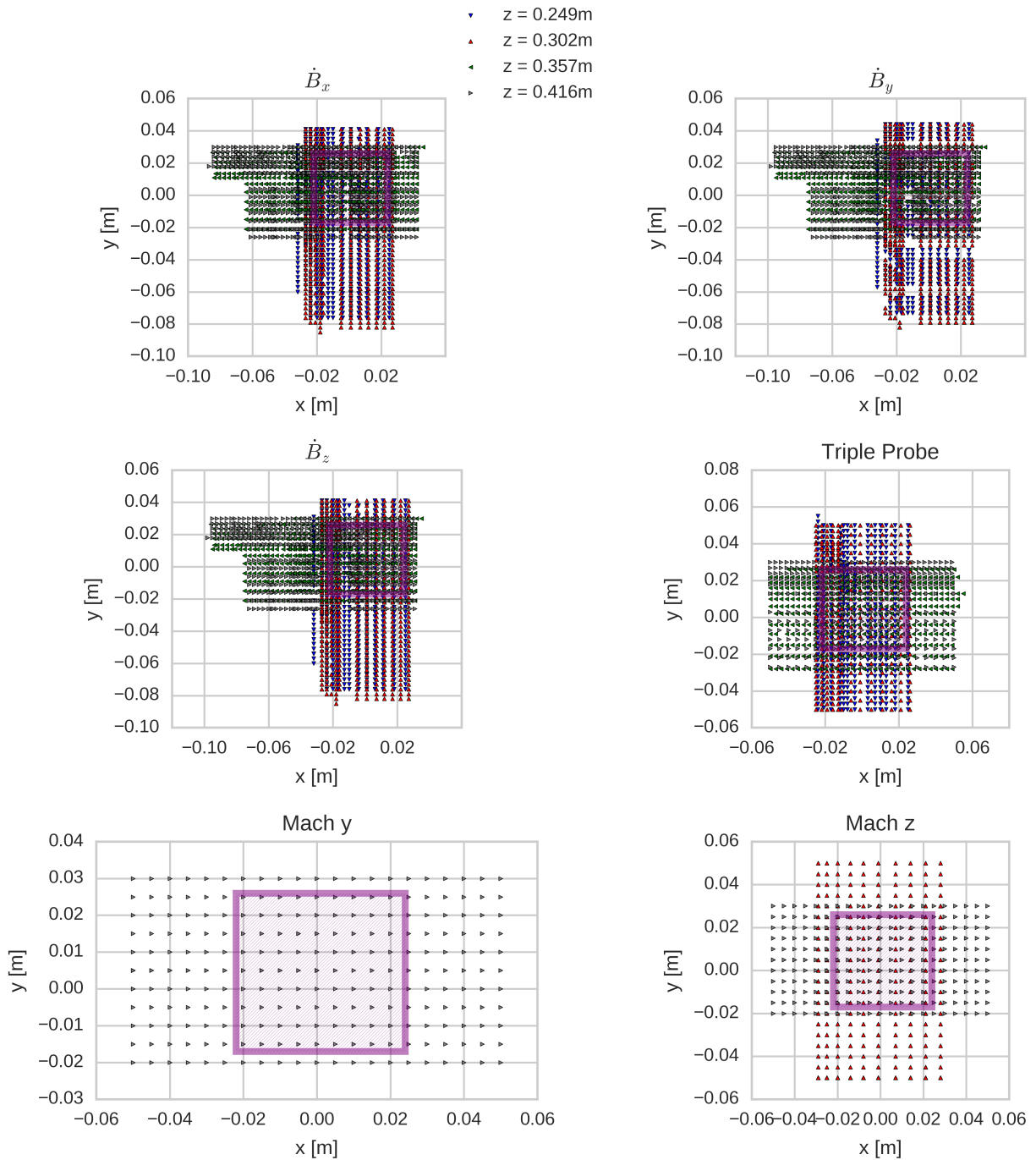


Figure 5.5: Points at which measurements were taken in the coherent shot set with \dot{B} , triple, and Mach probes. The (purple hatched) region is the union of measurement spaces which is used to reconstruct canonical flux tubes and their helicity.

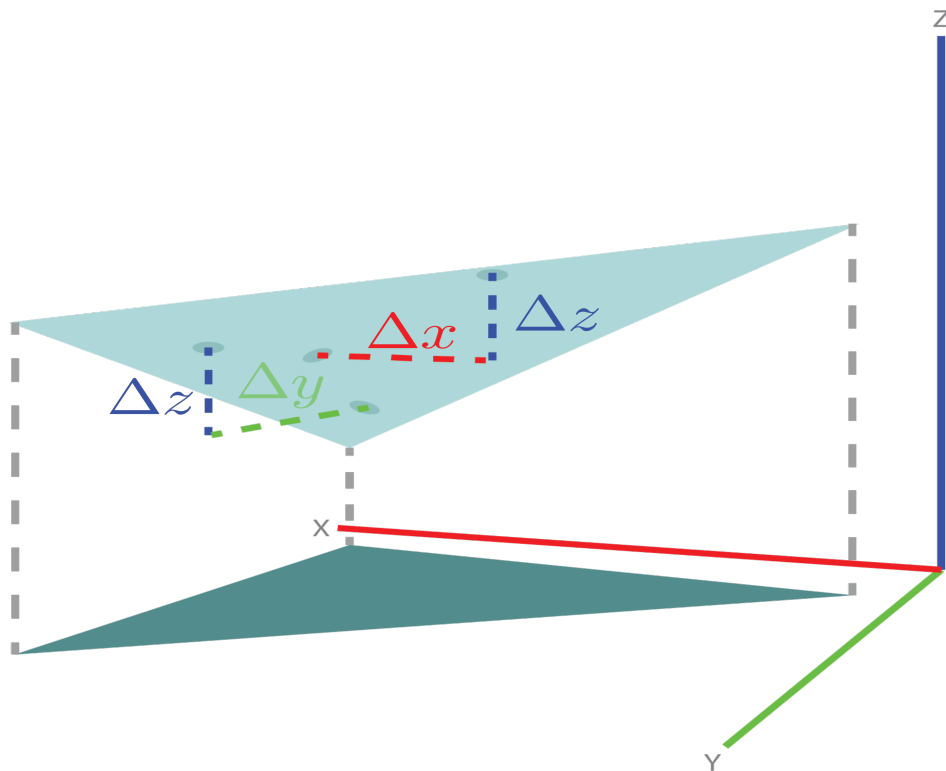


Figure 5.6: Linear barycentric interpolation: for interpolation on a 2D grid the vertices of a triangle are weighted by the z values. Each triangle has a uniform slope in the x and y directions ($\Delta z/\Delta x$ and $\Delta z/\Delta y$). The RSX data is on a 3D grid, so tetrahedrons are used.

5.4 Step 2: Reconstruct and interpret canonical flux tubes

If a vector field is divergence-less, field lines launched from the boundary of any 2D surface will trace out a tube of constant flux. To visualize canonical flux tubes the appropriate vector field definition and launching surfaces must be chosen. Species canonical flux is defined by eq. (2.3). However, the goal of the flux tube visualization is to develop intuition for canonical helicity. Since chapter 2 showed that canonical helicity is independent of the density gradient term in the canonical circulation (eq. (2.2)), the density gradient term will be dropped, reducing the canonical flux to eq. (2.4). In RSX the difference between current and ion flow vectors is small, so that the electron canonical flux tubes reduce to magnetic flux tubes. Three field quantities are needed to calculate the ion and electron canonical circulation: the density, the magnetic field, and the ion flow vorticity. The density and magnetic field have already been determined; the ion flow vorticity is determined by constructing the curl of ion flow from the slopes of the barycentric simplices. This study is interested in the dynamics of the gyrating current-carrying canonical flux tubes, so a launching surface should follow the gyration path.

5.4.1 Gyration path

The field null of the x and y components of the magnetic field has been identified as a tracer of the rotation. The x and y components of the magnetic field are shown in fig. 5.7 (left) together with their magnitudes. The field null is recognizable as the center around which the magnetic vectors circulate close to the peak of the magnetic field magnitude. However, since the magnetic field is asymmetric this is not the maxima of the curl of the magnetic field. An iterative scheme of fitting circles to integrated field lines of the x and y magnetic field and moving towards the circle center, determines the field null position for each time step. The starting point for the iteration scheme is the maximum of the x - y magnetic field magnitude. At each iteration, the field line integration launch point is moved towards the center of the least squares fitted circle by 10% of the radius. The iteration scheme continues until the fitted radius falls below 1 mm or the launch point falls outside of the common x - y magnetic field

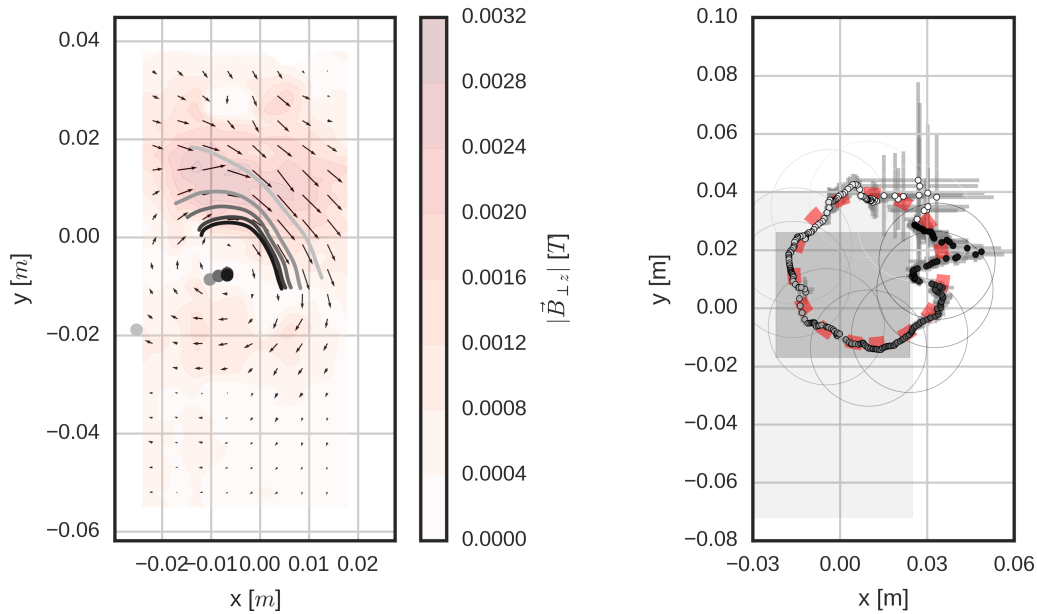


Figure 5.7: Left) Field null iteration scheme. \vec{B} and $|\vec{B}|$ at time $t = 8.5 \mu\text{s}$ in the $z = 25 \text{ cm}$ plane. A field line (successive steps from light gray to black) is integrated in both directions starting from the peak of $|\vec{B}|$, a circle is least squares fitted to the field line, and a new integration starting point is determined by moving 10% of the radius towards the circle center (successive steps from light gray to black). Right) Field nulls over one gyration period of $17 \mu\text{s}$ (white to black). Error bars (light gray) are determined by repeating the field null iteration scheme with successively stronger filtered data, averaging across shots. The field null gyration lies on a circle (dashed red). Circles with 2 cm radius are plotted around every 25th field null. 2 cm is the radius at which current and density drop of by $1/e$ [65]. Light gray region is the space in which both measurements of B_x and B_y were made. Dark gray region is the joint measurement space of all diagnostics used for flux tube reconstruction and helicity integrals.

measurement surface. Fig. 5.7 shows the gyration path of the field null in the $z = 0.25 \text{ cm}$ plane. The points and error bars are the averages and standard deviations of nine runs, the field null finding algorithm, one with unfiltered magnetic field interpolations and the others

with filtered magnetic field interpolation, where the standard deviation of the Gaussian filter kernel increases from 0.5 mm to 4.5 mm . The kernel is truncated at three times the standard deviation. The error bars account for both uncertainty due to the shot-to-shot variation of the measurements and the sensitivity of the fitting algorithm. The error is largest when the field null lies outside of the B_x and B_y measurement space, i.e. when the field null position has to be extrapolated from far away measurements. The field null positions with error bars lie on a circle (dashed red) centered at $x = 1\text{ cm}$ and $y = 1.3\text{ cm}$, and radius 2.5 cm .

5.4.2 Canonical Flux Tubes

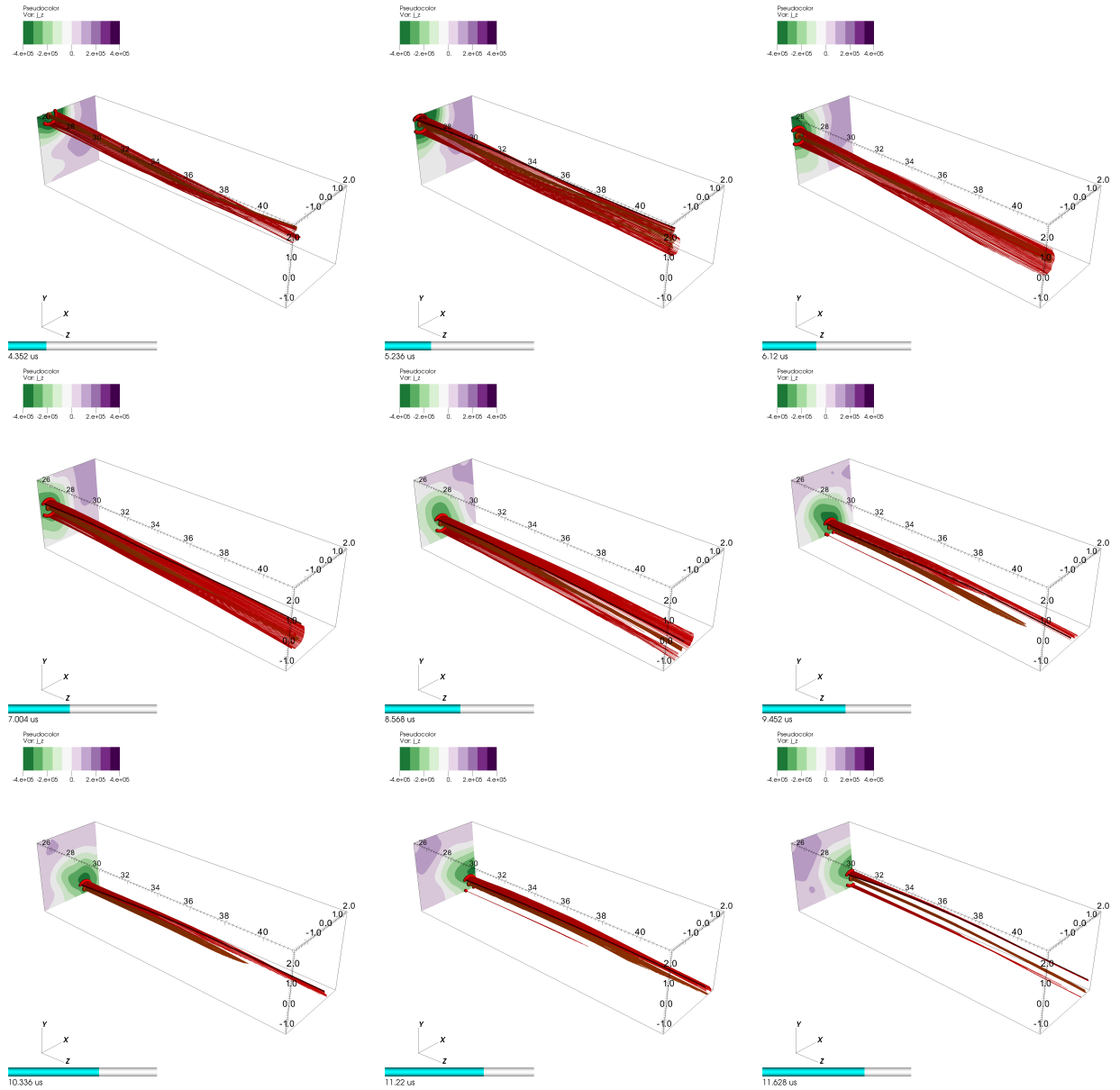


Figure 5.8: Gyrating electron canonical flux tubes. $n\vec{B}$ ($\vec{\Omega}_e$) field lines trace two electron canonical flux tubes over one gyration period of $17 \mu\text{s}$ in the joint measurement volume. The field lines are launched from circles of 1 mm (orange) and 5 mm (red) radii centered at the null of B_x and B_y in the $z = 25 \text{ cm}$ plane. A single field line (dark red) on the outer flux tube helps visualize the twist. Contours of j_z are plotted in the $z = 25 \text{ cm}$ plane, the colorbar units are $\frac{\text{A}}{\text{m}^2}$. The field null is inside the joint measurement from $t = 4.1 \mu\text{s}$ to $t = 12 \mu\text{s}$.

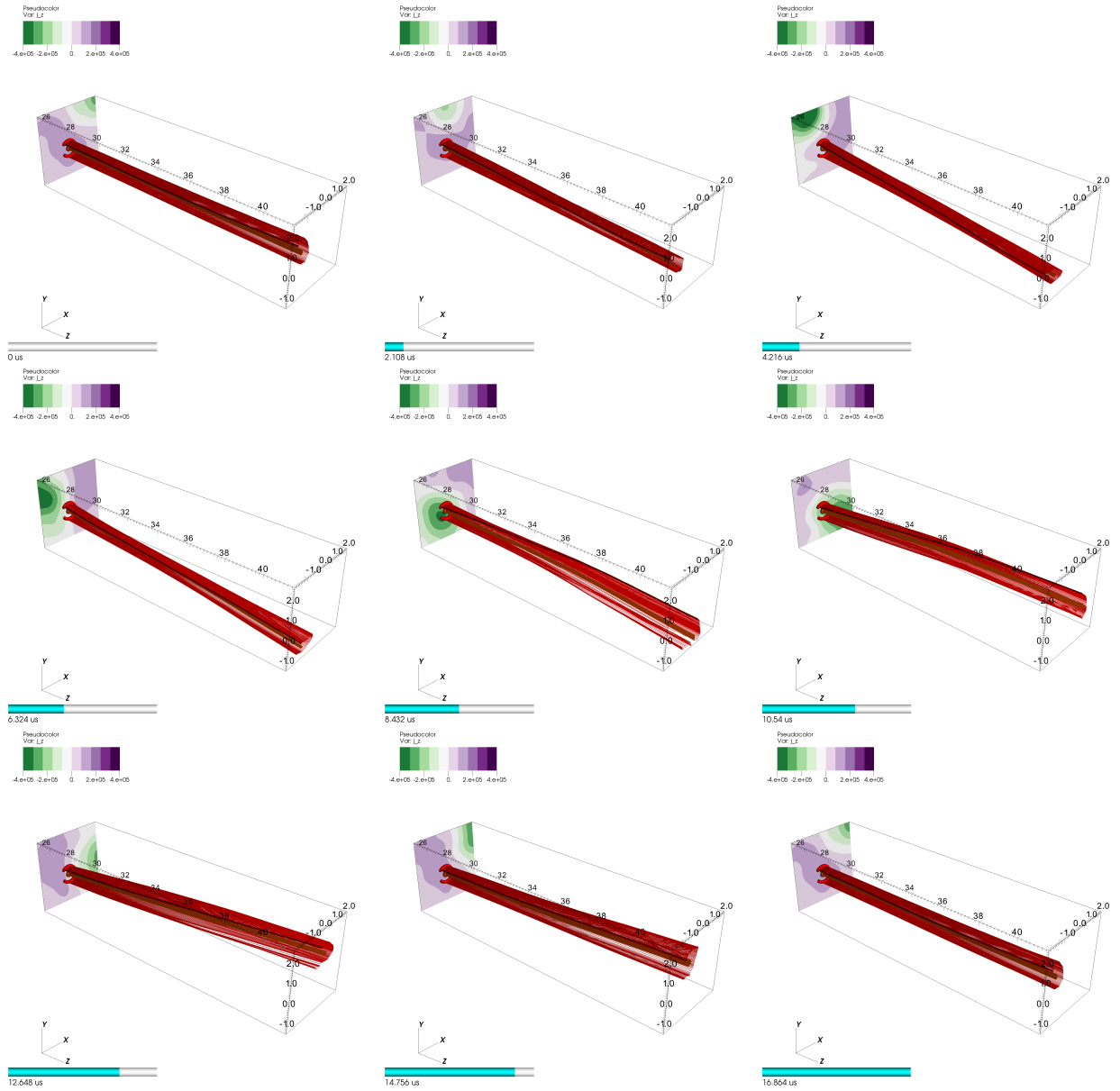


Figure 5.9: Stationary electron canonical flux tubes. $n\vec{B}$ ($\vec{\Omega}_e$) field lines tracing out two electron canonical flux tubes over one gyration period of $17 \mu\text{s}$. The field lines are launched from circles of 1 mm (orange) and 5 mm (red) radii centered at $x = 0$ and $y = 0$. A single field line (dark red) on the outer flux tube helps to visualize the twist. Contours of j_z are plotted in the $z = 25 \text{ cm}$ plane, the colorbar units are $\frac{\text{A}}{\text{m}^2}$.

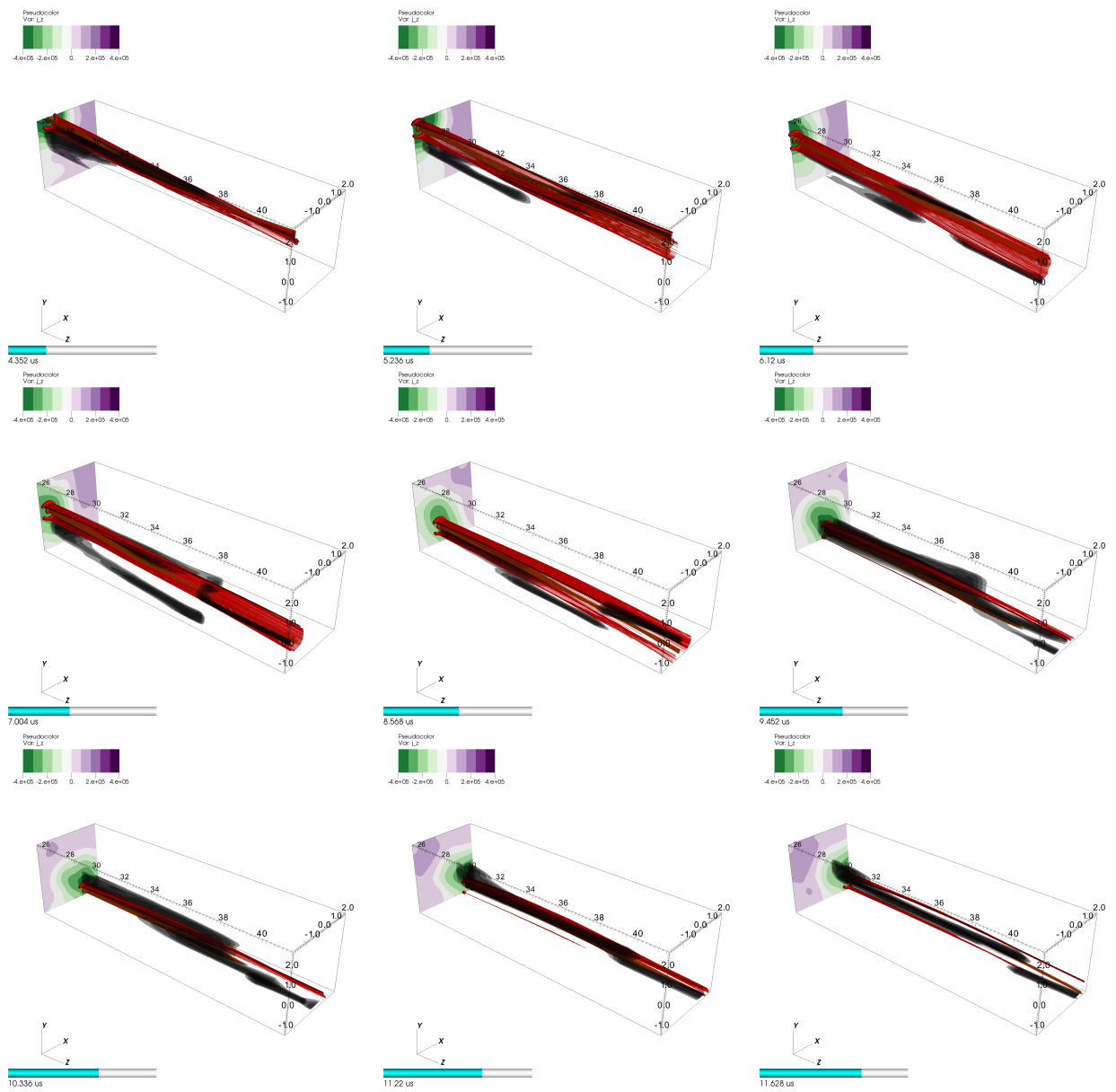


Figure 5.10: Isosurfaces of n normalized by the peak value in each of the x-y measurement plane over one gyration period of $17 \mu\text{s}$. The last isosurface encloses the top 10% of n . For comparison, electron canonical flux tubes and j_z from fig. 5.8 are plotted.

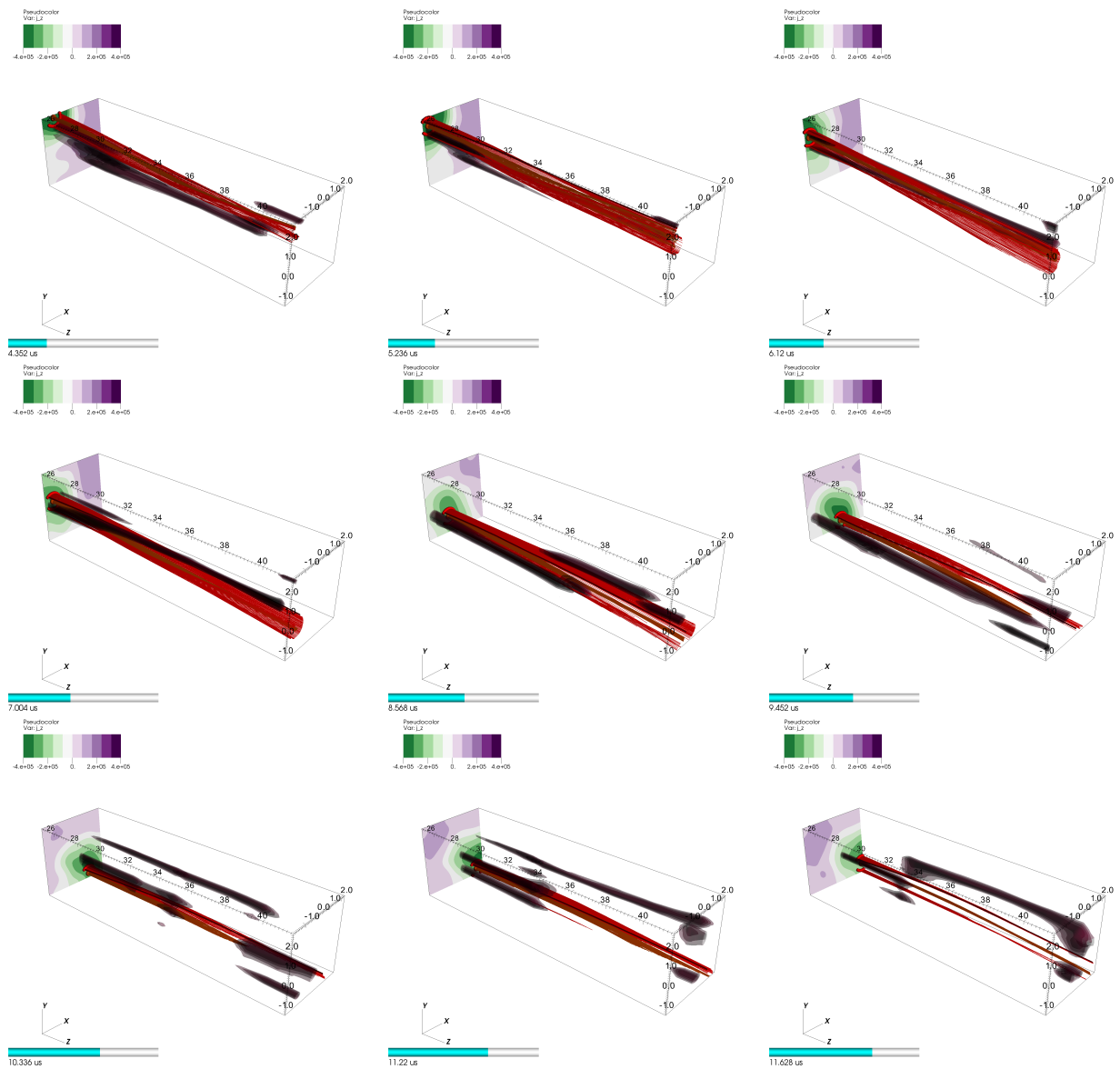


Figure 5.11: Isosurfaces of T_e normalized by the peak value in each x - y measurement plane over one gyration period of $17 \mu\text{s}$. The last isosurface encloses the top 10% of T_e . For comparison, electron canonical flux tubes and j_z from fig. 5.8 are plotted.

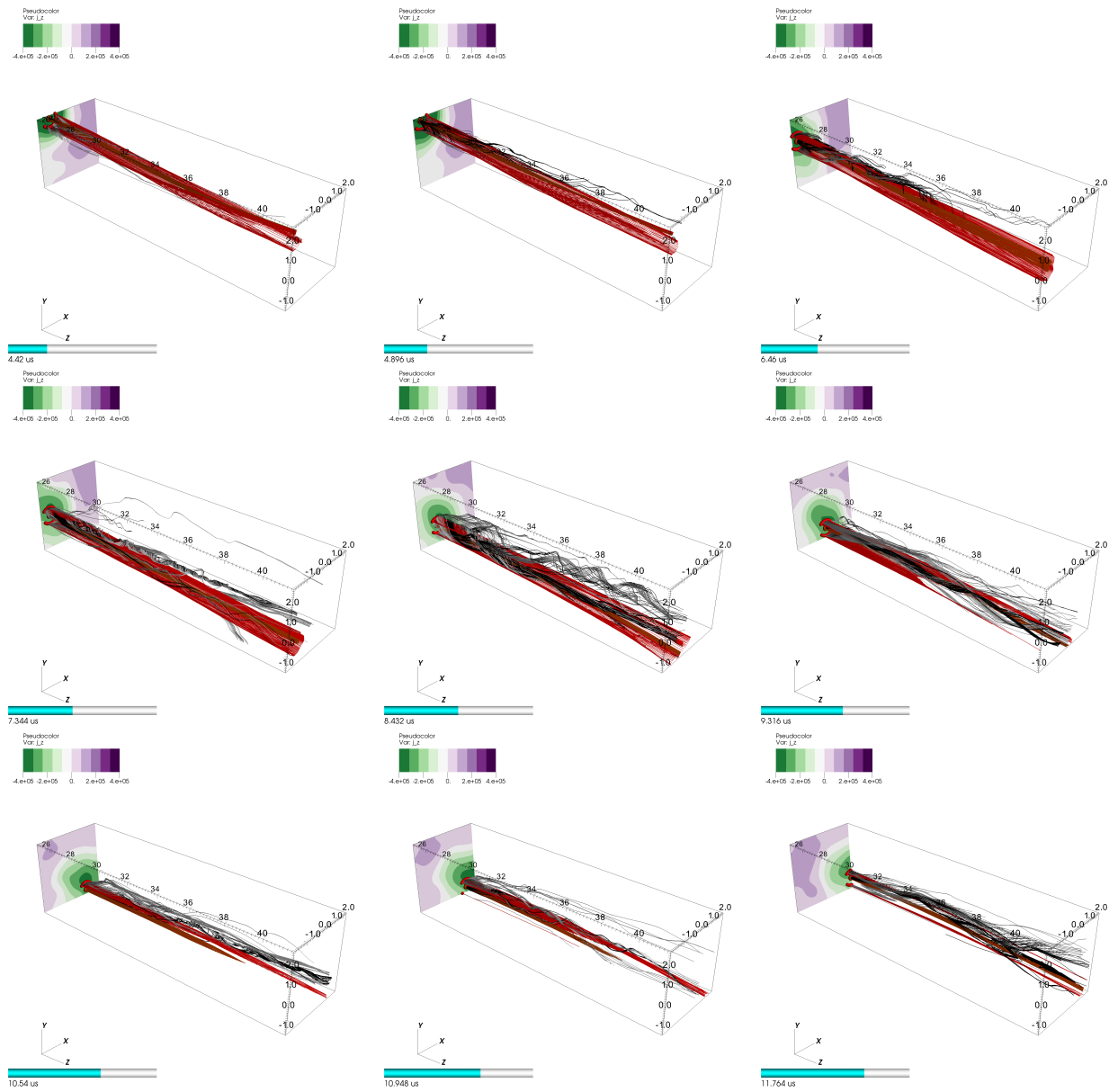


Figure 5.12: Gyrating ion canonical flux tubes. $\vec{\Omega}_i$ field lines trace out two ion canonical flux tubes over one gyration period of $17 \mu\text{s}$. The field lines are launched from circles of 1 mm (black) and 5 mm (grey) radii centered at the null of B_x and B_y in the $z = 25 \text{ cm}$ plane. For comparison \vec{B} flux tubes and j_z from fig. 5.8 are plotted.

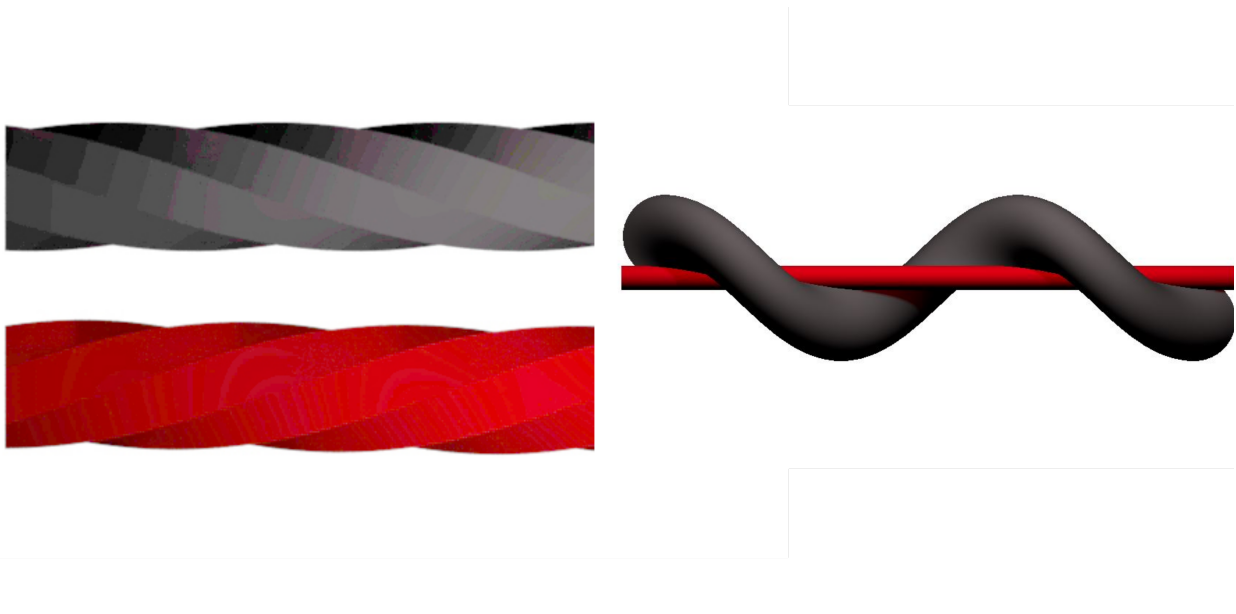


Figure 5.13: Schematics of twists and writhe. The positive axial direction is from left to right. Left) A right-handed twist (black) and a left-handed twist (red). Right) The black tube writhes with right-handed sense around the red tube.

Fig. 5.8 shows the evolution of two electron canonical flux tube during one gyration period. Field lines are launched from circles centered at the field nulls of B_x and B_y with 1 mm (orange) and 5 mm (red) radii. The electron canonical flux tube shape is dominated by the axial bias magnetic field which is an order of magnitude larger than the magnetic field due to internal currents. There is a reverse current that gyrates into the joint measurement volume as the field null is leaving the volume. This reverse current was identified as an eddy current in ref. [65], it is localized to $z \approx 25\text{--}35\text{ cm}$. A single field line is plotted in dark red on the surface of the outer flux tube. The single field line raps in a clockwise direction around the flux tube, indicating that canonical electron helicity is negative. The twist of the electron canonical flux and helicity in the measurement volume switches sign as the field null leaves the volume and the reverse current is centered in the volume as can be seen by following the single field line plotted on top of the stationary outer flux tube in fig. 5.9 (compare fig. 5.13). The field null tends to

be slightly below and to the left of the centroid of axial current j_z . If the plasma column were axisymmetric the field null would lie on the current centroid, however, since the column has kinked the current profile has a 3D structure, it is neither radially or azimuthally symmetric. Figs. 5.10 and 5.11 show that the position of the field null and the electron canonical flux tube are correlated with the peaks of density and electron temperature. These figures plot the gyrating electron canonical flux tube with isosurfaces of the top 10% of the maximum density and electron temperature values, respectively. The density and temperature were normalized in each plane prior to plotting so that the isosurfaces would be continuous. The peak density overlaps with field null, or at times, is below and to the right of the field null 'leading' the field null gyration. Since there is no extrapolation of the density the peak must be inside the joint measurement volume, even when the field null leaves the volume. The co-motion of the density and electron canonical flux tubes is evidence of the MHD frozen-in flux condition. The peak electron temperature overlaps with the field null, or at times, is above and to the left of the field null 'lagging' the field null gyration. Both density and electron temperature isosurfaces follow the axial structure of the electron canonical flux tubes bending downward at higher z . The leading and lagging of the peak density and temperature may be due to positional uncertainty in the probes or may be the result of the plasma not being in equilibrium. Ref. [65] found a 25% discrepancy in the magnitudes of $\vec{J} \times \vec{B}$ and ∇p terms of the MHD force balance and suggested Coriolis forces from the gyration flows may be responsible for the discrepancy. The Alfvén transit time along the gyration path length ($2\pi \cdot 2.5 \text{ cm}$) is $\sim 2 \mu\text{s}$, using the axial magnetic field 0.02 T and peak density $3 \cdot 10^{19} \text{ m}^{-3}$. $2 \mu\text{s}$ is almost an order of magnitude smaller than the gyration period. This suggests that the system should be in a gyrating pseudo-equilibrium. However, ref. [65] notes that the pseudo-equilibrium would be irreducibly 3D as the current and magnetic field profiles are radially asymmetric and the reverse current disappears in the $z = 42 \text{ cm}$ plane. In Fig. 5.12 the electron canonical flux tubes are plotted together with ion canonical flux tubes. The ion canonical flux tubes vary rapidly because the ion vorticity has a larger amount of error due to amplification of noise when taking the derivatives required for determining the curl of ion flow. The noise makes the ion canonical flux vary rapidly and

without strong tubular structure. Since the ion canonical vorticity is calculated from a curl it is practically divergence-less. The divergence of the ion canonical circulation is on the order of $10^{-16} \text{ kg s}^{-1} \text{ m}^{-1}$ (without multiplying by density n), which is double-precision floating point accuracy. Hence, the field lines should trace cross-sections of constant flux, however it is the cross-sections themselves that are varying rapidly. The divergence of the magnetic field varies between 0.1 T/m , when the field null is inside the measurement volume, and 0.01 T/m , when the field null is outside the measurement volume. The divergence stems from interpolation and instrument error in the magnetic probes. This means that the field lines do not strictly trace out cross-sections of constant flux, however since the axial vacuum magnetic field dominates the dynamic magnetic field by an order of magnitude, a tubular structure is preserved. The ion canonical flux tubes show significant right-handed twist and at some time steps ($7.344 \mu\text{s}$, $8.432 \mu\text{s}$, $9.316 \mu\text{s}$) writhe around the magnetic flux tubes (compare fig. 5.13). The right-handed twist and writhes indicate that the total ion canonical helicity is positive and exceeds the magnetic helicity which must be due to cross or fluid helicity. These plots represent the first reconstruction of canonical flux tubes from experimental measurements.

5.5 Step 3: Determine vector potential and reference fields

Helicity is the volume integral of vector potential of the flux quantity of interest dotted with its circulation. Relative canonical helicity has to be used since intersections of ion and electron canonical flux tubes and the open system boundaries will add a gauge dependence to the non-relative forms of canonical helicity. The relative canonical helicity integrals require choosing suitable reference circulation fields and determining the reference vector potential fields. This section will discuss methods for determining reference fields \vec{B}_{ref} and $\vec{\omega}_{iref}$ and vector potentials \vec{A} , \vec{A}_{ref} , and \vec{u}_{iref} .

5.5.1 Comparing vector fields

To test the methods developed in this section their solutions will be compared to known vector potentials and reference fields, however, vector fields are non-trivial to compare. Two scalar fields can be similar in certain regions and differ in others. In addition to regional differences, two vectors fields can have similar directions but different magnitudes and vice versa. To evaluate the reference field and vector potential calculation methods it is useful to quantify what effect they have on the helicity integrals. Ref. [97] developed the Taylor diagram that plots the scalar field characteristics: Pearson correlation coefficient, root mean squared field difference, and standard deviations of the scalar fields combined into a single polar diagram using a cosine relationship. Ref. [98] extended the Taylor diagram to vector fields introducing new characteristics: vector similarity coefficient, root mean square vector difference, and root mean square length. The vector similarity coefficient can be understood as a normalized helicity density sum between two vector fields and will be called the latter going forward. The normalized helicity density sum between two vectors \vec{A} and \vec{B} is defined as

$$\tilde{K} = \frac{\sum_{i=1}^N \vec{A}_i \cdot \vec{B}_i}{\sqrt{\sum_{i=1}^N |A_i|^2} \sqrt{\sum_{i=1}^N |B_i|^2}}, \quad (5.3)$$

where the sums are over all N spatial elements i . The normalized helicity density sum \tilde{K} measures the pattern similarity of vector fields and depends on both their length and directions. \tilde{K} does not change when either vector field is multiplied by a constant. The normalized helicity density sum varies between -1 and 1 . A positive (negative) \tilde{K} indicates that the angles between the vector fields are generally smaller (larger) than 90° . When the two vector fields are equal (equal and opposite), \tilde{K} is 1 (-1). The root mean square vector difference $RMSVD$ between two vector fields \vec{A} and \vec{B} is defined as

$$RMSVD = \sqrt{\frac{1}{N} \sum_{i=1}^N |\vec{A}_i - \vec{B}_i|^2}. \quad (5.4)$$

RMSVD quantifies the average difference in lengths of the two vector fields. The root mean square vector length L_A of a vector field \vec{A} is defined as

$$L_A = \sqrt{\frac{1}{N} \sum_{i=1}^N |\vec{A}_i|^2}. \quad (5.5)$$

The normalized helicity density sum \tilde{K} , the root mean square vector difference *RMSVD*, and the root mean square lengths L_A and L_B can be expressed in a law of cosines

$$RMSVD^2 = L_A^2 + L_B^2 - 2L_A L_B \tilde{K}, \quad (5.6)$$

where \tilde{K} acts as the angle between the L_A and L_B sides of a triangle and *RMSVD* is opposite to \tilde{K} . The three quantities can be plotted in a polar plot where \tilde{K} is the azimuthal angle, L is the radius, and *RMSVD* is the distance between two points. Testing numerical techniques by plotting their solutions together with known solutions helps quantify the effect the numerical error has on helicity calculations. The effect on helicity can be separated between the effect from differences in the normalized helicity density sum \tilde{K} and from differences in the root mean squared vector difference *RMSVD*.

5.5.2 Reference fields: Solving Laplace equation with fast Fourier methods

The conditions on the reference fields for canonical helicity (eq. 2.19) setup a Laplace problem with Neumann boundary conditions. The Laplace problem can be solved for a scalar potential ϕ of which the gradient is the reference circulation field. The Laplace problem is defined as

$$\begin{aligned} \nabla^2 \phi &= 0 \\ \frac{\partial \phi}{\partial \hat{n}} \Big|_s &= -\vec{\Omega}_\sigma \cdot \hat{n} \Big|_s, \end{aligned} \quad (5.7)$$

where \hat{n} is the surface normal. Since all quantities have been interpolated on a regular rectangular grid the problem can be expressed as a finite difference formulation and solved with fast Fourier methods [99, 100]. On a 3D grid with indices j_1 , j_2 , and j_3 , varying from 0 to J_n the Laplace equation can be expressed in finite differences

$$\phi_{j_1+1, j_2, j_3} + \phi_{j_1-1, j_2, j_3} + \phi_{j_1, j_2-1, j_3} + \phi_{j_1, j_2+1, j_3} + \phi_{j_1, j_2, j_3-1} + \phi_{j_1, j_2, j_3+1} + 6\phi_{j_1, j_2, j_3} = 0, \quad (5.8)$$

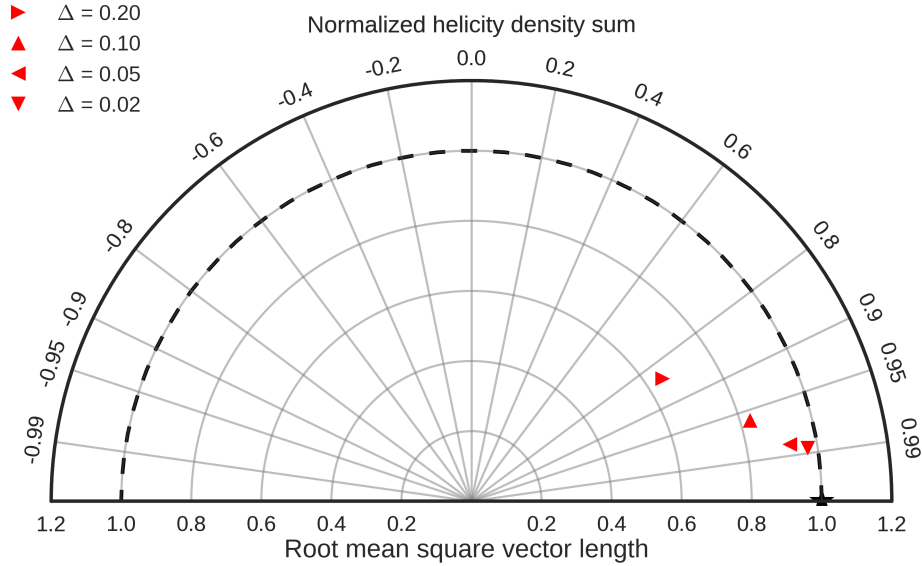


Figure 5.14: Taylor plot comparing known vacuum magnetic field (black star) with gradient of scalar potential (red triangles) obtained for 4 grid resolutions with the discrete cosine transform method for solving the Laplace problem. The known vacuum field is in the upper right quadrant of a x-y coordinate system with the conductor at its center. The known magnetic field is used as Neumann boundary condition for the Laplace solver.

with boundary condition on the lower x side

$$\frac{\phi_{-1,j_2,j_3} + \phi_{1,j_2,j_3}}{2\Delta_x} = -\vec{\Omega}_\sigma \cdot \hat{x}|_s, \quad (5.9)$$

where Δ_x is the spatial discretization in the x direction. The boundary conditions on the other edges are analogous. Discrete cosine transforms (DCT) use multiples of half-period cosines as basis functions. These functions have the convenient property that they impose homogeneous Neumann conditions $\partial \tilde{\phi} / \partial n = 0$. The inhomogeneous Neumann conditions can be treated by adding $2\Delta - \vec{\Omega}_\sigma \cdot \hat{x}|_s$ to the left hand side of eq. (5.8) at the edges [99]. The algorithm of the Laplace solver is 1) apply the DCT to the modified left hand side of eq. (5.8) ($2\Delta(-\vec{\Omega}_\sigma \cdot \hat{x}|_s)$), 2) solve for $\tilde{\phi}$ by dividing the transformed left hand side by the right hand side, and 3) apply the inverse DCT to obtain ϕ [101]. There are multiple possible definitions of the DCT. This

study chooses what is commonly referred to as the DCT-1

$$\tilde{f}_k = f_0 + (-1)^k f_{n-1} + 2 \sum_{j=1}^{J-2} f_j \cos(\pi j k / (J-1)). \quad (5.10)$$

The inverse DCT is eq. (5.10) multiplied by $1/(2(J-1))$. For 3D grids the DCT has to be applied three times for each dimension. This study uses the scientific Python (scipy) implementation of the DCT [95, 102]. The divisor in step 2) can be expressed as

$$\lambda = - \left(\frac{\pi^3 (k_1 + 1)(k_2 + 1)(k_3 + 1)}{K_1 K_2 K_3} \right)^2. \quad (5.11)$$

Fig. 5.14 compares three Laplace solutions for a magnetic vacuum field outside a current-carrying conductor. The normalized helicity density sum and the ratio of root mean square lengths of the known solution and the gradient of the computed scalar potential approach 0.95 and 1, respectively, with increasing resolution.

5.5.3 Two-component vector potential

The choice of a convenient gauge can simplify the calculation of the vector potential. Several coronal loop studies and simulations have identified setting the axial field component to zero $A_z = 0$ as part of a convenient gauge choice [103, 69]. The curl of \vec{A} becomes

$$\nabla \times \vec{A} = -\frac{\partial A_y}{\partial z} \hat{x} + \frac{\partial A_x}{\partial z} \hat{y} + \left(\frac{\partial A_y}{\partial x} - \frac{\partial A_x}{\partial y} \right) \hat{z}. \quad (5.12)$$

For a region of interest bounded by $[x_1 : x_2, y_1 : y_2, z_1 : z_2]$ the vector potential can be expressed as integrals along z

$$A_x(x, y, z) = A_{0x}(x, y) + \int_{z_1}^z B_y(x, y, z') dz' \quad (5.13)$$

and

$$A_y(x, y, z) = A_{0y}(x, y) - \int_{z_1}^z B_x(x, y, z') dz'. \quad (5.14)$$

The choice of A_{0x} and A_{0y} is constrained by the third term of eq. 5.12, one valid choice is

$$A_{0x}(x, y) = -\frac{1}{2} \int_{y_1}^y B_z(x, y', z = z_1) dy' \quad (5.15)$$

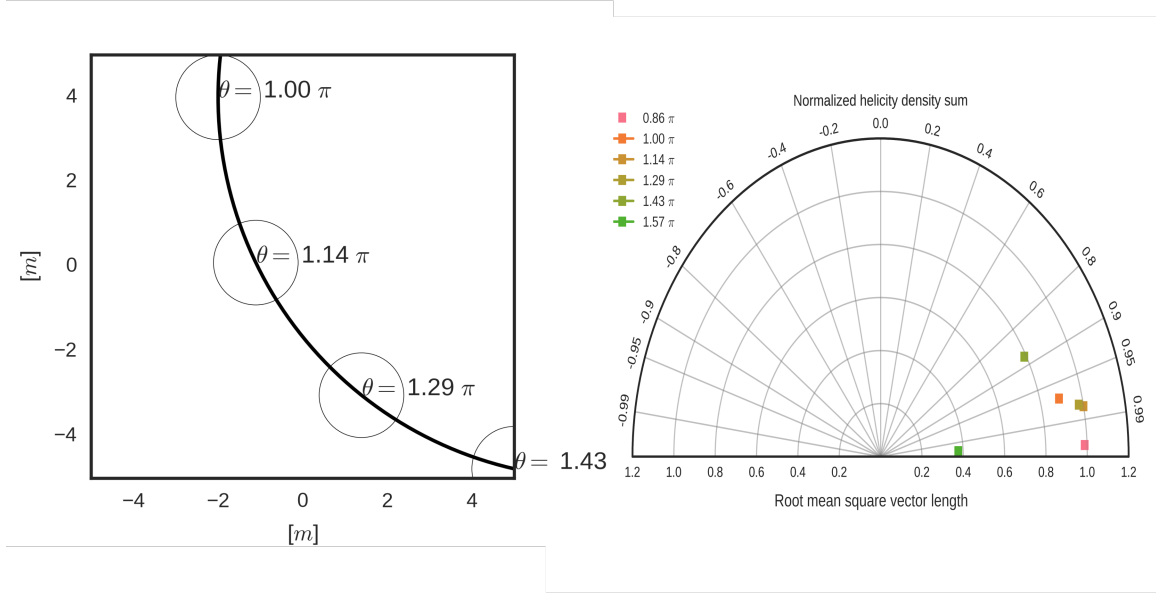


Figure 5.15: Left) Test problem setup for the two-component vector potential solver. The known test fields are the magnetic fields from a gyrating current-carrying cylindrical conductor at several angles. Right) Taylor plot comparing known magnetic fields from gyrating current-carrying conductor at various angles with curl of vector potential solutions obtained with the two-component vector potential method (squares).

and

$$A_{0y}(x, y) = \frac{1}{2} \int_{x_1}^x B_z(x', y, z = z_1) dx'. \quad (5.16)$$

The eqs. (5.15), (5.16), and $A_z = 0$ define the gauge. Fig. 5.15 shows that this method of determining the vector field performs well for the test problem of a uniform current-carrying conductor, which is gyrating in the x - y plane. The normalized helicity density sum of the curl of the calculated vector potentials and the known magnetic field are above 0.85. The two-component vector potential method performs well even when the current-carrying conductor is at the boundary, i.e. the boundary conditions have strong non-periodicity, which is in contrast to a method based on inverting the curl in (periodic) Fourier space, proposed in ref. [92].

5.6 Step 4: Reconstruct and interpret canonical helicity

Now that all necessary quantities are known, the dot products of the three-helicity expression of relative ion canonical helicity (eq. 2.20) are integrated with the trapezoidal method. Fig. 5.16 shows the evolution of magnetic (red), cross (green), fluid (blue) helicity, and their sum, which is the total ion canonical helicity (black), in the joint measurement volume during one gyration period. The gauge-dependent magnetic helicity is positive when the field null is outside the measurement volume, decreases as the field null enters the measurement volume, reaches its peak magnitude and increases again to a positive value as the field null exits the measurement volume. The gauge-dependent cross helicity is always positive and is anticorrelated with the gauge-dependent magnetic helicity, although the gauge-dependent cross helicity starts increasing $\sim 2 \mu s$ after the the magnitude of the gauge-dependent magnetic helicity starts increasing. The signs of helicities agree with the handedness of the twist of the electron and ion canonical flux tubes in figs. 5.8, 5.9, and 5.12. The density weighting of helicity increases the magnitude of the helicities when the field null, which co-gyrates with the peak density is inside the joint measurement volume. The strong twist and writhing visible on the ion canonical flux tubes must be due to the cross helicity as it is an order of magnitude larger than the fluid helicity. The relative canonical helicities have smaller magnitudes than their gauge-dependent counterparts. They exhibit increased noise due to the differentiation step in determining the relative helicity, which is taking the gradient of the reference potential field. The magnitude of the relative fluid helicity barely exceeds the noise, it may be negligible. The ratio of peaks of the relative magnetic helicity and relative cross helicity is 0.12 which agrees roughly with the following dimensional analysis: Using ion mass $m_0 = 1.7 \cdot 10^{-27} \text{ kg}$, the elementary charge $q_0 = 1.6 \cdot 10^{-19} \text{ C}$, the perpendicular magnetic field $B_0 = 0.002 \text{ T}$, the radial current and density e-folding length $l_0 = 0.02 \text{ m}$, and the peak ion velocity $u_0 = 2.5 \cdot 10^4 \text{ m/s}$, the ratio of magnetic helicity over cross helicity becomes

$$\frac{\mathcal{X}_{i\text{rel}}}{\mathcal{X}_{i\text{rel}}} = \frac{q_i^2 \int n (\vec{A}_- \cdot \vec{B}_+) dV}{q_i m_i \int n (\vec{u}_{i-} \cdot \vec{B}_+ + \vec{B}_- \cdot \vec{u}_{i+}) dV} \approx \frac{q_0 B_0 l_0}{2 m_0 u_0} \approx 0.08. \quad (5.17)$$

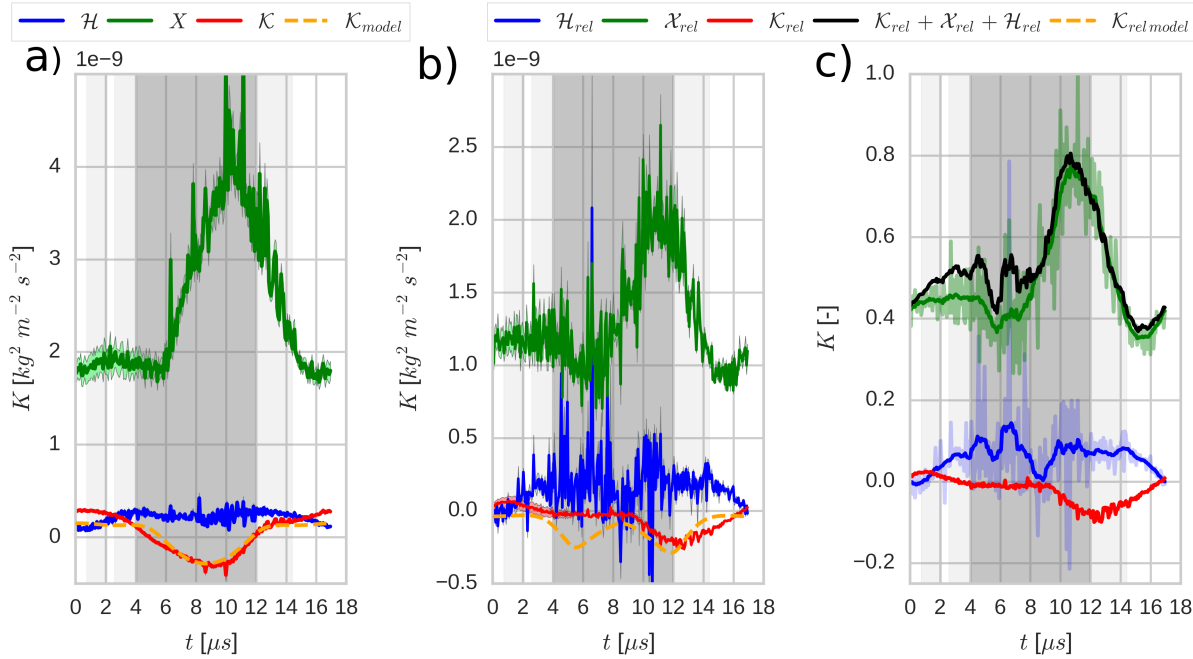


Figure 5.16: Magnetic (red), cross (green), flow (blue), and total ion canonical (black) helicity in the joint measurement volume identified in figs. 5.7 and 5.5. a) Gauge-dependent helicities with real units. b) Relative helicities with real units. c) Boxcar ($1.02 \mu\text{s}$ width) filtered relative helicities, normalized to the maximum relative cross helicity. Dark gray shading marks the time the field null is inside the joint measurement volume. Light gray shading marks the time at which the field null is inside the region with both B_x and B_y measurements shown in fig. 5.7. Dashed orange shows the magnetic helicity of a simplified model problem. The model problem consists of a cylindrical conductor with 0.02 m radius and uniform current density $j = 140 \text{ kA/m}^2$ with an exponential density cloud, $n(r) = 1.3 \cdot 10^{19} e^{r/(0.02 \text{ m})} \text{ m}^{-3}$, where r is the radius. The conductor is gyrating along the red dashed circle fitted to the field null path in fig. 5.7. All helicities are the mean determined from running the analysis nine times with successively increasing the standard deviation of the Gaussian kernel filtering of the interpolated measurements. The standard deviation of the runs is plotted as an envelope around the helicity curves, however, the helicity calculations are insensitive to this filtering and the envelope is only partially visible.

The increases in the magnitudes of the relative magnetic and cross helicities are better aligned in time than the increases of their gauge-dependent counterparts. To understand the time offset between the field null entering the joint measurement volume and the increase in helicity magnitudes, it is helpful to reduce the problem to the approximation of a current-carrying cylindrical conductor, parallel to the z -axis, gyrating along the circle fit to the field null gyration in fig. 5.7 through vacuum. Choosing the e-folding length of the current and density (0.02 m) as the radius of the conductor, a uniform current density of $j = 140\text{ kA/m}^2$ (compare current density in fig. 5.8) and an exponential density cloud given by $n = 1.3 \cdot 10^{19} e^{r/(0.02\text{ m})} \text{ m}^{-3}$, where r is the radius, yields a gauge-dependent magnetic helicity (dashed orange) consistent with the gauge-dependent magnetic helicity calculated from the RSX data. However, there is a discrepancy in the relative magnetic helicities calculated from gyrating conductor and the RSX magnetic fields. While the magnitude of relative magnetic helicity of the model problem has two peaks, the magnitude of helicity calculated from the RSX magnetic fields only has a single peak, which closely follows the second peak of the model. Looking at the canonical flux tube evolution (fig. 5.8), the discrepancy may be due to the reverse eddy current and the offset between the current-carrying canonical flux tube and the peak density. From $t = 4\ \mu\text{s}$ when the field null enters the joint measurement volume to about $t = 7\ \mu\text{s}$ the reverse current encompasses more than half the measurement volume with a peak of about $1/3$ of the magnitude of the negative axial current. The reverse current is in the $+z$ direction, generating a counter-clockwise azimuthal field which together with the positive axial magnetic bias field gives a right-handed (positive) helicity. This positive helicity counteracts the negative helicity from the main (negative) axial current. The axial bending of the canonical flux tubes and current path may also have an effect on the helicity. It should be possible to identify the contributing factors by expanding the simple current-carrying conductor model to include more features of the RSX current-carrying canonical flux tubes.

Since most measurement locations in fig. 5.5 only have a single measurement, it is important to test if the helicity calculations are sensitive to the shot-to-shot variation. The helicities plotted are the averages of nine runs of the data analysis described in this chapter. One run

starts with unfiltered interpolated values of B , n , T_e , and Mach numbers, the other runs start with filtered interpolations, where the standard deviation of the Gaussian filter kernel increases from 0.5 mm to 4.5 mm . The Gaussian kernel is truncated at three times the standard deviation. This averages across measurements at the cost of a coarser grid. The standard deviations of these runs are plotted as envelopes around the helicity curves. However, the helicities are not sensitive to the filtering of the interpolations. To reduce the shot variability in gyration amplitude it may be possible to average measurements over several periods of gyration, or repeat the helicity analysis with a limited subset of shots with a more limited spectral power distribution. A significant source of noise and uncertainty in the cross and fluid helicities is the curl of the linearly interpolated velocity. The noise could be reduced by fitting higher order functions to the measurements. Since the measurements are on a mostly rectilinear grid with only a few gaps, linear interpolation could be applied selectively to the gaps, followed by tri-cubic interpolation across the whole rectilinear grid. In addition, it may be possible to take advantage of cross-correlation between the four measurement quantities with a form of Gaussian process regression [104].

Since the RSX plasma motion becomes exceptionally coherent once the kink has saturated, this study has focused on calculating the helicity evolution during this time period. The variations in the helicities during the saturated kink seem to be explained by different sections of the current distribution gyrating in and out of the joint measurement volume. However, since the current structure in RSX is on the scale of the ion inertial length, there may be a conversion between destabilizing magnetic helicity and cross helicity as the kink develops and saturates. Indeed, a kinetic simulation of a periodic current-carrying magnetic flux tube with similar parameters to RSX develops forces and dynamics on kinetic scales and identifies possible reconnection sites [105]. If the helicities could be reconstructed in the current ramp-up phase it may be possible to observe a reduction in magnetic helicity together with an increase in cross helicity during onset of the kink. Cross-spectral data analysis techniques [106] could identify coherent mode structures between the fiducial and translatable probes at specific frequencies [107].

5.7 Conclusion

Canonical flux tubes and relative canonical helicity have been reconstructed from the Mach, triple, and \dot{B} probe measurements from 2,369 shots of kinked, gyrating canonical flux tubes. The electron and ion canonical flux tubes co-gyrate together with peak density and temperature. The electron and ion canonical flux tubes twist in left-handed and right-handed sense, respectively; in addition, the ion canonical flux tube writhes around the electron canonical flux tube. The signs of the twist agrees with the signs of the calculated relative magnetic and cross helicities. The magnetic and cross helicities are anticorrelated and increase and decrease in magnitude as the flux tubes gyrate in and out of the joint measurement volume. An offset in the increase of the relative magnetic and cross helicity magnitudes and the entry of the field null into the joint measurement volume may be due to the reverse eddy current and the helical shape of the canonical flux tube. While minimum energy states resulting from magnetic helicity conservation have been widely explored, there have been few direct experimental calculations without symmetry assumptions due to lack of 3D measurements [34, 108]. Researchers at the LAPD experiment at UCLA have calculated magnetic and cross helicity of gyrating and merging plasma columns, however, not in a gauge-independent relative form [109]. This work is the first calculation of relative canonical helicity in a dynamic system.

Chapter 6

CONCLUSION AND OUTLOOK

Observations indicate that the dynamics of plasmas in our cosmos, the heliosphere, and terrestrial experiments can involve coupling and conversions between magnetic and kinetic energies, such as in reconnection and dynamo behavior. Recent theoretical work [39] provides a geometrical picture of these dynamics as conversions between electron (magnetic) and ion canonical (magnetic, cross, and fluid) helicity, while conserving their sum. Experimental validation of the theory of canonical helicity transport could extend the quasi-static theory of magnetic helicity relaxation to phenomena with fast reconnection and multiscale dynamics, such as coronal eruptions, sawteeth in reverse field pinches and tokamaks, and could elucidate how destabilizing magnetic twist converts to shear flow in astrophysical jets and compact toroid merging. Sheared flows have been observed to be stabilizing in Z-pinches [40] and are thought to play a role in transport barriers in H-mode tokamaks [110]. Understanding canonical helicity injection may lead to methods for driving shear flow in fusion experiments analogous to how coaxial [111] and inductive [112] magnetic helicity injection drives current. To improve the understanding of canonical helicity transport, the theory needs to be tested and compared to experimental observations.

This thesis presents the first application of the theory of canonical helicity transport to design a laboratory canonical flux tube experiment and develops methods to measure a large volumetric dataset, to reconstruct the 3D dynamics of canonical flux tubes, and to interpret the canonical helicity evolution. A sausage-kink instability cascade has been identified in an idealized lengthening current-carrying magnetic flux tube. If the flux tube's current-to-magnetic flux ratio can be increased faster than the inverse aspect ratio decreases, and the ratio of the flux tube radius over the ion skin depth is kept below two, the instability cascade may couple

the MHD system to smaller scales at which conversions between species helicities are expected to occur. Experiment control and high-throughput FPGA based digitizers for the Mochi.Labjet experiment provide the means to measure the large volumetric datasets needed to calculate helicity volume integrals. Ion and electron canonical flux tubes and their helicity have been visualized and calculated from a volumetric dataset of Mach, triple, and \dot{B} probe measurements at over 10,000 spatial locations of a gyrating kinked plasma column in a subvolume of the RSX experiment. The flux tubes are launched from the field null of the perpendicular magnetic field and co-gyrate with the peak density and electron temperature on a circular path in and out of the subvolume. The electron and ion flux tubes twist with opposite handedness and the ion canonical flux tube writhes around the electron canonical flux tube. The cross helicity between the magnetic and ion flow vorticity flux tubes dominates the ion canonical helicity and is anticorrelated with the magnetic helicity.

The Mochi.Labjet experiment described in this thesis is currently exploring the $\bar{k} - \bar{\lambda}$ stability space of current-carrying magnetic flux tubes. A high-density 3D magnetic probe array and vector tomography based on ion Doppler spectroscopy measurements will provide the data necessary to calculate canonical helicity and investigate possible conversion during an instability cascade.

The data analysis techniques developed in this thesis can be applied to other experiments with potential for interactions between magnetic, cross, and fluid helicities. The decreasing cost of high-speed digitizers with high-channel count and high speed cameras will make the collection of large sets of electrical and spectroscopic data feasible on a variety of experiments.

For example, the Magnetic Reconnection Experiment (MRX) team observed an arched magnetic flux tube self-organize into a lower energy state while undergoing a torus instability; a decrease in toroidal current and associated poloidal field generates a stabilizing increase in the toroidal field, conserving magnetic helicity [29]. However, the relaxation process can also be interrupted by a kink instability with a violent conversion of magnetic energy into kinetic energy, mimicking a coronal loop eruption. While MRX focuses on measurements in a 2D plane its successor experiment FLARE aims to record 3D magnetic field and ion flow measurements

[113].

One configuration of the Large Plasma Device (LAPD) generates multiple plasma columns, which rotate around each other and periodically bounce and collide [114]. In the experiment the magnetic helicity and the magnetic field line squashing factor oscillate, with peaks of magnetic helicity corresponding to onsets of magnetic field squashing factor growth [115].

Reversed-field pinches (RFP) are relaxed minimum energy states constrained by magnetic helicity. An RFP exhibits a periodic sawtooth cycle characterized by a slow peaking of the current profile followed by a sudden global relaxation of current and density gradients, representing a discrete relaxation event in time. Magnetic helicity evolution has been measured indirectly during sawtooth crashes at the Madison Symmetric Torus (MST) by using a neural network to infer internal magnetic profiles from other measured plasma quantities [34]. Magnetic helicity varies slower than magnetic energy as MHD theories predict, however, the magnetic helicity decay is larger than expected. Simulations, though unable to reach the Lundquist numbers of lab plasmas, find that magnetic helicity is degraded when two-fluid effects are included [116]. Insertable Mach and magnetic probes can survive in the edge plasma and acquire measurements of sawteeth events at the $q = 0$ surface. The presence of ion flows on inertial length scales [117] suggests the possibility of conversion of magnetic helicity into cross helicity. Calculating the canonical helicity could reveal if part of the magnetic helicity is converted into cross helicity.

Applying the analysis techniques developed in this thesis to 3D measurements of magnetic fields and ion flows at these experiments could probe if the magnetic helicity is converted to cross or fluid helicity and if helicity injection and dissipation terms can be identified and quantified.

BIBLIOGRAPHY

- [1] J. A. Bittencourt. *Fundamentals of Plasma Physics*. New York: Springer-Verlag, 2004. DOI: 10.1007/978-1-4757-4030-1.
- [2] D. A. Gurnett and A. Bhattacharjee. *Introduction to Plasma Physics*. Cambridge, UK: Cambridge University Press, 2005. DOI: 10.1017/cbo9780511809125.
- [3] Richard Dendy, ed. *Plasma Physics: An Introductory Course*. Cambridge, UK: Cambridge University Press, 1994. ISBN: 0521433096.
- [4] Toshiki Tajima and Kazunari Shibata. *Plasma Astrophysics (Frontiers in Physics)*. Boulder, CO: Westview Press, 2002. ISBN: 0813339960.
- [5] Toshiki Tajima. *Computational Plasma Physics: With Applications to Fusion and Astrophysics (Frontiers in Physics, Vol. 72)*. Redwood City, CA: Addison-Wesley, 1989. ISBN: 0201164116.
- [6] P. M. Bellan. *Fundamentals of Plasma Physics*. Cambridge, UK: Cambridge University Press, 2006. ISBN: 978-0-521-52800-9. DOI: 10.1017/cbo9780511807183.
- [7] Micheal D. Smith. *Astrophysical Jets and Beams*. Cambridge, UK: Cambridge University Press, 2012.
- [8] C. Goddi, G. Surcis, L. Moscadelli, H. Imai, W. H. T. Vlemmings, H. J. van Langevelde, and A. Sanna. “Measuring magnetic fields from water masers in the synchrotron protostellar jet in W3(H₂O)”. In: *Astronomy & Astrophysics* 597 (2016), A43. DOI: 10.1051/0004-6361/201629321.
- [9] G. R. Gupta, Durgesh Tripathi, and Helen E. Mason. “Spectroscopic observations of a coronal loop: basic physical plasma parameters along the full loop length”. In: *The Astrophysical Journal* 800.2 (2015), p. 140. DOI: 10.1088/0004-637x/800/2/140.

- [10] C. Carrasco-Gonzalez, L. F. Rodriguez, G. Anglada, J. Marti, J. M. Torrelles, and M. Osorio. “A Magnetized Jet from a Massive Protostar”. In: *Science* 330.6008 (2010), pp. 1209–1212. DOI: 10.1126/science.1195589.
- [11] J.-F. Donati, I. D. Howarth, M. M. Jardine, P. Petit, C. Catala, J. D. Landstreet, J.-C. Bouret, E. Alecian, J. R. Barnes, T. Forveille, F. Paletou, and N. Manset. “The surprising magnetic topology of Sco: fossil remnant or dynamo output?” In: *Monthly Notices of the Royal Astronomical Society* 370.2 (2006), pp. 629–644. DOI: 10.1111/j.1365-2966.2006.10558.x.
- [12] D. Coffey, F. Bacciotti, J. Woitas, T.P. Ray, and J. EislÄuffel. “Rotation of Jets From T-Tauri Stars: New Clues From HST/STIS Observations”. In: *Astrophysics and Space Science* 292.1-4 (2004), pp. 553–558. DOI: 10.1023/b:astr.0000045062.71787.34.
- [13] Avery E. Broderick and Abraham Loeb. “Signatures of relativistic helical motion in the rotation measures of active galactic nucleus jets”. In: *The Astrophysical Journal* 703.2 (2009), pp. L104–L108. DOI: 10.1088/0004-637x/703/2/1104.
- [14] John Bally, Steve Heathcote, Bo Reipurth, Jon Morse, Patrick Hartigan, and Richard Schwartz. “Hubble Space Telescope Observations of Proper Motions in Herbig-Haro Objects 1 and 2”. In: *The Astronomical Journal* 123.5 (2002), pp. 2627–2657. DOI: 10.1086/339837.
- [15] U. Shumlak and C. Hartman. “Sheared Flow Stabilization of the $m=1$ Kink Mode in Z Pinches”. In: *Phys. Rev. Lett.* 75.18 (1995), pp. 3285–3288. DOI: 10.1103/PhysRevLett.75.3285.
- [16] Eric Sander Lavine and Setthivoine You. “The topology of canonical flux tubes in flared jet geometry”. In: *The Astrophysical Journal* 835.1 (2017), p. 89. DOI: 10.3847/1538-4357/835/1/89.

- [17] E. Priest. *Magnetohydrodynamics of the Sun*. Cambridge. UK: Cambridge University Press, 2014. ISBN: 9780521854719.
- [18] M. R. Brown, P.K. Browning, M. E. Dieckmann, I. Furno, and T. P. Intrator. “Microphysics of Cosmic Plasmas: Hierarchies of Plasma Instabilities from MHD to Kinetic”. In: *Space Sci Rev* 178.2-4 (2013), pp. 357–383. DOI: 10.1007/s11214-013-0005-7.
- [19] M. Yamada, R. Kulsrud, and H. Ji. “Magnetic reconnection”. In: *Reviews of Modern Physics* 82.1 (2010), pp. 603–664. DOI: 10.1103/revmodphys.82.603.
- [20] Ellen G. Zweibel and Masaaki Yamada. “Magnetic Reconnection in Astrophysical and Laboratory Plasmas”. In: *Annual Review of Astronomy and Astrophysics* 47.1 (2009), pp. 291–332. DOI: 10.1146/annurev-astro-082708-101726.
- [21] P. M. Bellan. “Why current-carrying magnetic flux tubes gobble up plasma and become thin as a result”. In: *Phys. Plasmas* 10.5 (2003), pp. 1999–1999. DOI: 10.1063/1.1558275.
- [22] S. You, G. Yun, and P. Bellan. “Dynamic and Stagnating Plasma Flow Leading to Magnetic-Flux-Tube Collimation”. In: *Phys. Rev. Lett.* 95.4 (2005), pp. 2–5. DOI: 10.1103/PhysRevLett.95.045002.
- [23] Auna L. Moser and Paul M. Bellan. “Magnetic reconnection from a multiscale instability cascade”. In: *Nat.* 482.7385 (2012), pp. 379–381. ISSN: 0028-0836, 1476-4687. DOI: 10.1038/nature10827.
- [24] P. M. Bellan. *Spheromaks A practical application of magnetohydrodynamic dynamos and plasma self-organization*. 1st ed. London, UK: Imperial College Press, 2000. ISBN: 1-86094-141-9.
- [25] J. B. O’Bryan and C. R. Sovinec. “Simulated flux-rope evolution during non-inductive startup in Pegasus”. In: *Plasma Phys. Controll. Fusion* 56.6 (2014), pp. 064005–064005. DOI: 10.1088/0741-3335/56/6/064005.

- [26] S. You. “A field theory approach to the evolution of canonical helicity and energy”. In: *Physics of Plasmas* 23.7 (2016), p. 072108. DOI: 10.1063/1.4956465.
- [27] ESA/Hubble & NASA Acknowledgement: Judy Schmidt. *The Twin Jet Nebula*. 2015.
- [28] E Kawamori, Y Murata, K Umeda, D Hirota, T Ogawa, T Sumikawa, T Iwama, K Ishii, T Kado, T Itagaki, M Katsurai, A Balandin, and Y Ono. “Ion kinetic effect on bifurcated relaxation to a field-reversed configuration in TS-4 CT experiment”. In: *Nucl. Fusion* 45.8 (2005), pp. 843–848. DOI: 10.1088/0029-5515/45/8/010.
- [29] Clayton E. Myers, Masaaki Yamada, Hantao Ji, Jongsoo Yoo, William Fox, Jonathan Jara-Almonte, Antonia Savcheva, and Edward E. DeLuca. “A dynamic magnetic tension force as the cause of failed solar eruptions”. In: *Nature* 528.7583 (2015), pp. 526–529. DOI: 10.1038/nature16188.
- [30] J. F. Hansen, S. K. P. Tripathi, and P. M. Bellan. “Co- and counter-helicity interaction between two adjacent laboratory prominences”. In: *Physics of Plasmas* 11.6 (2004), pp. 3177–3185. DOI: 10.1063/1.1724831.
- [31] Michael R. Brown. “Experimental evidence of rapid relaxation to large-scale structures in turbulent fluids: selective decay and maximal entropy”. In: *Journal of Plasma Physics* 57.1 (1997), pp. 203–229. DOI: 10.1017/S0022377896005211.
- [32] T R Jarboe. “Review of spheromak research”. In: *Plasma Physics and Controlled Fusion* 36.6 (1994), pp. 945–990. DOI: 10.1088/0741-3335/36/6/002.
- [33] J.S. Sarff, A.F. Almagri, J.K. Anderson, M. Borchardt, W. Cappechi, D. Carmody, K. Caspary, B.E. Chapman, D.J. Den Hartog, J. Duff, S. Eilerman, A. Falkowski, C.B. Forest, M. Galante, J.A. Goetz, D.J. Holly, J. Koliner, S. Kumar, J.D. Lee, D. Liu, K.J. McCollam, M. McGarry, V.V. Mirnov, L. Morton, S. Munaretto, M.D. Nornberg, P.D. Nonn, S.P. Oliva, E. Parke, M.J. Pueschel, J.A. Reusch, J. Sauppe, A. Seltzman, C.R. Sovinec, D. Stone, D. Theucks, M. Thomas, J. Triana, P.W. Terry, J. Waksman, G.C. Whelan, D.L. Brower, W.X. Ding, L. Lin, D.R. Demers, P. Fimognari, J. Titus, F. Auriemma, S.

- Cappello, P. Franz, P. Innocente, R. Lorenzini, E. Martines, B. Momo, P. Piovesan, M. Puiatti, M. Spolaore, D. Terranova, P. Zanca, V.I. Davydenko, P. Deichuli, A.A. Ivanov, S. Polosatkin, N.V. Stupishin, D. Spong, D. Craig, H. Stephens, R.W. Harvey, M. Cianciosa, J.D. Hanson, B.N. Breizman, M. Li, and L.J. Zheng. “Overview of results from the MST reversed field pinch experiment”. In: *Nuclear Fusion* 55.10 (2015), p. 104006. DOI: 10.1088/0029-5515/55/10/104006.
- [34] H. Ji, S. C. Prager, and J. S. Sarff. “Conservation of Magnetic Helicity during Plasma Relaxation”. In: *Phys. Rev. Lett.* 74.15 (1995), pp. 2945–2948. DOI: 10.1103/PhysRevLett.74.2945.
- [35] Loren C Steinhauer, Hideaki Yamada, and Akio Ishida. “Two-fluid flowing equilibria of compact plasmas”. In: *Physics of Plasmas* 8.9 (2001), pp. 4053–4061. DOI: 10.1063/1.1388034.
- [36] Mayuko Tsuruda, Yasushi Ono, and Makoto Katsurai. “Comparative experiments of co- and counter-helicity merging in the compact toroid merging device TS-4”. In: *Electrical Engineering in Japan* 145.4 (2003), pp. 1–11. DOI: 10.1002/eej.10207.
- [37] Y. Ono, M. Yamada, T. Akao, T. Tajima, and R. Matsumoto. “Ion Acceleration and Direct Ion Heating in Three-Component Magnetic Reconnection”. In: *Physical Review Letters* 76.18 (1996), pp. 3328–3331. DOI: 10.1103/physrevlett.76.3328.
- [38] P. M. Bellan. “Collisionless reconnection using Alfvén wave radiation resistance”. In: *Physics of Plasmas* 5.9 (1998), pp. 3081–3088. DOI: 10.1063/1.873034.
- [39] S. You. “The transport of relative canonical helicity”. In: *Phys. Plasmas* 19.9 (2012), p. 092107. DOI: 10.1063/1.4752215.
- [40] U. Shumlak, B. A. Nelson, R. P. Golingo, S. L. Jackson, E. A. Crawford, and D. J. Den Hartog. “Sheared flow stabilization experiments in the ZaP flow Z pinch”. In: *Phys. Plasmas* 10.5 (2003), pp. 1683–1683. DOI: 10.1063/1.1558294.

- [41] Jens von der Linden and Setthivoine You. “Sausage instabilities on top of kinking lengthening current-carrying magnetic flux tubes”. In: *Physics of Plasmas* 24.5 (2017), p. 052105. DOI: 10.1063/1.4981231.
- [42] Jens von der Linden and Setthivoine You. *Sausage Instabilities on Top of Kinking Lengthening Current-Carrying Magnetic Flux Tubes - Code used for analysis and to generate figures 1-4*. 2017. DOI: 10.5281/zenodo.230489.
- [43] Jens von der Linden and Setthivoine You. *Sausage Instabilities on Top of Kinking Lengthening Current-Carrying Magnetic Flux Tubes - Data underlying figures 3 & 4*. 2017. DOI: 10.5281/zenodo.230611.
- [44] Margarita Ryutova. *Physics of Magnetic Flux Tubes*. Berlin Heidelberg, Germany: Springer, 2015. DOI: 10.1007/978-3-662-45243-1.
- [45] J. Freidberg. *Ideal MHD*. Cambridge, UK: Cambridge University Press, 2014.
- [46] M. Kruskal and J. L. Tuck. “The Instability of a Pinched Fluid with a Longitudinal Magnetic Field”. In: *Proc. R. Soc. A* 245.1241 (1958), pp. 222–237. DOI: 10.1098/rspa.1958.0079.
- [47] William A Newcomb. “Hydromagnetic stability of a diffuse linear pinch”. In: *Ann. Phys.* 10.2 (1960), pp. 232–267. ISSN: 0003-4916. DOI: 10.1016/0003-4916(60)90023-3.
- [48] I. B. Bernstein, E. A. Frieman, M. D. Kruskal, and R. M. Kulsrud. “An Energy Principle for Hydromagnetic Stability Problems”. In: *Proc. R. Soc. A* 244.1236 (1958), pp. 17–40. DOI: 10.1098/rspa.1958.0023.
- [49] G. Benford. “The electrodynamic ‘snake’ at the Galactic Centre”. In: *Mon. Not. R. Astron. Soc.* 285.3 (1997), pp. 573–579. DOI: 10.1093/mnras/285.3.573.
- [50] S. Hsu and P. Bellan. “Experimental Identification of the Kink Instability as a Poloidal Flux Amplification Mechanism for Coaxial Gun Spheromak Formation”. In: *Phys. Rev. Lett.* 90.21 (2003), pp. 1–4. DOI: 10.1103/PhysRevLett.90.215002.

- [51] B. I. Cohen, C. A. Romero-Talamá, D. D. Ryutov, E. B. Hooper, L. L. LoDestro, H. S. McLean, T. L. Stewart, and R. D. Wood. “The role of the $n_\phi=1$ column mode in spheromak formation”. In: *Phys. Plasmas* 16.4 (2009), pp. 042501–042501. DOI: 10.1063/1.3097909.
- [52] Philippa Browning and Alex Lazarian. “Notes on Magnetohydrodynamics of Magnetic Reconnection in Turbulent Media”. In: *Space Sci. Rev.* 178.2-4 (2013), pp. 325–355. ISSN: 0038-6308, 1572-9672. DOI: 10.1007/s11214-013-0022-6.
- [53] G. S. Yun, H. K. Park, W. Lee, M. J. Choi, G. H. Choe, S. Park, Y. S. Bae, K. D. Lee, S. W. Yoon, Y. M. Jeon, C. W. Domier, N. C. Luhmann, B. Tobias, A. J. H. Donnelly, and KSTAR Team. “Appearance and Dynamics of Helical Flux Tubes under Electron Cyclotron Resonance Heating in the Core of KSTAR Plasmas”. In: *Phys. Rev. Lett.* 109.14 (2012), p. 145003. DOI: 10.1103/PhysRevLett.109.145003.
- [54] D. D. Ryutov, R. H. Cohen, and L. D. Pearlstein. “Stability of a finite-length screw pinch revisited”. In: *Phys. Plasmas* 11.10 (2004), pp. 4740–4740. DOI: 10.1063/1.1781624.
- [55] I. Furno, T. P. Intrator, G. Lapenta, L. Dorf, S. Abbate, and D. D. Ryutov. “Effects of boundary conditions and flow on the kink instability in a cylindrical plasma column”. In: *Phys. Plasmas* 14.2 (2007), pp. 022103–022103. DOI: 10.1063/1.2435306.
- [56] Bergen Suydam. “Stability of a Linear Pinch”. In: *Proc. Second U. N. Internatl. Conf. Peac. Use Atomic Energy*. Geneva, 1958.
- [57] Paul M Bellan. *Fundamentals of Plasma Physics*. Cambridge, UK: Cambridge University Press, 2008. ISBN: 978-0-521-52800-9.
- [58] R J Tayler. “The Influence of an Axial Magnetic Field on the Stability of a Constricted Gas Discharge”. In: *Proceedings of the Physical Society. Section B* 70.11 (1957), pp. 1049–1063. DOI: 10.1088/0370-1301/70/11/305.
- [59] Travis E. Oliphant. “Python for Scientific Computing”. In: *Comput. Sci. Eng.* 9.3 (2007), pp. 10–20. ISSN: 1521-9615. DOI: 10.1109/MCSE.2007.58.

- [60] J. P. Goedbloed and S. Poedts. *Principles of Magnetohydrodynamics: With Applications to Laboratory and Astrophysical Plasmas*. Cambridge, UK: Cambridge University Press, 2004.
- [61] A. K. Srivastava, R. Erdélyi, Durgesh Tripathi, V. Fedun, N. C. Joshi, and P. Kayshap. “Observational Evidence of Sausage-Pinch Instability in Solar Corona By SDO/AIA”. In: *Astrophys. J.* 765.2 (2013), pp. L42–L42. DOI: 10.1088/2041-8205/765/2/L42.
- [62] L. M. Zelenyi, H. V. Malova, A. V. Artemyev, V. Yu Popov, and A. A. Petrukovich. “Thin current sheets in collisionless plasma: Equilibrium structure, plasma instabilities, and particle acceleration”. In: *Plasma Phys. Rep.* 37.2 (2011), pp. 118–160. ISSN: 1063-780X. DOI: 10.1134/S1063780X1102005X.
- [63] M. R. Weis, P. Zhang, Y. Y. Lau, P. F. Schmit, K. J. Peterson, M. Hess, and R. M. Gilgenbach. “Coupling of sausage, kink, and magneto-Rayleigh-Taylor instabilities in a cylindrical liner”. In: *Phys. Plasmas* 22.3 (2015), p. 032706. ISSN: 1070-664X, 1089-7674. DOI: 10.1063/1.4915520.
- [64] Oscar A. Anderson, William R. Baker, Stirling A. Colgate, John Ise, and Robert V. Pyle. “Neutron Production in Linear Deuterium Pinches”. In: *Phys. Rev.* 110.6 (1958), pp. 1375–1387. DOI: 10.1103/physrev.110.1375.
- [65] J. Sears, Y. Feng, T. P. Intrator, T. E. Weber, and H. O. Swan. “Flux rope dynamics in three dimensions”. In: *Plasma Phys. Control. Fusion* 56.9 (2014), p. 095022. ISSN: 0741-3335. DOI: 10.1088/0741-3335/56/9/095022.
- [66] B. Dattner, B. Lehnert, and S. Lundquist. “Liquid Conductor Model of Instabilities in a Pinched Discharge”. In: *Proc. Second U. N. Internatl. Conf. Peac. Use Atomic Energy*. Geneva, 1958.
- [67] W. Bergerson, C. Forest, G. Fiksel, D. Hannum, R. Kendrick, J. Sarff, and S. Stambler. “Onset and Saturation of the Kink Instability in a Current-Carrying Line-Tied Plasma”.

- In: *Phys. Rev. Lett.* 96.1 (2006), pp. 015004–015004. DOI: 10.1103/PhysRevLett.96.015004.
- [68] A. Schmidt, V. Tang, and D. Welch. “Fully Kinetic Simulations of Dense Plasma Focus Z-Pinch Devices”. In: *Phys. Rev. Lett.* 109.20 (2012), p. 205003. DOI: 10.1103/physrevlett.109.205003.
- [69] Gherardo Valori, Etienne Pariat, Sergey Anfinogentov, Feng Chen, Manolis K. Georgoulis, Yang Guo, Yang Liu, Kostas Moraitis, Julia K. Thalmann, and Shangbin Yang. “Magnetic Helicity Estimations in Models and Observations of the Solar Magnetic Field. Part I: Finite Volume Methods”. In: *Space Science Reviews* 201.1-4 (2016), pp. 147–200. DOI: 10.1007/s11214-016-0299-3.
- [70] Y. Guo, M. D. Ding, X. Cheng, J. Zhao, and E. Pariat. “Twist accumulation and topology structure of a solar magnetic flux rope”. In: *The Astrophysical Journal* 779.2 (2013), p. 157. DOI: 10.1088/0004-637x/779/2/157.
- [71] E. Pariat, P. Démoulin, and M. A. Berger. “Photospheric flux density of magnetic helicity”. In: *Astronomy and Astrophysics* 439.3 (2005), pp. 1191–1203. DOI: 10.1051/0004-6361:20052663.
- [72] Jens von der Linden, Alexander Card, and Setthivoine You. *MochiControl: LabVIEW experiment control with MDSplus data storage*. 2017. DOI: 10.5281/zenodo.495643.
- [73] Alexander Card. *MochiModel: MDSplus tree for MochiLab & Mochi.Labjet*. 2017. DOI: 10.5281/zenodo.495631.
- [74] Jens von der Linden. *MochiFPGAcontrol: High-throughput FPGA code for NI-5752 digitizers*. 2017. DOI: 10.5281/zenodo.495787.
- [75] Evan Carroll. “Driving flows in laboratory astrophysical plasma jets : The Mochi.LabJet experiment”. MA thesis. University of Washington, 2016.

- [76] Vernon H Chaplin and Paul M Bellan. “Fast Ignitron Trigger Circuit Using Insulated Gate Bipolar Transistors”. In: *IEEE Transactions on Plasma Science* 41.4 (2013), pp. 975–979. DOI: 10.1109/TPS.2013.2249113.
- [77] J. A. Stillerman, T. W. Fredian, K.A. Klare, and G. Manduchi. “MDSplus data acquisition system”. In: *Review of Scientific Instruments* 68.1 (1997), pp. 939–942. DOI: 10.1063/1.1147719.
- [78] G. Manduchi, E. De Marchi, and A. Mandelli. “A new LabVIEW interface for MDSplus”. In: *Fusion Engineering and Design* 88.6-8 (2013), pp. 1196–1199. DOI: 10.1016/j.fusengdes.2012.12.013.
- [79] *8-Channel Variable-Gain Amplifier (VGA) With Octal High-Speed ADC*. AFE5801. Texas Instruments. 2010.
- [80] Stéfan van der Walt, S Chris Colbert, and Gael Varoquaux. “The NumPy Array: A Structure for Efficient Numerical Computation”. In: *Computing in Science & Engineering* 13.2 (2011), pp. 22–30. DOI: 10.1109/mcse.2011.37.
- [81] Samuel Harrold. *ccd-utexas/tsphot: Time series photometry using astropy*. <https://github.com/ccd-utexas/tsphot>. 2015.
- [82] Henry W. Ott. *Electromagnetic Compatibility Engineering*. John Wiley & Sons, Inc., 2009. DOI: 10.1002/9780470508510.
- [83] *NI LabVIEW High-Performance FPGA Developer’s Guide*. National Instruments. 2014.
- [84] Jens von der Linden. *Investigating the dynamics of canonical flux tubes - Code*. 2017. DOI: 10.5281/zenodo.581197.
- [85] I. Furno, T. Intrator, E. Torbert, C. Carey, M. D. Cash, J. K. Campbell, W. J. Fienup, C. A. Werley, G. A. Wurden, and G. Fiksel. “Reconnection scaling experiment: A new device for three-dimensional magnetic reconnection studies”. In: *Review of Scientific Instruments* 74.4 (2003), pp. 2324–2331. DOI: 10.1063/1.1544051.

- [86] T. Intrator, X. Sun, L. Dorf, I. Furno, and G. Lapenta. “A three dimensional probe positionera”. In: *Review of Scientific Instruments* 79.10 (2008), 10F129. ISSN: 0034-6748, 1089-7623. DOI: 10.1063/1.2956746.
- [87] C. A. Romero-Talamás, P. M. Bellan, and S. C. Hsu. “Multielement magnetic probe using commercial chip inductors”. In: *Review of Scientific Instruments* 75.8 (2004), pp. 2664–2667. DOI: 10.1063/1.1771483.
- [88] Auna L Moser. “Dynamics of magnetically driven plasma jets: An instability of an instability, gas cloud impacts, shocks, and other deformations”. PhD thesis. California Institute of Technology, 2012.
- [89] I. H. Hutchinson. *Principles of Plasma Diagnostics*. Cambridge University Press, 11, 2005. ISBN: 052167574X.
- [90] Kyu-Sun Chung. “Why Is the Mach Probe Formula Expressed as $R = J_{up}/J_{dn} = \exp[KM_\infty]$?” In: *Japanese Journal of Applied Physics* 45.10A (2006), pp. 7914–7916. ISSN: 0021-4922, 1347-4065. DOI: 10.1143/JJAP.45.7914.
- [91] X. Zhang, D. Dandurand, T. Gray, M. R. Brown, and V. S. Lukin. “Calibrated cylindrical Mach probe in a plasma wind tunnel”. In: *Review of Scientific Instruments* 82.3 (2011), p. 033510. ISSN: 0034-6748, 1089-7623. DOI: 10.1063/1.3559550.
- [92] Eric Eugene Lawrence. “Colliding Magnetic Flux Ropes and Quasi-Separatrix Layers in a Laboratory Plasma”. PhD thesis. University of California, Los Angeles, 2010.
- [93] Kyu-Sun Chung. “Mach probes”. In: *Plasma Sources Sci. Technol.* 21.6 (2012), p. 063001. ISSN: 0963-0252. DOI: 10.1088/0963-0252/21/6/063001.
- [94] I. Furno, C. Theiler, A. Fasoli, and B. Labit. “Three-Dimensional Imaging of a Radially Propagating Plasma Blob Using Conditional Sampling Techniques”. In: *IEEE Transactions on Plasma Science* 39.11 (2011), pp. 3018–3019. ISSN: 0093-3813. DOI: 10.1109/TPS.2011.2162254.

- [95] Eric Jones, Travis Oliphant, Pearu Peterson, et al. *SciPy: Open source scientific tools for Python*. 2001–.
- [96] C. Bradford Barber, David P. Dobkin, and Hannu Huhdanpaa. “The quickhull algorithm for convex hulls”. In: *ACM Transactions on Mathematical Software* 22.4 (1996), pp. 469–483. DOI: 10.1145/235815.235821.
- [97] Karl E. Taylor. “Summarizing multiple aspects of model performance in a single diagram”. In: *Journal of Geophysical Research: Atmospheres* 106.D7 (2001), pp. 7183–7192. DOI: 10.1029/2000jd900719.
- [98] Zhongfeng Xu, Zhaolu Hou, Ying Han, and Weidong Guo. “A diagram for evaluating multiple aspects of model performance in simulating vector fields”. In: *Geoscientific Model Development* 9.12 (2016), pp. 4365–4380. DOI: 10.5194/gmd-9-4365-2016.
- [99] William H. Press. *Numerical Recipes*. Cambridge University Press, 2007. ISBN: 0521880688.
- [100] Roger W. Hockney and J. W. Eastwood. *Computer Simulation Using Particles*. Taylor & Francis Ltd, 1, 1988. 540 pp. ISBN: 0852743920.
- [101] V. Fuka. “PoisFFT – A free parallel fast Poisson solver”. In: *Applied Mathematics and Computation* 267 (2015), pp. 356–364. DOI: 10.1016/j.amc.2015.03.011.
- [102] J. Makhoul. “A fast cosine transform in one and two dimensions”. In: *IEEE Transactions on Acoustics, Speech, and Signal Processing* 28.1 (1980), pp. 27–34. DOI: 10.1109/tassp.1980.1163351.
- [103] C. Richard DeVore. “Magnetic Helicity Generation by Solar Differential Rotation”. In: *The Astrophysical Journal* 539.2 (2000), pp. 944–953. DOI: 10.1086/309274.
- [104] M. A. Chilenski, M. Greenwald, Y. Marzouk, N. T. Howard, A. E. White, J. E. Rice, and J. R. Walk. “Improved profile fitting and quantification of uncertainty in experimental measurements of impurity transport coefficients using Gaussian process regression”. In: *Nucl. Fusion* 55.2 (2015), p. 023012. ISSN: 0029-5515. DOI: 10.1088/0029-5515/55/2/023012.

- [105] A. L. Restante, S. Markidis, G. Lapenta, and T. Intrator. “Geometrical investigation of the kinetic evolution of the magnetic field in a periodic flux rope”. In: *Physics of Plasmas* 20.8 (2013), p. 082501. DOI: 10.1063/1.4817167.
- [106] D.E. Smith, E.J. Powers, and G.S. Caldwell. “Fast-Fourier-Transform Spectral-Analysis Techniques as a Plasma Fluctuation Diagnostic Tool”. In: *IEEE Transactions on Plasma Science* 2.4 (1974), pp. 261–272. ISSN: 0093-3813. DOI: 10.1109/TPS.1974.4316849.
- [107] S. K. P. Tripathi, B. Van Compernelle, W. Gekelman, P. Pribyl, and W. Heidbrink. “Excitation of shear Alfvén waves by a spiraling ion beam in a large magnetoplasma”. In: *Physical Review E* 91.1 (2015). DOI: 10.1103/physreve.91.013109.
- [108] E. Pariat, G. Valori, P. Démoulin, and K. Dalmasse. “Testing magnetic helicity conservation in a solar-like active event”. In: *Astronomy & Astrophysics* 580 (2015), A128. DOI: 10.1051/0004-6361/201525811.
- [109] T. Dehaas. “Helicity Transformation under the Collision and Merging of Magnetic Flux Ropes”. In: *APS Meeting Abstracts*. 2016. DOI: 10.1103/BAPS.2016.DPP.DI2.1.
- [110] K. H. Burrell. “Effects of $E \times B$ velocity shear and magnetic shear on turbulence and transport in magnetic confinement devices”. In: *Physics of Plasmas (1994-present)* 4.5 (1997), pp. 1499–1518. ISSN: 1070-664X, 1089-7674. DOI: 10.1063/1.872367.
- [111] R. Raman, T. R. Jarboe, B. A. Nelson, V. A. Izzo, R. G. O’Neill, A. J. Redd, and R. J. Smith. “Demonstration of Plasma Startup by Coaxial Helicity Injection”. In: *Physical Review Letters* 90.7 (2003). DOI: 10.1103/physrevlett.90.075005.
- [112] B. S. Victor, T. R. Jarboe, A. C. Hossack, D. a. Ennis, B. A. Nelson, R. J. Smith, C. Akcay, C. J. Hansen, G. J. Marklin, N. K. Hicks, and J. S. Wrobel. “Evidence for Separatrix Formation and Sustainment with Steady Inductive Helicity Injection”. In: *Physical Review Letters* 107.16 (2011), pp. 165005–165005. DOI: 10.1103/PhysRevLett.107.165005.

- [113] H. Ji, A. Bhattacharjee, S. Prager, W. Daughton, S. Bale, T. Carter, N. Crocker, J. Drake, J. Egedal, J. Sarff, J. Wallace, Y. Chen, R. Cutler, W. Fox, P. Heitzenroeder, M. Kalish, J. Jara-Almonte, C. Myers, Y. Ren, M. Yamada, and J. Yoo. “Status and Plans for the FLARE (Facility for Laboratory Reconnection Experiments) Project”. In: *APS Meeting Abstracts*. 2015.
- [114] W. Gekelman, E. Lawrence, A. Collette, S. Vincena, B. Van Compernelle, P. Pribyl, M. Berger, and J. Campbell. “Magnetic field line reconnection in the current systems of flux ropes and Alfvén waves”. In: *Phys. Scr.* 2010.T142 (2010), p. 014032. ISSN: 1402-4896. DOI: 10.1088/0031-8949/2010/T142/014032.
- [115] T. Dehaas, W. Gekelman, and B. van Compernelle. “Characteristic Dynamics of a Non-Linear Flux Rope”. In: *APS Meeting Abstracts*. 2015.
- [116] J. P. Sauppe and C. R. Sovinec. “Two-fluid and finite Larmor radius effects on helicity evolution in a plasma pinch”. In: *Physics of Plasmas* 23.3 (2016), p. 032303. DOI: 10.1063/1.4942761.
- [117] I. V. Khalzov, F. Ebrahimi, D. D. Schnack, and V. V. Mirnov. “Minimum energy states of the cylindrical plasma pinch in single-fluid and Hall magnetohydrodynamics”. In: *Physics of Plasmas* 19.1 (2012), pp. 012111–012111. DOI: 10.1063/1.3676600.

Appendix A

FLUXTUBE STABILITY CODE

This appendix contains the source code used in the analysis and to generate figs. 3.3, 3.4, 3.5, and 3.6 and instructions for setting up and running the code. The source code can also be found at Zenodo

<https://doi.org/10.5281/zenodo.230489> [42].

A.1 Dependencies

- python 2.7.12
- numpy 1.11.2
- numba 0.30.0
- scipy 0.18.1
- matplotlib 1.5.3
- seaborn 0.7.1
- sqlite 3.13
- gitpython 2.1.0

The dependencies can be installed with the anaconda python distribution. `gitpython` can be installed with `pip`.

A.2 Setup

Create three directories `figures`, `output`, `source`. Git clone the repository or copy the files into `source`.

A.3 Important files

`recreate_paper_data.sh` recreates the data underlying figs. 3.5 and 3.6.

`skin_core_scanner.py` is a script file that runs a stability scan over $\bar{k} - \bar{\lambda}$ space for an equilibrium defined by a core skin current profile of a given core current to total current ratio ϵ . This file has a command line interface. Help can be accessed with `python skin_core_scanner.py -help`. `newcomb.py` determines the external stability of a single equilibrium (single pair of \bar{k} and $\bar{\lambda}$).

`paper_figures.py` recreates the figs. 3.3, 3.4, 3.5, and 3.6. This file has a command line interface. Help can be accessed with `python paper_figures.py -help`.

A.4 Run

Run the bash script `recreate_paper_data.sh`. This will create a SQL database in `output` called `output.db` that keeps track of all runs and input parameters of `skin_core_scanner.py` and run `skin_core_scanner.py` three times to do a stability scan for three values of ϵ . The output data is stored in dated directories in `output`. `output.db` can be opened, e.g., with the Firefox extension SQLite Manager and the run parameters can be inspected.

Generate paper figures with `python paper_figures ../output/[timestamp] ../output/[timestamp] ../output/[timestamp]`, where `[timestamp]` is the dated directory name. The order should be from oldest to newest date.

A.5 *newcomb.py* description

Examines the equilibrium. If the equilibrium has a singularity, the Frobenius method is used to determine a small solution at an radius r greater than the radius of the singularity. If the singularity is Suydam unstable no attempt is made to calculate external stability. If there is no Suydam instability a Frobenius power series solution close to $r = 0$ is chosen or if the integration does not start at $r = 0$ a given ξ is used as boundary condition. Only the last interval is integrated. ξ and ξ' are plugged into the potential energy equation to determine stability.

A.6 Source code

A.6.1 *init_database.py*

```

1  # -*- coding: utf-8 -*-
2  """
3  Created on Wed Dec 21 13:53:21 2016
4
5  @author: jensv
6
7  Create sql run database.
8  """
9
10 import sqlite3
11 import os
12
13 assert os.path.exists('../output'), ("../output does not exist."
14                                     "Please place repo next to"
15                                     "'output' directory")
16 assert not os.path.exists('../output/output.db'), ("database "
17                                                    "../output/output.db "
18                                                    "already exists.")
19 connection = sqlite3.connect('../output/output.db')
20 cursor = connection.cursor()
21 cursor.execute("CREATE TABLE Runs(datetime TEXT, "
22              "points_core INTEGER, "
23              "points_transition INTEGER, "
24              "points_skin INTEGER, "
25              "core_radius REAL, "
26              "transition_width REAL, "
27              "skin_width REAL, k_bar_start REAL, "
28              "k_bar_end REAL, k_bar_num INTEGER, "
29              "lambda_bar_start REAL, "
30              "lambda_bar_end REAL, "
31              "lambda_bar_num INTEGER, epsilon REAL, "
32              "git_commit TEXT, python_call TEXT)")

```

```

33 cursor.close()
34 connection.commit()
35 connection.close()

```

A.6.2 *skin_core_scanner.py*

```

1   -*- coding: utf-8 -*-
2  """
3  Created on Sun Feb 15 22:05:21 2015
4
5  @author: jensv
6
7  Script to scan  $k_{\text{bar}}$ - $\lambda_{\text{bar}}$  stability space of profile type.
8  """
9
10 import equil_solver as es
11 import newcomb as new
12 import numpy as np
13 from copy import deepcopy
14 from datetime import datetime
15 import os
16 import json
17 import sys
18 import call_provenance as cp
19 import sqlite3
20 import argparse
21
22
23 def scan_lambda_k_space(lambda_bar_space, k_bar_space,
24                        xi_factor=1., magnetic_potential_energy_ratio=1.,
25                        offset=1E-3, r_0=0., init_value=(0.0, 1.0),
26                        rtol=None, max_step=1E-2,
27                        nsteps=1000, method='lsoda', suppress_output=True,
28                        diagnose=False, stiff=False, use_jac=True,
29                        adapt_step_size=True, sing_search_points=1000,
30                        profile_type='default', no_git=False,
31                        **kwargs):
32     r"""
33     Scans space given by lambda_a_space and k_a_space for m=0, 1 stability and
34     saves several 2D numpy arrays (stability maps) to an npz file.
35     """
36     lambda_a_space = lambda_bar_space
37     k_a_space = k_bar_space
38     call_parameters = locals()
39     func_name = 'scan_lambda_k_space'
40
41     suydam_end_offset = offset
42
43     k_a_points = np.linspace(k_a_space[0], k_a_space[1], num=k_a_space[2])
44     lambda_a_points = np.linspace(lambda_a_space[0], lambda_a_space[1],
45                                  num=lambda_a_space[2])
46
47     lambda_a_mesh, k_a_mesh = np.meshgrid(lambda_a_points, k_a_points)
48

```



```

106         results = new.stability(params, offset, suydam_end_offset,
107                                 sing_search_points=sing_search_points,
108                                 suppress_output=suppress_output,
109                                 xi_given=init_value,
110                                 rtol=rtol, max_step=max_step,
111                                 nsteps=nsteps, method=method,
112                                 diagnose=diagnose, stiff=stiff,
113                                 use_jac=use_jac,
114                                 adapt_step_size=adapt_step_size)
115     stable_external = results[0]
116     stable_suydam = results[1]
117     delta_w = results[2]
118     xi = results[4]
119     xi_der = results[5]
120
121     delta = xi_der[-1] / xi[-1]
122
123     delta_map[m][j][i] = delta
124
125     if delta_w is not None:
126         stability_maps['d_w'][m][j][i] = delta_w
127         stability_maps['d_w_raw'][m][j][i] = delta_w
128     else:
129         stability_maps['d_w'][m][j][i] = np.nan
130         stability_maps['d_w_raw'][m][j][i] = np.nan
131
132     if not stable_external:
133         stability_maps['external'][m][j][i] = 0.
134     if stable_external and delta_w is None:
135         stability_maps['external'][m][j][i] = -1.
136     if not stable_suydam:
137         stability_maps['suydam'][m][j][i] = 0.
138
139     #normalize
140     for m in [-1, 0]:
141         stability_maps['d_w'][m] = (stability_maps['d_w'][m] /
142                                     np.nanmax(np.abs(stability_maps['d_w'][m])))
143
144     params_wo_splines.update({'lambda_a_space': lambda_a_space,
145                              'k_a_space': k_a_space,
146                              'sing_search_points': sing_search_points,
147                              'offset': offset,
148                              'suydam_end_offset': suydam_end_offset})
149     params_wo_splines.update(kwargs)
150
151     date = datetime.now().strftime('%Y-%m-%d-%H-%M')
152     if os.getcwd().endswith('ipython_notebooks'):
153         path = '../output/' + date
154         sql_db = '../output/output.db'
155     else:
156         path = './output/' + date
157         sql_db = './output/output.db'
158     os.mkdir(path)
159
160     track_provenance(sql_db, func_name, call_parameters, date, params,
161                    lambda_a_space, k_a_space, no_git)
162

```

```

163     params_wo_splines.pop('dr', None)
164     with open(path+'/params.txt', 'w') as params_file:
165         json.dump(params_wo_splines, params_file)
166     np.savez(path+'/meshes.npz', lambda_a_mesh=lambda_a_mesh,
167            k_a_mesh=k_a_mesh,
168            external_m_neg_1=stability_maps['external'][-1],
169            external_m_0=stability_maps['external'][0],
170            d_w_m_neg_1=stability_maps['d_w'][-1],
171            d_w_m_0=stability_maps['d_w'][0],
172            d_w_raw_m_neg_1=stability_maps['d_w_raw'][-1],
173            d_w_raw_m_0=stability_maps['d_w_raw'][0],
174            suydam_m_0=stability_maps['suydam'][0],
175            suydam_m_neg_1=stability_maps['suydam'][-1],
176            delta_m_0=delta_map[0],
177            delta_m_neg_1=delta_map[-1]
178         )
179
180     print('Saved in Directory:' + str(date))
181
182     return lambda_a_mesh, k_a_mesh, stability_maps
183
184 def track_provenance(sql_db, func_name, call_parameters, date, params,
185                    lambda_a_space, k_a_space, no_git):
186     r"""
187     Save parameters, call, and git commit to make results reproducible and allow
188     easy scanning.
189     """
190     call = func_name + '('
191     for key in call_parameters.keys():
192         call += key + '=' + str(call_parameters[key]) + ', '
193     call = call[:-2] + ')'
194     if no_git:
195         git_commit = None
196     else:
197         call, git_commit = cp.call_and_git_commit(call=call, call_path=os.getcwd())
198     assert os.path.exists(sql_db), ("Run database does not exist."
199                                     "Try running init_database.py")
200     connection = sqlite3.connect(sql_db)
201     cursor = connection.cursor()
202     cursor.execute("INSERT INTO Runs(datetime, points_core, points_transition"+
203                  ", points_skin, core_radius, transition_width, skin_width,"+
204                  "k_bar_start, k_bar_end, k_bar_num, lambda_bar_start, " +
205                  "lambda_bar_end, lambda_bar_num, epsilon, git_commit, " +
206                  "python_call) " +
207                  "VALUES(?, ?, ?, ?, ?, ?, ?, ?, ?, ?, ?, ?, ?, ?, ?"+
208                  ")", (
209         date,
210         params['points_core'],
211         params['points_transition'],
212         params['points_skin'],
213         params['core_radius'],
214         params['transition_width'],
215         params['skin_width'],
216         k_a_space[0],
217         k_a_space[1],
218         int(k_a_space[2]),
219         lambda_a_space[0],

```



```

277         default=False, action='store_true')
278     parser.add_argument('--stiff', help="flag to pass stiff flag to integrator",
279                        default=False, action='store_true')
280     parser.add_argument('--use_jac', help="flag to use Jacobian"
281                        "with integrator",
282                        action="store_true")
283     parser.add_argument('--adapt_step_size',
284                        help="flag to adapt the stepsize requirements"
285                        "for the integrator to the fluxtube region",
286                        action="store_true")
287     parser.add_argument('--sing_search_points',
288                        help="number of points to divide fluxtube radius by in"
289                        "search for singularities",
290                        type=int, default=1000)
291
292     args = parser.parse_args()
293     args.k_bar_space[2] = int(args.k_bar_space[2])
294     args.lambda_bar_space[2] = int(args.lambda_bar_space[2])
295     return args
296
297 def main(args):
298     r"""
299     Run skin_core_scanner from command line call.
300     """
301     scan_lambda_k_space(**vars(args))
302
303 if __name__ == "__main__":
304     args = parse_args()
305     main(args)

```

A.6.3 *paper_figures.py*

```

1  import numpy as np
2  from scipy.special import kv, kvp
3
4  import matplotlib.pyplot as plt
5  from matplotlib import colors
6  import seaborn as sns
7  sns.set_style('ticks')
8  sns.set_context('paper')
9
10 import argparse
11 import os
12 import lambda_k_plotting as plot
13 reload(plot)
14 import analytic_condition as ac
15 from analytic_condition import conditions
16 import equil_solver as es
17
18
19 """parser = argparse.ArgumentParser(description='make paper plots')
20 parser.add_argument('high_epsilon_path',
21                    help="path of high epsilon profile stability results")
22 parser.add_argument('mid_epsilon_path',

```

```

23             help="path of mid epsilon profile stability results")
24 parser.add_argument('low_epsilon_path',
25                     help="path of low epsilon profile stability results")
26 args = parser.parse_args()
27 high_epsilon_path = os.path.join(args.high_epsilon_path,
28                                 'meshes.npz')
29 mid_epsilon_path = os.path.join(args.mid_epsilon_path,
30                                 'meshes.npz')
31 low_epsilon_path = os.path.join(args.low_epsilon_path,
32                                 'meshes.npz')
33 ""
34
35 ## Figure 1 ##
36 #####
37
38 fig, axes = plt.subplots(2, 2,
39                          figsize=(6.69, 6.69),
40                          sharex=False,
41                          sharey=False)
42
43 example_ax = axes[0][0]
44 kink_ax = axes[0][1]
45 sausage_ax = axes[1][0]
46 delta_ax = axes[1][1]
47
48 ## Example Plot ##
49 #####
50
51 lambda_bar = np.linspace(0, 4.25, 500)
52 k_bar = np.linspace(0, 1.5, 500)
53 mesh = np.meshgrid(lambda_bar, k_bar)
54 lambda_bar_mesh, k_bar_mesh = mesh[0], mesh[1]
55
56
57 d_w_sausage = conditions(k_bar_mesh,
58                          lambda_bar_mesh,
59                          epsilon=0.1,
60                          m=0,
61                          delta=0.1)
62 d_w_kink = conditions(k_bar_mesh,
63                       lambda_bar_mesh,
64                       epsilon=0.1,
65                       m=1,
66                       delta=0.1)
67
68 stability_sausage = d_w_sausage < 0
69 stability_kink = d_w_kink < 0
70 stability = stability_kink.astype(float)
71 stability[stability_sausage] = 2
72
73
74 cmap = colors.ListedColormap(['white',
75                               'lightgrey',
76                               'lightgrey'])
77
78 example_ax.contourf(lambda_bar_mesh, k_bar_mesh, stability, cmap=cmap,
79                    levels=[0., 0.5, 1.5, 2.], hatches=[None, '/', 'x'])

```

```

80 contour_lines = example_ax.contour(lambda_bar_mesh, k_bar_mesh, stability,
81                                   levels=[0., 1.5, 2.], colors='black', linewidths=2)
82
83 example_ax.clabel(contour_lines,
84                  manual=[[1.5, 1.1],
85                          [2.5, 0.75]],
86                  fmt={0.: 'Kink Boundary ', 1.5: 'Sausage Boundary '}, fontsize=10)
87
88 kruskal_shafranov = lambda_bar_mesh > 2 * k_bar_mesh
89
90 contour_lines = example_ax.contour(lambda_bar_mesh, k_bar_mesh, kruskal_shafranov,
91                                   levels=[0.5], colors='black', linewidths=2)
92 contour_lines.collections[0].set_linestyle('--')
93 example_ax.clabel(contour_lines,
94                  manual=[[1.8, 0.95]],
95                  fmt={0.5: 'Kruskal-Shafranov'}, fontsize=10)
96
97 #example_ax.plot([0, 3], [0., 1.5], '--', c='black', lw=5)
98
99 example_ax.set_xlabel(r'$\bar{\lambda}$')
100 #example_ax.xaxis.labelpad = 20
101 plt.setp(example_ax.get_xticklabels())
102 example_ax.set_xticks(np.arange(0., 5, 1.))
103
104 example_ax.set_ylabel(r'$\bar{k}$', rotation='horizontal')
105 plt.setp(example_ax.get_yticklabels())
106 example_ax.set_yticks(np.arange(0., 2.0, 0.5))
107
108 example_ax.plot(2*np.sqrt(2), 0.0, 'o', lw=2, color='black')
109 example_ax.annotate('Tayler', color='black',
110                   xy=(2*np.sqrt(2), 0),
111                   xytext=(2*np.sqrt(2) + 0.025, 0.25),
112                   rotation=45, fontsize=10)
113
114 sns.despine()
115
116 """
117 ## Kink Plot ##
118 #####
119
120 delta = 0.0
121 stability = np.zeros(lambda_bar_mesh.shape) - 0.2
122 for i, epsilon in enumerate(np.arange(0.1, 1.9, 0.3)):
123
124     d_w_kink = conditions(k_bar_mesh,
125                          lambda_bar_mesh,
126                          epsilon=epsilon,
127                          m=1,
128                          delta=delta)
129
130     stability_epsilon = d_w_kink < 0
131     stability[stability_epsilon] = epsilon
132
133 levels = np.arange(0.1, 1.9, 0.3)
134 contour = kink_ax.contourf(lambda_bar_mesh,
135                            k_bar_mesh,
136                            stability,

```

```

137             levels=levels)
138 contour.cmap.set_over(sns.xkcd_rgb['red brown'])
139 contour.cmap.set_under('white')
140 contour.set_clim(-0.1, 0.)
141 colors_list = ['grey', 'white', 'white', 'white', 'white']
142 contour_lines = kink_ax.contour(lambda_bar_mesh,
143                                k_bar_mesh,
144                                stability,
145                                levels=levels,
146                                colors=colors_list,
147                                linewidths=2)
148 kink_ax.clabel(contour_lines,
149               manual=[[1.6, 1.3],
150                      [2.1, 1.2],
151                      [2.3, 1.1],
152                      [2.4, 0.8],
153                      [2.4, 0.5]],
154               fmt=r'$ \epsilon = %.1f $', colors=colors_list,
155               fontsize=12)
156 for line in contour_lines.collections:
157     line.set_linestyle('solid')
158
159 line_x = np.linspace(0, 3, 50)
160 line_y = np.linspace(0, 1.5, 50)
161
162 line_y_masked = np.ma.masked_inside(line_y, 1.05, 1.18)
163
164 kink_ax.plot(line_x, line_y_masked, '--', c='black', lw=2)
165
166
167 kink_ax.plot([0, 3], [0., 1.5], '--', c='black', lw=2)
168 kink_ax.set_xlabel(r'$\bar{\lambda}$')
169 #kink_ax.xaxis.labelpad = 20
170 plt.setp(kink_ax.get_xticklabels())
171 kink_ax.set_xticks(np.arange(0., 5, 1.))
172
173 kink_ax.set_ylabel(r'$\bar{k}$', rotation='horizontal')
174 plt.setp(kink_ax.get_yticklabels())
175 kink_ax.set_yticks(np.arange(0., 2.0, 0.5))
176
177 sns.despine()
178
179 ## Sausage Plot ##
180 #####
181
182 delta = -0.7
183 stability = np.zeros(lambda_bar_mesh.shape) - 0.2
184 for i, epsilon in enumerate(np.arange(0, 1.2, 0.2)):
185
186     d_w_sausage = conditions(k_bar_mesh,
187                             lambda_bar_mesh,
188                             epsilon=epsilon,
189                             m=0,
190                             delta=delta)
191
192     stability_epsilon = d_w_sausage < 0
193     stability[stability_epsilon] = epsilon

```

```

194
195 levels = np.arange(0., 1.2, 0.2)
196 contour = sausage_ax.contourf(lambda_bar_mesh,
197                               k_bar_mesh,
198                               stability,
199                               levels=levels)
200 contour.cmap.set_over('darkgreen')
201 contour.cmap.set_under('white')
202 contour.set_clim(-0.2, -0.1)
203
204 colors_list = ['grey', 'white', 'white', 'white']
205
206 contour_lines = sausage_ax.contour(lambda_bar_mesh,
207                                   k_bar_mesh,
208                                   stability,
209                                   levels=levels,
210                                   colors=colors_list,
211                                   linewidths=2)
212 for line in contour_lines.collections:
213     line.set_linestyle('solid')
214
215
216 sausage_ax.clabel(contour_lines,
217                  manual=([2.3, 1.3],
218                          [1.75, 0.55],
219                          [2.0, 0.4],
220                          [2.1, 0.2]),
221                  fmt=r'$ \epsilon = %.1f$', fontsize=12)
222
223 sausage_ax.plot([0, 3.], [0., 1.5], '--', c='black', lw=2)
224 sausage_ax.set_xlabel(r'$\bar{\lambda}$')
225 #sausage_ax.xaxis.labelpad = 20
226 plt.setp(sausage_ax.get_xticklabels())
227 sausage_ax.set_xticks(np.arange(0., 5, 1.))
228
229 sausage_ax.set_ylabel(r'$\bar{k}$', rotation='horizontal')
230 plt.setp(sausage_ax.get_yticklabels())
231 sausage_ax.set_yticks(np.arange(0., 2.0, 0.5))
232 sns.despine()
233
234
235 ## Delta dependence ##
236 #####
237
238 epsilon = 0.2
239 stability = np.zeros(lambda_bar_mesh.shape) - 1.2
240 for i, delta in enumerate(np.arange(-1.0, 1.6, 0.5)):
241
242     d_w_delta = conditions(k_bar_mesh,
243                           lambda_bar_mesh,
244                           epsilon=epsilon,
245                           m=0,
246                           delta=delta)
247
248     stability_delta = d_w_delta < 0
249     stability[stability_delta] = delta
250

```



```

365             transition_width_norm=0.175,
366             skin_width_norm=0.05)
367
368 lgd = normalized_single_plot(profile, axes1, 1.8, 'a', legend_loc=[0.51, 1.8])
369
370 profile = es.UnITLESSSmoothedCoreSkin(k_bar=1, lambda_bar=1, epsilon=0.5,
371             core_radius_norm=0.6,
372             transition_width_norm=0.175,
373             skin_width_norm=0.05)
374
375 normalized_single_plot(profile, axes2, 1.8, 'b')
376
377 profile = es.UnITLESSSmoothedCoreSkin(k_bar=1, lambda_bar=1, epsilon=0.1,
378             core_radius_norm=0.6,
379             transition_width_norm=0.175,
380             skin_width_norm=0.05)
381
382 normalized_single_plot(profile, axes3, 1.8, 'c')
383 #axes1.legend(loc='best')
384 #axes2.legend(loc='best')
385 #axes3.legend(loc='best')
386 #plt.figlegend([l1, l2, l3],
387 #             [r'$\bar{k}_j$',
388 #             r'$\bar{B}_\theta$',
389 #             r'$\bar{p}$'], 'upper left',
390 #             bbox_to_anchor = (0.5, 0.5))
391
392 #plt.tight_layout()
393 plt.figtext(-0.0, 0.90, '(a)')
394 plt.figtext(-0.0, 0.60, '(b)')
395 plt.figtext(-0.0, 0.30, '(c)')
396 #plt.show()
397 fig.subplots_adjust(hspace=0.75)
398 sns.despine()
399 plt.savefig('../figures/figure2.eps', dpi=300,
400             bbox_extra_artists=(lgd,), bbox_inches='tight')
401
402 ## Fig 3 Numerical Stability Space ##
403 #####
404
405 from mpl_toolkits.axes_grid1 import make_axes_locatable
406
407 from matplotlib.colors import SymLogNorm, BoundaryNorm
408 from matplotlib.ticker import FormatStrFormatter, FixedFormatter
409 import matplotlib.patches as patches
410 import matplotlib.ticker as ticker
411
412 def plot_lambda_k_space_dw(axes, filename, epsilon, name, mode_to_plot='m_neg_1',
413             show_points=False, lim=None, levels=None, log=True,
414             linthresh=1E-7, bounds=(1.5, 3.0), norm=True,
415             analytic_compare=False,
416             label_pos=((0.5, 0.4), (2.1, 0.4), (2.8, 0.2)),
417             delta_values=[-1,0,1],
418             interpolate=False,
419             cmap=None, hatch=False,
420             figsize=None,
421             save_as=None,

```

```

422         return_ax=False,
423         hatch_sausage_gap=False):
424
425     epsilon_case = np.load(filename)
426     lambda_a_mesh = epsilon_case['lambda_a_mesh']
427     k_a_mesh = epsilon_case['k_a_mesh']
428     external_m_neg_1 = epsilon_case['d_w_m_neg_1']
429     external_sausage = epsilon_case['d_w_m_0']
430     epsilon_case.close()
431
432     if hatch_sausage_gap:
433         external_sausage_gap = np.where((lambda_a_mesh > 3.) & (external_sausage > 0))
434         external_sausage[external_sausage_gap] = np.nan
435
436     instability_map = {'m_0': external_sausage,
437                      'm_neg_1': external_m_neg_1}
438
439
440     kink_pal = sns.blend_palette([sns.xkcd_rgb["dandelion"],
441                                sns.xkcd_rgb["white"]], 7, as_cmap=True)
442     kink_pal = sns.diverging_palette(73, 182, s=72, l=85, sep=1, n=9, as_cmap=True)
443     sausage_pal = sns.blend_palette(['orange', 'white'], 7, as_cmap=True)
444     sausage_pal = sns.diverging_palette(49, 181, s=99, l=78, sep=1, n=9, as_cmap=True)
445
446     if cmap:
447         instability_palette = {'m_0': cmap,
448                               'm_neg_1': cmap}
449     else:
450         instability_palette = {'m_0': sausage_pal,
451                               'm_neg_1': kink_pal}
452
453
454
455
456     if interpolate:
457         instability_map['m_neg_1'] = interpolate_nans(lambda_a_mesh,
458                                                     k_a_mesh,
459                                                     instability_map['m_neg_1']
460                                                     )
461
462     values = instability_map[mode_to_plot]
463
464     if norm:
465         values = values / np.nanmax(np.abs(values))
466     else:
467         values = values
468
469     if levels:
470         if log:
471             plot = axes.contourf(lambda_a_mesh, k_a_mesh, values,
472                                cmap=instability_palette[mode_to_plot],
473                                levels=levels, norm=SymLogNorm(linthresh))
474             divider = make_axes_locatable(axes)
475             cax = divider.append_axes("right", size="5%", pad=0.1)
476             cbar = plt.colorbar(plot, cax=cax, label=r'$\delta W$')
477             cbar.ax.yaxis.set_ticks_position('right')
478             cbar.set_label(label=r'$\delta W$', size=10, rotation=0, labelpad=1)

```

```

479         contourlines = axes.contour(lambda_a_mesh, k_a_mesh,
480                                     values, levels=levels,
481                                     colors='grey',
482                                     norm=SymLogNorm(linthresh), linewidths=0.8)
483
484     else:
485         norm = BoundaryNorm(levels, 256)
486         plot = axes.contourf(lambda_a_mesh, k_a_mesh, values,
487                             cmap=instability_palette[mode_to_plot],
488                             levels=levels, norm=norm)
489         divider = make_axes_locatable(axes)
490         cax = divider.append_axes("right", size="5%", pad=0.1)
491         cbar = plt.colorbar(plot, cax=cax, label=r'$\delta W$')
492         cbar.set_label(label=r'$\delta W$', size=10, rotation=0, labelpad=1)
493         contourlines = axes.contour(lambda_a_mesh, k_a_mesh,
494                                     values, levels=levels,
495                                     colors='grey', linewidths=0.8)
496
497     if log:
498         plot = axes.contourf(lambda_a_mesh, k_a_mesh, values,
499                             cmap=instability_palette[mode_to_plot],
500                             norm=SymLogNorm(linthresh))
501         divider = make_axes_locatable(axes)
502         cax = divider.append_axes("right", size="5%", pad=0.1)
503         cbar = plt.colorbar(plot, cax=cax, label=r'$\delta W$')
504         cbar.set_label(label=r'$\delta W$', size=10, rotation=0, labelpad=1)
505         contourlines = axes.contour(lambda_a_mesh, k_a_mesh,
506                                     values, colors='grey',
507                                     norm=SymLogNorm(linthresh), linewidths=0.8)
508
509     else:
510         plot = plt.contourf(lambda_a_mesh, k_a_mesh, values,
511                             cmap=instability_palette[mode_to_plot])
512         divider = make_axes_locatable(axes)
513         cax = divider.append_axes("right", size="5%", pad=0.1)
514         cbar = plt.colorbar(plot, cax=cax, label=r'$\delta W$')
515         cbar.set_label(label=r'$\delta W$', size=10, rotation=0, labelpad=1)
516         contourlines = axes.contour(lambda_a_mesh, k_a_mesh,
517                                     values, colors='grey', linewidths=0.8)
518
519     if lim:
520         plot.set_clim(lim)
521
522     cbar.add_lines(contourlines)
523
524     cbar_lines = cbar.lines[0]
525     number_of_lines = len(cbar_lines.get_linewidths())
526
527     linewidths = []
528     linestyle = []
529     cbar_zero_line = 4
530     for line in xrange(number_of_lines):
531         if line < cbar_zero_line:
532             linewidths.append(0.8)
533             linestyle.append('--')
534         elif line == cbar_zero_line:
535             linewidths.append(0.8)
536             linestyle.append('--')

```

```

536         else:
537             linewidths.append(0.8)
538             linestyles.append('-')
539
540 cbar_lines.set_linewidths(linewidths)
541 cbar_lines.set_linestyles(linestyles)
542
543 axes.plot([0.01, 0.1, 1.0, 2.0, 3.0],
544           [0.005, 0.05, 0.5, 1.0, 1.5], color='black', lw=1.5)
545
546 axes.set_axis_bgcolor(sns.xkcd_rgb['white'])
547
548 lambda_bar_analytic = np.linspace(0.01, 4., 750)
549 k_bar_analytic = np.linspace(0.01, 1.5, 750)
550 (lambda_bar_mesh_analytic,
551  k_bar_mesh_analytic) = np.meshgrid(lambda_bar_analytic, k_bar_analytic)
552
553 if analytic_compare:
554     analytic_comparison(mode_to_plot, k_bar_mesh_analytic,
555                        lambda_bar_mesh_analytic, epsilon, label_pos)
556
557 if show_points:
558     axes.scatter(lambda_a_mesh, k_a_mesh, marker='o', c='b', s=2)
559
560 axes.set_ylim(0.01, bounds[0])
561 axes.set_xlim(0.01, bounds[1])
562 axes.set_xticks(np.arange(0., 4.5, 1.0))
563 axes.set_yticks(np.arange(0., 2.0, 0.5))
564 plt.setp(axes.get_xticklabels(), fontsize=10)
565 plt.setp(axes.get_yticklabels(), fontsize=10)
566 axes.set_ylabel(r'$\bar{k}$', rotation='horizontal', fontsize=10)
567 axes.set_xlabel(r'$\bar{\lambda}$', fontsize=10)
568 cbar.ax.tick_params(labelsize=8)
569
570 def my_formatter_fun(x):
571     if x == 0:
572         return r'$0$'
573     if np.sign(x) > 0:
574         return r'$10^{\%i}$' % np.int(np.log10(x))
575     else:
576         return r'$-10^{\%i}$' % np.int(np.log10(np.abs(x)))
577 labels = [my_formatter_fun(level) for level in levels]
578 cbar.ax.set_yticklabels(labels)
579 sns.despine(ax=axes)
580
581 if hatch:
582     xmin, xmax = axes.get_xlim()
583     ymin, ymax = axes.get_ylim()
584     xy = (xmin, ymin+0.1)
585     width = xmax - xmin
586     height = ymax - ymin
587     p = patches.Rectangle(xy, width, height, hatch='X'*2,
588                          zorder=-10, edgecolor='#FEFF00',
589                          facecolor='#6C2605')
590     axes.add_patch(p)
591 if hatch_sausage_gap:
592     xmin, xmax = axes.get_xlim()

```



```

650             hatch=True,
651             bounds=(1.5, 4.3))
652
653
654 plot_lambda_k_space_dw(sausage_ax2, mid_epsilon_path,
655                       1., 'ep12-m1', mode_to_plot='m_0',
656                       levels=[-1, -1e-1, -1e-2, -1e-3,
657                               0, 1e-3, 1e-2, 1e-1, 1],
658                       norm=True, analytic_compare=False,
659                       log=True,
660                       label_pos=None,
661                       interpolate=False, cmap="YlGn_r",
662                       hatch_sausage_gap=True,
663                       bounds=(1.5, 4.3))
664
665
666
667
668 ## Low epsilon
669 plot_lambda_k_space_dw(kink_ax3, low_epsilon_path,
670                       1., 'ep12-m1', mode_to_plot='m_neg_1',
671                       levels=[-1, -1e-1, -1e-2, -1e-3,
672                               0, 1e-3, 1e-2, 1e-1, 1],
673                       norm=True, analytic_compare=False,
674                       log=True,
675                       label_pos=None,
676                       interpolate=False, cmap="YlOrBr_r",
677                       bounds=(1.5, 4.3),
678                       hatch=True)
679
680 plot_lambda_k_space_dw(sausage_ax3, low_epsilon_path,
681                       1., 'ep12-m1', mode_to_plot='m_0',
682                       levels=[-1, -1e-1, -1e-2, -1e-3,
683                               0, 1e-3, 1e-2, 1e-1, 1],
684                       norm=True, analytic_compare=False,
685                       log=True,
686                       label_pos=None,
687                       bounds=(1.5, 4.3),
688                       interpolate=False, cmap="YlGn_r",
689                       hatch=True)
690
691
692
693 plt.tight_layout(pad=0.5, w_pad=0.1, h_pad=0.5)
694
695 plt.figtext(0.01, 0.98, '(a)', fontsize=10)
696 plt.figtext(0.01, 0.655, '(b)', fontsize=10)
697 plt.figtext(0.01, 0.33, '(c)', fontsize=10)
698 plt.figtext(0.49, 0.98, '(d)', fontsize=10)
699 plt.figtext(0.49, 0.655, '(e)', fontsize=10)
700 plt.figtext(0.49, 0.33, '(f)', fontsize=10)
701
702 plt.savefig('../figures/figure3.eps', dpi=300)
703
704 ### Ratio Plots ###
705 #####
706

```

```

707 def sausage_kink_ratio(axes, filename, xy_limits=None, cmap=None, save_as=None,
708                       levels=None, zero_line=2, label_lines=False, cbar_zero_line=2):
709     r"""
710     Plot ratio of sausage and kink potential energies.
711     """
712     meshes = np.load(filename)
713     lambda_bar_mesh = meshes['lambda_a_mesh']
714     k_bar_mesh = meshes['k_a_mesh']
715     external_m_neg_1 = meshes['d_w_m_neg_1']
716     external_sausage = meshes['d_w_m_0']
717     meshes.close()
718
719     sausage_stable_region = np.invert((external_sausage < 0))
720     ratio = np.abs(external_sausage / external_m_neg_1)
721     ratio[sausage_stable_region] = np.nan
722     ratio_log = np.log10(ratio)
723
724     if not cmap:
725         cmap = sns.light_palette(sns.xkcd_rgb['red orange'],
726                                as_cmap=True)
727
728     if levels:
729         contours = axes.contourf(lambda_bar_mesh, k_bar_mesh,
730                                ratio_log, cmap=cmap, levels=levels)
731     else:
732         contours = axes.contourf(lambda_bar_mesh, k_bar_mesh,
733                                ratio_log, cmap=cmap)
734
735     divider = make_axes_locatable(axes)
736     cax = divider.append_axes("right", size="5%", pad=0.1)
737     colorbar = plt.colorbar(contours, cax=cax, format=FormatStrFormatter(r'$10^{%i}$'))
738     colorbar.set_label(r'$\frac{\delta W_{m=0}}{\delta W_{m=1}}$', rotation=0,
739                      labelpad=10,
740                      fontsize=10)
741
742     if levels:
743         lines = axes.contour(lambda_bar_mesh, k_bar_mesh,
744                             ratio_log, colors='black', levels=levels, linewidths=1)
745     else:
746         lines = axes.contour(lambda_bar_mesh, k_bar_mesh,
747                             ratio_log, colors='black', linewidths=1)
748
749     plt.setp(lines.collections[zero_line], linewidth=2)
750     colorbar.add_lines(lines)
751
752     cbar_lines = colorbar.lines[0]
753     number_of_lines = len(cbar_lines.get_linewidths())
754
755     linewidths = []
756     linestyles = []
757     for line in xrange(number_of_lines):
758         if line < cbar_zero_line:
759             linewidths.append(1)
760             linestyles.append('--')
761         elif line == cbar_zero_line:
762             linewidths.append(2)
763             linestyles.append('-')
764         else:
765             linewidths.append(1)
766             linestyles.append('-')

```

```

764
765     cbar_lines.set_linewidths(linewidths)
766     cbar_lines.set_linestyles(linestyles)
767
768     axes.plot([0, 3.], [0., 1.5], '--', c='black', lw=2)
769     axes.set_xlabel(r'$\bar{\lambda}$', fontsize=10)
770     plt.setp(axes.get_xticklabels(), fontsize=10)
771     axes.set_xticks(np.arange(0., 4.5, 1.0))
772
773     axes.set_ylabel(r'$\bar{k}$', rotation='horizontal', fontsize=10)
774     plt.setp(axes.get_yticklabels(), fontsize=10)
775     axes.set_yticks(np.arange(0., 2.0, 0.5))
776
777     if label_lines:
778         plt.clabel(lines)
779
780     if xy_limits:
781         axes.set_ylim((xy_limits[0], xy_limits[1]))
782         axes.set_xlim((xy_limits[2], xy_limits[3]))
783     plt.setp(axes.get_xticklabels(), fontsize=10)
784     plt.setp(axes.get_yticklabels(), fontsize=10)
785     axes.set_xlim((0, 4.3))
786     sns.despine(ax=axes)
787     colorbar.ax.yaxis.set_ticks_position('right')
788     colorbar.ax.tick_params(labelsize=8)
789
790 fig = plt.figure(figsize=(3.75,6.69))
791
792 ratio_ax1 = plt.subplot2grid((9, 3), (0, 0), colspan=3, rowspan=3)
793 ratio_ax2 = plt.subplot2grid((9, 3), (3, 0), colspan=3, rowspan=3)
794 ratio_ax3 = plt.subplot2grid((9, 3), (6, 0), colspan=3, rowspan=3)
795
796 sausage_kink_ratio(ratio_ax1, high_epsilon_path,
797                    cmap="Greys",
798                    zero_line=2, label_lines=False,
799                    cbar_zero_line=2)
800
801 sausage_kink_ratio(ratio_ax2, mid_epsilon_path,
802                    cmap="Greys",
803                    zero_line=1, label_lines=False,
804                    cbar_zero_line=1)
805
806 sausage_kink_ratio(ratio_ax3, low_epsilon_path,
807                    cmap="Greys",
808                    levels=[-4, -2, 0, 2, 4, 6, 15],
809                    zero_line=2, label_lines=False,
810                    cbar_zero_line=2)
811 plt.tight_layout()
812
813 plt.figtext(0.05, 0.96, '(a)', fontsize=10)
814 plt.figtext(0.05, 0.64, '(b)', fontsize=10)
815 plt.figtext(0.05, 0.32, '(c)', fontsize=10)
816 plt.savefig('./figures/figure4.eps', dpi=300)
817
818 ## Critical Lambda Bar Plot ##
819 #####
820

```

```

821 def lambda_crit(s_star):
822     return 2.*s_star/np.sqrt(4. - s_star**2)
823
824 fig, axes = plt.subplots(figsize=(3.37,3.37))
825 s_star = np.linspace(0, 5, 200)
826 critical_value = np.zeros(s_star.size)
827 critical_value[s_star < 2] = lambda_crit(s_star[s_star < 2])
828 critical_value[s_star >= 2] = np.nan
829 axes.plot(s_star, critical_value, color='black', lw=2)
830 axes.set_xlabel(r'$S^{\ast}$')
831 axes.set_ylabel(r'$\bar{\lambda}_{crit}$')
832 axes.set_ylim(0, 5)
833 axes.axhline(2*np.sqrt(2), linestyle='--', color='black', lw=2)
834 rectangle = patches.Rectangle((-1, 2.25), 10, 10, hatch='/',
835                               facecolor='none', edgecolor='grey')
836 axes.add_patch(rectangle)
837 plt.tight_layout()
838 plt.savefig('../figures/figure5.eps', dpi=300)
839 """

```

A.6.4 call_provenance.py

```

1  # -*- coding: utf-8 -*-
2  """
3  Created on Sat Oct 24 13:01:44 2015
4
5  @author: jensv
6  """
7
8  from git import Repo
9  import os
10
11
12 def call_and_git_commit(call='', call_path=None):
13     """
14     Returns a program call and git HEAD commit hash of a git repo located in
15     the supplied call directory. If no directory is passed the current
16     directory is used.
17     """
18     if call_path is None:
19         call_path = os.getcwd()
20     repo = Repo(path=call_path, search_parent_directories=True)
21     commit = repo.commit('HEAD')
22     git_commit = commit.hexsha
23     return call, git_commit

```

A.6.5 equil_solver.py

```

1  # -*- coding: utf-8 -*-
2  """
3  Created on Fri May 23 10:19:28 2014

```

```

4
5 @author: Jens von der Linden
6
7 Create various profiles.
8 The analysis in the paper exclusively focuses on UnitlessSmoothedCoreSkin
9 profile.
10
11 ParabolicNu2, NuCurrentProfile recreate the profiles from Wesson's
12 Tokamak book. In the large aspect ratio limit  $k \rightarrow 0$  these should
13 allow to recreate his stability plots.
14 The HardCoreZPinch is discussed in Freidberg's Ideal MHD book.
15 """
16
17
18 from __future__ import print_function, unicode_literals, division
19 from __future__ import absolute_import
20 from future import standard_library, utils
21 from future.builtins import (ascii, bytes, chr, dict, filter, hex, input,
22                             int, map, next, oct, open, pow, range, round,
23                             str, super, zip)
24 """Python 3.x compatability"""
25
26 import sys
27 import numpy as np
28 from numpy import atleast_1d
29 from scipy.interpolate import splev
30 import sympy as sp
31 from collections import OrderedDict
32 import scipy.interpolate as interp
33 import scipy.integrate as inte
34
35
36 class EquilSolver(object):
37     r"""
38     General Equilibrium Solver parent implements spline generation and safety
39     factor calculation for various profiles.
40     """
41
42     def set_splines(self, param_points):
43         r"""
44         Returns Splines requested with a dictionary of spline names and point
45         generating functions.
46         """
47         splines = {}
48         r = self.r
49         for key, value in param_points.items():
50             splines[key] = interp.InterpolatedUnivariateSpline(r,
51                                                             value(self.r),
52                                                             k=3)
53         self.splines = splines
54
55     def get_splines(self):
56         r"""
57         Returns splines of instance.
58         """
59         return self.splines
60

```

```

61 def get_tckSplines(self):
62     r"""
63     Returns tck splines lists , to be used with scipy procedural spline
64     interface.
65     """
66     return self.tckSplines
67
68 def q(self, r):
69     r"""
70     Returns safety factor evaluated at points.
71     """
72     if r[0] == 0.:
73         q_to_return = np.ones(r.size)*self.q0
74         q_to_return[1:] = r[1:]*self.k*self.b_z(r[1:])/self.b_theta(r[1:])
75     else:
76         q_to_return = r*self.k*self.b_z(r)/self.b_theta(r)
77     return q_to_return
78
79 def rho(self, r):
80     r"""
81     Return density. Set to one evrywhere. Density plays no role for
82     Newcomb. However, the general eigenvalue problem has stability issues.
83     """
84     return np.ones(r.size)
85
86 def convert_spline_objects_to_tck(self, spline_dict):
87     r"""
88     Returns tck tuples for use with procedural scipy spline interface ,
89     which is slightly faster than the object-oriented interface.
90
91     Parameters
92     -----
93     spline_dict: dict
94         dict of splines
95
96     Returns
97     -----
98     splines_tck: dict
99         dict of tckSplines
100     """
101     tckSplines = {}
102     for key in spline_dict.keys():
103         tck = spline_dict[key]._eval_args
104         tckSplines.update({key: tck})
105     return tckSplines
106
107
108 class ParabolicNu2(EquilSolver):
109     r"""
110     Creates splines for parabolic current profile pinch.
111     """
112
113     def __init__(self, a=1, points=500, q0=1.0, k=1, b_z0=1, temp=1.0,
114                 qa=None, mu_0=1.):
115         r"""
116         Initalize parameters defining parabolic pinch and create splines .
117         """

```

```

118     self.r = np.linspace(0, a, points)
119     if qa is not None:
120         q0 = qa/3.
121     self.q0 = q0
122     self.mu_0 = mu_0
123     self.k = k
124     self.b_z0 = b_z0
125     self.temp = temp
126     self.j0 = self.get_j0()
127     param_points = {'j_z': self.j_z, 'b_theta': self.b_theta,
128                    'b_z': self.b_z, 'p_prime': self.p_prime,
129                    'pressure': self.pressure, 'q': self.q,
130                    'rho': self.rho}
131     self.set_splines(param_points)
132
133     def get_j0(self):
134         r"""
135         Return j0 for a b_z and q0 paramters of pinch.
136         """
137         self.j0 = 1
138         return self.k*2.*self.b_z(0)/(self.q0*self.mu_0)
139
140     def j_z(self, r):
141         r"""
142         Return parabolic axial current profile.
143         """
144         return self.j0*(1 - r**2)**2
145
146     def b_theta(self, r):
147         r"""
148         Return azimuthhal magnetic field for a parabolic current profile pinch.
149         """
150         j0 = self.j0
151         return self.mu_0*(j0*r/2 - j0*r**3/2. + j0*r**5/6.)
152
153     def b_z(self, r):
154         r"""
155         Return constant axial magnetic field.
156         """
157         b_z0 = self.b_z0
158         r = np.asarray(r)
159         return np.ones(r.size) * b_z0
160
161     def p_prime(self, r):
162         r"""
163         Returns pressure_prime profile for a arabolic current profile pinch.
164         """
165         j0 = self.j0
166         return self.mu_0*(-j0**2*r/2. + 3.*j0**2*r**3/2.
167                        - 5.*j0**2*r**5/3. + 5.*j0**2*r**7/6.
168                        - j0**2*r**9/6.)
169
170     def pressure(self, r):
171         r"""
172         Returns pressure profile for a arabolic current profile pinch.
173         """
174         j0 = self.j0

```

```

175         return self.mu_0*(47.*j0**2/720. - j0**2*r**2/4. + 3.*j0**2*r**4/8.
176             - 5.*j0**2*r**6/18. + 5.*j0**2*r**8/48.
177             - j0**2*r**10/60.)
178
179
180 class NuCurrentConstructor(object):
181     r"""
182     Constructors for arbitrary nu current profiles.
183     """
184     def __init__(self, a=1., nu=2):
185         j0, r, mu_0, k, b_z, q0, qa = sp.symbols('j_0 r mu_0 k b_z \
186             q_0 q_a')
187         current_sym = j0*(1 - r**2)**nu
188         b_theta_sym = mu_0*sp.integrate(current_sym*r, r, conds='none')/r
189         p_prime_sym = -current_sym*b_theta_sym
190         pressure_sym = sp.integrate(p_prime_sym, r, conds='none')
191         pressure_norm_sym = pressure_sym - pressure_sym.subs(r, a)
192         q_sym = sp.cancel(r*k*b_z/b_theta_sym)
193         q0_sym = q_sym.subs(r, 0)
194         qa_sym = q_sym.subs(r, a)
195         j0_defined_by_q0_sym = sp.solve(q0_sym - q0, j0)[0]
196         j0_defined_by_qa_sym = sp.solve(qa_sym - qa, j0)[0]
197
198         # create lambda functions of expressions
199         self.current_func = sp.lambdify((r, j0), current_sym,
200             modules=str('numpy'))
201         self.b_theta_func = sp.lambdify((r, j0, mu_0), sp.cancel(b_theta_sym),
202             modules=str('numpy'))
203         self.p_prime_func = sp.lambdify((r, j0, mu_0), sp.cancel(p_prime_sym),
204             modules=str('numpy'))
205         self.pressure_func = sp.lambdify((r, j0, mu_0), pressure_norm_sym,
206             modules=str('numpy'))
207         self.q_func = sp.lambdify((r, k, b_z, j0, mu_0), q_sym,
208             modules=str('numpy'))
209         self.j0_defined_by_q0_func = sp.lambdify((k, b_z, mu_0, q0),
210             j0_defined_by_q0_sym,
211             modules=str('numpy'))
212         self.j0_defined_by_qa_func = sp.lambdify((k, b_z, mu_0, qa),
213             j0_defined_by_qa_sym,
214             modules=str('numpy'))
215
216
217 class NuCurrentProfile(EquilSolver):
218     r"""
219     Nu current profiles as described in Wesson's Tokamak book under
220     large aspect ratio tokamak limit.
221     """
222
223     def __init__(self, nu_constructor=NuCurrentConstructor(), nu=2, a=1,
224         points=500, q0=1.0, k=1., b_z0=1., temp=1.0, qa=None, mu_0=1.):
225         r"""
226
227         """
228
229         self.get_j_z = nu_constructor.current_func
230         self.get_b_theta = nu_constructor.b_theta_func
231         self.get_p_prime = nu_constructor.p_prime_func

```

```

232     self.get_pressure = nu_constructor.pressure_func
233     self.get_q = nu_constructor.q_func
234     self.get_j0_given_q0 = nu_constructor.j0_defined_by_q0_func
235     self.get_j0_given_qa = nu_constructor.j0_defined_by_qa_func
236
237     self.r = np.linspace(0, a, points)
238     self.nu = nu
239     if qa is not None:
240         self.j0 = self.get_j0_given_qa(k, b_z0, mu_0, qa)
241     else:
242         self.j0 = self.get_j0_given_q0(k, b_z0, mu_0, q0)
243     self.q0 = q0
244     self.mu_0 = mu_0
245     self.k = k
246     self.b_z0 = b_z0
247     self.temp = temp
248     param_points = {'j_z': self.j_z, 'b_theta': self.b_theta,
249                    'b_z': self.b_z, 'p_prime': self.p_prime,
250                    'pressure': self.pressure, 'q': self.q,
251                    'rho': self.rho}
252     self.set_splines(param_points)
253
254     def j_z(self, r):
255         r"""
256         Return nu axial current profile.
257         """
258         j_z_value = self.get_j_z(r, self.j0)
259         if isinstance(j_z_value, int) or isinstance(j_z_value, float):
260             j_z_value = np.ones(r.size)*j_z_value
261         return j_z_value
262
263     def b_theta(self, r):
264         r"""
265         Return azimuthal magnetic field for a nu current profile pinch.
266         """
267         return self.get_b_theta(r, self.j0, self.mu_0)
268
269     def b_z(self, r):
270         r"""
271
272         """
273         b_z0 = self.b_z0
274         r = np.asarray(r)
275         return np.ones(r.size) * self.b_z0
276
277     def p_prime(self, r):
278         r"""
279
280         """
281         return self.get_p_prime(r, self.j0, self.mu_0)
282
283     def pressure(self, r):
284         r"""
285
286         """
287         return self.get_pressure(r, self.j0, self.mu_0)
288

```

```

289     def q(self, r):
290         r"""
291         Returns safety factor evaluated at points.
292         """
293         q_value = self.get_q(r, self.k, self.b_z0, self.j0, self.mu_0)
294         if isinstance(q_value, int) or isinstance(q_value, float):
295             q_value = np.ones(r.size)*q_value
296         return q_value
297
298
299     class NewcombConstantPressure(EquilSolver):
300         """
301         Creates splines describing the constant pressure profile at the end of
302         Newcomb's 1960 paper.
303         """
304
305         def __init__(self, a=0.1, r_0i=0.5, k=1, b_z0=0.1, b_thetai=0.1,
306                     points=500):
307             r"""
308             Initialize parameters defining parabolic pinch and create splines.
309             """
310             self.r = np.linspace(a, r_0i, points)
311             self.a = a
312             self.r_0i = r_0i
313             self.k = k
314             self.b_z0 = b_z0
315             self.b_thetai = b_thetai
316             self.beta_0 = 0.
317             r = self.r
318             param_points = {'j_z': self.get_j_z, 'b_theta': self.b_theta,
319                             'b_z': self.b_z, 'p_prime': self.p_prime,
320                             'pressure': self.pressure, 'q': self.q,
321                             'rho': self.rho}
322
323             self.set_splines(param_points)
324
325             b_theta_prime = self.splines['b_theta'].derivative()
326             b_theta_prime_prime = b_theta_prime.derivative()
327             b_z_prime = self.splines['b_z'].derivative()
328             q_prime = self.splines['q'].derivative()
329
330             self.splines.update({'b_theta_prime': b_theta_prime,
331                                 'b_theta_prime_prime': b_theta_prime_prime,
332                                 'b_z_prime': b_z_prime, 'q_prime': q_prime})
333
334
335             self.tck_splines = self.convert_spline_objects_to_tck(self.splines)
336
337         def get_j_z(self, r):
338             r"""
339             Return zero current.
340             """
341             r = np.asarray(r)
342             return np.zeros(r.size)
343
344         def b_theta(self, r):
345             r"""

```

```

346         Return b_theta current profile as given in Newcomb's paper.
347         """
348         return self.b_theta*self.r_0i/r
349
350     def b_z(self, r):
351         r"""
352         Return constant b_z field.
353         """
354         return np.ones(r.size)*self.b_z0
355
356     def p_prime(self, r):
357         r"""
358         Return pressure_prime profile.
359         """
360         r = np.asarray(r)
361         return np.zeros(r.size)
362
363     def pressure(self, r):
364         r"""
365         Return pressure.
366         """
367         r = np.asarray(r)
368         return np.ones(r.size)
369
370
371     class SmoothedCoreSkin(EquilSolver):
372         r"""
373         Creates splines describing a smooth skin and core current profile.
374         """
375         def __init__(self, points_core=20, points_transition=50, points_skin=20,
376                     core_radius=0.7, transition_width=0.1, skin_width=0.1, k=1.,
377                     j_core=0.1, epsilon=0.3, lambda_bar=0.5, mu_0=1., q0=1.1,
378                     b_z0=0.1, determinant='j_core'):
379             r"""
380             Initialize parameters defining smooth skin and core profile
381             and create splines.
382             """
383             self.mu_0 = mu_0
384             self.q0 = q0
385
386             self.points_core = points_core
387             self.points_transition = points_transition
388             self.points_skin = points_skin
389             self.core_radius = core_radius
390             self.transition_width = transition_width
391             self.skin_width = skin_width
392
393             mask = np.ones(points_transition + 2, dtype=bool)
394             mask[[0, -1]] = False
395             self.r1 = np.linspace(0., core_radius, points_core)
396             r2 = np.linspace(core_radius, core_radius + transition_width,
397                             points_transition + 2)
398             self.r2 = r2[mask]
399             self.r3 = np.linspace(core_radius + transition_width,
400                                 core_radius + transition_width + skin_width,
401                                 points_skin)
402             r4 = np.linspace(core_radius + transition_width + skin_width,

```

```

403         core_radius + 2*transition_width + skin_width,
404         points_transition + 2)
405     self.r4 = r4[mask]
406     self.r = np.concatenate((self.r1, self.r2, self.r3, self.r4))
407
408     self.k = k
409     self.epsilon = epsilon
410     self.lambda_bar = lambda_bar
411
412     if determinant == 'q0':
413         self.b_z0 = b_z0
414         self.j_core = self.get_j_z_core()
415         self.ratio = self.get_ratio()
416         self.j_skin = j_core*self.ratio
417         self.j_skin = self.get_j_z_skin()
418
419     if determinant == 'j_core':
420         self.j_core = j_core
421         self.ratio = self.get_ratio()
422         self.j_skin = j_core*self.ratio
423         self.current = self.get_current()
424         self.b_z0 = self.get_b_z()
425
426     param_points = OrderedDict([( 'j_z', self.j_z),
427                                ( 'b_theta', self.b_theta),
428                                ( 'b_z', self.b_z),
429                                ( 'p_prime', self.p_prime),
430                                ( 'pressure', self.pressure),
431                                ( 'q', self.q),
432                                ( 'rho', self.rho)])
433
434     self.set_splines(param_points)
435
436     def smooth(self, x1, x2, g1, g2, x):
437         """
438         Smoothing method by Alan Glasser.
439         """
440         delta_x = (x2 - x1) / 2.
441         x_bar = (x2 + x1) / 2.
442         delta_g = (g2 - g1) / 2.
443         g_bar = (g1 + g2) / 2.
444         z = (x - x_bar) / delta_x
445         return g_bar + self.smooth_f(z)*delta_g
446
447     def smooth_f(self, z):
448         r"""
449         Smoothing polynomial by Alan Glasser.
450         """
451         return z/8.*(3.*z**4 - 10.*z**2 + 15.)
452
453     def get_j_z_core(self):
454         r"""
455         """
456         return (2.*self.b_z0*self.k/(self.mu_0*self.q0))
457
458     def get_ratio(self):
459         r"""

```

```

460     Returns j_z_skin based on j_z_core, geometry and epsilon of pinch.
461     """
462     a = self.core_radius + 2*self.transition_width + self.skin_width
463     term1 = -7.*a**2
464     term2 = 7.*a*self.skin_width
465     term3 = 14.*a*self.transition_width
466     term4 = 7.*a**2*self.epsilon
467     term5 = -14.*a*self.skin_width*self.epsilon
468     term6 = 7.*self.skin_width**2*self.epsilon
469     term7 = -21.*a*self.transition_width*self.epsilon
470     term8 = 21.*self.skin_width*self.transition_width*self.epsilon
471     term9 = 16.*self.transition_width**2*self.epsilon
472     denominator = (7.*(2.*a - self.skin_width -
473                    2.*self.transition_width) *
474                   (self.skin_width + self.transition_width) *
475                    self.epsilon)
476     return -(term1 + term2 + term3 + term4 + term5 + term6 +
477            term7 + term8 + term9) / denominator
478
479 def get_current(self):
480     r """
481     """
482     a = self.core_radius + 2*self.transition_width + self.skin_width
483     term1 = 7.*a**2*self.j_core
484     term2 = -14.*a*self.skin_width*self.j_core
485     term3 = 14.*a*self.skin_width*self.j_skin
486     term4 = -21.*a*self.transition_width*self.j_core
487     term5 = 14.*a*self.transition_width*self.j_skin
488     term6 = 7.*self.skin_width**2*self.j_core
489     term7 = -7.*self.skin_width**2*self.j_skin
490     term8 = 21.*self.skin_width*self.transition_width*self.j_core
491     term9 = -21.*self.skin_width*self.transition_width*self.j_skin
492     term10 = 16.*self.transition_width**2*self.j_core
493     term11 = -14.*self.transition_width**2*self.j_skin
494     return np.pi/7.*(term1 + term2 + term3 + term4 + term5 + term6 +
495                    term7 + term8 + term9 + term10 + term11)
496
497 def get_b_z(self):
498     r """
499     Returns b_z based on j_z, geometry and lambda_bar of pinch.
500     """
501     a = self.core_radius + 2*self.transition_width + self.skin_width
502     return self.current*self.mu_0/(np.pi*a**2*self.lambda_bar)
503
504 def j_z(self, dummy_r):
505     r """
506     For now always returns complete j_z.
507     """
508     total_points = (self.points_core + 2*self.points_transition +
509                    self.points_skin)
510
511     points1 = self.points_core
512     points2 = self.points_core + self.points_transition
513     points3 = self.points_core + self.points_transition + self.points_skin
514     points4 = (self.points_core + 2*self.points_transition +
515               self.points_skin)
516

```

```

517     boundary1 = self.core_radius
518     boundary2 = self.core_radius + self.transition_width
519     boundary3 = self.core_radius + self.transition_width + self.skin_width
520     boundary4 = (self.core_radius + 2*self.transition_width +
521                 self.skin_width)
522
523     j_z = np.zeros(total_points)
524     j_z[:points1] = self.j_core
525     j_z[points1:points2] = self.smooth(boundary1, boundary2, self.j_core,
526                                     self.j_skin,
527                                     self.r[points1:points2])
528     j_z[points2:points3] = self.j_skin
529     j_z[points3:points4] = self.smooth(boundary3, boundary4, self.j_skin,
530                                     0., self.r[points3:points4])
531     return j_z
532
533 def b_theta(self, r):
534     r"""
535     Return b_theta at given r values.
536     """
537     b_theta_r_integrator = inte.ode(b_theta_r_prime_func)
538     b_theta_r_integrator.set_integrator('lsoda')
539     b_theta_r_integrator.set_f_params(self.splines['j_z'], self.mu_0)
540     b_theta_r_integrator.set_initial_value(0., t=0.)
541     b_theta_array = np.empty(r.size)
542     b_theta_array[0] = 0.
543     for i, position in enumerate(r[1:]):
544         if b_theta_r_integrator.successful():
545             b_theta_r_integrator.integrate(position)
546             b_theta_array[i+1] = (b_theta_r_integrator.y/position)
547         else:
548             break
549     return np.array(b_theta_array)
550
551 def b_z(self, r):
552     r"""
553     Returns constant axial magnetic field.
554     """
555     return np.ones(r.size)*self.b_z0
556
557 def p_prime(self, r):
558     r"""
559     Return pressure_prime at given r values. To be used for integration.
560     """
561     return -self.splines['b_theta'](r)*self.splines['j_z'](r)
562
563 def pressure(self, r):
564     r"""
565     Return pressure_prime at given r values. To be used for integration.
566     """
567     pressure_integrator = inte.ode(p_prime_func)
568     pressure_integrator.set_integrator('lsoda')
569     pressure_integrator.set_initial_value(0., 0.)
570     pressure_integrator.set_f_params(self.splines['j_z'],
571                                     self.splines['b_theta'])
572     pressure_unnorm = np.empty(r.size)
573     pressure_unnorm[0] = 0.

```

```

574     for i, position in enumerate(r[1:]):
575         if pressure_integrator.successful():
576             pressure_integrator.integrate(t=position)
577             pressure_unnorm[i+1] = pressure_integrator.y
578         else:
579             break
580     pressure_norm = pressure_unnorm - pressure_unnorm[-1]
581     return pressure_norm
582
583 def get_beta(self, r):
584     r"""
585     """
586     beta_numerator = 2.*self.mu_0*self.splines['pressure'](self.r)
587     beta_denominator = ((self.splines['b_z'](self.r))**2 +
588                        (self.splines['b_theta'](self.r))**2)
589     return interp.InterpolatedUnivariateSpline(self.r, beta_numerator/beta_denominator)
590
591 def get_beta_average(self, r):
592     pass
593
594 def q(self, r):
595     r"""
596     Returns safety factor evaluated at points.
597     """
598     if r[0] == 0.:
599         q0 = self.k*self.b_z0/(0.5*self.mu_0*self.j_core)
600         q_to_return = np.ones(r.size)*q0
601         q_to_return[1:] = (r[1:]*self.k*self.splines['b_z'](r[1:]) /
602                          self.splines['b_theta'](r[1:]))
603     else:
604         q_to_return = (r*self.k*self.splines['b_z'](r) /
605                      self.splines['b_theta'](r))
606     return q_to_return
607
608
609 class UnitlessSmoothedCoreSkin(EquilSolver):
610     r"""
611     Creates splines describing a smooth skin and core current profile.
612     """
613     def __init__(self, points_core=20, points_transition=50, points_skin=20,
614                 core_radius_norm=0.7, transition_width_norm=0.1,
615                 skin_width_norm=0.1, k_bar=1.,
616                 epsilon=0.3, lambda_bar=0.5):
617         r"""
618         Initialize parameters defining smooth skin and core profile
619         and create splines.
620         """
621         self.points_core = points_core
622         self.points_transition = points_transition
623         self.points_skin = points_skin
624         self.core_radius = core_radius_norm
625         self.transition_width = transition_width_norm
626         self.skin_width = skin_width_norm
627         self.r_bar = self.core_radius + 2*self.transition_width + self.skin_width
628         self.r = self.r_points()
629
630         self.k_bar = k_bar

```

```

631     self.epsilon = epsilon
632     self.lambda_bar = lambda_bar
633
634     self.splines = {}
635
636     self.b_z0 = 1.
637     self.make_spline('b_z', self.r, self.b_z(self.r))
638
639     self.j_core = 1.
640     self.j_skin = self.get_j_skin_norm()
641     self.make_spline('j_z', self.r, self.j_z(self.r))
642
643     self.b_theta_integrand_array = self.b_theta_integrand(self.r)
644
645     self.A = self.get_A()
646
647     self.make_spline('b_theta', self.r, self.b_theta(self.r))
648
649     self.make_spline('pressure', self.r, self.pressure(self.r))
650     self.make_spline('p_prime', self.r, self.p_prime(self.r))
651
652     self.q_0 = self.get_q_0()
653     self.make_spline('q', self.r, self.q(self.r))
654     self.make_spline('beta', self.r, self.beta(self.r))
655
656     self.make_spline('rho', self.r, self.rho(self.r))
657
658     b_theta_prime = self.splines['b_theta'].derivative()
659     b_theta_prime_prime = b_theta_prime.derivative()
660     b_z_prime = self.splines['b_z'].derivative()
661     q_prime = self.splines['q'].derivative()
662
663     self.splines.update({'b_theta_prime': b_theta_prime,
664                         'b_theta_prime_prime': b_theta_prime_prime,
665                         'b_z_prime': b_z_prime, 'q_prime': q_prime})
666
667     self.tck_splines = self.convert_spline_objects_to_tck(self.splines)
668
669
670 def r_points(self):
671     r"""
672     """
673     (points_core, points_transition,
674     points_skin) = (self.points_core,
675                   self.points_transition,
676                   self.points_skin)
677     (core_radius, transition_width,
678     skin_width) = (self.core_radius,
679                  self.transition_width,
680                  self.skin_width)
681     mask1 = np.ones(points_transition + 2, dtype=bool)
682     mask2 = np.ones(points_transition + 2, dtype=bool)
683     mask1[[0, -1]] = False
684     mask2[0] = False
685     self.r1 = np.linspace(0., core_radius, points_core)
686     r2 = np.linspace(core_radius, core_radius +
687                     transition_width, points_transition + 2)

```

```

688     self.r2 = r2[mask1]
689     self.r3 = np.linspace(core_radius + transition_width ,
690                          core_radius + transition_width +
691                          skin_width, points_skin)
692     r4 = np.linspace(core_radius + transition_width +
693                    skin_width,
694                    core_radius + 2*transition_width +
695                    skin_width, points_transition + 2)
696     self.r4 = r4[mask2]
697     r = np.concatenate((self.r1, self.r2, self.r3, self.r4))
698     return r
699
700 def make_spline(self, key, r, values):
701     r """
702     """
703     self.splines[key] = interp.InterpolatedUnivariateSpline(r,
704                                                            values,
705                                                            k=3)
706 def smooth(self, x1, x2, g1, g2, x):
707     """
708     Smoothing method by Alan Glasser.
709     """
710     delta_x = (x2 - x1) / 2.
711     x_bar = (x2 + x1) / 2.
712     delta_g = (g2 - g1) / 2.
713     g_bar = (g1 + g2) / 2.
714     z = (x - x_bar) / delta_x
715     return g_bar + self.smooth_f(z)*delta_g
716
717 def smooth_f(self, z):
718     r """
719     Smoothing polynomial by Alan Glasser.
720     """
721     return z/8.*(3.*z**4 - 10.*z**2 + 15.)
722
723 def get_j_skin_norm(self):
724     r """
725     Returns j_z_skin based on j_z_core, geometry and epsilon of pinch.
726     """
727     (epsilon, skin_width,
728      transition_width, r_bar) = (self.epsilon, self.skin_width,
729                                 self.transition_width, self.r_bar)
730
731     term1 = 16.*skin_width**2*epsilon
732     term2 = 21.*skin_width*transition_width*epsilon
733     term3 = -21*skin_width*epsilon*r_bar
734     term4 = 14.*skin_width*r_bar
735     term5 = 7.*transition_width**2*epsilon
736     term6 = -14.*transition_width*r_bar*epsilon
737     term7 = 7.*transition_width*r_bar
738     term8 = 7.*epsilon*r_bar**2
739     term9 = -7.*r_bar**2
740     numerator = (term1 + term2 + term3 + term4 + term5 + term6 + term7 +
741                term8 + term9)
742
743     factor1 = 7.*epsilon
744     factor2 = (skin_width + transition_width)

```

```

745     factor3 = (2.*skin_width + transition_width - 2.*r_bar)
746
747     denominator = factor1*factor2*factor3
748
749     return self.j_core*numerator/denominator
750
751 def j_z(self, dummy_r):
752     r"""
753     For now always returns complete j_z.
754     """
755     total_points = (self.points_core + 2*self.points_transition +
756                   self.points_skin)+1
757
758     points1 = self.points_core
759     points2 = self.points_core + self.points_transition
760     points3 = self.points_core + self.points_transition + self.points_skin
761     points4 = (self.points_core + 2*self.points_transition +
762              self.points_skin)+1
763
764     boundary1 = self.core_radius
765     boundary2 = self.core_radius + self.transition_width
766     boundary3 = self.core_radius + self.transition_width + self.skin_width
767     boundary4 = (self.core_radius + 2*self.transition_width +
768                self.skin_width)
769
770     j_z = np.zeros(total_points)
771     j_z[:points1] = self.j_core
772     j_z[points1:points2] = self.smooth(boundary1, boundary2, 1.,
773                                     self.j_skin,
774                                     self.r[points1:points2])
775     j_z[points2:points3] = self.j_skin
776     j_z[points3:points4] = self.smooth(boundary3, boundary4, self.j_skin,
777                                     0., self.r[points3:points4])
778     return j_z
779
780 def b_theta_integrand(self, r):
781     r"""
782     """
783     b_theta_r_integrator = inte.ode(b_theta_r_prime_func)
784     b_theta_r_integrator.set_integrator('lsoda')
785     b_theta_r_integrator.set_f_params(self.splines['j_z'], _eval_args, 1.0)
786     b_theta_r_integrator.set_initial_value(0., t=0.)
787     b_theta_integrand_array = np.empty(r.size)
788     b_theta_integrand_array[0] = 0.
789     for i, position in enumerate(r[1:]):
790         if b_theta_r_integrator.successful():
791             b_theta_r_integrator.integrate(position)
792             b_theta_integrand_array[i+1] = (b_theta_r_integrator.y/position)
793         else:
794             break
795     return b_theta_integrand_array
796
797 def get_A(self):
798     return self.lambda_bar*self.b_z0/(2*self.b_theta_integrand_array[-1])
799
800 def get_q_0(self):
801     r"""

```

```

802     """
803     return 2.*self.k_bar*self.b_z0/(self.A*self.j_core)
804
805 def b_theta(self, r):
806     r"""
807     Return b_theta at given r values.
808     """
809     b_theta_array = self.b_theta_integrand_array*self.A
810     return b_theta_array
811
812 def b_z(self, r):
813     r"""
814     Returns constant axial magnetic field.
815     """
816     return np.ones(r.size)*self.b_z0
817
818 def p_prime(self, r):
819     r"""
820     Return pressure_prime at given r values. To be used for integration.
821     """
822     return -self.B*self.splines['b_theta'](r)*self.splines['j_z'](r)
823
824 def pressure(self, r):
825     r"""
826     Return pressure_prime at given r values. To be used for integration.
827     """
828     pressure_integrator = inte.ode(p_prime_func_reverse)
829     pressure_integrator.set_integrator('lsoda')
830     pressure_integrator.set_initial_value(0., 0.)
831     pressure_integrator.set_f_params(self.splines['j_z']._eval_args,
832                                     self.splines['b_theta']._eval_args)
833     pressure_reverse = np.empty(r.size)
834     pressure_reverse[0] = 0.
835     r_reverse_diffs = np.cumsum(np.diff(self.r)[::-1])
836     for i, position in enumerate(r_reverse_diffs):
837         if pressure_integrator.successful():
838             pressure_integrator.integrate(t=position)
839             pressure_reverse[i+1] = pressure_integrator.y
840         else:
841             break
842     pressure = pressure_reverse[::-1]
843     self.B = 1./pressure[0]
844     pressure_norm = pressure*self.B
845     return pressure_norm
846
847 def beta_0(self):
848     r"""
849     """
850     return 2.*self.A/(self.b_z0**2*self.B)*self.splines['pressure'](0)
851
852 def beta(self, r):
853     r"""
854     """
855     return 2.*self.A/(self.b_z0**2*self.B)*self.splines['pressure'](r)
856
857 def q(self, r):
858     r"""

```

```

859     Returns safety factor evaluated at points.
860     """
861     if r[0] == 0.:
862         q_to_return = np.ones(r.size)*self.q_0
863         q_to_return[1:] = (r[1:]*self.k_bar*self.splines['b_z'](r[1:]) /
864                         self.splines['b_theta'](r[1:]))
865     else:
866         q_to_return = (r*self.k_bar*self.splines['b_z'](r) /
867                       self.splines['b_theta'](r))
868     return q_to_return
869
870
871 class UnitlessSmoothedCoreSkinLinearBz(EquilSolver):
872     r"""
873     Creates splines describing a smooth skin and core current profile.
874     """
875     def __init__(self, points_core=20, points_transition=50, points_skin=20,
876                 core_radius_norm=0.7, transition_width_norm=0.1,
877                 skin_width_norm=0.1, k_bar=1.,
878                 epsilon=0.3, lambda_bar=0.5, b_z_factor=0.9):
879         self.points_core = points_core
880         self.points_transition = points_transition
881         self.points_skin = points_skin
882         self.core_radius = core_radius_norm
883         self.transition_width = transition_width_norm
884         self.skin_width = skin_width_norm
885         self.r_bar = self.core_radius + 2*self.transition_width + self.skin_width
886         self.r = self.r_points()
887
888         self.k_bar = k_bar
889         self.epsilon = epsilon
890         self.lambda_bar = lambda_bar
891
892         self.splines = {}
893
894         self.b_z_factor = b_z_factor
895         self.b_z0 = 1.*b_z_factor
896         self.make_spline('b_z', self.r, self.b_z(self.r))
897
898         self.j_core = 1.
899         self.j_skin = self.get_j_skin_norm()
900         self.make_spline('j_z', self.r, self.j_z(self.r))
901
902         self.b_theta_integrand_array = self.b_theta_integrand(self.r)
903
904         self.A = self.get_A()
905
906         self.make_spline('j_theta', self.r, self.j_theta(self.r))
907
908         self.make_spline('b_theta', self.r, self.b_theta(self.r))
909
910         self.make_spline('pressure', self.r, self.pressure(self.r))
911         self.make_spline('p_prime', self.r, self.p_prime(self.r))
912
913         self.q_0 = self.get_q_0()
914         self.make_spline('q', self.r, self.q(self.r))
915         self.make_spline('beta', self.r, self.beta(self.r))

```

```

916
917     self.make_spline('rho', self.r, self.rho(self.r))
918
919     b_theta_prime = self.splines['b_theta'].derivative()
920     b_theta_prime_prime = b_theta_prime.derivative()
921     b_z_prime = self.splines['b_z'].derivative()
922     q_prime = self.splines['q'].derivative()
923
924     self.splines.update({'b_theta_prime': b_theta_prime,
925                         'b_theta_prime_prime': b_theta_prime_prime,
926                         'b_z_prime': b_z_prime, 'q_prime': q_prime})
927
928     self.tck_splines = self.convert_spline_objects_to_tck(self.splines)
929
930
931 def r_points(self):
932     r"""
933     """
934     (points_core, points_transition,
935      points_skin) = (self.points_core,
936                    self.points_transition,
937                    self.points_skin)
938     (core_radius, transition_width,
939      skin_width) = (self.core_radius,
940                   self.transition_width,
941                   self.skin_width)
942     mask1 = np.ones(points_transition + 2, dtype=bool)
943     mask2 = np.ones(points_transition + 2, dtype=bool)
944     mask1[[0, -1]] = False
945     mask2[0] = False
946     self.r1 = np.linspace(0., core_radius, points_core)
947     r2 = np.linspace(core_radius, core_radius +
948                    transition_width, points_transition + 2)
949     self.r2 = r2[mask1]
950     self.r3 = np.linspace(core_radius + transition_width,
951                          core_radius + transition_width +
952                          skin_width, points_skin)
953     r4 = np.linspace(core_radius + transition_width +
954                    skin_width,
955                    core_radius + 2*transition_width +
956                    skin_width, points_transition + 2)
957     self.r4 = r4[mask2]
958     r = np.concatenate((self.r1, self.r2, self.r3, self.r4))
959     return r
960
961 def make_spline(self, key, r, values):
962     r"""
963     """
964     self.splines[key] = interp.InterpolatedUnivariateSpline(r,
965                                                            values,
966                                                            k=3)
967
968 def smooth(self, x1, x2, g1, g2, x):
969     """
970     Smoothing method by Alan Glasser.
971     """
972     delta_x = (x2 - x1) / 2.
973     x_bar = (x2 + x1) / 2.

```

```

973     delta_g = (g2 - g1) / 2.
974     g_bar = (g1 + g2) / 2.
975     z = (x - x_bar) / delta_x
976     return g_bar + self.smooth_f(z)*delta_g
977
978 def smooth_f(self, z):
979     r"""
980     Smoothing polynomial by Alan Glasser.
981     """
982     return z/8.*(3.*z**4 - 10.*z**2 + 15.)
983
984 def get_j_skin_norm(self):
985     r"""
986     Returns j_z_skin based on j_z_core, geometry and epsilon of pinch.
987     """
988     (epsilon, skin_width,
989      transition_width, r_bar) = (self.epsilon, self.skin_width,
990                                 self.transition_width, self.r_bar)
991
992     term1 = 16.*skin_width**2*epsilon
993     term2 = 21.*skin_width*transition_width*epsilon
994     term3 = -21.*skin_width*epsilon*r_bar
995     term4 = 14.*skin_width*r_bar
996     term5 = 7.*transition_width**2*epsilon
997     term6 = -14.*transition_width*r_bar*epsilon
998     term7 = 7.*transition_width*r_bar
999     term8 = 7.*epsilon*r_bar**2
1000    term9 = -7.*r_bar**2
1001    numerator = (term1 + term2 + term3 + term4 + term5 + term6 + term7 +
1002                term8 + term9)
1003
1004    factor1 = 7.*epsilon
1005    factor2 = (skin_width + transition_width)
1006    factor3 = (2.*skin_width + transition_width - 2.*r_bar)
1007
1008    denominator = factor1*factor2*factor3
1009
1010    return self.j_core*numerator/denominator
1011
1012 def j_z(self, dummy_r):
1013     r"""
1014     For now always returns complete j_z.
1015     """
1016     total_points = (self.points_core + 2*self.points_transition +
1017                    self.points_skin)+1
1018
1019     points1 = self.points_core
1020     points2 = self.points_core + self.points_transition
1021     points3 = self.points_core + self.points_transition + self.points_skin
1022     points4 = (self.points_core + 2*self.points_transition +
1023               self.points_skin)+1
1024
1025     boundary1 = self.core_radius
1026     boundary2 = self.core_radius + self.transition_width
1027     boundary3 = self.core_radius + self.transition_width + self.skin_width
1028     boundary4 = (self.core_radius + 2*self.transition_width +
1029                 self.skin_width)

```

```

1030
1031     j_z = np.zeros(total_points)
1032     j_z[:points1] = self.j_core
1033     j_z[points1:points2] = self.smooth(boundary1, boundary2, 1.,
1034                                     self.j_skin,
1035                                     self.r[points1:points2])
1036     j_z[points2:points3] = self.j_skin
1037     j_z[points3:points4] = self.smooth(boundary3, boundary4, self.j_skin,
1038                                     0., self.r[points3:points4])
1039     return j_z
1040
1041     def b_theta_integrand(self, r):
1042         r"""
1043         """
1044         b_theta_r_integrator = inte.ode(b_theta_r_prime_func)
1045         b_theta_r_integrator.set_integrator('lsoda')
1046         b_theta_r_integrator.set_f_params(self.splines['j_z']._eval_args, 1.0)
1047         b_theta_r_integrator.set_initial_value(0., t=0.)
1048         b_theta_integrand_array = np.empty(r.size)
1049         b_theta_integrand_array[0] = 0.
1050         for i, position in enumerate(r[1:]):
1051             if b_theta_r_integrator.successful():
1052                 b_theta_r_integrator.integrate(position)
1053                 b_theta_integrand_array[i+1] = (b_theta_r_integrator.y/position)
1054             else:
1055                 break
1056         return b_theta_integrand_array
1057
1058     def get_A(self):
1059         return self.lambdabar*self.b_z0/(2*self.b_theta_integrand_array[-1])
1060
1061     def get_q_0(self):
1062         r"""
1063         """
1064         return 2.*self.k_bar*self.b_z0/(self.A*self.j_core)
1065
1066     def j_theta(self, r):
1067         return 1./self.A*self.splines['b_z'].derivative()(r)
1068
1069     def b_theta(self, r):
1070         r"""
1071         Return b_theta at given r values.
1072         """
1073         b_theta_array = self.b_theta_integrand_array*self.A
1074         return b_theta_array
1075
1076     def b_z(self, r):
1077         r"""
1078         Returns constant axial magnetic field.
1079         """
1080         return (1.-self.b_z_factor)/(1.)*r+self.b_z_factor
1081
1082     def p_prime(self, r):
1083         r"""
1084         Return pressure_prime at given r values. To be used for integration.
1085         """
1086         return self.B*(self.splines['b_z'](r)*self.splines['j_theta'](r) -

```

```

1087         self.splines['b_theta'](r)*self.splines['j_z'](r))
1088
1089     def pressure(self, r):
1090         r"""
1091         Return pressure_prime at given r values. To be used for integration.
1092         """
1093         pressure_integrator = integrate.ode(p_prime_func_reverse_j_theta)
1094         pressure_integrator.set_integrator('lsoda')
1095         pressure_integrator.set_initial_value(0., 0.)
1096         pressure_integrator.set_f_params(self.splines['j_z']._eval_args,
1097                                         self.splines['b_theta']._eval_args,
1098                                         self.splines['j_theta']._eval_args,
1099                                         self.splines['b_z']._eval_args)
1100
1101         pressure_reverse = np.empty(r.size)
1102         pressure_reverse[0] = 0.
1103         r_reverse_diffs = np.cumsum(np.diff(self.r)[::-1])
1104         for i, position in enumerate(r_reverse_diffs):
1105             if pressure_integrator.successful():
1106                 pressure_integrator.integrate(t=position)
1107                 pressure_reverse[i+1] = pressure_integrator.y
1108             else:
1109                 break
1110         pressure = pressure_reverse[::-1]
1111         self.B = 1./pressure[0]
1112         pressure_norm = pressure*self.B
1113         return pressure_norm
1114
1115     def beta_0(self):
1116         r"""
1117         """
1118         return 2.*self.A/(self.b_z**2*self.B)*self.splines['pressure'](0)
1119
1120     def beta(self, r):
1121         r"""
1122         """
1123         return 2.*self.A/(self.b_z**2*self.B)*self.splines['pressure'](r)
1124
1125     def q(self, r):
1126         r"""
1127         Returns safety factor evaluated at points.
1128         """
1129         if r[0] == 0.:
1130             q_to_return = np.ones(r.size)*self.q_0
1131             q_to_return[1:] = (r[1:]*self.k_bar*self.splines['b_z'](r[1:])/
1132                             self.splines['b_theta'](r[1:]))
1133         else:
1134             q_to_return = (r*self.k_bar*self.splines['b_z'](r)/
1135                             self.splines['b_theta'](r))
1136         return q_to_return
1137
1138     class UnitlessSmoothedCoreSkinSmoothJTheta(EquilibriumSolver):
1139         r"""
1140         Creates splines describing a smooth skin and core current profile.
1141         """
1142         def __init__(self, points_core=20, points_transition=50, points_skin=20,
1143                     core_radius_norm=0.7, transition_width_norm=0.1,

```

```

1144         skin_width_norm=0.1, k_bar=1.,
1145         epsilon=0.3, lambda_bar=0.5, j_theta_peak=1., j_theta_start=0., j_theta_peak_pos=0.5):
1146     self.points_core = points_core
1147     self.points_transition = points_transition
1148     self.points_skin = points_skin
1149     self.core_radius = core_radius_norm
1150     self.transition_width = transition_width_norm
1151     self.skin_width = skin_width_norm
1152     self.r_bar = self.core_radius + 2*self.transition_width + self.skin_width
1153     self.r = self.r_points()
1154
1155     self.k_bar = k_bar
1156     self.epsilon = epsilon
1157     self.lambda_bar = lambda_bar
1158
1159     self.splines = {}
1160
1161     self.b_z0 = 1.
1162
1163     self.j_core = 1.
1164     self.j_skin = self.get_j_skin_norm()
1165     self.make_spline('j_z', self.r, self.j_z(self.r))
1166
1167     self.b_theta_integrand_array = self.b_theta_integrand(self.r)
1168
1169     self.A = self.get_A()
1170
1171     self.j_theta_peak = j_theta_peak
1172     self.j_theta_start = j_theta_start
1173     self.j_theta_peak_pos = j_theta_peak_pos
1174     self.make_spline('j_theta', self.r, self.j_theta(self.r))
1175     self.make_spline('b_z', self.r, self.b_z(self.r))
1176
1177     self.make_spline('b_theta', self.r, self.b_theta(self.r))
1178
1179     self.make_spline('pressure', self.r, self.pressure(self.r))
1180     self.make_spline('p_prime', self.r, self.p_prime(self.r))
1181
1182     self.q_0 = self.get_q_0()
1183     self.make_spline('q', self.r, self.q(self.r))
1184     self.make_spline('beta', self.r, self.beta(self.r))
1185
1186     self.make_spline('rho', self.r, self.rho(self.r))
1187
1188     b_theta_prime = self.splines['b_theta'].derivative()
1189     b_theta_prime_prime = b_theta_prime.derivative()
1190     b_z_prime = self.splines['b_z'].derivative()
1191     q_prime = self.splines['q'].derivative()
1192
1193     self.splines.update({'b_theta_prime': b_theta_prime,
1194                        'b_theta_prime_prime': b_theta_prime_prime,
1195                        'b_z_prime': b_z_prime, 'q_prime': q_prime})
1196
1197     self.tck_splines = self.convert_spline_objects_to_tck(self.splines)
1198
1199
1200 def r_points(self):

```

```

1201     r"""
1202     """
1203     (points_core, points_transition,
1204      points_skin) = (self.points_core,
1205                     self.points_transition,
1206                     self.points_skin)
1207     (core_radius, transition_width,
1208      skin_width) = (self.core_radius,
1209                    self.transition_width,
1210                    self.skin_width)
1211     mask1 = np.ones(points_transition + 2, dtype=bool)
1212     mask2 = np.ones(points_transition + 2, dtype=bool)
1213     mask1[[0, -1]] = False
1214     mask2[0] = False
1215     self.r1 = np.linspace(0., core_radius, points_core)
1216     r2 = np.linspace(core_radius, core_radius +
1217                     transition_width, points_transition + 2)
1218     self.r2 = r2[mask1]
1219     self.r3 = np.linspace(core_radius + transition_width,
1220                           core_radius + transition_width +
1221                           skin_width, points_skin)
1222     r4 = np.linspace(core_radius + transition_width +
1223                     skin_width,
1224                     core_radius + 2*transition_width +
1225                     skin_width, points_transition + 2)
1226     self.r4 = r4[mask2]
1227     r = np.concatenate((self.r1, self.r2, self.r3, self.r4))
1228     return r
1229
1230 def make_spline(self, key, r, values):
1231     r"""
1232     """
1233     self.splines[key] = interp.InterpolatedUnivariateSpline(r,
1234                                                             values,
1235                                                             k=3)
1236
1237 def smooth(self, x1, x2, g1, g2, x):
1238     """
1239     Smoothing method by Alan Glasser.
1240     """
1241     delta_x = (x2 - x1) / 2.
1242     x_bar = (x2 + x1) / 2.
1243     delta_g = (g2 - g1) / 2.
1244     g_bar = (g1 + g2) / 2.
1245     z = (x - x_bar) / delta_x
1246     return g_bar + self.smooth_f(z)*delta_g
1247
1248 def smooth_f(self, z):
1249     r"""
1250     Smoothing polynomial by Alan Glasser.
1251     """
1252     return z/8.*(3.*z**4 - 10.*z**2 + 15.)
1253
1254 def get_j_skin_norm(self):
1255     r"""
1256     Returns j_z_skin based on j_z_core, geometry and epsilon of pinch.
1257     """

```

```

1258     (epsilon, skin_width,
1259      transition_width, r_bar) = (self.epsilon, self.skin_width,
1260                                  self.transition_width, self.r_bar)
1261
1262     term1 = 16.*skin_width**2*epsilon
1263     term2 = 21.*skin_width*transition_width*epsilon
1264     term3 = -21.*skin_width*epsilon*r_bar
1265     term4 = 14.*skin_width*r_bar
1266     term5 = 7.*transition_width**2*epsilon
1267     term6 = -14.*transition_width*r_bar*epsilon
1268     term7 = 7.*transition_width*r_bar
1269     term8 = 7.*epsilon*r_bar**2
1270     term9 = -7.*r_bar**2
1271     numerator = (term1 + term2 + term3 + term4 + term5 + term6 + term7 +
1272                  term8 + term9)
1273
1274     factor1 = 7.*epsilon
1275     factor2 = (skin_width + transition_width)
1276     factor3 = (2.*skin_width + transition_width - 2.*r_bar)
1277
1278     denominator = factor1*factor2*factor3
1279
1280     return self.j_core*numerator/denominator
1281
1282 def j_z(self, dummy_r):
1283     r """
1284     For now always returns complete j_z.
1285     """
1286     total_points = (self.points_core + 2*self.points_transition +
1287                    self.points_skin)+1
1288
1289     points1 = self.points_core
1290     points2 = self.points_core + self.points_transition
1291     points3 = self.points_core + self.points_transition + self.points_skin
1292     points4 = (self.points_core + 2*self.points_transition +
1293               self.points_skin)+1
1294
1295     boundary1 = self.core_radius
1296     boundary2 = self.core_radius + self.transition_width
1297     boundary3 = self.core_radius + self.transition_width + self.skin_width
1298     boundary4 = (self.core_radius + 2*self.transition_width +
1299                 self.skin_width)
1300
1301     j_z = np.zeros(total_points)
1302     j_z[:points1] = self.j_core
1303     j_z[points1:points2] = self.smooth(boundary1, boundary2, 1.,
1304                                       self.j_skin,
1305                                       self.r[points1:points2])
1306     j_z[points2:points3] = self.j_skin
1307     j_z[points3:points4] = self.smooth(boundary3, boundary4, self.j_skin,
1308                                       0., self.r[points3:points4])
1309
1310     return j_z
1311
1312 def b_theta_integrand(self, r):
1313     r """
1314
1315     b_theta_r_integrator = inte.ode(b_theta_r_prime_func)

```

```

1315     b_theta_r_integrator.set_integrator('lsoda')
1316     b_theta_r_integrator.set_f_params(self.splines['j_z'], _eval_args, 1.0)
1317     b_theta_r_integrator.set_initial_value(0., t=0.)
1318     b_theta_integrand_array = np.empty(r.size)
1319     b_theta_integrand_array[0] = 0.
1320     for i, position in enumerate(r[1:]):
1321         if b_theta_r_integrator.successful():
1322             b_theta_r_integrator.integrate(position)
1323             b_theta_integrand_array[i+1] = (b_theta_r_integrator.y/position)
1324         else:
1325             break
1326     return b_theta_integrand_array
1327
1328 def get_A(self):
1329     return self.lambda_bar*self.b_z0/(2*self.b_theta_integrand_array[-1])
1330
1331 def get_q_0(self):
1332     r"""
1333     """
1334     return 2.*self.k_bar*self.b_z0/(self.A*self.j_core)
1335
1336 def j_theta(self, r):
1337     peak = np.where(r>self.j_theta_peak_pos)[0][0]
1338     start = np.where(r>self.j_theta_start)[0][0]
1339     j_theta = np.zeros(r.shape)
1340     j_theta[start:peak] = self.smooth(self.j_theta_start,
1341                                     self.j_theta_peak_pos, 0.,
1342                                     self.j_theta_peak, r[start:peak])
1343     j_theta[peak:] = self.smooth(self.j_theta_peak_pos, 1.,
1344                                 self.j_theta_peak, 0, r[peak:])
1345     return j_theta
1346
1347 def b_theta(self, r):
1348     r"""
1349     Return b_theta at given r values.
1350     """
1351     b_theta_array = self.b_theta_integrand_array*self.A
1352     return b_theta_array
1353
1354 def b_z(self, r):
1355     r"""
1356     Returns constant axial magnetic field.
1357     """
1358     b_z_integrator = inte.ode(j_theta_func)
1359     b_z_integrator.set_integrator('lsoda')
1360     b_z_integrator.set_f_params(self.splines['j_theta'], 1.0)
1361     b_z_integrator.set_initial_value(0, t=0.)
1362     b_z = np.ones(r.size)*self.b_z0
1363     for i, position in enumerate(r):
1364         if b_z_integrator.successful():
1365             b_z_integrator.integrate(position)
1366             b_z[i] += self.A*b_z_integrator.y
1367         else:
1368             break
1369     return b_z
1370
1371 def p_prime(self, r):

```

```

1372     r"""
1373     Return pressure_prime at given r values. To be used for integration.
1374     """
1375     return self.B*(self.splines['b_z'](r)*self.splines['j_theta'](r) -
1376                  self.splines['b_theta'](r)*self.splines['j_z'](r))
1377
1378 def pressure(self, r):
1379     r"""
1380     Return pressure_prime at given r values. To be used for integration.
1381     """
1382     pressure_integrator = inte.ode(p_prime_func_reverse_j_theta)
1383     pressure_integrator.set_integrator('lsoda')
1384     pressure_integrator.set_initial_value(0., 0.)
1385     pressure_integrator.set_f_params(self.splines['j_z']._eval_args,
1386                                     self.splines['b_theta']._eval_args,
1387                                     self.splines['j_theta']._eval_args,
1388                                     self.splines['b_z']._eval_args)
1389     pressure_reverse = np.empty(r.size)
1390     pressure_reverse[0] = 0.
1391     r_reverse_diffs = np.cumsum(np.diff(self.r)[::-1])
1392     for i, position in enumerate(r_reverse_diffs):
1393         if pressure_integrator.successful():
1394             pressure_integrator.integrate(t=position)
1395             pressure_reverse[i+1] = pressure_integrator.y
1396         else:
1397             break
1398     pressure = pressure_reverse[::-1]
1399     self.B = 1./pressure[0]
1400     pressure_norm = pressure*self.B
1401     return pressure_norm
1402
1403 def beta_0(self):
1404     r"""
1405     """
1406     return 2.*self.A/(self.b_z0**2*self.B)*self.splines['pressure'](0)
1407
1408 def beta(self, r):
1409     r"""
1410     """
1411     return 2.*self.A/(self.b_z0**2*self.B)*self.splines['pressure'](r)
1412
1413 def q(self, r):
1414     r"""
1415     Returns safety factor evaluated at points.
1416     """
1417     if r[0] == 0.:
1418         q_to_return = np.ones(r.size)*self.q_0
1419         q_to_return[1:] = (r[1:]*self.k_bar*self.splines['b_z'](r[1:]) /
1420                          self.splines['b_theta'](r[1:]))
1421     else:
1422         q_to_return = (r*self.k_bar*self.splines['b_z'](r) /
1423                       self.splines['b_theta'](r))
1424     return q_to_return
1425
1426
1427 class UnitlessExponentialDecaySkin(UnitlessSmoothedCoreSkin):
1428     r"""

```

```

1429     Creates splines describing a smooth skin and core current profile.
1430     """
1431     def __init__(self, points_core=20, points_skin=20, k_bar=1.,
1432                 epsilon=0.3, lambda_bar=0.5):
1433         r"""
1434         Initialize parameters defining smooth skin and core profile
1435         and create splines.
1436         """
1437         self.points_core = points_core
1438         self.points_skin = points_skin
1439         self.core_radius = 0.6
1440         self.skin_width = 0.4
1441         self.r_bar = self.core_radius + self.skin_width
1442         self.r = self.r_points()
1443
1444         self.k_bar = k_bar
1445         self.epsilon = epsilon
1446         self.lambda_bar = lambda_bar
1447
1448         self.splines = {}
1449
1450         self.b_z0 = 1.
1451         self.make_spline('b_z', self.r, self.b_z(self.r))
1452
1453         self.j_core = 1.
1454         self.j_skin = self.get_j_skin_norm(epsilon)
1455         self.make_spline('j_z', self.r, self.j_z(self.r))
1456
1457         self.b_theta_integrand_array = self.b_theta_integrand(self.r)
1458
1459         self.A = self.get_A()
1460
1461         self.make_spline('b_theta', self.r, self.b_theta(self.r))
1462
1463         self.make_spline('pressure', self.r, self.pressure(self.r))
1464         self.make_spline('p_prime', self.r, self.p_prime(self.r))
1465
1466         self.q_0 = self.get_q_0()
1467         self.make_spline('q', self.r, self.q(self.r))
1468         self.make_spline('beta', self.r, self.beta(self.r))
1469
1470         self.make_spline('rho', self.r, self.rho(self.r))
1471
1472         b_theta_prime = self.splines['b_theta'].derivative()
1473         b_theta_prime_prime = b_theta_prime.derivative()
1474         b_z_prime = self.splines['b_z'].derivative()
1475         q_prime = self.splines['q'].derivative()
1476
1477         self.splines.update({'b_theta_prime': b_theta_prime,
1478                             'b_theta_prime_prime': b_theta_prime_prime,
1479                             'b_z_prime': b_z_prime, 'q_prime': q_prime})
1480
1481         self.tck_splines = self.convert_spline_objects_to_tck(self.splines)
1482
1483     def r_points(self):
1484         r"""
1485         """

```

```

1486     (points_core ,
1487      points_skin) = (self.points_core ,
1488                     self.points_skin)
1489     (core_radius ,
1490      skin_width) = (self.core_radius ,
1491                    self.skin_width)
1492     self.r1 = np.linspace(0. , core_radius , points_core , endpoint=False)
1493     self.r2 = np.linspace(core_radius , core_radius + skin_width ,
1494                           points_skin)
1495     #print('r_points_build ', core_radius , poin)
1496     r = np.concatenate((self.r1 , self.r2))
1497     return r
1498
1499     def get_j_skin_norm(self , epsilon ,
1500                       i_core=0.806207671074 ,
1501                       slope=1.0053096491487337 ,
1502                       offset=0.18521395596186707):
1503         r"""
1504         Returns j_z_skin based on j_z_core , geometry and epsilon of pinch.
1505         """
1506         return (i_core/epsilon - i_core - offset) / slope
1507
1508     def j_z(self , dummy_r):
1509         r"""
1510         """
1511
1512         r = self.r
1513         (core_radius ,
1514          skin_width) = (self.core_radius ,
1515                        self.skin_width)
1516         skin_peak = skin_width/2
1517         skin_peak_radius = core_radius + skin_peak
1518         radius = core_radius + skin_width
1519         core = self.j_core * np.exp(-2*r**2)
1520         skin = interp.BPoly.from_derivatives([core_radius ,
1521                                             skin_peak_radius ,
1522                                             radius] ,
1523                                             [[np.exp(-2*core_radius**2) ,
1524                                               -4*core_radius*np.exp(-2*core_radius**2)] ,
1525                                              [self.j_skin , 0.] , [0. ,0.]])
1526         j_z = core
1527         indexes = np.where(r >= core_radius)
1528         j_z[indexes] = skin(r[indexes])
1529         return j_z
1530
1531
1532     class UnitlessTanhCoreSkin(EquilSolver):
1533         r"""
1534         Creates splines describing a smooth skin and core current profile.
1535         """
1536         def __init__(self , points_core=100 , points_transition=100 , points_skin=100 ,
1537                     core_radius_norm=0.7 , transition_width_norm=0.1 ,
1538                     skin_width_norm=0.1 , k_bar=1. ,
1539                     epsilon=0.3 , lambda_bar=0.5):
1540             r"""
1541             Initialize parameters defining smooth skin and core profile
1542             and create splines.

```

```

1543     """
1544     self.points_core = points_core
1545     self.points_transition = points_transition
1546     self.points_skin = points_skin
1547     self.core_radius = core_radius_norm
1548     self.transition_width = transition_width_norm
1549     self.skin_width = skin_width_norm
1550     self.r_bar = self.core_radius + 2*self.transition_width + self.skin_width
1551     self.r = self.r_points()
1552
1553     self.k_bar = k_bar
1554     self.epsilon = epsilon
1555     self.lambda_bar = lambda_bar
1556
1557     self.splines = {}
1558
1559     self.b_z0 = 1.
1560     self.make_spline('b_z', self.r, self.b_z(self.r))
1561
1562     self.j_core = 1.
1563     self.j_skin = self.get_j_skin_norm()
1564     self.make_spline('j_z', self.r, self.j_z(self.r))
1565
1566     self.b_theta_integrand_array = self.b_theta_integrand(self.r)
1567
1568     self.A = self.get_A()
1569
1570     self.make_spline('b_theta', self.r, self.b_theta(self.r))
1571
1572     self.make_spline('pressure', self.r, self.pressure(self.r))
1573     self.make_spline('p_prime', self.r, self.p_prime(self.r))
1574
1575     self.q_0 = self.get_q_0()
1576     self.make_spline('q', self.r, self.q(self.r))
1577     self.make_spline('beta', self.r, self.beta(self.r))
1578
1579     self.make_spline('rho', self.r, self.rho(self.r))
1580
1581
1582     def r_points(self):
1583         r """
1584         """
1585         (points_core, points_transition,
1586          points_skin) = (self.points_core,
1587                          self.points_transition,
1588                          self.points_skin)
1589         (core_radius, transition_width,
1590          skin_width) = (self.core_radius,
1591                         self.transition_width,
1592                         self.skin_width)
1593         mask1 = np.ones(points_transition + 2, dtype=bool)
1594         mask2 = np.ones(points_transition + 2, dtype=bool)
1595         mask1[[0, -1]] = False
1596         mask2[0] = False
1597         self.r1 = np.linspace(0., core_radius, points_core)
1598         r2 = np.linspace(core_radius, core_radius +
1599                          transition_width, points_transition + 2)

```

```

1600     self.r2 = r2[mask1]
1601     self.r3 = np.linspace(core_radius + transition_width ,
1602                          core_radius + transition_width +
1603                          skin_width, points_skin)
1604     r4 = np.linspace(core_radius + transition_width +
1605                    skin_width,
1606                    core_radius + 2*transition_width +
1607                    skin_width, points_transition + 2)
1608     self.r4 = r4[mask2]
1609     r = np.concatenate((self.r1, self.r2, self.r3, self.r4))
1610     return r
1611
1612 def make_spline(self, key, r, values):
1613     r """
1614     """
1615     self.splines[key] = interp.InterpolatedUnivariateSpline(r,
1616                                                            values,
1617                                                            k=3)
1618 def smooth(self, x1, x2, g1, g2, x):
1619     """
1620     Smoothing method by Alan Glasser.
1621     """
1622     delta_x = (x2 - x1) / 2.
1623     x_bar = (x2 + x1) / 2.
1624     delta_g = (g2 - g1) / 2.
1625     g_bar = (g1 + g2) / 2.
1626     z = (x - x_bar) / delta_x
1627     return g_bar + self.smooth_f(z)*delta_g
1628
1629 def smooth_f(self, z):
1630     r """
1631     Smoothing polynomial by Alan Glasser.
1632     """
1633     return z/8.*(3.*z**4 - 10.*z**2 + 15.)
1634
1635 def get_j_skin_norm(self):
1636     r """
1637     Returns j_z_skin based on j_z_core, geometry and epsilon of pinch.
1638     """
1639     (epsilon, skin_width,
1640      transition_width, r_bar) = (self.epsilon, self.skin_width,
1641                                 self.transition_width, self.r_bar)
1642
1643     term1 = 16.*skin_width**2*epsilon
1644     term2 = 21.*skin_width*transition_width*epsilon
1645     term3 = -21*skin_width*epsilon*r_bar
1646     term4 = 14.*skin_width*r_bar
1647     term5 = 7.*transition_width**2*epsilon
1648     term6 = -14.*transition_width*r_bar*epsilon
1649     term7 = 7.*transition_width*r_bar
1650     term8 = 7.*epsilon*r_bar**2
1651     term9 = -7.*r_bar**2
1652     numerator = (term1 + term2 + term3 + term4 + term5 + term6 + term7 +
1653                term8 + term9)
1654
1655     factor1 = 7.*epsilon
1656     factor2 = (skin_width + transition_width)

```

```

1657     factor3 = (2.*skin_width + transition_width - 2.*r_bar)
1658
1659     denominator = factor1*factor2*factor3
1660
1661     return self.j_core*numerator/denominator
1662
1663 def j_z(self, dummy_r):
1664     r"""
1665     For now always returns complete j_z.
1666     """
1667     total_points = (self.points_core + 2*self.points_transition +
1668                    self.points_skin)+1
1669
1670     points1 = self.points_core
1671     points2 = self.points_core + self.points_transition
1672     points3 = self.points_core + self.points_transition + self.points_skin
1673     points4 = (self.points_core + 2*self.points_transition +
1674               self.points_skin)+1
1675
1676     boundary1 = self.core_radius
1677     boundary2 = self.core_radius + self.transition_width
1678     boundary3 = self.core_radius + self.transition_width + self.skin_width
1679     boundary4 = (self.core_radius + 2*self.transition_width +
1680                self.skin_width)
1681
1682     j_z = np.zeros(total_points)
1683     j_z[:points1] = self.j_core
1684     j_z[points1:points2] = np.tanh((self.r[points1:points2]-boundary1)/(self.transition_width)*4*np.pi-2*np.pi)*(self.j_skin - self.j_core)/2. + 1. *(self.j_skin - self.j_core)/2. + self.j_core
1685     j_z[points2:points3] = self.j_skin
1686     j_z[points3:points4] = np.tanh((self.r[points3:points4]-boundary3)/(self.transition_width)*4*np.pi-2*np.pi)*(0. - self.j_skin)/2. + 1. *(0. - self.j_skin)/2. + self.j_skin
1687     return j_z
1688
1689 def b_theta_integrand(self, r):
1690     r"""
1691     """
1692     b_theta_r_integrator = inte.ode(b_theta_r_prime_func)
1693     b_theta_r_integrator.set_integrator('lsoda')
1694     b_theta_r_integrator.set_f_params(self.splines['j_z'], 1.0)
1695     b_theta_r_integrator.set_initial_value(0., t=0.)
1696     b_theta_integrand_array = np.empty(r.size)
1697     b_theta_integrand_array[0] = 0.
1698     for i, position in enumerate(r[1:]):
1699         if b_theta_r_integrator.successful():
1700             b_theta_r_integrator.integrate(position)
1701             b_theta_integrand_array[i+1] = (b_theta_r_integrator.y/position)
1702         else:
1703             break
1704     return b_theta_integrand_array
1705
1706 def get_A(self):
1707     return self.lambdas_bar*self.b_z0/(2*self.b_theta_integrand_array[-1])
1708
1709 def get_q_0(self):
1710     r"""
1711     """

```

```

1712         return 2.*self.k_bar*self.b_z0/(self.A*self.j_core)
1713
1714     def b_theta(self, r):
1715         r"""
1716         Return b_theta at given r values.
1717         """
1718         b_theta_array = self.b_theta_integrand_array*self.A
1719         return b_theta_array
1720
1721     def b_z(self, r):
1722         r"""
1723         Returns constant axial magnetic field.
1724         """
1725         return np.ones(r.size)*self.b_z0
1726
1727     def p_prime(self, r):
1728         r"""
1729         Return pressure_prime at given r values. To be used for integration.
1730         """
1731         return -self.B*self.splines['b_theta'](r)*self.splines['j_z'](r)
1732
1733     def pressure(self, r):
1734         r"""
1735         Return pressure_prime at given r values. To be used for integration.
1736         """
1737         pressure_integrator = inte.ode(p_prime_func_reverse)
1738         pressure_integrator.set_integrator('lsoda')
1739         pressure_integrator.set_initial_value(0., 0)
1740         pressure_integrator.set_f_params(self.splines['j_z'],
1741                                         self.splines['b_theta'])
1742         pressure_reverse = np.empty(r.size)
1743         pressure_reverse[0] = 0.
1744         r_reverse_diffs = np.cumsum(np.diff(self.r)[::-1])
1745         for i, position in enumerate(r_reverse_diffs):
1746             if pressure_integrator.successful():
1747                 pressure_integrator.integrate(t=position)
1748                 pressure_reverse[i+1] = pressure_integrator.y
1749             else:
1750                 print('integration failed')
1751                 break
1752         pressure = pressure_reverse[::-1]
1753         self.B = 1./pressure[0]
1754         pressure_norm = pressure*self.B
1755         return pressure_norm
1756
1757     def beta_0(self):
1758         r"""
1759         """
1760         return 2.*self.A/(self.b_z0**2*self.B)*self.splines['pressure'](0)
1761
1762     def beta(self, r):
1763         r"""
1764         """
1765         return 2.*self.A/(self.b_z0**2*self.B)*self.splines['pressure'](r)
1766
1767     def q(self, r):
1768         r"""

```

```

1769     Returns safety factor evaluated at points.
1770     """
1771     if r[0] == 0.:
1772         q_to_return = np.ones(r.size)*self.q_0
1773         q_to_return[1:] = (r[1:]*self.k_bar*self.splines['b_z'](r[1:]) /
1774             self.splines['b_theta'](r[1:]))
1775     else:
1776         q_to_return = (r*self.k_bar*self.splines['b_z'](r) /
1777             self.splines['b_theta'](r))
1778     return q_to_return
1779
1780
1781 class HardcoreZPinch(EquilSolver):
1782     r"""
1783     Create profiles for the Hard-Core Z-pinch as described in Freidberg Ideal
1784     MHD.
1785     """
1786     def __init__(self, i_c=0.1, i_p=0.2, r_c=0.1, r_a=1.0, k=1.0, points=500,
1787         mu_0=1.):
1788         self.k = k
1789         self.i_c = i_c
1790         self.i_p = i_p
1791         self.r_c = r_c
1792         self.r_a = r_a
1793         self.current = i_c + i_p
1794         self.k_p = 3./2.*(5./3.)*(5./2.)
1795         self.k_i = mu_0*((i_c + i_p)/(2.*np.pi*r_c))**2
1796         self.mu_0 = mu_0
1797
1798         self.r = np.linspace(r_c, r_a, points)
1799
1800         param_points = {'j_z': self.j_z,
1801             'b_theta': self.b_theta,
1802             'b_z': self.b_z,
1803             'p_prime': self.p_prime,
1804             'pressure': self.pressure,
1805             'q': self.q,
1806             'rho': self.rho,
1807             'stability': self.stability_criterion}
1808
1809         self.set_splines(param_points)
1810
1811     def b_z(self, r):
1812         r"""
1813         Returns axial field.
1814         """
1815         r = np.asarray(r)
1816         return np.zeros(r.size)
1817
1818     def b_theta(self, r):
1819         r"""
1820         Returns azimuthal field.
1821         """
1822         r = np.asarray(r)
1823         x = r**2 / self.r_c**2
1824         b_theta = np.sqrt(self.k_i/x - 2.*self.mu_0*self.k_p*(9.*x-5.) /
1825             (3*x***(3./2.)))

```

```

1826         return b_theta
1827
1828     def pressure(self, r):
1829         r"""
1830         Returns pressure.
1831         """
1832         r = np.asarray(r)
1833         x = r**2 / self.r_c**2
1834         return self.k_p*(x - 1.)/x**(5./2.)
1835
1836     def p_prime(self, r):
1837         r"""
1838         Returns derivative of pressure.
1839         """
1840         r = np.asarray(r)
1841         r_sym, r_c, k_p = sp.symbols('r r_c K_p')
1842         x = r_sym**2 / self.r_c**2
1843         pressure_sym = k_p*(x - 1)/x**(2.5)
1844         p_prime_func = sp.lambdify((r_sym, r_c, k_p),
1845                                     sp.diff(pressure_sym, r_sym), modules=np)
1846         return p_prime_func(r, self.r_c, self.k_p)
1847
1848     def j_z(self, r):
1849         r"""
1850         Returns axial current.
1851         """
1852         r = np.asarray(r)
1853
1854         r_sym, r_c, k_p, k_i = sp.symbols('r r_c K_p K_i')
1855         x = r_sym**2 / r_c**2
1856         b_theta = sp.sqrt(k_i/x - 2.*k_p*(9.*x - 5.)/(3*x*x**(1.5)))
1857         j_z_sym = sp.diff(r_sym*b_theta, r_sym)/(r_sym*self.mu_0)
1858         j_z_func = sp.lambdify((r_sym, r_c, k_p, k_i), j_z_sym,
1859                                 modules=np)
1860         return j_z_func(r, self.r_c, self.k_p, self.k_i)
1861
1862     def beta(self, r):
1863         r"""
1864         Returns Beta
1865         """
1866         r = np.asarray(r)
1867         return 32./2.*np.pi**2*self.r_c**2/(self.mu_0*self.current)*self.k_p
1868
1869     def stability_criterion(self, r):
1870         r"""
1871         Returns stability criterion. If array is greater than 0 any where the
1872         profile is unstable.
1873         """
1874         r = np.asarray(r)
1875         x_sym, r_c, current, k_p = sp.symbols('x r_c I K_p')
1876         beta = 32./3.*sp.pi**2*r_c**2/(self.mu_0*current**2)*k_p
1877         b_theta_norm_sq = 1. - beta/4. * (9.*x_sym - 5.)/x_sym**(1.5)
1878         stab_sym = sp.diff(b_theta_norm_sq/x_sym**(0.5), x_sym)
1879         stab_func = sp.lambdify((x_sym, r_c, k_p, current), stab_sym,
1880                                 modules=np)
1881         return stab_func(r**2/self.r_c**2, self.r_c, self.k_p, self.current)
1882

```

```

1883
1884 class SharpCoreSkin(EquilSolver):
1885     pass
1886
1887
1888 def b_theta_r_prime_func(r, y, j_z, mu_0):
1889     r"""
1890     Return b_theta_r_prime at given r values. To be used for integration.
1891     """
1892     r_arr = np.asarray(r)
1893     r_arr = atleast_1d(r_arr).ravel()
1894     return splev(r_arr, j_z)*r_arr*mu_0
1895
1896
1897 def p_prime_func(r, y, j_z, b_theta):
1898     r"""
1899     Return pressure_prime at given r values. To be used for integration.
1900     """
1901     return -splev(r, b_theta)*splev(r, j_z)
1902
1903 def p_prime_func_reverse_j_theta(r, y, j_z, b_theta, j_theta, b_z):
1904     r"""
1905     Return negative pressure_prime at given r values. To be used for reverse integration.
1906     """
1907     r_arr = np.asarray(r)
1908     r_arr = atleast_1d(r_arr).ravel()
1909     return splev(1.-r_arr, b_theta)*splev(1.-r_arr, j_z) - splev(1.-r_arr, b_z)*splev(1.-r_arr, j_theta)
1910
1911 def p_prime_func_reverse(r, y, j_z, b_theta):
1912     r"""
1913     Return negative pressure_prime at given r values. To be used for reverse integration.
1914     """
1915     r_arr = np.asarray(r)
1916     r_arr = atleast_1d(r_arr).ravel()
1917     return splev(1.-r_arr, b_theta)*splev(1.-r_arr, j_z)
1918
1919 def j_theta_func(r, y, j_theta_spline):
1920     return j_theta_spline(r)

```

A.6.6 newcomb.py

```

1  -*- coding: utf-8 -*-
2  """
3  Created on Sun Feb 08 15:36:58 2015
4
5  @author: Jens von der Linden
6  """
7
8  from __future__ import print_function
9  from __future__ import division
10 from __future__ import absolute_import
11 from future.builtins import (ascii, bytes, chr, dict, filter, hex, input,
12                             int, map, next, oct, open, pow, range, round,
13                             str, super, zip)

```

```

14 """Python 3.x compatibility"""
15
16 import sys
17 from scipy.interpolate import splev
18
19 import numpy as np
20 from numpy import atleast_1d
21 import scipy.integrate
22
23 import newcomb_init as init
24 import singularity_frobenius as frob
25 import find_singularities as find_sing
26 import external_stability as ext
27 import newcomb_f as new_f
28 import newcomb_g as new_g
29
30
31
32 def stability(params, offset, suydam_offset, suppress_output=False,
33             method='lsoda', rtol=None, max_step=None, nsteps=None,
34             xi_given=[0., 1.], diagnose=False, sing_search_points=10000,
35             f_func=new_f.newcomb_f_16, g_func=new_g.newcomb_g_18_dimless_wo_q,
36             skip_external_stability=False, stiff=False, use_jac=True,
37             adapt_step_size=False, adapt_min_steps=500):
38     r"""
39     Determine external stability.
40
41     Parameters
42     -----
43     params: dict
44         equilibrium parameters including spline coefficients
45     offset : float
46         offset after which to start integrating after singularities
47     suydam_offset : float
48         offset after which to start integrating after suydam unstable
49         singularities
50     suppress_output: boolean
51         flag to suppress diagnostic print statements
52     method: string
53         integration method to use. Either an integrator in scipy.integrate.ode
54         or 'odeint' for scipy.integrate.odeint
55     rtol : float
56         passed to ode solver relative tolerance setting for ODE integrator
57     max_step: float
58         option passed to ode solver, limit for max step size
59     nsteps: int
60         option passed to ode solver, maximum number of steps allowed during call
61         to solver.
62     xi_given: tuple of floats
63         Initial condition used for xi if equilibrium does not start at r=0
64     diagnose: bool
65         flag to print out more diagnostic statements during integration
66     sing_search_points: int
67         number of points to divide domain by in search for singularities
68     f_func: function
69         python function to use to calculate f
70     g_func: function

```

```

71     python function to use to calculate given
72 skip_external_stability: bool
73     flag to skip external stability
74 stiff: bool
75     flag to indicate stiff equation to integrator
76 use_jac: bool
77     flag to have integrator use Jacobian
78 adapt_step_size: bool
79     flag to use adaptive step size integrator
80 adapt_min_steps: int
81     specify minimum number of steps
82 Returns
83 -----
84 stable_external : bool
85     True if  $\Delta_w > 0$ 
86 suydam_stable : bool
87     True if all singularities (except  $r=0$ ) are Suydam stable
88 delta_w : float
89     total perturbed potential energy
90 missing_end_params:
91     diagnostic output no longer used.
92 xi : ndarray
93     xi at interval boundary (only last element is relevant)
94 xi_der : ndarray
95     derivative of xi at interval boundary (only last element is relevant)
96 r_array : ndarray
97     array of r values at which xi is integrated
98 Notes
99 -----
100 Examines the equilibrium. If the equilibrium has a singularity, the
101 Frobenius method is used to determine a small solution at an  $r >$  than
102 instability. If the singularity is suydam unstable no attempt is made to
103 calculate external stability.
104 If there is no Frobenius instability power series solution
105 close to  $r=0$  is chosen or if the integration does not start at  $r=0$  a given
106 xi is used as boundary condition.
107 Only the last interval is integrated.
108 To save time xi and xi_der are only evaluated at  $r=a$  (under the hood the
109 integrator is evaluating xi and xi_der across the interval).
110 Xi and xi_der are plugged into the potential energy equation to determine
111 stability.
112 """
113 params.update({'f_func': f_func, 'g_func': g_func})
114 missing_end_params = None
115
116 if params['m'] == -1:
117     sing_params = {'a': params['r_0'], 'b': params['a'],
118                  'points': sing_search_points, 'k': params['k'],
119                  'm': params['m'], 'b_z_spl': params['b_z'],
120                  'b_z_prime_spl': params['b_z_prime'],
121                  'b_theta_spl': params['b_theta'],
122                  'b_theta_prime_spl': params['b_theta_prime'],
123                  'p_prime_spl': params['p_prime'], 'offset': offset,
124                  'tol': 1E-2, 'beta_0': params['beta_0']}
125
126     (interval,
127      starts_with_sing,
128      suydam_stable,

```

```

128         suydam_unstable_interval) = intervals_with_singularities(suppress_output,
129                                                                 **sing_params)
130     else:
131         suydam_stable = True
132         starts_with_sing = False
133         suydam_unstable_interval = False
134         interval = [params['r_0'], params['a']]
135
136     interval, init_value = setup_initial_conditions(interval, starts_with_sing,
137                                                  offset, suydam_offset,
138                                                  xi_given=xi_given,
139                                                  **params)
140     if not suydam_unstable_interval:
141         if skip_external_stability:
142             (xi, xi_der, r_array) = newcomb_int(params, interval,
143                                              init_value, method,
144                                              diagnose, max_step,
145                                              nsteps, rtol,
146                                              skip_external_stability=True,
147                                              stiff=stiff,
148                                              use_jac=use_jac,
149                                              adapt_step_size=adapt_step_size,
150                                              adapt_min_steps=adapt_min_steps)
151             return xi, xi_der
152
153         (stable_external, delta_w,
154          missing_end_params, xi, xi_der,
155          r_array) = newcomb_int(params, interval, init_value, method,
156                               diagnose, max_step, nsteps, rtol,
157                               stiff=stiff, use_jac=use_jac,
158                               adapt_step_size=adapt_step_size,
159                               adapt_min_steps=adapt_min_steps)
160     else:
161         msg = ("Last singularity is suydam unstable. " +
162              "Unable to determine external instability at k = %.3f."
163              % params['k'])
164         print(msg)
165         delta_w = None
166         stable_external = None
167         xi = np.asarray([np.nan])
168         xi_der = np.asarray([np.nan])
169         r_array = np.asarray([np.nan])
170     return (stable_external, suydam_stable, delta_w, missing_end_params, xi,
171           xi_der, r_array)
172
173
174 def newcomb_der(r, y, k, m, b_z_spl, b_z_prime_spl, b_theta_spl,
175               b_theta_prime_spl, p_prime_spl, q_spl, q_prime_spl,
176               f_func, g_func, beta_0):
177     r"""
178     Returns derivatives of Newcomb's Euler-Lagrange equation expressed as a set
179     of 2 first order ODEs.
180
181     Parameters
182     -----
183     r : float
184         radius for which to find derivative

```

```

185     y : ndarray (2)
186         values of :math:'\xi' and :math:'f \xi''
187     k : float
188         axial periodicity number
189     m : float
190         azimuthal periodicity number
191     b_z_spl : scipy spline tck tuple
192         axial magnetic field
193     b_theta_spl : scipy spline tck tuple
194         azimuthal magnetic field
195     b_theta_prime_spl: scipy spline tck tuple
196         radial derivative of azimuthal magnetic field
197     p_prime_spl : scipy spline tck tuple
198         derivative of pressure
199     q_spl : scipy spline tck tuple
200         safety factor
201     f_func : function
202         function which returns f of Newcomb's Euler-Lagrange equation
203     g_func : function
204         function which returns g of Newcomb's Euler-Lagrange equation
205     beta_0 : float
206         pressure ratio on axis
207
208     Returns
209     -----
210     y_prime : ndarray of floats (2)
211         derivatives of y
212
213     Notes
214     -----
215     The system of ODEs representing the Euler-Lagrange equations is
216
217     .. math::
218
219         \frac{d \xi}{dr} \&= \xi' \ \backslash\
220         \frac{d (f \xi')}{dr} \&= g \xi
221
222     Reference
223     -----
224     Newcomb (1960) Hydromagnetic Stability of a diffuse linear pinch.
225     """
226     y_prime = np.zeros(2)
227
228     r_arr = np.asarray(r)
229     r_arr = atleast_1d(r_arr).ravel()
230
231     g_params = {'r': r, 'k': k, 'm': m, 'b_z': splev(r_arr, b_z_spl),
232                'b_theta': splev(r_arr, b_theta_spl),
233                'p_prime': splev(r_arr, p_prime_spl),
234                'beta_0': beta_0}
235
236     f_params = {'r': r, 'k': k, 'm': m, 'b_z': splev(r_arr, b_z_spl),
237                'b_theta': splev(r_arr, b_theta_spl), 'q': splev(r_arr, q_spl)}
238
239     y_prime[0] = y[1] / f_func(**f_params)
240     y_prime[1] = y[0]*g_func(**g_params)
241     return y_prime

```

```

242
243 def newcomb_jac(r, y, k, m, b_z_spl, b_z_prime_spl, b_theta_spl,
244                b_theta_prime_spl, p_prime_spl, q_spl, q_prime_spl,
245                f_func, g_func, beta_0):
246     r"""
247     Jacobian of Newcomb's Euler-Lagrange equation.
248     """
249     r_arr = np.asarray(r)
250     r_arr = atleast_1d(r_arr).ravel()
251     g_params = {'r': r, 'k': k, 'm': m, 'b_z': splev(r_arr, b_z_spl),
252               'b_theta': splev(r_arr, b_theta_spl),
253               'p_prime': splev(r_arr, p_prime_spl),
254               'beta_0': beta_0}
255
256     f_params = {'r': r, 'k': k, 'm': m, 'b_z': splev(r_arr, b_z_spl),
257               'b_theta': splev(r_arr, b_theta_spl), 'q': splev(r_arr, q_spl)}
258
259     jac = np.zeros((2,2))
260     jac[0,1] = 1. / f_func(**f_params)
261     jac[1,0] = g_func(**g_params)
262     return jac
263
264 def newcomb_der_for_odeint(y, r, *args):
265     r"""
266     odeint uses a derivative function with y and r passed as arguments in
267     reverse order.
268     """
269     return newcomb_der(r, y, *args)
270
271
272 def divide_by_f(r, xi_der_f, k, m, b_z_spl, b_theta_spl, q_spl, f_func):
273     r"""
274     Divides  $y[1]=f \xi$  by f to recover  $\xi$ .
275     """
276     r_arr = np.asarray(r)
277     r_arr = atleast_1d(r_arr).ravel()
278     f_params = {'r': r, 'k': k, 'm': m, 'b_z': splev(r_arr, b_z_spl),
279               'b_theta': splev(r_arr, b_theta_spl), 'q': splev(r_arr, q_spl)}
280     return xi_der_f / f_func(**f_params)
281
282
283 def intervals_with_singularities(suppress_output, **sing_params):
284     r"""
285     Determines if an interval starts with a singularity, is Suydam unstable.
286     """
287     starts_with_sing = False
288     suydam_unstable_interval = False
289     suydam_stable = False
290     interval = [sing_params['a'], sing_params['b']]
291     (sings,
292      sings_wo_0, intervals) = find_sing.identify_singularities(**sing_params)
293
294     if not sings_wo_0.size == 0:
295         if not suppress_output:
296             print("Non-geometric singularities identified at r =", sings_wo_0)
297         interval = [sings_wo_0[-1], sing_params['b']]
298         starts_with_sing = True

```



```

356         init_value = init.init_xi_given(xi_given, interval[0], **init_params)
357     return interval, init_value
358
359
360 def check_suydam(r, b_z_spl, b_z_prime_spl, b_theta_spl, b_theta_prime_spl,
361                p_prime_spl, beta_0, **kwargs):
362     r"""
363     Return radial positions at which the Euler–Lagrange equation is singular
364     and Suydam’s criterion is violated.
365
366     Parameters
367     -----
368     r : ndarray of floats (M)
369         positions at which f=0.
370     b_z_spl : scipy spline object
371         axial magnetic field
372     b_theta_spl : scipy spline object
373         azimuthal magnetic field
374     p_prime_spl : scipy spline object
375         derivative of pressure
376     beta_0 : float
377         beta on axis
378     Returns
379     -----
380     unstable_r : ndarray of floats (N)
381         positions at which plasma column is suydam unstable
382     """
383     params = {'r': r, 'b_z_spl': b_z_spl, 'b_z_prime_spl': b_z_prime_spl,
384             'b_theta_spl': b_theta_spl,
385             'b_theta_prime_spl': b_theta_prime_spl,
386             'p_prime_spl': p_prime_spl, 'beta_0': beta_0}
387     unstable_mask = np.invert(frob.sings_suydam_stable(**params))
388     return r[unstable_mask]
389
390
391 def newcomb_int(params, interval, init_value, method, diagnose, max_step,
392               nsteps, rtol, skip_external_stability=False, stiff=False,
393               use_jac=True, adapt_step_size=False, adapt_min_steps=500):
394     r"""
395     Integrates newcomb’s euler Lagrange equation in a given interval with lsoda
396     either with the scipy.ode object oriented interface or with scipy.odeint.
397     """
398     missing_end_params = None
399     #print('k_bar', params['k'], 'interval:', interval[0], interval[1], init_value)
400     args = (params['k'], params['m'], params['b_z'], params['b_z_prime'],
401           params['b_theta'], params['b_theta_prime'], params['p_prime'],
402           params['q'], params['q_prime'], params['f_func'], params['g_func'],
403           params['beta_0'])
404
405     if adapt_step_size:
406         interval_list = [interval]
407         max_step_list = [10.**((np.floor(np.log10(1 - params['core_radius']))-1)]
408         nsteps_for_list = 10.**((np.abs(np.log10(max_step_list[0]))+5) * (1 - params['core_radius']))
409         nsteps_for_list = adapt_min_steps if nsteps_for_list < adapt_min_steps else nsteps_for_list
410         nsteps_list = [nsteps_for_list]
411         if interval[0] < params['core_radius']:
412             interval_list.insert(0, [interval[0], params['core_radius']])

```

```

413         interval_list[1] = [params['core_radius'], interval[1]]
414         max_step_list.insert(0, max_step)
415         nsteps_list.insert(0, nsteps)
416     else:
417         interval_list = [interval]
418         max_step_list = [max_step]
419         nsteps_list = [nsteps]
420
421
422     for i, interval in enumerate(interval_list):
423         max_step = max_step_list[i]
424         nsteps = nsteps_list[i]
425         if diagnose:
426             r_array = np.linspace(interval[0], interval[1], 250)
427         else:
428             r_array = np.asarray(interval)
429
430
431     if method == 'lsoda_odeint':
432         if 'core_radius' in params.keys():
433             transition_points = np.asarray([params['core_radius'],
434                                             params['core_radius'] +
435                                             params['transition_width'],
436                                             params['core_radius'] +
437                                             params['transition_width'] +
438                                             params['skin_width']])
439             tcrit = np.asarray(transition_points[np.less(interval[0], transition_points)])
440         else:
441             tcrit = None
442
443         integrator_args = {}
444         if rtol is not None:
445             integrator_args['rtol'] = rtol
446         if nsteps is not None:
447             integrator_args['mxstep'] = nsteps
448         if max_step is not None:
449             integrator_args['hmax'] = max_step
450         if use_jac:
451             results = scipy.integrate.odeint(newcomb_der_for_odeint,
452                                             np.asarray(init_value),
453                                             np.asarray(r_array),
454                                             Dfun=newcomb_jac,
455                                             tcrit=tcrit,
456                                             args=args,
457                                             **integrator_args)
458         else:
459             results = scipy.integrate.odeint(newcomb_der_for_odeint,
460                                             np.asarray(init_value),
461                                             np.asarray(r_array),
462                                             tcrit=tcrit,
463                                             args=args,
464                                             **integrator_args)
465         xi = np.asarray([results[:, 0]]).ravel()
466         xi_der_f = np.asarray([results[:, 1]]).ravel()
467     else:
468         if use_jac:
469             integrator = scipy.integrate.ode(newcomb_der, jac=newcomb_jac)

```

```

470         else:
471             integrator = scipy.integrate.ode(newcomb_der)
472
473         integrator_args = {}
474         if rtol is not None:
475             integrator_args['rtol'] = rtol
476         if nsteps is not None:
477             integrator_args['nsteps'] = nsteps
478         if max_step is not None:
479             integrator_args['max_step'] = max_step
480         if stiff:
481             integrator_args['method'] = 'bdf'
482
483         integrator.set_integrator(method, **integrator_args)
484         integrator.set_f_params(*args)
485         integrator.set_jac_params(*args)
486         integrator.set_initial_value(init_value, interval[0])
487         results = np.empty((r_array.size, 2))
488         results[0] = init_value
489         for i, r in enumerate(r_array[1:]):
490             integrator.integrate(r)
491             results[i+1, :] = integrator.y
492             if not integrator.successful():
493                 results[i+1:, :] = [np.nan, np.nan]
494             break
495         xi = results[:, 0]
496         xi_der_f = results[:, 1]
497         init_value = [xi[-1], xi_der_f[-1]]
498
499         xi_der = divide_by_f(r_array,
500                             xi_der_f,
501                             params['k'],
502                             params['m'],
503                             params['b_z'],
504                             params['b_theta'],
505                             params['q'],
506                             params['f_func'])
507
508         if np.all(np.isfinite(results[-1])):
509             if skip_external_stability:
510                 return xi, xi_der, r_array
511             (stable_external,
512              delta_w) = ext.external_stability_from_analytic_condition(params,
513                                                                      xi[-1],
514                                                                      xi_der[-1],
515                                                                      without_sing=True,
516                                                                      dim_less=True)
517             #print(delta_w)
518         else:
519             msg = ("Integration to plasma edge did not succeed. " +
520                  "Can not determine external stability at k = %.3f."
521                  % params['k'])
522             print(msg)
523             missing_end_params = params
524             stable_external = None
525             delta_w = None
526         return (stable_external, delta_w, missing_end_params, xi, xi_der, r_array)

```

A.6.7 newcomb_init.py

```

1  # -*- coding: utf-8 -*-
2  """
3  Created on Mon Aug 18 11:31:46 2014
4
5  @author: Jens von der Linden
6
7  Collection of init functions to set initial xi and xi prime for newcomb
8  integrations.
9  """
10
11 from __future__ import print_function
12 from __future__ import division
13 from __future__ import absolute_import
14 from future.builtins import (ascii, bytes, chr, dict, filter, hex, input,
15                             int, map, next, oct, open, pow, range, round,
16                             str, super, zip)
17 """Python 3.x compatibility"""
18
19 import numpy as np
20
21 def init_geometric_sing(r, k, m, b_z, b_theta, q, f_func, xi_factor, *args, **kwargs):
22     r"""
23     Return xi found from Frobenius method at a geometric singularity (i.e. r=0)
24
25     Parameters
26     -----
27     r : float
28         radius
29     k : float
30         axial periodicity number
31     m : float
32         azimuthal periodicity number
33     b_z : float
34         axial magnetic field
35     b_z_prime : float
36         derivative of axial magnetic field
37     b_theta : float
38         azimuthal magnetic field
39     b_theta_prime : float
40         derivative of azimuthal magnetic field
41     p_prime : float
42         derivative of pressure
43     q : float
44         safety factor
45     q_prime : float
46         derivative of safety factor
47     f_func : function
48         function used to return Newcomb's g
49
50     Returns

```

```

51  -----
52  y : ndarray of floats (2)
53      initial values for linear set of ODEs representing Euler–Lagrange
54      equation. :math:'y(0)=\xi'' and :math:'y(1)=f\backslash\xi''
55
56  Notes
57  -----
58  The expressions for xi and xi_prime are from power series expansion as
59  described in the Newcomb's paper, Goedbloed and Freidberg's MHD books.
60  """
61  y = np.zeros(2)
62
63  f_params = {'r': r, 'k': k, 'm': m, 'b_z': b_z, 'b_theta': b_theta, 'q': q}
64
65  if m == 0:
66      y[0] = r
67      y[1] = 1.
68  else:
69      y[0] = r**(abs(m) - 1.)
70      y[1] = (abs(m) - 1.)*r**(abs(m) - 2.)
71      #y[0] = r**(m - 1)
72      #y[1] = (m - 1)*r**(m - 2)
73
74  y[1] = f_func(**f_params)*y[1]
75  return y*xi_factor
76
77
78  def init_xi_given(xi, r, k, m, b_z, b_theta, q, f_func, xi_factor, *args, **kwargs):
79      r"""
80      Return y intialized with given xi and xi_prime.
81
82      Parameters
83      -----
84      r : float
85          radius
86      k : float
87          axial periodicity number
88      m : float
89          azimuthal periodicity number
90      b_z : float
91          axial magnetic field
92      b_z_prime : float
93          derivative of axial magnetic field
94      b_theta : float
95          azimuthal magnetic field
96      b_theta_prime : float
97          derivative of azimuthal magnetic field
98      p_prime : float
99          derivative of pressure
100     q : float
101         safety factor
102     q_prime : float
103         derivative of safety factor
104     f_func : function
105         function used to return Newcomb's f
106
107     Returns

```

```

108  _____
109  y : ndarray of floats (2)
110      initial values for linear set of ODEs representing Euler–Lagrange
111      equation. :math:'y(0)=\xi'' and :math:'y(1)=f\xi''
112
113  Notes
114  _____
115  The expressions for xi and xi_prime are from power series expansion as
116  described in the Newcomb's paper, Goedbloed and Freidberg's MHD books.
117  """
118  y = np.zeros(2)
119
120  f_params = {'r': r, 'k': k, 'm': m, 'b_z': b_z, 'b_theta': b_theta, 'q': q}
121
122  y[0] = xi[0]
123  y[1] = xi[1] * f_func(**f_params)
124
125  return y*xi_factor
126
127
128  def init_r_sing_glasser(r, k, m, b_z, b_theta, xi_factor, *args, **kwargs):
129      r"""
130      Returns initial condition for r close to zero.
131
132      Parameters
133      _____
134      r : float
135          radial position
136
137      k : float
138          axial periodicity number
139
140      m : float
141          azimuthal periodicity number
142
143      b_z : scipy spline
144          axial magnetic field
145
146      b_theta : scipy spline
147          azimuthal magnetic field
148
149      Returns
150      _____
151      xi : ndarray
152          newcomb's xi
153
154      Notes
155      _____
156      Implements initial condition Alan used in his code.
157
158      .. math ::
159          u(0) \&= r^{\{m - 1\}} \ \
160          u(1) \&= u(0) \frac{\{(k B_{\{z\}} r + m B_{\{\theta\}})^{\{2\}}\}m^{\{2\}}}{(m-1)}
161
162      Reference
163      _____
164      Alan Glasser's newcomb.f code.

```

```

165     """
166     xi = np.zeros(2)
167     xi[0] = r**(m - 1)
168     xi[1] = xi[0]*((k*b_z(r)*r + m*b_theta(r))/m)**2*(m - 1)
169     return xi*xi_factor

```

A.6.8 newcomb_f.py

```

1  # -*- coding: utf-8 -*-
2  """
3  Created on Wed Aug 06 13:43:55 2014
4
5  @author: Jens von der Linden
6  """
7
8  from __future__ import print_function
9  from __future__ import division
10 from __future__ import absolute_import
11 from future.builtins import (ascii, bytes, chr, dict, filter, hex, input,
12                             int, map, next, oct, open, pow, range, round,
13                             str, super, zip)
14 """Python 3.x compatibility"""
15
16 from numba import jit, float64
17
18
19 def newcomb_f_16(r, k, m, b_z, b_theta, **kwargs):
20     r"""
21     Return f from Newcomb's paper.
22
23     Parameters
24     -----
25     r : ndarray of floats
26         radius
27     k : float
28         axial periodicity number
29     m : float
30         azimuthal periodicity number
31     b_z : ndarray of floats
32         axial magnetic field
33     b_theta : ndarray of floats
34         azimuthal magnetic field
35
36     Returns
37     -----
38     f : ndarray of floats
39         f from Newcomb's paper
40
41     Notes
42     -----
43     Implements equation:
44     :math: f = \frac{r}{(k r B_z + m B_{\theta})^2} (k^2 r^2 + m^2)'
```

```

47     Reference
48     -----
49     Newcomb (1960) Hydromagnetic Stability of a Diffuse Linear Pinch
50     Equation (16)
51     """
52     params_num = {'r': r, 'k': k, 'm': m, 'b_z': b_z, 'b_theta': b_theta}
53     params_denom = {'r': r, 'k': k, 'm': m}
54     #if type(r) == float:
55     #    all_f_g.all_f.append([r, r*f_num_wo_r(**params_num)/f_denom(**params_denom)])
56     return r*f_num_wo_r(**params_num)/f_denom(**params_denom)
57
58
59 def jardin_f_8_78(r, k, m, b_z, b_theta, q):
60     r"""
61     Return f from Newcomb's paper.
62
63     Parameters
64     -----
65     r : ndarray of floats
66         radius
67     k : float
68         axial periodicity number
69     m : float
70         azimuthal periodicity number
71     b_z : ndarray of floats
72         axial magnetic field
73     b_theta : ndarray of floats
74         azimuthal magnetic field
75     q: ndarray of floats
76         safety factor
77
78     Returns
79     -----
80     f : ndarray of floats
81         f from Newcomb's paper
82
83     Reference
84     -----
85     Jardin (2010) Computational Methods in Plasma Physics
86     Equation (8.78)
87     """
88     return r*b_theta**2*(m - k*q)**2/(k**2*r**2 + m**2)
89
90
91 #@jit(float64(float64, float64, float64))
92 @jit
93 def f_denom(r, k, m):
94     r"""
95     Return denominator of f from Newcomb's paper.
96
97     Parameters
98     -----
99     r: ndarray of floats
100         radius
101     k: float
102         axial periodicity number
103     m: float

```

```

104         azimuthal periodicity number
105
106     Returns
107     -----
108     f_denom: ndarray of floats
109         denominator of f from Newcomb's paper
110
111     Notes
112     -----
113     f denominator :math:'k^{2}r^{2}+m^{2}'
114
115     Reference
116     -----
117     Newcomb (1960) Hydromagnetic Stability of a Diffuse Linear Pinch
118     Equation (16)
119     """
120     return k**2*r**2 + m**2
121
122
123 #@jit(float64(float64, float64, float64, float64, float64))
124 @jit
125 def f_num_wo_r(r, k, m, b_z, b_theta):
126     r """
127     Return numerator of f without r from Newcomb's paper.
128
129     Parameters
130     -----
131     r : ndarray of floats
132         radius
133     k : float
134         axial periodicity number
135     m : float
136         azimuthal periodicity number
137     b_z : ndarray of floats
138         axial magnetic field
139     b_theta : ndarray of floats
140         azimuthal magnetic field
141
142     Returns
143     -----
144     f_num_wo_r : ndarray of floats
145         numerator of f without r from Newcomb's paper
146
147     Notes
148     -----
149     f numerator without r: :math:'(k r B_{z}+m B_{\theta})^{2}'
150
151     Reference
152     -----
153     Newcomb (1960) Hydromagnetic Stability of a Diffuse Linear Pinch
154     Equation (16)
155     """
156     return (k*r*b_z + m*b_theta)**2
157
158
159 def f_prime(r, k, m, b_z, b_theta, b_theta_prime, **kwargs):
160     r """

```

```

161     return f_prime
162     """
163     term1 = -2.*k**2*r**2/(k**2*r**2 + m**2)**2 * (b_z*k*r + m*b_theta)**2
164     term2 = r/(k**2*r**2 + m**2)*(2.*b_z*k + 2.*m*b_theta_prime)*(b_z*k*r + m*b_theta)
165     term3 = 1./(k**2*r**2 + m**2)*(b_z*k*r + m*b_theta)**2
166     return term1 + term2 + term3

```

A.6.9 newcomb_g.py

```

1   -*- coding: utf-8 -*-
2  """
3  Created on Wed Aug 06 14:39:57 2014
4
5  @author: Jens von der Linden
6  """
7
8  from __future__ import print_function
9  from __future__ import division
10 from __future__ import absolute_import
11 from future.builtins import (ascii, bytes, chr, dict, filter, hex, input,
12                             int, map, next, oct, open, pow, range, round,
13                             str, super, zip)
14  """Python 3.x compatibility """
15
16 from newcomb_f import f_denom, f_num_wo_r
17 from numba import jit, float64
18
19
20 def jardin_g_8_80(r, k, m, b_z, b_z_prime, b_theta, b_theta_prime, p_prime, q,
21                 q_prime):
22      r """
23      Return g from Newcomb's paper.
24
25      Parameters
26      -----
27      r : ndarray of floats
28          radius
29      k : float
30          axial periodicity number
31      m : float
32          azimuthal periodicity number
33      b_z : ndarray of floats
34          axial magnetic field
35      b_theta : ndarray of floats
36          azimuthal magnetic field
37      b_theta_prime: ndarray of floats
38          azimuthal magnetic field
39      p_prime : ndarray of floats
40          pressure prime
41      q : ndarray of floats
42          safety factor
43      q_prime : ndarray of floats
44          derivative of safety factor
45      mu_0 : float

```

```

46         magnetic permeability of free space
47
48     Returns
49     -----
50     g : ndarray of floats
51         g from Newcomb's paper
52
53     Reference
54     -----
55     Jardin (2010) Computational Methods in Plasma Physics
56     Equation (8.80)
57     """
58     term1 = (2.*k**2*r**2)/(k**2*r**2+m**2)*p_prime
59     term2 = b_theta**2/r*(m-k*q)**2*(k**2*r**2+m**2-1.)/(k**2*r**2+m**2)
60     term3 = 2*k**2*r*b_theta**2/(k**2*r**2+m**2)**2*(k**2*q**2-m**2)
61     return term1 + term2 + term3
62
63
64 def jardin_g_8_79(r, k, m, b_z, b_z_prime, b_theta, b_theta_prime, p_prime, q,
65                 q_prime):
66     r"""
67     Return g from Newcomb's paper.
68
69     Parameters
70     -----
71     r : ndarray of floats
72         radius
73     k : float
74         axial periodicity number
75     m : float
76         azimuthal periodicity number
77     b_z : ndarray of floats
78         axial magnetic field
79     b_theta : ndarray of floats
80         azimuthal magnetic field
81     b_theta_prime: ndarray of floats
82         azimuthal magnetic field
83     p_prime : ndarray of floats
84         pressure prime
85     q : ndarray of floats
86         safety factor
87     q_prime : ndarray of floats
88         derivative of safety factor
89     mu_0 : float
90         magnetic permeability of free space
91
92     Returns
93     -----
94     g : ndarray of floats
95         g from Newcomb's paper
96
97     Reference
98     -----
99     Jardin (2010) Computational Methods in Plasma Physics
100    Equation (8.79)
101    """
102    term1 = 1./r*b_theta**2/(k**2*r**2+m**2)*(k*q + m)**2

```

```

103 term2 = b_theta**2/r*(m - k*q)
104 term3 = 2.*b_theta/r*(r*b_theta_prime + b_theta)
105 der_term1 = -2.*k**2*r*b_theta**2/(k**2*r**2 + m**2)**2*(k**2*q**2 -
106                                     m**2)
107 der_term2 = 2.*k**2*b_theta**2/(k**2*r**2 + m**2)*q_prime
108 der_term3 = 2.*b_theta_prime/(k**2*r**2 + m**2)*((k**2*q**2 - m**2) *
109                                     b_theta)
110 return term1 + term2 - term3 - der_term1 - der_term2 - der_term3
111
112
113 def newcomb_g_17(r, k, m, b_z, b_z_prime, b_theta, b_theta_prime, p_prime, q,
114                 q_prime):
115     r"""
116     Return g from Newcomb's paper.
117
118     Parameters
119     -----
120     r : ndarray of floats
121         radius
122     k : float
123         axial periodicity number
124     m : float
125         azimuthal periodicity number
126     b_z : ndarray of floats
127         axial magnetic field
128     b_theta : ndarray of floats
129         azimuthal magnetic field
130     b_theta_prime: ndarray of floats
131         azimuthal magnetic field
132     p_prime : ndarray of floats
133         pressure prime
134     q : ndarray of floats
135         safety factor
136     q_prime : ndarray of floats
137         derivative of safety factor
138     mu_0 : float
139         magnetic permeability of free space
140
141     Returns
142     -----
143     g : ndarray of floats
144         g from Newcomb's paper
145
146     Reference
147     -----
148     Newcomb (1960) Hydromagnetic Stability of a Diffuse Linear Pinch
149     Equation (17)
150     """
151     term1 = 1./r*(k*r*b_z - m*b_theta)**2/(k**2*r**2 + m**2)
152     term2 = 1./r*(k*r*b_z - m*b_theta)**2
153     term3 = 2.*b_theta/r*(r*b_theta_prime + b_theta)
154     der_term1 = -2.*k**2*r/(k**2*r**2 + m**2)**2*(k**2*r**2*b_z**2 -
155                                     m**2*b_theta**2)
156     der_term2 = 1./(k**2*r**2 + m**2)*(2.*k**2*r**2*b_z*b_z_prime +
157                                     2.*k**2*r*b_z**2 -
158                                     2.*m**2*b_theta*b_theta_prime)
159     return term1 + term2 - term3 - der_term1 - der_term2

```

```

160
161
162 def newcomb_g_18(r, k, m, b_z, b_theta, p_prime, mu_0, **kwargs):
163     r"""
164     Return g from Newcomb's paper.
165
166     Parameters
167     -----
168     r : ndarray of floats
169         radius
170     k : float
171         axial periodicity number
172     m : float
173         azimuthal periodicity number
174     b_z : ndarray of floats
175         axial magnetic field
176     b_theta : ndarray of floats
177         azimuthal magnetic field
178     p_prime : ndarray of floats
179         pressure prime
180     q : ndarray of floats
181         safety factor
182     mu_0 : float
183         magnetic permeability of free space
184
185     Returns
186     -----
187     g : ndarray of floats
188         g from Newcomb's paper
189
190     Notes
191     -----
192     Implements equation
193
194     .. math::
195         \frac{2}{r} k^2 r^2 \{k^2 r^2 + m^2\} \frac{dP}{dr} +
196         \frac{1}{r} (k r B_z + m B_{\theta})^2
197         \frac{k^2 r^2 + m^2 - 1}{k^2 r^2 + m^2} +
198         \frac{2k^2 r}{(k^2 r^2 + m^2)^2}
199         (k^2 r^2 B_z^2 - m^2 B_{\theta}^2)
200
201     Reference
202     -----
203     Newcomb (1960) Hydromagnetic Stability of a Diffuse Linear Pinch
204     Equation (18)
205     """
206     term1 = 2.*k**2*r**2/(f_denom(r, k, m))*p_prime*mu_0
207     term2 = (1./r*f_num_wo_r(r, k, m, b_z, b_theta)*(k**2*r**2+m**2-1.) /
208             f_denom(r, k, m))
209     term3 = (2.*k**2*r/f_denom(r, k, m)**2 *
210             (k**2*r**2*b_z**2 - m**2*b_theta**2))
211     #if type(r) == float:
212     #    all_f_g.all_g.append([r, term1 + term2 + term3])
213     return term1 + term2 + term3
214
215
216 def newcomb_g_18_dimless(r, k, m, b_z, p_prime, q, beta_0, **kwargs):

```

```

217     r"""
218     Return g from Newcomb's paper in dimensionless form. g only depends on b_z,
219     b_theta is cacluated from q and b_z.
220
221     Parameters
222     -----
223     r : float
224         radial position
225     k : float
226         axial periodicity number
227     m : float
228         azimuthal periodicity number
229     b_z : float
230         axial magnetic field
231     p_prime : float
232         pressure gradient
233     q : safety factor
234     beta_0 : float
235         beta on axis
236
237     Returns
238     -----
239     g : dimensionless g
240
241     Notes
242     -----
243     Implements equation
244
245     .. math::
246         \frac{\beta_0}{k} \frac{r^2}{r^2 + m^2} \frac{dr}{dr} +
247         r(k B_z)^2 \frac{r^2 + m^2 - 1}{k^2 r^2 + m^2} \frac{dr}{dr} +
248         \frac{1}{m} B_{\theta}^2 \frac{r^2 + m^2 - 1}{k^2 r^2 + m^2} \frac{dr}{dr} +
249         2k B_z B_{\theta} \frac{r^2 + m^2 - 1}{k^2 r^2 + m^2} \frac{dr}{dr} +
250         \frac{2k^4 r^3 B_z}{k^2 r^2 + m^2} -
251         \frac{2k^2 m^2 r B_{\theta}^2}{k^2 r^2 + m^2}
252
253     """
254     term1 = beta_0*k**2*r**2/f_denom(r, k, m)*p_prime
255     term2 = r*(k*b_z)**2*(k**2*r**2 + m**2-1.)/f_denom(r, k, m)
256     term3 = m**2*1./r*(b_z*r*k/q)**2*(k**2*r**2+m**2-1.)/ f_denom(r, k, m)
257     term4 = 2.*m*k**2*r*b_z**2/q*(k**2*r**2 + m**2-1.)/(k**2*r**2 + m**2)
258     term5 = 2*k**4*r**3*b_z**2/f_denom(r, k, m)**2
259     term6 = -m**2*2.*k**4*r**3*b_z**2/(q**2*f_denom(r, k, m)**2)
260     #if type(r) == float:
261     #    all_f_g.all_g.append([r, term1 + term2 + term3 + term4 + term5 + term6])
262     #    all_f_g.all_g_term1.append([r, term1])
263     #    all_f_g.all_g_term2.append([r, term2])
264     #    all_f_g.all_g_term3.append([r, term3])
265     #    all_f_g.all_g_term4.append([r, term4])
266     #    all_f_g.all_g_term5.append([r, term5])
267     #    all_f_g.all_g_term6.append([r, term6])
268     return term1 + term2 + term3 + term4 + term5 + term6
269
270
271     #@jit(float64(float64, float64, float64, float64, float64, float64, float64))
272     #@jit
273     def newcomb_g_18_dimless_wo_q(r, k, m, b_z, b_theta, p_prime, beta_0):

```

```

274     r"""
275     Return g from Newcomb's paper in dimensionless form.
276
277     Parameters
278     -----
279     r : float
280         radial position
281     k : float
282         axial periodicity number
283     m : float
284         azimuthal periodicity number
285     b_z : float
286         axial magnetic field
287     p_prime: float
288         pressure gradient
289     beta_0 : float
290         beta on axis
291
292     Returns
293     -----
294     g : dimensionless g
295
296     Notes
297     -----
298     Implements equation
299
300     .. math::
301         \frac{2}{r} k^2 r^2 \{k^2 r^2 + m^2\} \frac{dP}{dr} +
302         \frac{1}{r} (k r B_z + m B_{\theta})^2
303         \frac{k^2 r^2 + m^2 - 1}{k^2 r^2 + m^2} +
304         \frac{2k^2 r}{(k^2 r^2 + m^2)^2}
305         (k^2 r^2 B_z^2 - m^2 B_{\theta}^2) \text{return g from Newcomb's paper in dimensionless form.}
306     """
307     term1 = beta_0 * k**2 * r**2 / f_denom(r, k, m) * p_prime
308     term2 = r * (k * b_z)**2 * (k**2 * r**2 + m**2 - 1.) / f_denom(r, k, m)
309     term3 = 1. / r * (m * b_theta)**2 * (k**2 * r**2 + m**2 - 1.) / f_denom(r, k, m)
310     term4 = 2. * m * k * b_z * b_theta * (k**2 * r**2 + m**2 - 1.) / f_denom(r, k, m)
311     term5 = 2. * k**4 * r**3 * b_z**2 / f_denom(r, k, m)**2
312     term6 = -2. * k**2 * m**2 * r * b_theta**2 / f_denom(r, k, m)**2
313     #if type(r) == type(r):
314     #    all_f_g.all_g.append([r, term1 + term2 + term3 + term4 + term5 + term6])
315     #    all_f_g.all_g_term1.append([r, term1])
316     #    all_f_g.all_g_term2.append([r, term2])
317     #    all_f_g.all_g_term3.append([r, term3])
318     #    all_f_g.all_g_term4.append([r, term4])
319     #    all_f_g.all_g_term5.append([r, term5])
320     #    all_f_g.all_g_term6.append([r, term6])
321     #    all_f_g.all_pressure_prime.append([r, p_prime])
322     #    all_f_g.all_b_theta.append([r, b_theta])
323     #    all_f_g.all_b_z.append([r, b_z])
324     #    all_f_g.all_beta_0.append([r, beta_0])
325     #    all_f_g.all_m.append([r, m])
326     #    all_f_g.all_k.append([r, k])
327     return term1 + term2 + term3 + term4 + term5 + term6

```

A.6.10 `find_singularities`

```

1  # -*- coding: utf-8 -*-
2  """
3  Created on Mon Sep 22 20:27:04 2014
4
5  @author: Jens von der Linden
6
7  Identify singularities in Euler-Lagrange
8  by searching for zeros of  $f$ .
9  """
10
11 from __future__ import print_function
12 from __future__ import division
13 from __future__ import absolute_import
14 from future.builtins import (ascii, bytes, chr, dict, filter, hex, input,
15                             int, map, next, oct, open, pow, range, round,
16                             str, super, zip)
17 """Python 3.x compatibility"""
18
19 import numpy as np
20 import scipy.optimize as opt
21 from scipy.interpolate import splev
22
23
24 def identify_singularities(a, b, points, k, m, b_z_spl, b_theta_spl, offset,
25                          tol, **kwargs):
26     """
27     Return list of singular points.
28
29     Parameters
30     -----
31     a : float
32         radial start of pinch
33     b : float
34         radial end of pinch
35     points : int
36         number of points through which to divide  $f$ 
37     k : float
38         axial periodicity number
39     m : float
40         azimuthal periodicity number
41     b_z_spl : scipy spline object
42         axial magnetic field
43     b_theta_spl : scipy spline object
44         azimuthal magnetic field
45
46     Returns
47     -----
48     zero_positions: ndarray of floats (M)
49         radial positions at which  $r$  equals zero.
50
51     Notes
52     -----
53     Singular points are found by dividing  $f$  into intervals checking for sign
54     changes and then running a zero finding method from the scipy optimize

```

```

55     module.
56     """
57     params = (k, m, b_z_spl, b_theta_spl)
58     r = np.linspace(a, b, points)
59     zero_positions = []
60
61     sign = np.sign(f_relevant_part(r, k, m, b_z_spl, b_theta_spl))
62     for i in range(points-1):
63         if abs(sign[i] + sign[i+1]) < 1e-8:
64             zero_pos = opt.brentq(f_relevant_part, r[i], r[i+1], args=params)
65             zero = f_relevant_part(r[i], k, m, b_z_spl, b_theta_spl)
66             if np.isnan(zero) or abs(zero) > tol:
67                 continue
68             else:
69                 zero_positions.append(zero_pos)
70
71     sings = np.array(zero_positions)
72
73     if not sings.size == 0 and abs(sings[0]) < 1e-8:
74         sings_wo_0 = np.delete(sings, 0)
75     else:
76         sings_wo_0 = sings
77
78     integration_points = np.insert((float(a), float(b)), 1, sings_wo_0)
79     intervals = [[integration_points[i],
80                  integration_points[i+1]]
81                 for i in range(integration_points.size-1)]
82
83     return sings, sings_wo_0, intervals
84
85
86 def f_relevant_part(r, k, m, b_z_spl, b_theta_spl):
87     """
88     Return relevant part of f for singularity detection.
89
90     Parameters
91     -----
92     r : ndarray of floats
93         radial points
94     k : float
95         axial periodicity number
96     m : float
97         azimuthal periodicity number
98     b_z_spl : scipy spline object
99         axial magnetic field
100    b_theta_spl : scipy spline object
101        azimuthal magnetic field
102
103    Returns
104    -----
105    f_relevant_part : ndarray of floats
106        The relevant part of eigenfunctions = []
107    eigen_ders = []
108    rs_list = [] f Newcomb's f for determining f=0. The term that can
109        make f=0 when :math:'r \neq 0'
110
111    Notes

```

```

112  -----
113  The relevant part of f is:
114  .. math::
115      $k r B_{\{z\}} + m B_{\{\theta\}}$ 
116  """
117  b_theta = splev(r, b_theta_spl)
118  b_z = splev(r, b_z_spl)
119  return f_relevant_part_func(r, k, m, b_z, b_theta)
120
121
122  def f_relevant_part_func(r, k, m, b_z, b_theta):
123  """
124  Return relevant part of f for singularity detection. Could be compiled be
125  with numba.
126
127  Parameters
128  -----
129  r : ndarray of floats
130     radial points
131  k : float
132     axial periodicity number
133  m : float
134     azimuthal periodicity number
135  b_z : ndarray of floats
136     axial magnetic field
137  b_theta : ndarray of floats
138     azimuthal magnetic field
139
140  Returns
141  -----
142  f_relevant_part : ndarray of floats
143     The relevant part of Newcomb's f for determining f=0. The term that can
144     make f=0 when :math:'r \neq 0'
145
146  Notes
147  -----
148  The relevant part of f is:
149  .. math::
150      $k r B_{\{z\}} + m B_{\{\theta\}}$ 
151  """
152  return k*r*b_z + m*b_theta
153
154
155  def f_relevant_part_der(r, k, m, b_z_spl, b_theta_prime_spl):
156  r"""
157  Prefunction to derivative of f_relevant_part.
158  """
159  b_z = b_z_spl(r)
160  b_theta_prime = splev(r, b_theta_prime_spl)
161  return f_relevant_part_der_func(r, k, m, b_z, b_theta_prime)
162
163
164  def f_relevant_part_der_func(r, k, m, b_z, b_theta_prime):
165  r"""
166  Derivative of f_relevant_part.
167  """
168  return k*b_z + m*b_theta_prime

```

```

169
170
171 def f_relevant_part_der_2(r, m, b_theta_prime_prime_spl):
172     r"""
173     Prefunction to Second derivative of f_relevant_part.
174     """
175     b_theta_prime_prime = splev(r, b_theta_prime_prime_spl)
176     return f_relevant_part_der_2_func(r, m, b_theta_prime_prime)
177
178
179 def f_relevant_part_der_2_func(r, m, b_theta_prime_prime):
180     r"""
181     Second derivative of f_relevant_part.
182     """
183     return m*b_theta_prime_prime

```

A.6.11 singularity_frobenius.py

```

1  # -*- coding: utf-8 -*-
2  """
3  Created on Thu Aug 21 13:23:31 2014
4
5  @author: Jens von der Linden
6
7  Implements Frobenius expansion around a singularity to determine the "small"
8  solution and check the Suydam condition.
9  """
10
11 from __future__ import print_function
12 from __future__ import division
13 from __future__ import absolute_import
14 from future.builtins import (ascii, bytes, chr, dict, filter, hex, input,
15                             int, map, next, oct, open, pow, range, round,
16                             str, super, zip)
17 """Python 3.x compatibility"""
18
19 import numpy as np
20 from scipy.interpolate import splev
21
22
23 def alpha_func(r, b_z, b_z_prime, b_theta, b_theta_prime, **kwargs):
24     r"""
25     Return alpha for Frobenius solution.
26
27     Parameters
28     -----
29     r : ndarray of floats
30         radial position of singularity
31     b_z : ndarray of floats
32         axial magnetic field
33     b_z_prime : ndarray of floats
34         derivative of axial magnetic field
35     b_theta : ndarray of floats
36         azimuthal magnetic field

```

```

37     b_theta_prime : ndarray of floats
38         derivative of azimuthal magnetic field
39
40     Returns
41     -----
42     alpha : ndarray of floats
43         beta of quadratic equation for the exponents of the Frobenius solutions
44     """
45     mu = b_theta/(r*b_z)
46     mu_prime = (r*b_z*b_theta_prime - b_theta*(b_z + r*b_z_prime)) / (r*b_z)**2
47     return r*b_theta**2*b_z**2/(b_theta**2 + b_z**2)*(mu_prime / mu)**2
48
49
50 def beta_func(b_z, b_theta, p_prime, beta_0, **kwargs):
51     r"""
52     Return beta for Frobenius solution.
53
54     Parameters
55     -----
56     b_z : ndarray of floats
57         axial magnetic field
58     b_theta: ndarray of floats
59         azimuthal magnetic field
60     p_prime : ndarray of floats
61         derivative of pressure
62     Returns
63     -----
64     beta : ndarray of floats
65         beta of quadratic equation for the exponents of the Frobenius solutions
66     """
67     return 2.*beta_0*b_theta**2/(b_theta**2 + b_z**2) * p_prime
68
69
70 def nu_1_2(alpha, beta, imaginary=False, **kwargs):
71     r"""
72     Return exponents of Frobenius solution.
73
74     Paramters
75     -----
76     alpha : ndarray of floats
77         alpha of quadratic equation for the exponents of the Frobenius
78         solutions
79     beta : ndarray of floats
80         beta of quadratic equation for the exponents of the Frobenius solutions
81     Returns
82     -----
83     nu_1 : ndarray of floats
84         exponent 1 of Frobenius solution
85     nu_2 : ndarray of floats
86         exponent 1 of Frobenius solution
87     """
88     nu_1 = -0.5 + np.emath.sqrt(0.25 + beta/alpha)
89     nu_2 = -0.5 - np.emath.sqrt(0.25 + beta/alpha)
90     return nu_1, nu_2
91
92
93 def sings_alpha_beta(r, b_z_spl, b_z_prime_spl, b_theta_spl, b_theta_prime_spl,

```

```

94         p_prime_spl, beta_0):
95     r"""
96     Returns alpha and beta at the singularity.
97
98     Parameters
99     -----
100    r : ndarray of floats
101         positions of singularities
102    b_z_spl : scipy spline object
103         axial magnetic field
104    b_theta_spl : scipy spline object
105         azimuthal magnetic field
106    p_prime_spl : scipy spline object
107         derivative of pressure
108
109     Returns
110     -----
111    alpha : ndarray of floats
112         alpha of quadratic equation for the exponents of the Frobenius
113         solutions
114    beta : ndarray of floats
115         beta of quadratic equation for the exponents of the Frobenius solutions
116    """
117    if r.size == 0:
118        return np.empty(0), np.empty(0)
119    else:
120        b_z = splev(r, b_z_spl)
121        b_z_prime = splev(r, b_z_prime_spl)
122        b_theta = splev(r, b_theta_spl)
123        b_theta_prime = splev(r, b_theta_prime_spl)
124        p_prime = splev(r, p_prime_spl)
125        params = {'r': r, 'b_z': b_z, 'b_z_prime': b_z_prime,
126                'b_theta': b_theta, 'b_theta_prime': b_theta_prime,
127                'p_prime': p_prime, 'beta_0': beta_0}
128        alpha = alpha_func(**params)
129        beta = beta_func(**params)
130        return alpha, beta
131
132
133 def sings_suydam_stable(r, b_z_spl, b_z_prime_spl, b_theta_spl,
134                        b_theta_prime_spl, p_prime_spl, beta_0):
135     r"""
136     Returns bool array. True for singularities that are Suydam stable and False
137     for unstable singularities.
138
139     Parameters
140     -----
141    r : ndarray of floats
142         singularity positions
143    b_z_spl : scipy spline object
144         axial magnetic field
145    b_theta_spl : scipy spline object
146         azimuthal magnetic field
147    p_prime_spl : scipy spline object
148         derivative of pressure
149
150     Returns

```

```

151  _____
152  stable_mask : ndarray of bool
153      bool array of Suydam stable singularities can be used as a mask for
154      indexing.
155  """
156  alpha, beta = sings_alpha_beta(r, b_z_spl, b_z_prime_spl, b_theta_spl,
157                                b_theta_prime_spl, p_prime_spl, beta_0)
158  return suydam_stable(alpha, beta)
159
160
161  def sing_small_solution(r_sing, offset, b_z_spl, b_z_prime_spl, b_theta_spl,
162                        b_theta_prime_spl, p_prime_spl, q_spl, f_func, beta_0,
163                        r_request=None):
164      r """
165      Returns small solution of Frobenius expansion near singularity in y form of
166      ODE set.
167
168      Parameters
169      _____
170      r_sing : ndarray of floats
171          position of singularities
172      offset : float
173          offset from singularity for integration
174      b_z_spl : scipy spline object
175          axial magnetic field
176      b_theta_spl : scipy spline object
177          azimuthal magnetic field
178      p_prime_spl : scipy spline object
179          derivative of pressure
180      q_spl : scipy spline object
181          safety factor
182      f_func : function
183          function
184
185      Returns
186      _____
187      small_sol : ndarray of floats (2)
188          small solution xi and xi_prime to be used in an init function.
189
190      References
191      _____
192      Newcomb (1960) Hydromagnetic Stability of a Diffuse Linear Pinch
193      """
194      alpha, beta = sings_alpha_beta(r_sing, b_z_spl, b_z_prime_spl, b_theta_spl,
195                                    b_theta_prime_spl, p_prime_spl, beta_0)
196
197      nu_1, nu_2 = nu_1_2(alpha, beta)
198      if not r_request:
199          r = r_sing + offset
200      else:
201          r = r_request
202      small_sol = small_solution(r_sing + offset, r_sing, nu_1, nu_2)
203      return small_sol
204
205
206  def suydam_stable(alpha, beta):
207      r """

```

```

208     Returns suydam condition.
209
210     Parameters
211     -----
212     alpha : ndarray of floats
213         alpha of quadratic equation for the exponents of the Frobenius
214         solutions
215     beta : scipy spline
216         beta of quadratic equation for the exponents of the Forbenius solutions
217
218     Returns
219     -----
220     suydam : ndarray of bool
221         suydam stable
222
223     Notes
224     -----
225     This ithe criterion for oscillatory solutions near singularity.
226
227     Reference
228     -----
229     Newcomb (1960) Hydromagnetic Stability of a Diffuse Linear Pinch
230     eq (5).
231     Jardin (2010) Computational Mehtods in Plasma Physics. eq (8.84)
232     """
233     return alpha + 4.*beta > 0.
234
235
236 def small_solution(r, r_sing, nu_1, nu_2):
237     r"""
238     Returns xi and f*xi_der of the small solution close to a singularity.
239
240     Parameters
241     -----
242     r : float
243         position at which small solution is desired
244     r_sing : float
245         position of singularity
246     nu_1 : float
247         exponent 1 of Frobenius solution
248     nu_2 : float
249         exponent 2 of Frobenius solution
250
251     Returns
252     -----
253     small_sol : ndarry of floats (2)
254         small solution near singularity
255
256     Reference
257     -----
258     Newcomb (1960) Hydromagnetic Stability of a Diffuse Linear Pinch (p. 243)
259     """
260     x = np.abs(r - r_sing)
261     if nu_1 < nu_2:
262         return np.array([np.real(x**nu_2), np.real(nu_2*x**(nu_2 - 1.))])
263     else:
264         return np.array([np.real(x**nu_1), np.real(nu_1*x**(nu_1 - 1.))])

```

A.6.12 external_stability.py

```

1  # -*- coding: utf-8 -*-
2  """
3  Created on Mon Sep 08 20:42:30 2014
4
5  @author: Jens von der Linden
6
7  Calculate dW and determine external stability.
8  """
9
10 from __future__ import print_function
11 from __future__ import division
12 from __future__ import absolute_import
13 from future.builtins import (ascii, bytes, chr, dict, filter, hex, input,
14                             int, map, next, oct, open, pow, range, round,
15                             str, super, zip)
16 """Python 3.x compatibility"""
17
18 import scipy.special as spec
19 from scipy.interpolate import splev
20 import analytic_condition as ac
21
22 def external_stability(params, xi, xi_der, dim_less=False):
23     r"""
24     Returns external external stability and dW.
25     """
26     a = params['a']
27     b_z = splev(a, params['b_z'])
28     b_theta = splev(a, params['b_theta'])
29     m = params['m']
30     k = params['k']
31     magnetic_potential_energy_ratio = params['magnetic_potential_energy_ratio']
32
33     if params['b'] == 'infinity':
34         lambda_term = lambda_infinity(**{'a': a, 'k': k, 'm': m})
35     else:
36         assert isinstance(params['b'], float), "b must be 'infinity' or of \
37             type float."
38         lambda_term = lambda_boundary(**{'a': a, 'b': b, 'k': k, 'm': m})
39     f_term = capital_f(**{'a': a, 'k': k, 'm': m, 'b_theta': b_theta,
40                        'b_z': b_z})
41     f_adjoint_term = f_adjoint(**{'a': a, 'k': k, 'm': m, 'b_theta': b_theta,
42                                'b_z': b_z})
43     k_0_sq_term = k_0(**{'k': k, 'm': m, 'a': a})
44
45     term1 = f_term**2*a*xi_der/(k_0_sq_term*xi)
46     term2 = f_term*f_adjoint_term/(k_0_sq_term)
47     term3 = a**2*f_term**2*lambda_term
48     delta_w = (term1+term2*term3)*xi**2
49     if dim_less:
50         delta_w = magnetic_potential_energy_ratio * delta_w

```

```

51     stable = delta_w > 0
52     return stable, delta_w
53
54 def lambda_infinity(a, k, m):
55     r"""
56     Return lambda term for wall at infinity.
57     """
58     k_a = spec.kv(m, abs(k)*a)
59     k_a_prime = spec.kvp(m, abs(k)*a)
60
61     return -k_a/(abs(k*a)*k_a_prime)
62
63
64 def lambda_boundary(a, b, k, m):
65     r"""
66     Return lambda term for wall at radius b.
67     """
68     k_a = spec.kv(m, abs(k)*a)
69     k_a_prime = spec.kvp(m, abs(k)*a)
70     k_b_prime = spec.kvp(m, abs(k)*b)
71     i_a = spec.iv(m, abs(k)*a)
72     i_a_prime = spec.ivp(m, abs(k)*a)
73     i_b_prime = spec.ivp(m, abs(k)*b)
74
75     factor1 = -k_a/(abs(k*a)*k_a_prime)
76     factor2_num = 1. - k_b_prime*i_a/(i_b_prime*k_a)
77     factor2_denom = 1. - k_b_prime*i_a_prime/(i_b_prime*k_a_prime)
78     return factor1*factor2_num/factor2_denom
79
80
81 def k_0(k, m, a):
82     r"""
83     Return k_0 term.
84     """
85     return k**2 + m**2 / a**2
86
87
88 def f_adjoint(a, k, m, b_theta, b_z):
89     r"""
90     Return adjoint F.
91     """
92     return k*b_z - m*b_theta/a
93
94
95 def capital_f(a, k, m, b_theta, b_z):
96     r"""
97     Return F.
98     """
99     return k*b_z + m*b_theta/a
100
101
102 def external_stability_from_notes(params, xi, xi_der, dim_less=False):
103     a = params['a']
104     b_z = splev(a, params['b_z'])
105     b_theta = splev(a, params['b_theta'])
106     m = params['m']
107     k_bar = params['k']

```



```

165         dW = ac.conditions_without_interface(k_bar, lambda_bar, m, delta)
166     stable = dW > 0
167     return stable, dW

```

A.6.13 `lambda_k_plotting.py`

```

1  # -*- coding: utf-8 -*-
2  """
3  Created on Mon Feb 16 00:30:53 2015
4
5  @author: jensv
6
7  Module for examining stability spaces.
8  """
9
10 from __future__ import print_function, unicode_literals, division
11 from __future__ import absolute_import
12 from future import standard_library, utils
13 from future.builtins import (ascii, bytes, chr, dict, filter, hex, input,
14                             int, map, next, oct, open, pow, range, round,
15                             str, super, zip)
16
17 import numpy as np
18 from scipy.special import kv, kvp
19 import analytic_condition as ac
20 from scipy.interpolate import griddata
21
22 import matplotlib.pyplot as plt
23 from matplotlib.colors import SymLogNorm, BoundaryNorm
24 from matplotlib.ticker import FormatStrFormatter, FixedFormatter
25 import matplotlib.patches as patches
26 import matplotlib.ticker as ticker
27 import seaborn as sns
28 sns.set_style('white')
29 sns.set_context('poster')
30
31
32 def plot_lambda_k_space_dw(filename, epsilon, name, mode_to_plot='m_neg_1',
33                          show_points=False, lim=None, levels=None, log=True,
34                          lenthresh=1E-7, bounds=(1.5, 3.0), norm=True,
35                          analytic_compare=False,
36                          label_pos=((0.5, 0.4), (2.1, 0.4), (2.8, 0.2)),
37                          delta_values=[-1,0,1],
38                          interpolate=False,
39                          cmap=None, hatch=False,
40                          figsize=None,
41                          save_as=None,
42                          return_ax=False,
43                          axes=None):
44     r"""
45     Plot the delta_w of external instabilities in the lambda-k space.
46     """
47     if figsize:
48         fig = plt.figure(figsize=figsize)

```



```

106         cbar = plt.colorbar(label=r '$\delta W$')
107         cbar.set_label(label=r '$\delta W$', size=45, rotation=0, labelpad=30)
108         contourlines = plt.contour(lambda_a_mesh, k_a_mesh,
109                                   values, levels=levels,
110                                   colors='grey')
111     else:
112         if log:
113             plot = plt.contourf(lambda_a_mesh, k_a_mesh, values,
114                                 cmap=instability_palette[mode_to_plot],
115                                 norm=SymLogNorm(linthresh))
116             cbar = plt.colorbar(label=r '$\delta W$')
117             cbar.set_label(label=r '$\delta W$', size=45, rotation=0, labelpad=30)
118             contourlines = plt.contour(lambda_a_mesh, k_a_mesh,
119                                       values, colors='grey',
120                                       norm=SymLogNorm(linthresh))
121         else:
122             plot = plt.contourf(lambda_a_mesh, k_a_mesh, values,
123                                 cmap=instability_palette[mode_to_plot])
124             cbar = plt.colorbar(label=r '$\delta W$')
125             cbar.set_label(label=r '$\delta W$', size=45, rotation=0, labelpad=30)
126             contourlines = plt.contour(lambda_a_mesh, k_a_mesh,
127                                       values, colors='grey')
128
129     if lim:
130         plot.set_clim(lim)
131
132     cbar.add_lines(contourlines)
133
134     plt.plot([0.01, 0.1, 1.0, 2.0, 3.0],
135             [0.005, 0.05, 0.5, 1.0, 1.5], color='black')
136
137     axes = plt.gca()
138     axes.set_axis_bgcolor(sns.xkcd_rgb['white'])
139
140     lambda_bar_analytic = np.linspace(0.01, 3., 750)
141     k_bar_analytic = np.linspace(0.01, 1.5, 750)
142     (lambda_bar_mesh_analytic,
143      k_bar_mesh_analytic) = np.meshgrid(lambda_bar_analytic, k_bar_analytic)
144
145     if analytic_compare:
146         analytic_comparison(mode_to_plot, k_bar_mesh_analytic,
147                             lambda_bar_mesh_analytic, epsilon, label_pos)
148
149     if show_points:
150         plt.scatter(lambda_a_mesh, k_a_mesh, marker='o', c='b', s=5)
151
152     plt.ylim(0.01, bounds[0])
153     plt.xlim(0.01, bounds[1])
154     axes = plt.gca()
155     axes.set_xticks(np.arange(0., 4.5, 1.))
156     axes.set_yticks(np.arange(0., 2.0, 0.5))
157     plt.setp(axes.get_xticklabels(), fontsize=30)
158     plt.setp(axes.get_yticklabels(), fontsize=30)
159     plt.ylabel(r '$\bar{k}$', fontsize=40, rotation='horizontal', labelpad=30)
160     plt.xlabel(r '$\bar{\lambda}$', fontsize=40)
161     cbar.ax.tick_params(labelsize=30)
162     def my_formatter_fun(x):

```

```

163     if x == 0:
164         return r'$0$'
165     if np.sign(x) > 0:
166         return r'$10^{%i}$' % np.int(np.log10(x))
167     else:
168         return r'$-10^{%i}$' % np.int(np.log10(np.abs(x)))
169 labels = [my_formatter_fun(level) for level in levels]
170 cbar.ax.set_yticklabels(labels)
171 sns.despine(ax=axes)
172
173 if hatch:
174     xmin, xmax = axes.get_xlim()
175     ymin, ymax = axes.get_ylim()
176     xy = (xmin, ymin)
177     width = xmax - xmin
178     height = ymax - ymin
179     p = patches.Rectangle(xy, width, height, hatch='+', fill=None, zorder=-10)
180     axes.add_patch(p)
181
182 plt.tight_layout()
183 if return_ax:
184     return axes, cbar
185 else:
186     plt.savefig('../output/plots/' + name + '.png')
187     if save_as:
188         plt.savefig(save_as)
189     plt.show()
190
191
192 def interpolate_nans(lambda_a, k_a, quantity):
193     r"""
194     Return mesh with nans interpolated from neighboring values.
195     """
196     index_to_keep = np.isnan(quantity.ravel())
197     interp_values = quantity.ravel()[~index_to_keep]
198     interp_k = k_a.ravel()[~index_to_keep]
199     interp_lambda = lambda_a.ravel()[~index_to_keep]
200     return griddata((interp_lambda, interp_k),
201                    interp_values,
202                    (lambda_a, k_a),
203                    method='linear')
204
205
206 def plot_dW_given_delta(filename, epsilon, name, mode_to_plot='m_neg_1',
207                        show_points=False, lim=None, levels=None, log=False,
208                        linthresh=1E-7, bounds=(1.5, 3.0), floor_norm=False,
209                        analytic_compare=False,
210                        label_pos=((0.5, 0.4), (2.1, 0.4), (2.8, 0.2)),
211                        delta_values=[-1, 0, 1],
212                        interpolate=False, with_interface=False):
213     r"""
214     Plot the delta_w of external instabilities in the lambda-k space.
215     """
216     epsilon_case = np.load(filename)
217     lambda_a_mesh = epsilon_case['lambda_a_mesh']
218     k_a_mesh = epsilon_case['k_a_mesh']
219

```

```

220 delta_mesh_sausage = epsilon_case['delta_m_0']
221 delta_mesh_kink = epsilon_case['delta_m_neg_1']
222
223 epsilon_case.close()
224
225 if with_interface:
226     external_sausage_norm = ac.conditions(k_a_mesh, lambda_a_mesh, epsilon,
227                                         0, delta_mesh_sausage)
228     external_m_neg_1_norm = ac.conditions(k_a_mesh, lambda_a_mesh, epsilon,
229                                         1, delta_mesh_kink)
230 else:
231     external_sausage_norm = ac.conditions_without_interface(k_a_mesh,
232                                                            lambda_a_mesh,
233                                                            epsilon,
234                                                            0,
235                                                            delta_mesh_sausage)
236     external_m_neg_1_norm = ac.conditions_without_interface(k_a_mesh,
237                                                            lambda_a_mesh,
238                                                            epsilon,
239                                                            1,
240                                                            delta_mesh_kink)
241
242 instability_map = {'m_0': external_sausage_norm,
243                  'm_neg_1': external_m_neg_1_norm}
244
245 kink_pal = sns.blend_palette([sns.xkcd_rgb["dandelion"],
246                             sns.xkcd_rgb["white"]], 7, as_cmap=True)
247 kink_pal = sns.diverging_palette(73, 182, s=72, l=85, sep=1, n=9, as_cmap=True)
248 sausage_pal = sns.blend_palette(['orange', 'white'], 7, as_cmap=True)
249 sausage_pal = sns.diverging_palette(49, 181, s=99, l=78, sep=1, n=9, as_cmap=True)
250 instability_palette = {'m_0': sausage_pal,
251                      'm_neg_1': kink_pal}
252
253 if interpolate:
254     instability_map['m_neg_1'] = interpolate_nans(lambda_a_mesh,
255                                                  k_a_mesh,
256                                                  instability_map['m_neg_1']
257                                                  )
258
259 values = instability_map[mode_to_plot]
260
261 if floor_norm:
262     values = np.clip(values, -100., 100.)
263     values = values / -np.nanmin(values)
264     values = np.clip(values, -1., 1.)
265 else:
266     values = values / -np.nanmin(values)
267
268 if levels:
269     if log:
270         plot = plt.contourf(lambda_a_mesh, k_a_mesh, values,
271                             cmap=instability_palette[mode_to_plot],
272                             levels=levels, norm=SymLogNorm(linthresh))
273     else:
274         norm = BoundaryNorm(levels, 256)
275         plot = plt.contourf(lambda_a_mesh, k_a_mesh, values,
276                             cmap=instability_palette[mode_to_plot],

```

```

277         levels=levels, norm=norm)
278     cbar = plt.colorbar(label=r'$\delta W$',
279                        format=FormatStrFormatter('%0e'))
280     cbar.set_label(label=r'$\delta W$', size=45, rotation=0, labelpad=30)
281     contourlines = plt.contour(lambda_a_mesh, k_a_mesh, values,
282                               levels=levels[:-1], colors='grey')
283     cbar.add_lines(contourlines)
284 else:
285     if log:
286         plot = plt.contourf(lambda_a_mesh, k_a_mesh, values,
287                             cmap=instability_palette[mode_to_plot],
288                             norm=SymLogNorm(linthresh))
289     else:
290         plot = plt.contourf(lambda_a_mesh, k_a_mesh, values,
291                             cmap=instability_palette[mode_to_plot])
292
293     if lim:
294         plot.set_clim(lim)
295     plt.plot([0.01, 0.1, 1.0, 2.0, 3.0],
296            [0.005, 0.05, 0.5, 1.0, 1.5], color='black')
297
298     axes = plt.gca()
299     axes.set_axis_bgcolor(sns.xkcd_rgb['grey'])
300
301     lambda_bar = np.linspace(0.01, 3., 750)
302     k_bar = np.linspace(0.01, 1.5, 750)
303     lambda_bar_mesh, k_bar_mesh = np.meshgrid(lambda_bar, k_bar)
304
305     if analytic_compare:
306         analytic_comparison(mode_to_plot, k_bar_mesh, lambda_bar_mesh, epsilon,
307                             label_pos)
308
309     if show_points:
310         plt.scatter(lambda_a_mesh, k_a_mesh, marker='o', c='b', s=5)
311     plt.ylim(0.01, bounds[0])
312     plt.xlim(0.01, bounds[1])
313     axes = plt.gca()
314     plt.setp(axes.get_xticklabels(), fontsize=40)
315     plt.setp(axes.get_yticklabels(), fontsize=40)
316     plt.ylabel(r'$\bar{k}$', fontsize=45, rotation='horizontal', labelpad=30)
317     plt.xlabel(r'$\bar{\lambda}$', fontsize=45)
318     cbar.ax.tick_params(labelsize=40)
319     sns.despine(ax=axes)
320     plt.tight_layout()
321     plt.savefig('../output/plots/' + name + '.png')
322     plt.show()
323
324
325 def analytic_comparison_flex(mode_to_plot, k_bar_mesh, lambda_bar_mesh, epsilon,
326                             delta_values, label_pos):
327     r"""
328     Add red lines indicating stability boundaries from analytical model.
329     """
330     line_labels = FixedFormatter(delta_values)
331
332     assert (mode_to_plot == 'm_neg_1' or
333           mode_to_plot == 'm_0'), ("Please specify mode_to_plot as either " +

```

```

334         "m_neg_1 or m_0")
335
336     if mode_to_plot == 'm_neg_1':
337         m = 1
338         color = 'red'
339     if mode_to_plot == 'm_0':
340         m = 0
341         color = 'red'
342
343
344     stability_kink_given_delta = []
345
346     for delta in delta_values:
347         stability_kink_given_delta.append(ac.conditions(k_bar_mesh,
348                                                         lambda_bar_mesh,
349                                                         epsilon,
350                                                         m,
351                                                         delta))
352
353
354     stability_kink = stability_kink_given_delta[0] < 0
355     stability_kink = stability_kink.astype(float)
356     stability_kink[stability_kink_given_delta[0] >= 0] = -1.5
357     stability_kink[stability_kink_given_delta[0] < 0] = -0.5
358     value = 0.5
359
360     for i in range(len(delta_values[1:])):
361         stability_kink[stability_kink_given_delta[i] < 0] = value
362         value += 1.
363
364     levels = np.array(range(len(delta_values))) - 1
365
366     cs = plt.contour(lambda_bar_mesh, k_bar_mesh, stability_kink,
367                     levels=levels, colors=color, linewidths=5,
368                     linestyle='dotted')
369
370     line_labels = {}
371
372     for i, level in enumerate(levels):
373         line_labels.update({level: r'$\delta = $ %2.1f' % (delta_values[i])})
374     print(levels, value, line_labels)
375     plt.clabel(cs, fmt=line_labels, fontsize=40, manual=label_pos)
376     return cs
377
378
379 def single_analytic_comparison(mode_to_plot,
380                                k_bar_mesh,
381                                lambda_bar_mesh,
382                                epsilon,
383                                delta_value,
384                                label_pos):
385     """
386     Add contour of analytic stability condition.
387     """
388
389     line_labels = FixedFormatter(delta_value)
390

```

```

391     assert (mode_to_plot == 'm_neg_1' or
392            mode_to_plot == 'm_0'), ("Please specify mode_to_plot as either" +
393                                   "m_neg_1 or m_0")
394
395     if mode_to_plot == 'm_neg_1':
396         m = 1
397         color = 'red'
398     if mode_to_plot == 'm_0':
399         m = 0
400         color = 'red'
401
402
403     stability_kink_given_delta = []
404
405     stability_kink_given_delta.append(ac.conditions(k_bar_mesh,
406                                                    lambda_bar_mesh,
407                                                    epsilon,
408                                                    m,
409                                                    delta_value))
410
411
412     stability_kink = stability_kink_given_delta[0] < 0
413     stability_kink = stability_kink.astype(float)
414     stability_kink[stability_kink_given_delta[0] >= 0] = -1.5
415     stability_kink[stability_kink_given_delta[0] < 0] = -0.5
416
417     levels = [-1]
418
419     cs = plt.contour(lambda_bar_mesh, k_bar_mesh, stability_kink,
420                    levels=levels, colors=color, linewidths=5,
421                    linestyle='dotted')
422
423     line_labels = {}
424
425     #plt.clabel(cs, fmt={-1: '%2.1f' % delta_value}, fontsize=40, manual=label_pos)
426     return cs
427
428 def analytic_comparison(mode_to_plot, k_bar_mesh, lambda_bar_mesh, epsilon,
429                        label_pos, lines=None, colors=None):
430     r"""
431     Add red lines indicating stability boundaries from analytical model.
432     """
433     if not lines:
434         line_labels = FixedFormatter(['-1', '0', '1'])
435     else:
436         line_labels = FixedFormatter([str(line) for line in lines])
437
438     assert (mode_to_plot == 'm_neg_1' or
439            mode_to_plot == 'm_0'), ("Please specify mode_to_plot as either" +
440                                   "m_neg_1 or m_0")
441
442
443     if mode_to_plot == 'm_neg_1':
444         m = 1
445         if not colors:
446             color = 'red'
447         else:

```

```

448         color = colors
449     if mode_to_plot == 'm_0':
450         m = 0
451         if not colors:
452             color = 'red'
453         else:
454             color = colors
455
456     if not lines:
457         stability_kink_m_neg_1 = ac.conditions(k_bar_mesh, lambda_bar_mesh,
458                                             epsilon, m, -1.)
459         stability_kink_m_0 = ac.conditions(k_bar_mesh, lambda_bar_mesh,
460                                             epsilon, m, 0.)
461         stability_kink_m_1 = ac.conditions(k_bar_mesh, lambda_bar_mesh,
462                                             epsilon, m, 1)
463     else:
464         stability_kink_m_neg_1 = ac.conditions(k_bar_mesh, lambda_bar_mesh,
465                                             epsilon, m, lines[0])
466         stability_kink_m_0 = ac.conditions(k_bar_mesh, lambda_bar_mesh,
467                                             epsilon, m, lines[1])
468         stability_kink_m_1 = ac.conditions(k_bar_mesh, lambda_bar_mesh,
469                                             epsilon, m, lines[2])
470
471
472     stability_kink = stability_kink_m_neg_1 < 0
473     stability_kink = stability_kink.astype(float)
474     stability_kink[stability_kink_m_neg_1 >= 0] = -1.5
475     stability_kink[stability_kink_m_neg_1 < 0] = -0.5
476     stability_kink[stability_kink_m_0 < 0] = 0.5
477     stability_kink[stability_kink_m_1 < 0] = 1.5
478     cs = plt.contour(lambda_bar_mesh, k_bar_mesh, stability_kink,
479                    levels=[-1, 0, 1], colors=color, linewidths=10,
480                    linestyles='dotted')
481
482     if not lines:
483         plt.clabel(cs, fmt={-1: r'$\delta = -1$', 0: r'$\delta = 0$',
484                          1: r'$\delta = 1$'}, fontsize=40, manual=label_pos)
485     else:
486         plt.clabel(cs, fmt={-1: r'$\delta = $ %' % lines[0], 0: r'$\delta = $ %' % lines[1],
487                          1: r'$\delta = $ %' % lines[2]}, fontsize=40, manual=label_pos)
488     return cs
489
490 def plot_lambda_k_space_delta(filename, mode_to_plot,
491                              clip=False, delta_min=-1.5,
492                              delta_max=1., levels=None,
493                              interpolate=True, compare_analytic=False,
494                              epsilon=None, analytic_label_pos=None, lines=None,
495                              plot_numeric_boundary=False, cmap=None, analytic_color=None):
496     r"""
497     Plot values of delta in lambda k space.
498     """
499     data_meshes = np.load(filename)
500     lambda_mesh = data_meshes['lambda_a_mesh']
501     k_mesh = data_meshes['k_a_mesh']
502
503
504     if mode_to_plot == 0:

```

```

505     color = 'green'
506     delta_mesh = data_meshes['delta_m_0']
507     external_sausage = data_meshes['d_w_m_0']
508 else:
509     #color = sns.xkcd_rgb["dandelion"]
510     color = 'green'
511     delta_mesh = data_meshes['delta_m_neg_1']
512     external_kink = data_meshes['d_w_m_neg_1']
513
514 if interpolate:
515     delta_mesh = interpolate_nans(lambda_mesh,
516                                 k_mesh,
517                                 delta_mesh)
518
519
520 if clip:
521     delta_mesh = np.clip(delta_mesh, delta_min, delta_max)
522
523 if cmap:
524     colors = cmap
525 else:
526     colors = sns.light_palette(color, n_colors=6, reverse=True,
527                               as_cmap=True)
528
529 if levels:
530     plt.contourf(lambda_mesh, k_mesh, delta_mesh, cmap=colors,
531                 levels=levels)
532 else:
533     plt.contourf(lambda_mesh, k_mesh, delta_mesh, cmap=colors)
534
535 cbar = plt.colorbar(label=r'\delta$')
536 cbar.set_label(label=r'\delta(\bar{\lambda}),\bar{k}$', size=45, rotation=0, labelpad=30)
537
538 if levels:
539     contourlines = plt.contour(lambda_mesh, k_mesh, delta_mesh,
540                               colors='grey', levels=levels)
541 else:
542     contourlines = plt.contour(lambda_mesh, k_mesh, delta_mesh,
543                               colors='grey')
544
545 cbar.add_lines(contourlines)
546
547
548 if mode_to_plot == 0:
549     mode_to_plot = 'm_0'
550 else:
551     mode_to_plot = 'm_neg_1'
552
553 if compare_analytic:
554     if analytic_color:
555         analytic_comparison(mode_to_plot, k_mesh, lambda_mesh, epsilon,
556                             analytic_label_pos, lines=lines, colors=analytic_color)
557     else:
558         analytic_comparison(mode_to_plot, k_mesh, lambda_mesh, epsilon,
559                             analytic_label_pos, lines=lines)
560
561

```

```

562     if plot_numeric_boundary:
563         contour = plt.contour(lambda_mesh,
564                               k_mesh,
565                               external_sausage,
566                               levels=[0],
567                               colors='grey',
568                               linestyle='-.')
569
570
571
572     axes = plt.gca()
573     axes.set_axis_bgcolor(sns.xkcd_rgb['grey'])
574     plt.setp(axes.get_xticklabels(), fontsize=40)
575     plt.setp(axes.get_yticklabels(), fontsize=40)
576     plt.ylabel(r'$\bar{k}$', fontsize=45, rotation='horizontal', labelpad=30)
577     plt.xlabel(r'$\bar{\lambda}$', fontsize=45)
578     cbar.ax.tick_params(labelsize=40)
579     axes.set_xticks(np.arange(0., 5, 1.))
580     axes.set_yticks(np.arange(0., 2.0, 0.5))
581
582     plt.ylim(0.01, 1.5)
583     plt.xlim(0.01, 3.0)
584     sns.despine(ax=axes)
585     plt.tight_layout()
586
587 def sausage_kink_ratio(filename, xy_limits=None, cmap=None, save_as=None,
588                       levels=None, return_ax=False):
589     r"""
590     Plot ratio of sausage and kink potential energies.
591     """
592     meshes = np.load(filename)
593     lambda_bar_mesh = meshes['lambda_a_mesh']
594     k_bar_mesh = meshes['k_a_mesh']
595     external_m_neg_1 = meshes['d_w_m_neg_1']
596     external_sausage = meshes['d_w_m_0']
597     meshes.close()
598
599     sausage_stable_region = np.invert((external_sausage < 0))
600     ratio = np.abs(external_sausage / external_m_neg_1)
601     ratio[sausage_stable_region] = np.nan
602     ratio_log = np.log10(ratio)
603
604     if not cmap:
605         cmap = sns.light_palette(sns.xkcd_rgb['red orange'],
606                                 as_cmap=True)
607
608     if levels:
609         contours = plt.contourf(lambda_bar_mesh, k_bar_mesh,
610                                 ratio_log, cmap=cmap, levels=levels)
611     else:
612         contours = plt.contourf(lambda_bar_mesh, k_bar_mesh,
613                                 ratio_log, cmap=cmap)
614
615     colorbar = plt.colorbar(format=FormatStrFormatter(r'$10^{%i}$'))
616     colorbar.set_label(r'$\frac{\Delta W_{m=0}}{\Delta W_{m=-1}}$',
617                       size=35, rotation=0, labelpad=50)
618
619     if levels:
620         lines = plt.contour(lambda_bar_mesh, k_bar_mesh,

```

```

619         ratio_log, colors='grey', levels=levels)
620     else:
621         lines = plt.contour(lambda_bar_mesh, k_bar_mesh,
622                             ratio_log, colors='grey')
623     colorbar.add_lines(lines)
624
625     axes = plt.gca()
626     axes.plot([0, 3.], [0., 1.5], '—', c='black', lw=5)
627     axes.set_xlabel(r'$\bar{\lambda}$', fontsize=40)
628     plt.setp(axes.get_xticklabels(), fontsize=30)
629     axes.set_xticks(np.arange(0., 4.5, 0.5))
630
631     axes.set_ylabel(r'$\bar{k}$', fontsize=40)
632     plt.setp(axes.get_yticklabels(), fontsize=30)
633     axes.set_yticks(np.arange(0., 2.0, 0.5))
634
635     if xy_limits:
636         axes.set_ylim((xy_limits[0], xy_limits[1]))
637         axes.set_xlim((xy_limits[2], xy_limits[3]))
638
639     sns.despine()
640     colorbar.ax.yaxis.set_ticks_position('right')
641     colorbar.ax.tick_params(labelsize=30)
642     plt.tight_layout()
643     if return_ax:
644         return axes, colorbar
645     else:
646         if save_as:
647             plt.savefig(save_as)
648         plt.show()

```

A.6.14 *analytic_condition.py*

```

1  # -*- coding: utf-8 -*-
2  """
3  Created on Wed Nov 4 13:25:43 2015
4
5  @author: jensv
6
7  Analytic stability condition derived for lengthening
8  current-carrying magnetic flux tube with core and skin
9  currents.
10 """
11
12 import numpy as np
13 from scipy.special import kv, kvp
14
15 import matplotlib.pyplot as plt
16 from matplotlib import colors
17 import seaborn as sns
18 sns.set_style('ticks')
19 sns.set_context('poster')
20
21

```

```

22 def conditions(k_bar, lambda_bar, epsilon, m, delta):
23     r"""
24     Return analytic stability condition.
25
26     Parameters
27     -----
28     k_bar : float
29         normalized inverse aspect ratio
30     lambda_bar : float
31         normalized current-to-magnetic flux ratio
32     epsilon : float
33         core to total current ratio
34     m : float
35         azimuthal periodicity number
36     delta : float
37         abruptness parameter
38
39     Returns
40     -----
41     delta_w : float
42         perturbed potential energy of marginal stability case
43     """
44     term1 = conditions_plasma_term(k_bar, lambda_bar, epsilon, m, delta)
45     term2 = conditions_interface_term(k_bar, lambda_bar, epsilon, m, delta)
46     term3 = conditions_vacuum_term(k_bar, lambda_bar, m, delta)
47     return term1 + term2 - term3
48
49
50 def conditions_without_interface(k_bar, lambda_bar, m, delta):
51     r"""
52     Return analytic stability condition minus interface term (term2).
53
54     Parameters
55     -----
56     k_bar : float
57         normalized inverse aspect ratio
58     lambda_bar : float
59         normalized current-to-magnetic flux ratio
60     m : float
61         azimuthal periodicity number
62     delta : float
63         abruptness parameter
64
65     Returns
66     -----
67     delta_w_without_interface : float
68         perturbed potential energy without interface term.
69
70     Notes
71     -----
72     For profiles with current smoothly going to zero at the delta_w term is zero.
73     """
74     term1 = conditions_smooth_plasma_term(k_bar, lambda_bar, m, delta)
75     term3 = conditions_vacuum_term(k_bar, lambda_bar, m, delta)
76     return term1 - term3
77
78

```

```

79 def conditions_without_interface_wo_sing(k_bar, lambda_bar, m, xi,
80                                         xi_der, a):
81     r"""
82     Multiply analytic expression with xi squared to avoid singularity.
83
84     Parameters
85     -----
86     k_bar : float
87         normalized inverse aspect ratio
88     lambda_bar : float
89         normalized current-to-magnetic flux ratio
90     m : float
91         azimuthal periodicity number
92     xi : float
93         solution to Euler-Lagrange equation at boundary
94     xi_der : float
95         derivative of solution to Euler-Lagrange equation at boundary
96     a : float
97         radius of current-carrying magnetic flux tube
98     Returns
99     -----
100    delta_w_without_interface_wo_sing : float
101        perturbed potential energy without interface or singularity
102
103    Notes
104    -----
105    delta can be singular when xi goes through zero. This form is multiplied
106    by xi**2 to avoid singularity.
107    """
108    term1 = conditions_smooth_plasma_term_wo_sing(k_bar, lambda_bar,
109                                                m, xi, xi_der, a)
110    term3 = conditions_vacuum_term_wo_sing(k_bar, lambda_bar, m, xi)
111    return term1 - term3
112
113
114 def conditions_plasma_term(k_bar, lambda_bar, epsilon, m, delta):
115     r"""
116     Returns plasma term of analytic stability condition.
117
118     Parameters
119     -----
120     k_bar : float
121         normalized inverse aspect ratio
122     lambda_bar : float
123         normalized current-to-magnetic flux ratio
124     epsilon : float
125         core to total current ratio
126     m : float
127         azimuthal periodicity number
128     delta : float
129         abruptness parameter
130
131     Returns
132     -----
133     delta_w_plasma_term : float
134         perturbed potential energy plasma term due to internal
135         currents.

```

```

136 """
137 term1 = (2.*k_bar - m*epsilon*lambda_bar)*((delta + 1)*2.*k_bar -
138                                             (delta - 1)*m*epsilon *
139                                             lambda_bar)/(k_bar**2 + m**2)
140 return term1
141
142
143 def conditions_smooth_plasma_term_wo_sing(k_bar, lambda_bar, m, xi ,
144                                           xi_der, a):
145     r"""
146     Multiply analytic expression with xi squared to avoid singularity.
147
148     Parameters
149     -----
150     k_bar : float
151         normalized inverse aspect ratio
152     lambda_bar : float
153         normalized current-to-magnetic flux ratio
154     m : float
155         azimuthal periodicity number
156     xi : float
157         solution to Euler-Lagrange equation at boundary
158     xi_der : float
159         derivative of solution to Euler-Lagrange equation at boundary
160     a : float
161         radius of current-carrying magnetic flux tube
162
163     """
164     epsilon = 1.
165     term1 = (2.*k_bar - m*epsilon*lambda_bar)*((xi_der*a*xi + xi**2)*2.*k_bar -
166                                             (xi_der*a*xi - xi**2)*m*epsilon*
167                                             lambda_bar)/(k_bar**2 + m**2)
168     return term1
169
170
171 def conditions_smooth_plasma_term(k_bar, lambda_bar, m, delta):
172     r"""
173     Returns plasma term of analytic condition with epsilon set to 1. This
174     should be relevant for a profile that smoothly goes to zero current,
175     since  $b_v(a) = b_p(a)$  in that case.
176
177     Parameters
178     -----
179     k_bar : float
180         normalized inverse aspect ratio
181     lambda_bar : float
182         normalized current-to-magnetic flux ratio
183     m : float
184         azimuthal periodicity number
185     delta : float
186         abruptness parameter
187
188     """
189     epsilon = 1.
190     term1 = conditions_plasma_term(k_bar, lambda_bar, epsilon, m, delta)
191     return term1
192

```

```

193
194 def conditions_interface_term(k_bar, lambda_bar, epsilon, m, delta):
195     r"""
196     Returns interface term of analytic stability condition.
197
198     Parameters
199     -----
200     k_bar : float
201         normalized inverse aspect ratio
202     lambda_bar : float
203         normalized current-to-magnetic flux ratio
204     epsilon : float
205         core to total current ratio
206     m : float
207         azimuthal periodicity number
208     delta : float
209         abruptness parameter
210
211     """
212     term2 = (epsilon**2 - 1) * lambda_bar**2
213     return term2
214
215
216 def conditions_vacuum_term(k_bar, lambda_bar, m, delta):
217     r"""
218     Returns vacuum term of analytic stability condition.
219
220     Parameters
221     -----
222     k_bar : float
223         normalized inverse aspect ratio
224     lambda_bar : float
225         normalized current-to-magnetic flux ratio
226     m : float
227         azimuthal periodicity number
228     delta : float
229         abruptness parameter
230
231     """
232     term3 = (m*lambda_bar - 2.*k_bar)**2/k_bar*(kv(m, np.abs(k_bar)) /
233           kvp(m, np.abs(k_bar)))
234     return term3
235
236 def conditions_vacuum_term_wo_sing(k_bar, lambda_bar, m, xi):
237     r"""
238     Multiply analytic expression with xi squared to avoid singularity.
239
240     Parameters
241     -----
242     k_bar : float
243         normalized inverse aspect ratio
244     lambda_bar : float
245         normalized current-to-magnetic flux ratio
246     m : float
247         azimuthal periodicity number
248     xi : float
249         Euler-Lagrange solution
250
251     """

```

```

250     term3 = xi**2 * (m*lambda_bar - 2.*k_bar)**2/k_bar*(kv(m, np.abs(k_bar)) /
251                                     kvp(m, np.abs(k_bar)))
252     return term3
253
254
255 def condition_map(epsilon=0.5, delta=0.):
256     r"""
257     Draw filled contours of sausage (orange), kink(yellow), and stable (white)
258     regions for given epsilon and delta values.
259
260     Parameters
261     -----
262     epsilon : float
263         core to total current ratio
264     delta : float
265         abruptness parameter
266     """
267     fig = plt.figure(figsize=(10,10))
268     lambda_bar = np.linspace(0., 3., 750)
269     k_bar = np.linspace(0, 1.5, 750)
270     lambda_bar_mesh, k_bar_mesh = np.meshgrid(lambda_bar, k_bar)
271
272     stability_kink = conditions(k_bar_mesh, lambda_bar_mesh, epsilon, 1., delta)
273     stability_kink = stability_kink < 0
274     stability_sausage = conditions(k_bar_mesh, lambda_bar_mesh, epsilon, 0., delta)
275     stability_sausage = stability_sausage < 0
276     stability_kink = stability_kink.astype(float)
277     stability_kink[stability_sausage] = 2
278
279     cmap = colors.ListedColormap([sns.xkcd_rgb["white"],
280                                   sns.xkcd_rgb["yellow"], sns.xkcd_rgb["orange"]])
281     plt.contourf(lambda_bar_mesh, k_bar_mesh, stability_kink,
282                 cmap=cmap, levels=[0., 0.5, 1.5, 2.])
283     plt.contour(lambda_bar_mesh, k_bar_mesh, stability_kink,
284                 levels=[0., 0.5, 1.5, 2.], colors='grey')
285     plt.plot([0, 3.], [0., 1.5], '—', c='black', lw=5)
286     axes = plt.gca()
287
288     plt.setp(axes.get_xticklabels(), fontsize=40)
289     plt.setp(axes.get_yticklabels(), fontsize=40)
290     plt.ylabel(r'$\bar{k}$', fontsize=45, rotation='horizontal', labelpad=25)
291     plt.xlabel(r'$\bar{\lambda}$', fontsize=45)
292     sns.despine()
293
294
295 def condition_map_variable_delta(filename, mode=1, epsilon=0.5,
296                                 conditions_func=conditions_without_interface):
297     r"""
298     Draw filled contours of sausage (orange), kink(yellow), and stable (white)
299     regions for given epsilon and delta values.
300     Delta values are loaded from a .npz mesh file.
301
302     Parameters
303     -----
304     filename : string
305         filename from which to load lambda_bar, k_bar and delta values.
306     mode : int

```

```

307     azimuthal mode number 0 or 1
308     epsilon : float
309     core current to total current ratio
310     conditions_func : function
311     conditions function to use
312     """
313     data_mesheres = np.load(filename)
314     lambda_bar_mesh = data_mesheres['lambda_a_mesh']
315     k_bar_mesh = data_mesheres['k_a_mesh']
316     delta_mesh = data_mesheres['delta_m_0']
317
318     fig = plt.figure(figsize=(10,10))
319
320     cmap = colors.ListedColormap([sns.xkcd_rgb["white"],
321                                 sns.xkcd_rgb["yellow"],
322                                 sns.xkcd_rgb["orange"]])
323
324     stability_kink = conditions_func(k_bar_mesh, lambda_bar_mesh, epsilon, 1.,
325                                   delta_mesh)
326     stability_kink = stability_kink < 0
327     stability_sausage = conditions_func(k_bar_mesh, lambda_bar_mesh, epsilon, 0.,
328                                       delta_mesh)
329     stability_sausage = stability_sausage < 0
330
331     if mode == 0:
332         stability = stability_sausage
333         cmap = colors.ListedColormap([sns.xkcd_rgb["white"],
334                                     sns.xkcd_rgb["orange"]])
335     else:
336         stability = stability_kink
337         cmap = colors.ListedColormap([sns.xkcd_rgb["white"],
338                                     sns.xkcd_rgb["yellow"]])
339
340     plt.contourf(lambda_bar_mesh, k_bar_mesh, stability,
341                 cmap=cmap, levels=[0.5, 1.5])
342     plt.contour(lambda_bar_mesh, k_bar_mesh, stability,
343                levels=[0.5, 1.5], colors='grey')
344     plt.plot([0, 3.], [0., 1.5], '--', c='black', lw=5)
345     axes = plt.gca()
346
347     plt.setp(axes.get_xticklabels(), fontsize=40)
348     plt.setp(axes.get_yticklabels(), fontsize=40)
349     plt.ylabel(r'$\bar{k}$', fontsize=45, rotation='horizontal', labelpad=25)
350     plt.xlabel(r'$\bar{\lambda}$', fontsize=45)
351     sns.despine()
352     plt.show()

```

A.6.15 diagnostic_plots.py

```

1     """
2     Created on Tue Nov 22 11:12:58 2016
3
4     @author: Jens von der Linden
5     """

```

```

6
7 from __future__ import print_function
8 from __future__ import division
9 from __future__ import absolute_import
10 from future.builtins import (ascii, bytes, chr, dict, filter, hex, input,
11                             int, map, next, oct, open, pow, range, round,
12                             str, super, zip)
13 """Python 3.x compatibility"""
14
15 import sys
16
17 import scipy.integrate
18
19 import singularity_frobenius as frob
20
21 import matplotlib.pyplot as plt
22 import seaborn as sns
23 sns.set_style('whitegrid')
24 sns.set_context('poster')
25
26 def plot_all_profiles_suydam(profile, normalize=False,
27                             mu_0=None, axes=None, title=None):
28     r"""
29     Plot radial profiles of current, magnetic field, pressure, safety_factor,
30     and Suydam criterion.
31
32     Parameters
33     -----
34     profiles : profile_object
35         profile created with equi_solver
36     normalize : bool
37         boolean flag to normalize profiles to max values
38     mu_0 : float
39         magnetic permeability value (used for non-dimensionless profiles)
40     axes : matplotlib axes
41         plotting axes to use
42     title :
43         plot title
44     """
45     if not axes:
46         axes = plt.gca()
47     r = np.linspace(0, 1, 250)
48     splines = profile.get_splines()
49     j_z = splines['j_z'](r)
50     b_z = splines['b_z'](r)
51     b_z_prime = splines['b_z'].derivative()(r)
52     b_theta = splines['b_theta'](r)
53     b_theta_prime = splines['b_theta'].derivative()(r)
54     p_prime = splines['p_prime'](r)
55     p = splines['pressure'](r)
56     safety_factor = splines['q'](r)
57     safety_factor_prime = splines['q'].derivative()(r)
58     if mu_0:
59         beta_0 = mu_0
60     else:
61         beta_0 = profile.beta_0()
62     alpha = frob.alpha_func(r, b_z, b_z_prime, b_theta, b_theta_prime)

```

```

63     beta = frob.beta_func(b_z, b_theta, p_prime, beta_0)
64     suydam_mu = alpha + 4.*beta
65     suydam_q = r*b_z**2./(8. * beta_0)*(safety_factor_prime/safety_factor)**2. + p_prime
66     if 'j_theta' in splines.keys():
67         print('true')
68         j_theta = splines['j_theta'](r)
69     else:
70         print('false')
71         j_theta = None
72     if normalize:
73         j_z = j_z/np.max(np.abs(j_z))
74         b_theta = b_theta/np.max(np.abs(b_theta))
75         alpha = alpha/np.max(np.abs(alpha))
76         beta = beta/np.max(np.abs(beta))
77         suydam_q = suydam_q/np.max(np.abs(suydam_q))
78         suydam_mu = suydam_mu/np.nanmax(np.abs(suydam_mu))
79         p = p/np.max(np.abs(p))
80         p_prime = p_prime/np.max(np.abs(p_prime))
81         safety_factor_prime = safety_factor_prime/np.max(np.abs(safety_factor_prime))
82     if 'j_theta' in splines.keys():
83         j_theta = j_theta/np.nanmax(np.abs(j_theta))
84     axes.plot(r, j_z, c='#087804', label=r'$j_z$')
85     if 'j_theta' in splines.keys():
86         axes.plot(r, j_theta, c='#6fc276', label=r'$j_\theta$')
87     axes.plot(r, b_theta, c='#e50000', label=r'$B_\theta$')
88     axes.plot(r, p_prime, c='#7e1e9c', label=r"$p'$")
89     axes.plot(r, p, c='#bf77f6', label=r"$p$")
90     axes.plot(r, safety_factor, c='#000000', label=r"$q$")
91     axes.plot(r, safety_factor_prime, c='#7d7f7c', label=r"$q'$")
92     axes.plot(r[1:], suydam_q[1:], c='#acfffc', label=r"suydam_q")
93     #axes.plot(r[1:], suydam_mu[1:], c='#82cafc', label=r"suydam_mu")
94     if title:
95         axes.set_title(title)
96     axes.legend(loc='best')
97     return axes
98
99 def plot_suydam(profile, normalize=False):
100     r"""
101     Plot suydam stability conditions.
102
103     Parameters
104     _____
105     profiles : profile_object
106         profile created with equil_solver
107     normalize : bool
108         boolean flag to normalize profiles to max value
109     """
110     axes = plt.gca()
111     r = np.linspace(0, 1, 250)
112     splines = profile.get_splines()
113     j_z = splines['j_z'](r)
114     b_z = splines['b_z'](r)
115     b_z_prime = splines['b_z'].derivative()(r)
116     b_theta = splines['b_theta'](r)
117     b_theta_prime = splines['b_theta'].derivative()(r)
118     p_prime = splines['p_prime'](r)
119     p = splines['pressure'](r)

```



```

26
27
28 def teardown_func():
29     pass
30
31
32 @with_setup(setup_func, teardown_func)
33 def test_epsilon():
34     r"""
35     Test that ratio of b_theta gives epsilon.
36     """
37     r_core = test_equil.core_radius
38     a = (test_equil.core_radius + 2.*test_equil.transition_width +
39         test_equil.skin_width)
40     b_theta_tck = test_equil.get_tck_splines()['b_theta']
41     epsilon_from_b_theta_ratio = (splev(r_core, b_theta_tck) /
42         splev(a, b_theta_tck))
43     test.assert_approx_equal(epsilon_from_b_theta_ratio, test_equil.epsilon,
44         significant=3)
45
46
47 @with_setup(setup_func, teardown_func)
48 def test_lambda_bar():
49     r"""
50     Test that lambda bar is given by ratio of total current to magnetic flux.
51     """
52     a = (test_equil.core_radius + 2.*test_equil.transition_width +
53         test_equil.skin_width)
54     b_theta_tck = test_equil.get_tck_splines()['b_theta']
55     b_z_tck = test_equil.get_tck_splines()['b_z']
56     calculated_lambda = (2.*splev(a, b_theta_tck) /
57         (splev(a, b_z_tck)))
58     test.assert_approx_equal(calculated_lambda, test_equil.lambda_bar,
59         significant=3)

```

A.6.17 test_newcomb.py

```

1  # -*- coding: utf-8 -*-
2  """
3  Created on Tue May 20 14:05:57 2014
4
5  @author: Jens von der Linden
6
7  Tests based on relations in Goedbloed (2010) Principles of MHD, Jardin &
8  Newcomb paper.
9  All equation references are from these books unless otherwise noted.
10 """
11
12 from __future__ import print_function
13 from __future__ import division
14 from __future__ import absolute_import
15 from future.builtins import (ascii, bytes, chr, dict, filter, hex, input,
16                             int, map, next, oct, open, pow, range, round,
17                             str, super, zip)

```

```

18 """Python 3.x compatibility"""
19
20 import math
21 import numpy as np
22 from numpy import atleast_1d as d1
23 from numpy.testing import assert_allclose, assert_array_less
24 import newcomb_g as g
25 import newcomb_f as f
26
27
28 class TestParabolic(object):
29     r"""
30     Compare f and g outputs for a parabolic current profile.
31     """
32
33     def setUp(self):
34         r"""
35         Create a parabolic axial current equilibrium profile.
36         """
37         import equil_solver as es
38         parabolic = es.ParabolicNu2()
39         params = {'mu0': 1.0, 'k': (2*math.pi)/1.0, 'n': 1.0, 'm': 1.0,
40                 'a': 1.0, 'b': 10.0, 'omega_sq': -5.0, 'gamma': 1.0,
41                 'constant': 1.0}
42         splines = parabolic.get_splines()
43         params.update(splines)
44         self.params = params
45         self.delta = 10E-5
46
47     def test_jardin_f_negative(self):
48         r"""
49         Test that f is never negative for all r.
50         """
51         k, m, b_z, b_theta, q = map(self.params.get, ['k', 'm', 'b_z',
52                                                     'b_theta', 'q'])
53         r = np.linspace(0, 1, 100)
54         f_params = {'r': r, 'k': d1(k), 'm': d1(m),
55                   'b_z': b_z(r), 'b_theta': b_theta(r),
56                   'q': q(r)}
57
58         assert_array_less(-1E-14, f.jardin_f_8_78(**f_params))
59
60     def test_jardin_f_newcomb_f(self):
61         r"""
62         Test that the jardin_f and newcomb_f expressions are equivalent.
63         """
64         k, m, b_z, b_theta, q = map(self.params.get, ['k', 'm', 'b_z',
65                                                     'b_theta', 'q'])
66         r = np.linspace(0, 1, 100)
67         f_params = {'r': r, 'k': d1(k), 'm': d1(m),
68                   'b_z': b_z(r), 'b_theta': b_theta(r), 'q': q(r)}
69
70         assert_allclose(f.jardin_f_8_78(**f_params),
71                         f.newcomb_f_16(**f_params), rtol=0.5)
72
73     def test_jardin_g_8_79_and_8_80(self):
74         r"""

```

```

75     Test that the jardin equation (8.79) and jardin (8.80) equation
76     are equivalent.
77     """
78     (k, m, b_z, b_theta,
79      q, p_prime) = map(self.params.get, ['k', 'm', 'b_z', 'b_theta', 'q',
80                                       'p_prime'])
81
82     r = np.linspace(0, 1, 100)
83     g_params = {'r': r, 'k': d1(k), 'm': d1(m),
84                'b_z': b_z(r), 'b_z_prime': b_z.derivative()(r),
85                'b_theta': b_theta(r),
86                'b_theta_prime': b_theta.derivative()(r),
87                'p_prime': p_prime(r), 'q': q(r),
88                'q_prime': q.derivative()(r)}
89
90     assert_allclose(g.jardin_g_8_79(**g_params),
91                    g.jardin_g_8_80(**g_params), rtol=0.5)
92
93 def test_jardin_g_8_80_newcomb_g_18(self):
94     r"""
95     Test that the jardin g (8.80) and newcomb g (18) expressions are
96     equivalent.
97     """
98     (k, m, b_z, b_theta,
99      q, p_prime) = map(self.params.get, ['k', 'm', 'b_z', 'b_theta', 'q',
100                                       'p_prime'])
101
102     r = np.linspace(0, 1, 100)
103
104     g_params = {'r': r, 'k': d1(k), 'm': d1(m),
105                'b_z': b_z(r), 'b_z_prime': b_z.derivative()(r),
106                'b_theta': b_theta(r),
107                'b_theta_prime': b_theta.derivative()(r),
108                'p_prime': p_prime(r), 'q': q(r),
109                'q_prime': q.derivative()(r)}
110
111     assert_allclose(g.jardin_g_8_80(**g_params),
112                    g.newcomb_g_18(**g_params), rtol=0.5)
113
114 def test_jardin_g_8_79_newcomb_g_18(self):
115     r"""
116     Test that the jardin g (8.79) and newcomb g (18) expressions are
117     equivalent.
118     """
119     (k, m, b_z, b_theta,
120      q, p_prime) = map(self.params.get, ['k', 'm', 'b_z', 'b_theta', 'q',
121                                       'p_prime'])
122
123     r = np.linspace(0, 1, 100)
124     g_params = {'r': r, 'k': d1(k), 'm': d1(m),
125                'b_z': b_z(r), 'b_z_prime': b_z.derivative()(r),
126                'b_theta': b_theta(r),
127                'b_theta_prime': b_theta.derivative()(r),
128                'p_prime': p_prime(r), 'q': q(r),
129                'q_prime': q.derivative()(r)}
130
131     assert_allclose(g.jardin_g_8_79(**g_params),
132                    g.newcomb_g_18(**g_params), rtol=0.5)
133
134 def test_newcomb_g_17_newcomb_g_18(self):

```

```

132     r"""
133     Test that the newcomb g (17) and newcomb g (18) expressions are
134     equivalent.
135     """
136     (k, m, b_z, b_theta,
137      q, p_prime) = map(self.params.get, ['k', 'm', 'b_z', 'b_theta', 'q',
138                                       'p_prime'])
139     r = np.linspace(0, 1, 100)
140     g_params = {'r': r, 'k': d1(k), 'm': d1(m),
141               'b_z': b_z(r), 'b_z_prime': b_z.derivative()(r),
142               'b_theta': b_theta(r),
143               'b_theta_prime': b_theta.derivative()(r),
144               'p_prime': p_prime(r), 'q': q(r),
145               'q_prime': q.derivative()(r)}
146     assert_allclose(g.newcomb_g_17(**g_params),
147                   g.newcomb_g_18(**g_params), rtol=0.5)
148
149
150     def test_suydam_q_suydam_alpha_beta(self):
151         r"""
152         Not implemented
153         """
154         pass
155         # r = np.linspace(0, 1, 100)
156         # assert_almost_equal(suydam_q(), suydam_alpha_beta())
157
158     def test_suydam_q_suydam_mu(self):
159         r"""
160         Not implemented
161         """
162         pass
163         # r = np.linspace(0, 1, 100)
164         # assert_almost_equal(suydam_q(), suydam_mu())
165
166     def test_jardin_small_solution_goedbloed_small_solution(self):
167         r"""
168         Not implemented
169         """
170         pass
171         # r = np.linspace(0, 1, 100)
172         # assert_almost_equal(jardin_small_solution(), newcomb_small_solution())

```

Appendix B

MOCHICONTROL & MOCHIFPGACONTROL CODE

This appendix contains instructions for setting up and running the MochiControl and MochiFPGAControl LabVIEW applications. The source code can also be found at Zenodo <https://doi.org/10.5281/zenodo.495643> and <https://doi.org/10.5281/zenodo.495787> [72, 74]

B.1 MochiControl

Mochi Lab uses this flexible National Instruments LabVIEW experiment control application, based on the producer-consumer design pattern, to allow operators real-time control over all experimental settings, including 16 timing channels with a dynamic timing map, 120 digitizer channels, and a settings save and load interface powered by MDSplus. The hierarchical MDSplus tree stores all experiment settings such as capacitor bank voltages and discharge times together with all data acquired through National Instruments PXI-6133 and NI-5752 digitizer cards, Tektronix TDS-2024B oscilloscopes, and a Princeton Instruments PI-MAX 3 fast framing camera. The experiment control application can also access stored settings through the MDSplus LabVIEW interface which leverages the object oriented and multi-threaded features of MDSplus. To control the experiment the application switches digital outputs of a PXI-6602 timing card connected through fiber optics to relays in the bias coil and plasma gun capacitor banks to achieve the desired charging voltage. The application transmits the desired experiment timings to the PXI-6602 cards which use on board clocks to generate optically isolated trigger pulses for the gas puff valves, oscilloscopes, bias coil and plasma gun capacitor banks. The optical isolation is achieved with TTL-optical transmitter circuits, and DC and fast optical-TTL receiver circuits at the experiment (Carroll 2016).

B.1.1 Requirements

Software Dependencies

The following software can be downloaded from the National Instruments website.

- LabVIEW 2015 (or later)
- DAQmx
- NI-Sync
- MathScript
- LabVIEW FPGA module
- FlexRIO drivers
- FlexRIO adapter drivers

The following software can be downloaded from mdsplus.org.

- MDSplus (the directory with the Vis has to be copied to the LabVIEW directory)

Hardware Setup

This code is designed for this specific hardware.

- PXI-1042Q chassis with
 - PXI-MXI-4 (communication with PC)
 - PXI-6653 (synchronization card)
 - 2x PXI-6602 (Timing cards with 8 channels each)
 - 3x PXI-6133 (Digitizers each 8 channel 2.5 MS/s 14 bit)

- PXIe-1082 chassis with
 - PXIe-8375 (communication with PC)
 - 3x PXIe-7962R with NI-5752 (Digitizers each 32 channel 50MS/s 12 bit)
 - PXIe-6672 (synchronization card)

B.1.2 Important Files

Experiment_Control.lvproj project file this file should be opened with LabVIEW

`Modules/mochifpgacontrol/FPGA bitfiles/MochiFPGAControl_2016-11-29_generic_register_setting_5f6bfda_K10_digital_filters.lvbitx` this bitfile must be loaded on the FPGAs with NI-MAX

B.1.3 Setup

- The code is setup to synchronize two chassis (one leader, one follower). The synchronization cards, one in each chassis should be connected with two coax cables. One coax cable should connect PFI 0 of the leader to PFI 1 of the leader and the other cable PFI 2 of the leader to PFI 0 of the follower. The bitfile has to be loaded onto the FPGA, one way to do this is with NI MAX and the update firmware option.
- The bitfile has to be loaded onto the FPGA, one way to do this is with NI MAX and the update firmware option.
- The NI components have to be named in NI-MAX as follows:
 - PXIe-1082 -> Chassis 1
 - PXIe-7962R -> RIO[0-2]
 - PXIe-6672 -> Sync0
 - PXI-6653 -> Sync

- PXI-6602 -> Timing[0-1]
 - PXI-6133 -> DAQ[0-2]
- an MDSplus tree named 'op_tree' has to be created with the MochiModel software referenced below.

B.1.4 Adapting the code to new hardware

Adapting this code to new NI components requires significant work. Woodruff Scientific, Inc. designs and installs Controls, Data Access and Communication (CODAC) systems.

<http://www.woodruffscientific.com/codac>

B.1.5 Reference

- Jens von der Linden. (In preparation). Investigating the Dynamics of Canonical Flux Tubes (Doctoral dissertation). Chapter 4. University of Washington.
- Alexander Card. (In preparation). A new measurement of electron densities in the MOCHI LabJet experiment using an unequal path length, heterodyne interferometer (Master's thesis). University of Washington
- Alexander Card. (2017). MochiModel. Zenodo. <https://doi.org/10.5281/zenodo.495631>
- Jens von der Linden. (2017). MochiFPGAcontrol: High-throughput FPGA code for NI-5752 digitizers. Zenodo. <http://doi.org/10.5281/zenodo.439654>
- Evan Carroll (2016). Driving Flows in Laboratory Astrophysical Plasma Jets: The Mochi.LabJet Experiment (Master's thesis). University of Washington.

B.1.6 Acknowledgments

James Stuber and Woodruff Scientific, Inc. provided the lab with our initial NI hardware, code, and ongoing support.

B.1.7 Contact

Jens von der Linden jensv@uw.edu Alexander Card card@uw.edu

B.2 MochiFPGAControl

This LabVIEW project programs a PXIe-7962R field programmable arrays (FPGA) to read out 50Mhz 12 bit samples for 800 us from a NI-5752 digitizer.

The PXIe-7962R reads out the samples as 16-bit words, resulting in a data throughput of 3GB/s. This code achieves a throughput to the on board DRAM of 1.5 GB/s, limiting the acquisition time to 800us when the overflow data fills the on board block memory.

B.2.1 Requirements

Software Dependencies

All software can be downloaded from the National Instruments website.

- LabVIEW 2015 (or later)
- LabVIEW FPGA module
- FlexRIO drivers
- FlexRIO adapter drivers
- Xilinx Compile Tools
- NI-Sync

Hardware Requirements

This code is custom designed to this specific hardware. It can, however, serve as an example to be adapted to other NI FPGA based digitizers.

- NI-5752 digitizer
- PXIe-7962R FPGA
- Two NI chassis
- Two NI sync cards (e.g. PXIe 6672, PXI 6652)

The code is designed to work in a double chassis configuration with two synchronization cards. This double chassis requirement could be removed with minor edits in the host Vis.

B.2.2 Important Files

LabVIEW FPGA projects consist of FPGA VIs meant to be compiled to bitfiles and run on the FPGAs, and Host VIs to be run on a computer.

MochiFPGAControl.lvproj is the LabVIEW project file which should be opened with LabVIEW.

host_with_sub_vis_timed_pulse.vi is the recommended host test file. There are options to set the number of samples that should be acquired and to display the acquisition from one channel. An analog digital high pass filter can be set to on or off. It should be set to on. A digital high pass filter can be set with a binary number. The possible settings can be looked up in the AFE 5801.

FPGA Bitfiles/MOCHIFPGAControl_2016-11-29_generic_register_setting_5f6bfd_K10_digital_filters.lvbitx is the bitfile that has to be loaded onto the FPGA.

pxie_7962_fpga.vi is the FPGA vi. The bitfile is compiled from this file.

B.2.3 Setup

The HostVI is setup to synchronize two chassis (one leader, one follower) and trigger the FPGA. The FPGA should be located in the follower. The synchronization cards, one in each chassis should be connected with two coax cables. One coax cable should connect PFI 0 of the leader to PFI 1 of the leader and the other cable PFI 2 of the leader to PFI 0 of the follower. The bitfile has to be loaded onto the FPGA, one way to do this is with NI MAX and the update firmware option.

B.2.4 Reference

- Jens von der Linden. 2017. Investigating the Dynamics of Canonical Flux Tubes (Doctoral dissertation). Chapter 4. University of Washington.
- NI-5752 spec sheet.
- AFE-5801 (Texas Instruments) spec sheet. Each NI-5752 has 4x AFE-5801 ADC chips. The analog filter settings have to be set on ADC chip registers.
- NI LabVIEW High-Performance FPGA Developer's Guide. 2014.

B.2.5 Improvements

- Bitpacking the 16 bit words to 12 bits. This would reduce the data throughput to 2.25GB/s and increase the acquisition time. First steps are in the bitpacking branches in the GitHub repository (MochiLab/mochiFPGAcontrol).
- Use of K7 library to manage DRAM memory. There is a LabVIEW FPGA DRAM memory library that could simplify the read and write process to the DRAM. First steps are in the guys_version branch in the GitHub repository (MochiLab/mochiFPGAcontrol).

- Using digital outputs of the NI-5752 as counters. The clock in the digitizer adapter could be used as a driver for single-cycle timed loop. An upcount vi could count 20ns ticks and then turn on the digital output channels at given counts.

B.2.6 Acknowledgments

Thanks to Glenn Manlongat (National Instruments) for help specifying and selecting the hardware, and Guy McDonnell (National Instruments) for help and advice developing the FPGA code.

B.2.7 Contact

Jens von der Linden jensv@uw.edu

Appendix C

MOCHI.PSU1

This appendix contains figures and engineering drawings of the Mochi.PSU1 (power supply unit). Mochi.PSU1 consists of two identical capacitor banks of 30x $4\mu F$ NWL# 12094 capacitors. The capacitors are connected in parallel by two brass plates, one for the hot leads, and one for the ground leads. The brass plates are isolated from each other by two insulating high-density polyethylene (HDPE) plates which sandwich insulating hats for the capacitor bank leads, maximizing the tracking length between the leads. Each capacitor bank is switched by an individually triggered A size ignitron. Each ignitron is housed in a coaxial enclosure that is insulated from the bank and control electronics with an acrylic tube.

C.1 Overview figures

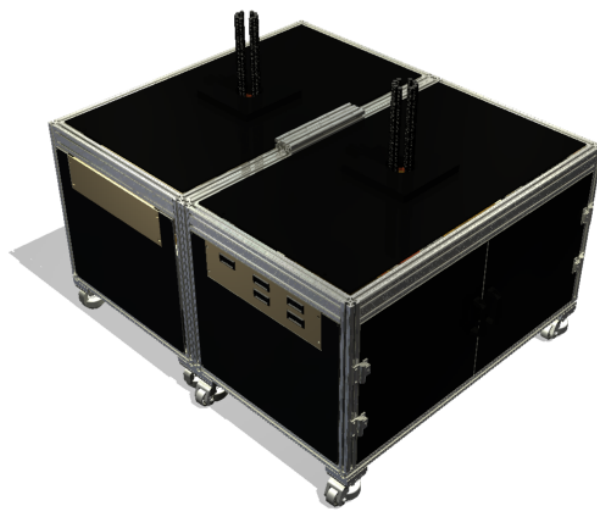


Figure C.1: Mochi.PSU1: Two capacitor banks in an 80-20 frame enclosed with ABS plastic panels.

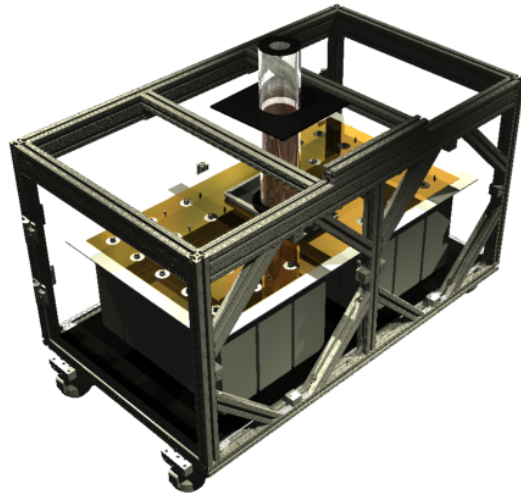


Figure C.2: One bank of PSU1: ABS panels have been removed. The acrylic tube around the ignitron coaxial housing is visible.

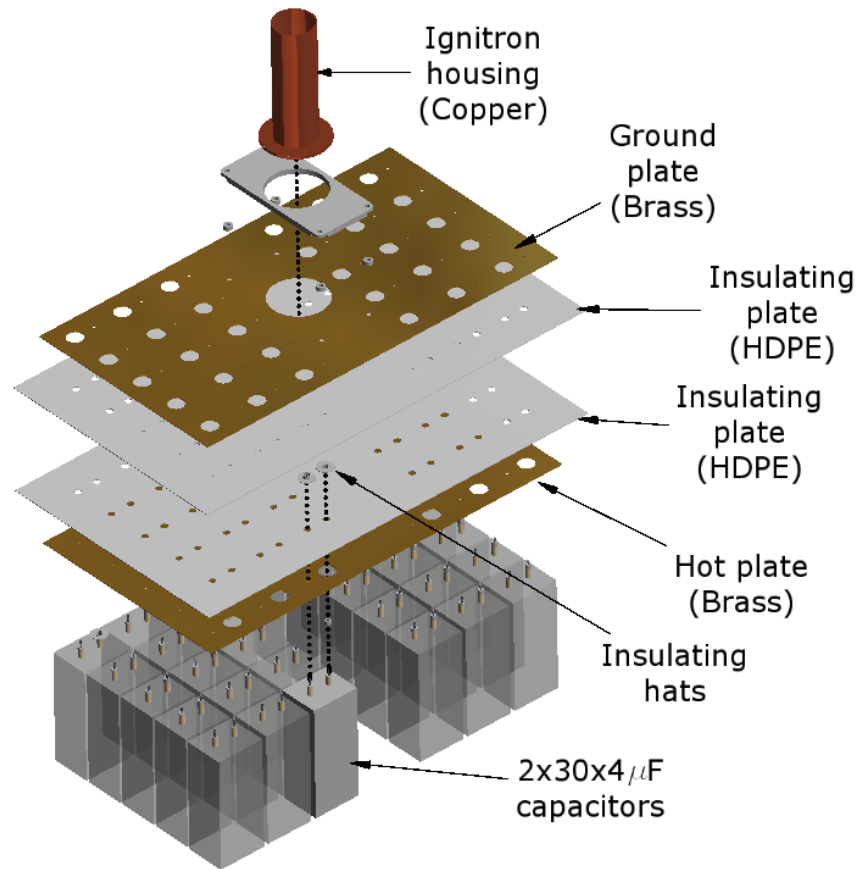
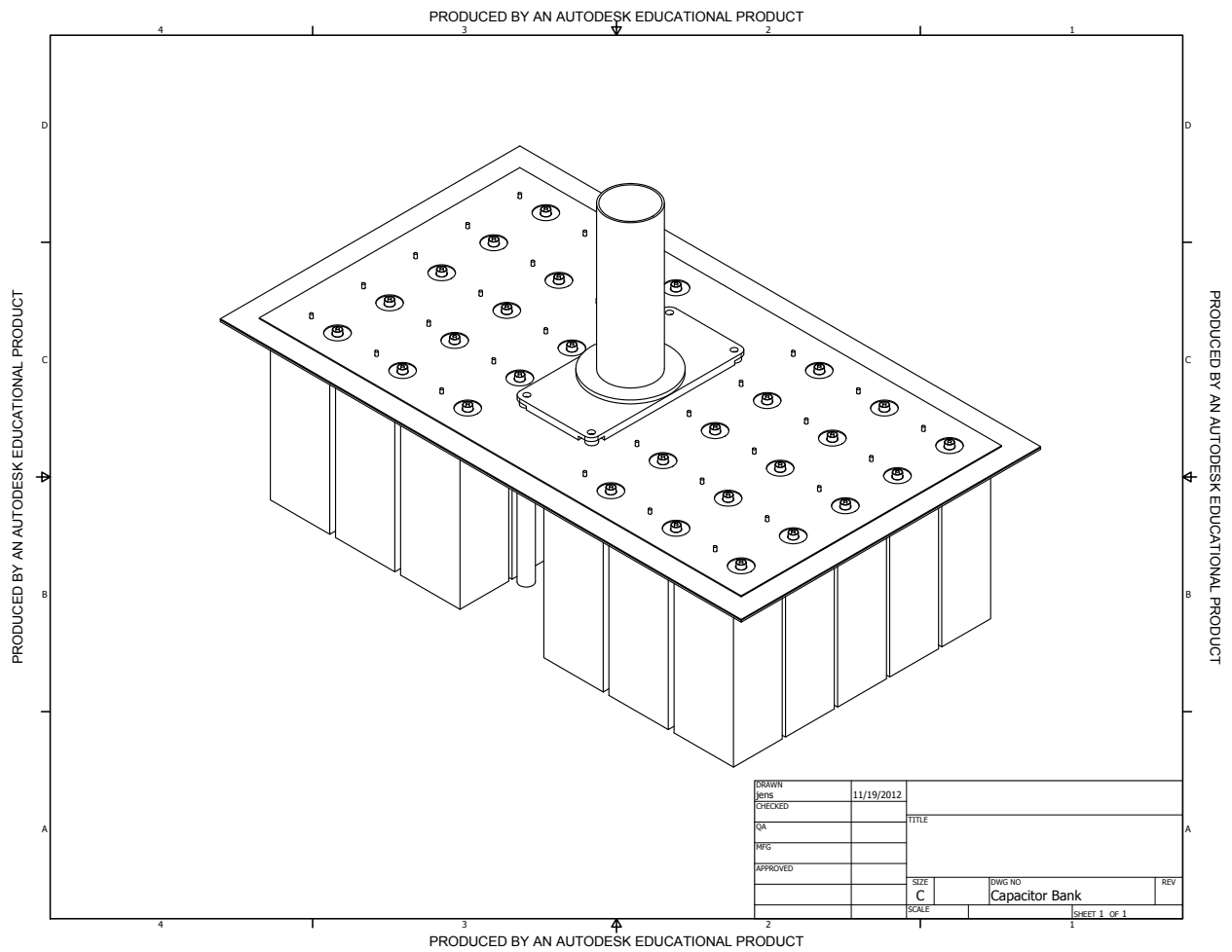


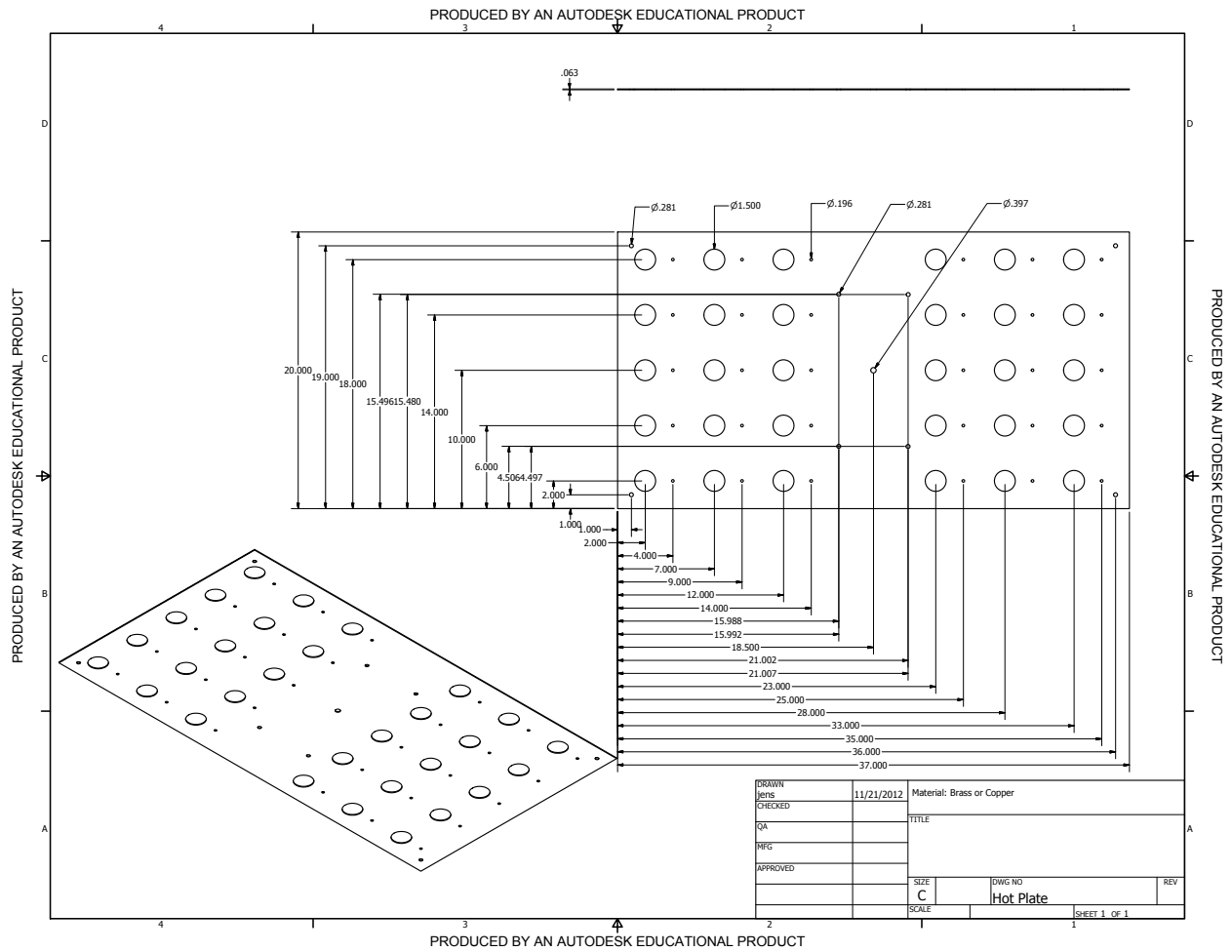
Figure C.3: Exploded view of capacitor bank assembly.

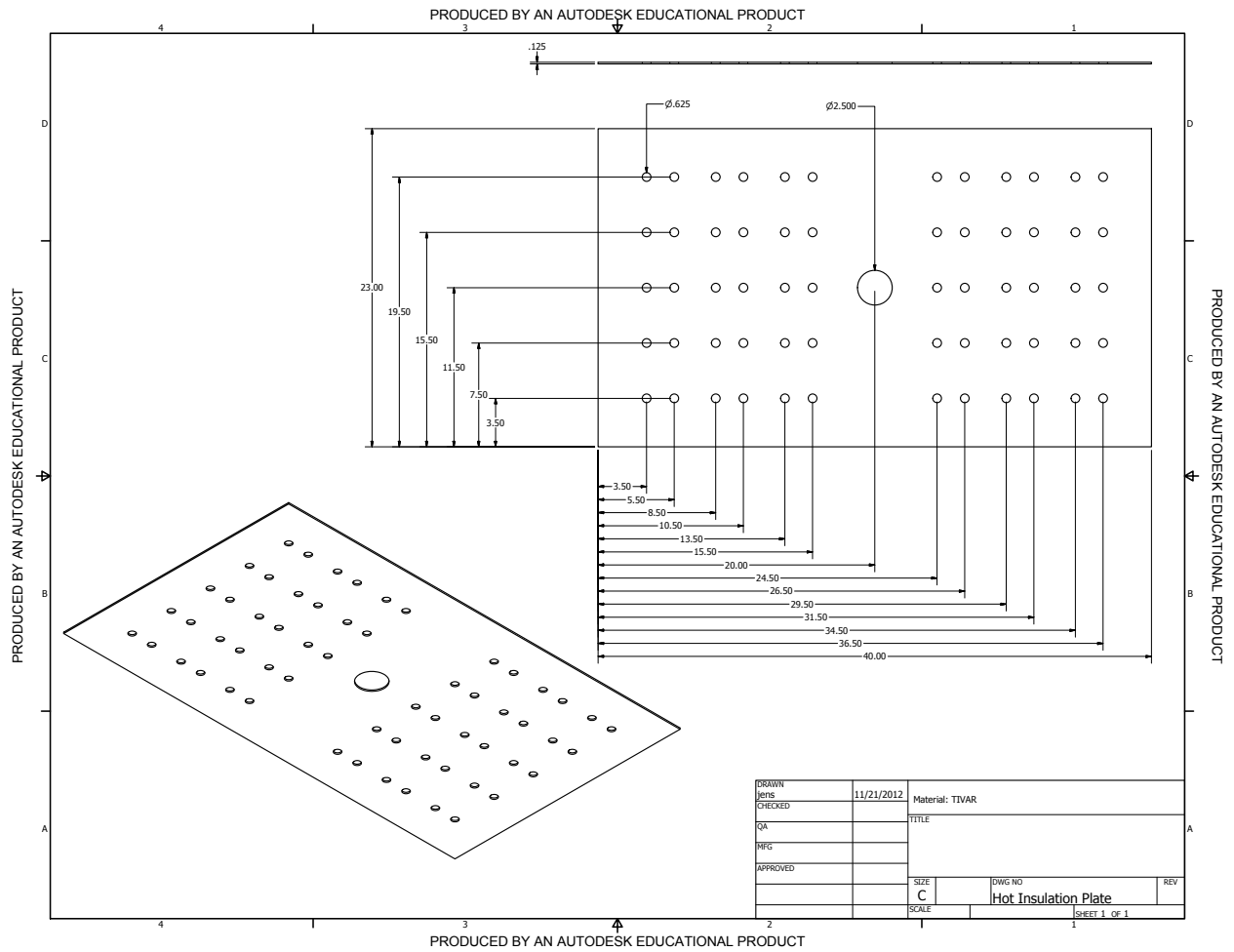
C.2 Drawings

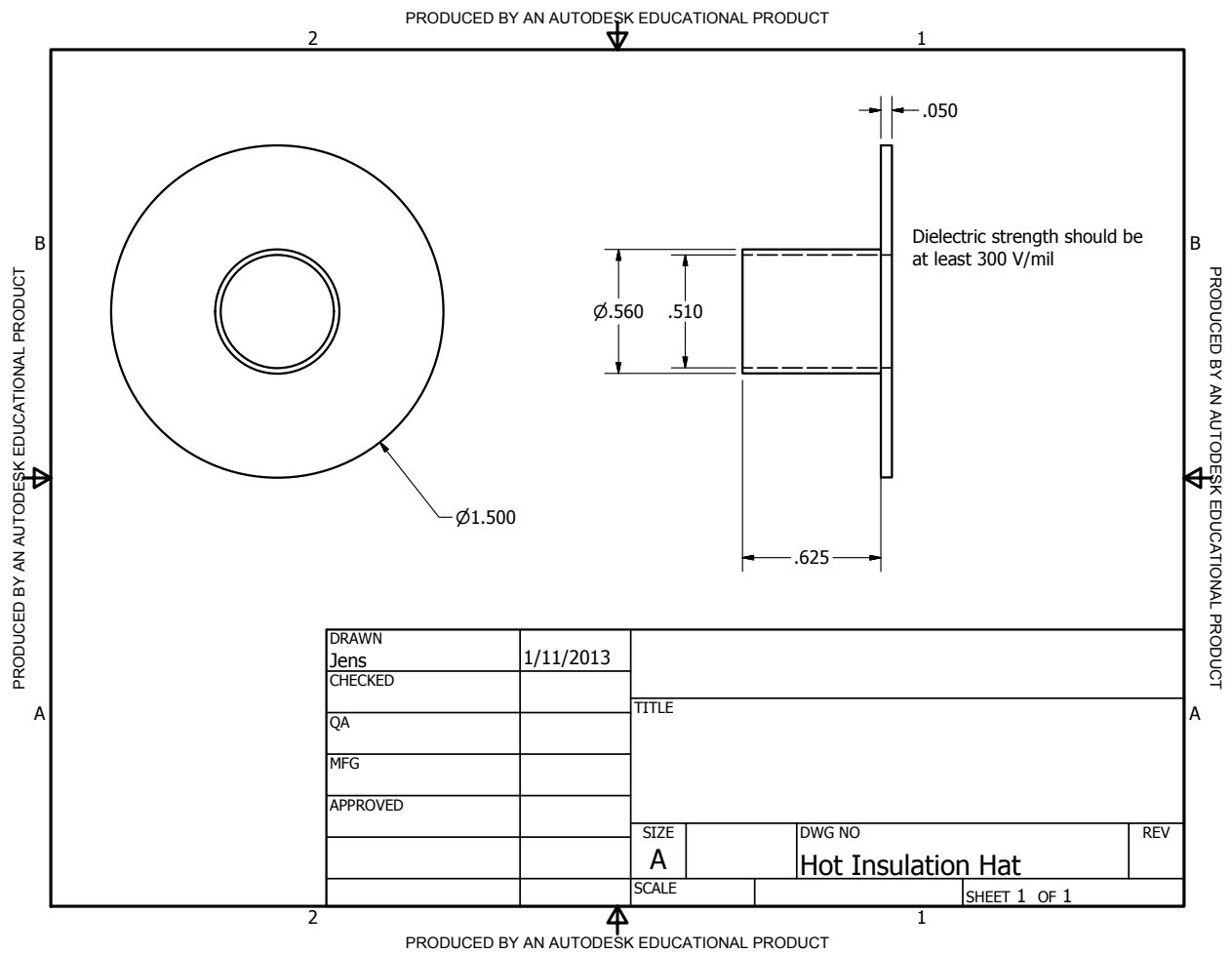
C.2.1 Capacitor Bank Assembly



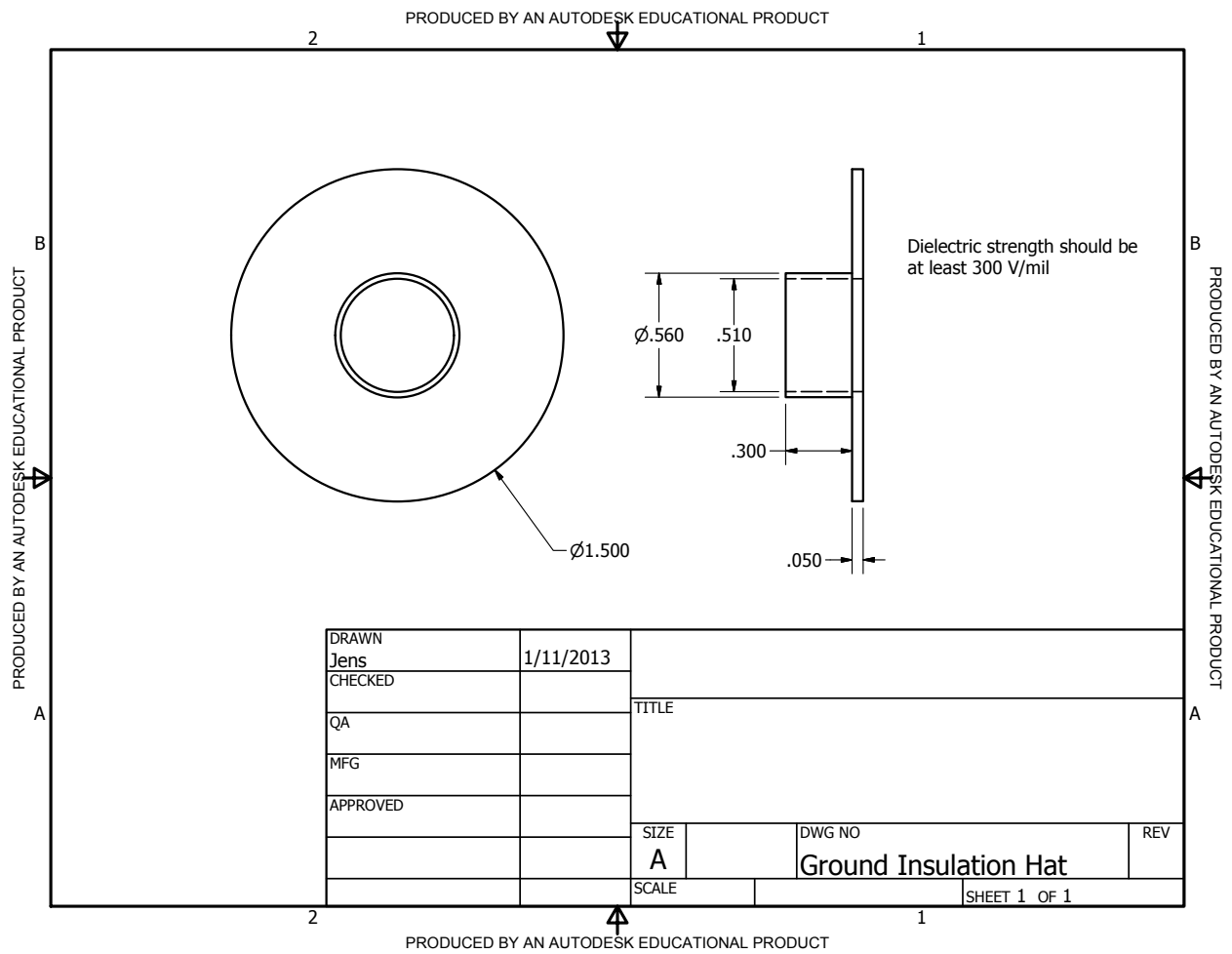
C.2.2 *Plates*



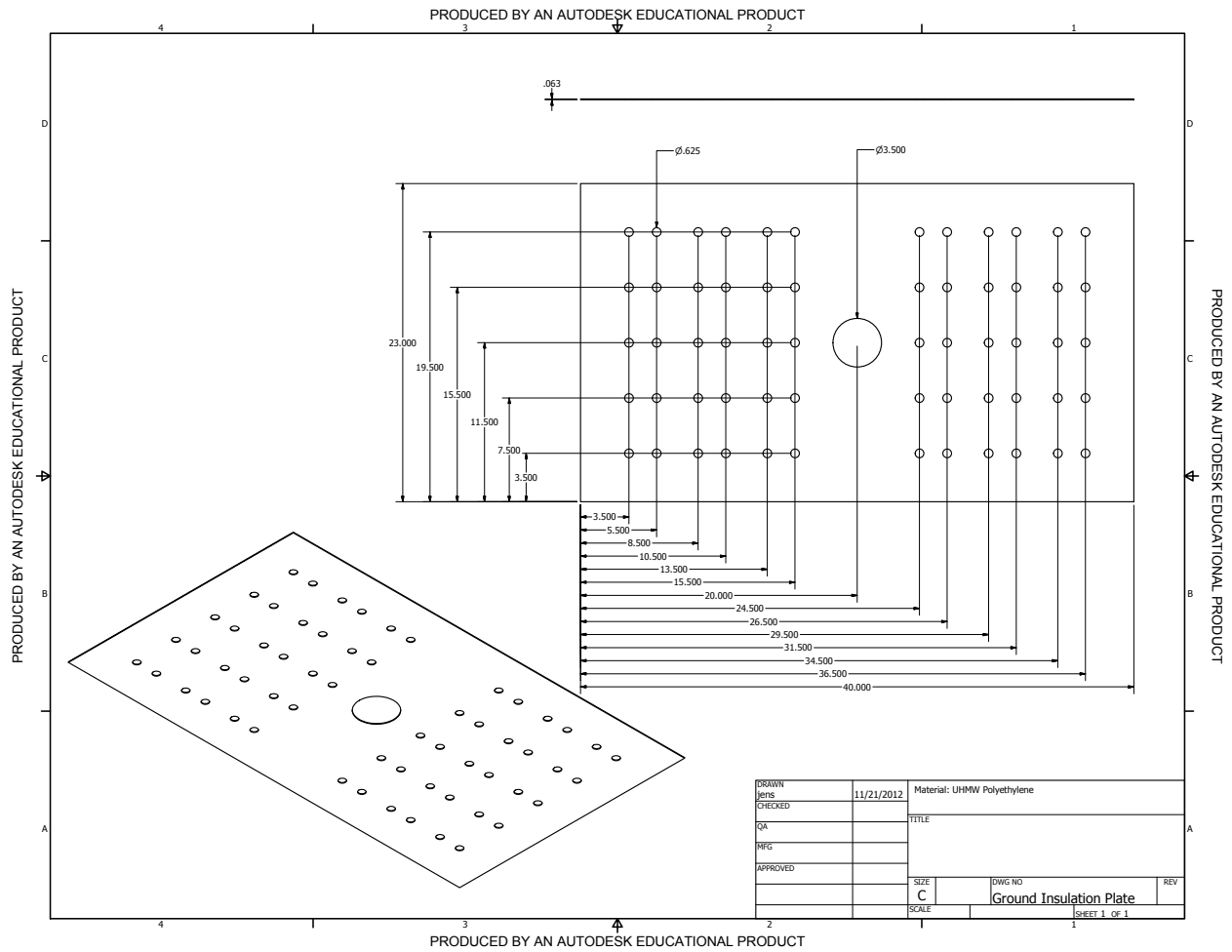


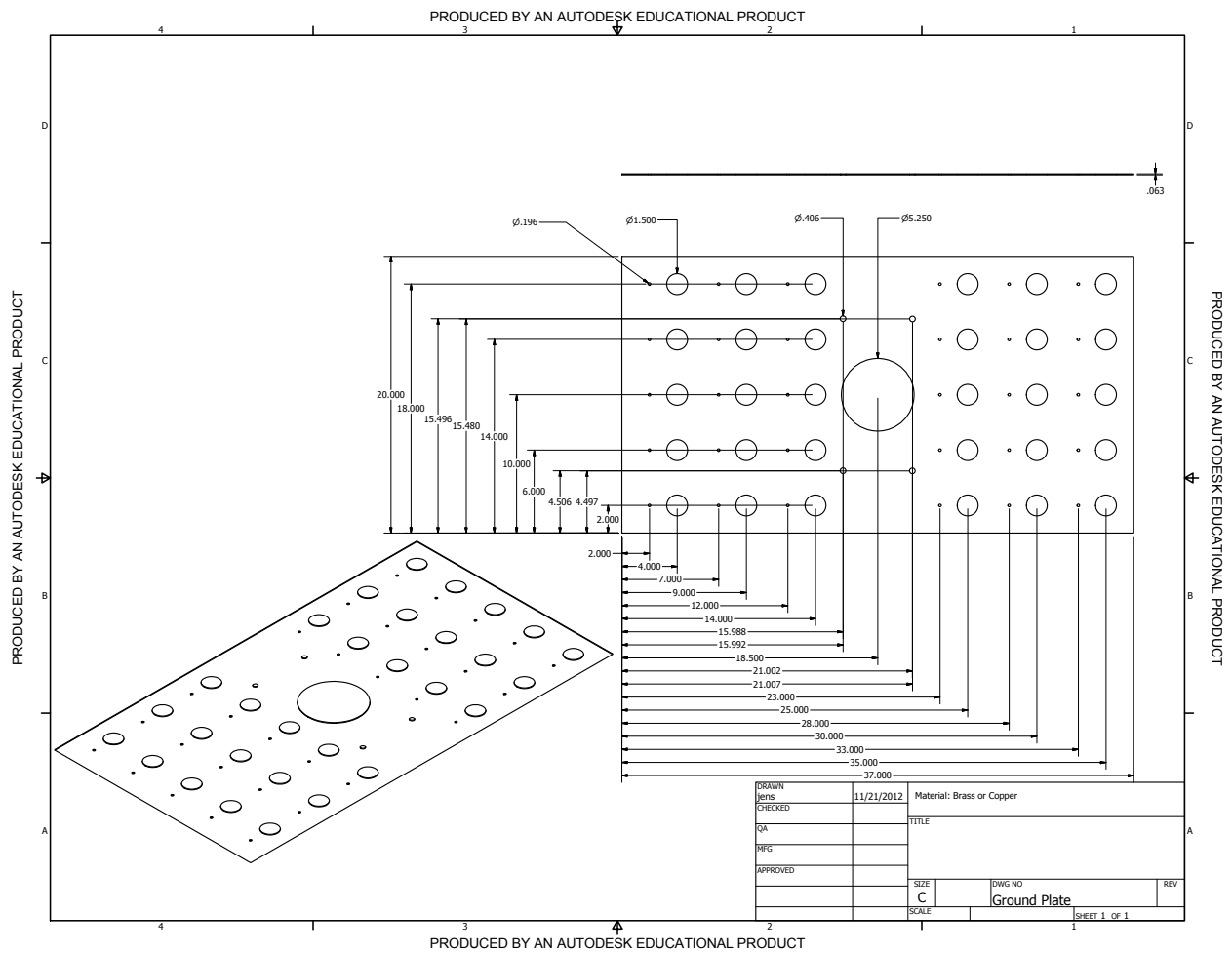


DRAWN	Jens	1/11/2013		
CHECKED			TITLE	
QA				
MFG				
APPROVED				
			SIZE	DWG NO
			A	Hot Insulation Hat
			SCALE	REV
				SHEET 1 OF 1

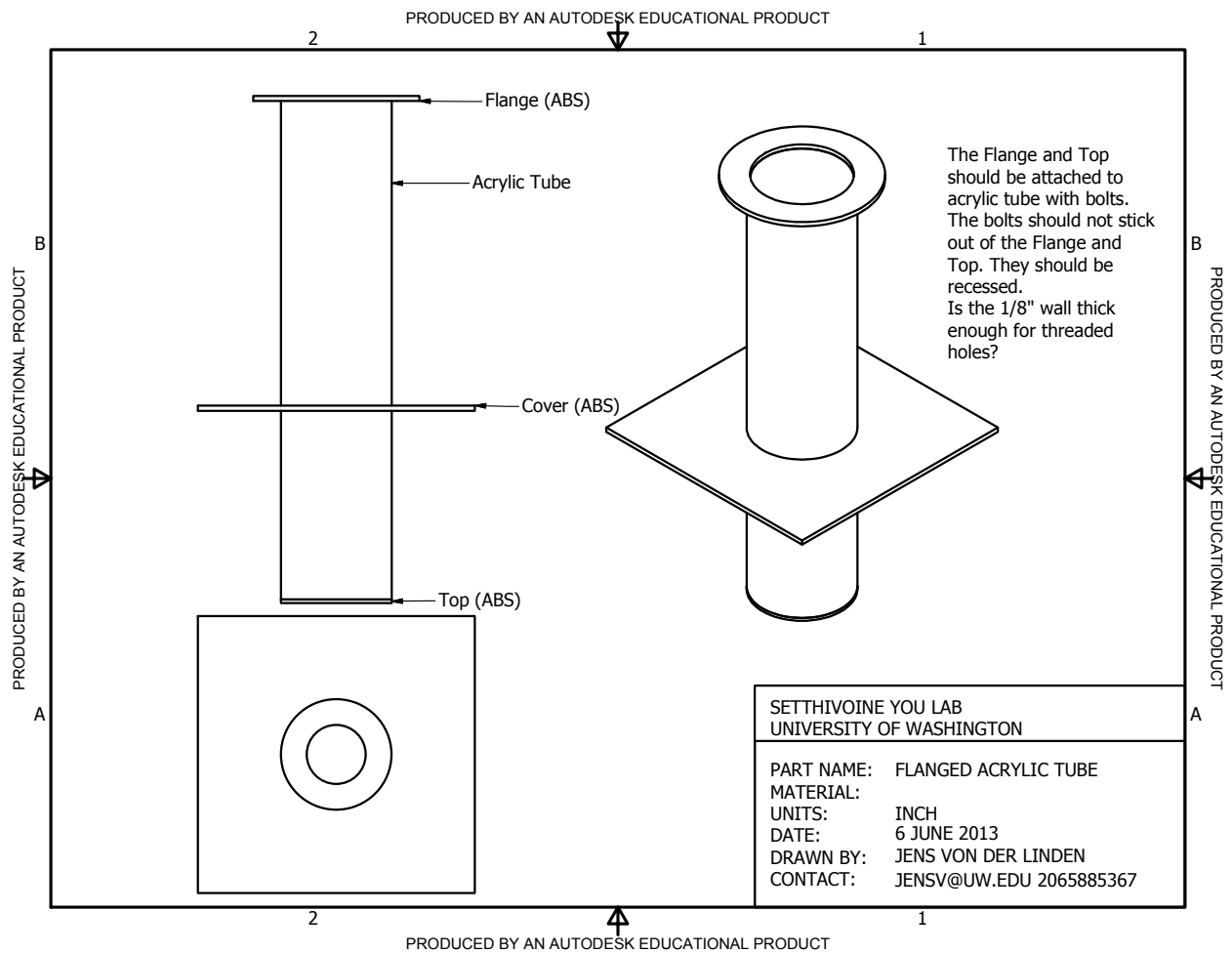


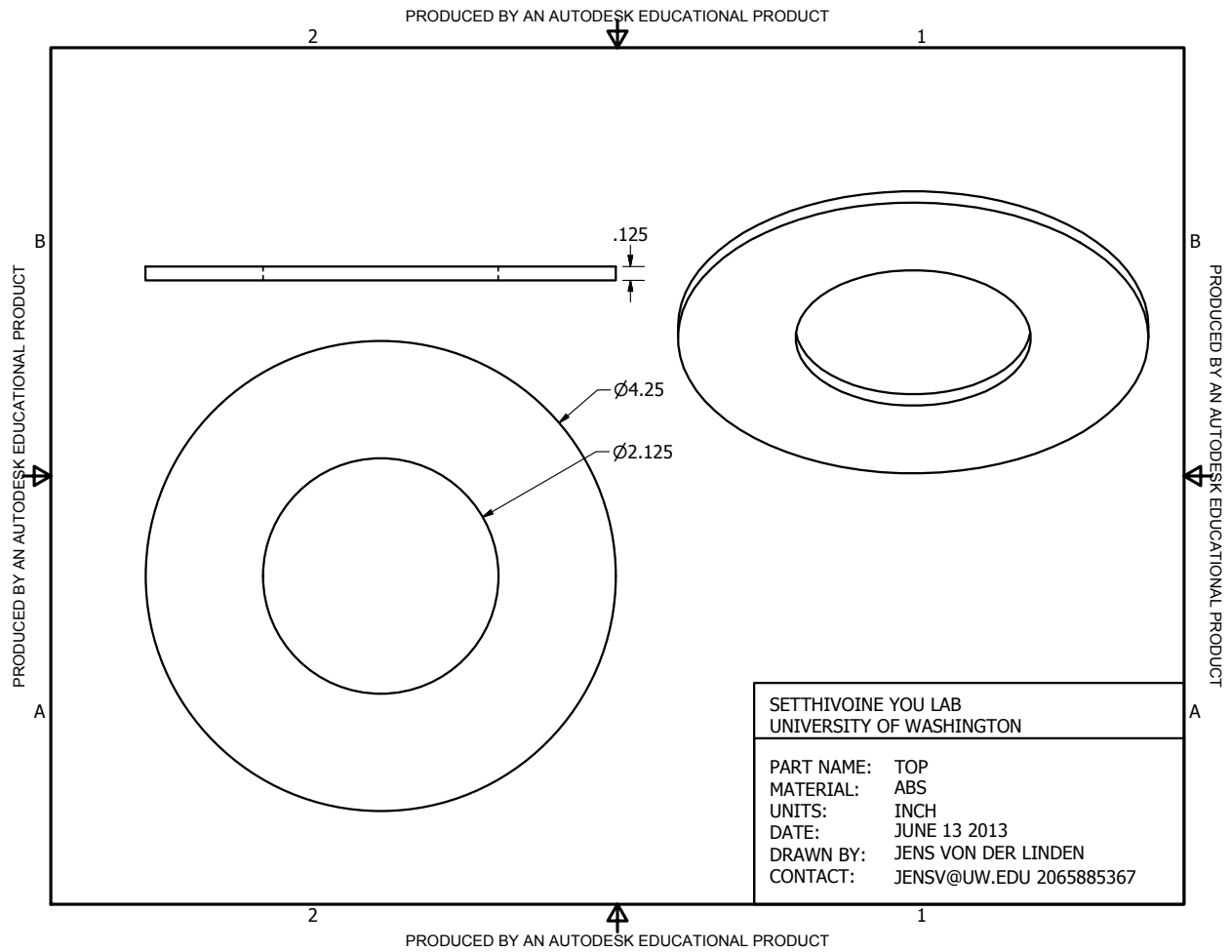
DRAWN	Jens	1/11/2013			
CHECKED			TITLE		
QA					
MFG					
APPROVED					
			SIZE	DWG NO	REV
			A	Ground Insulation Hat	
			SCALE		SHEET 1 OF 1

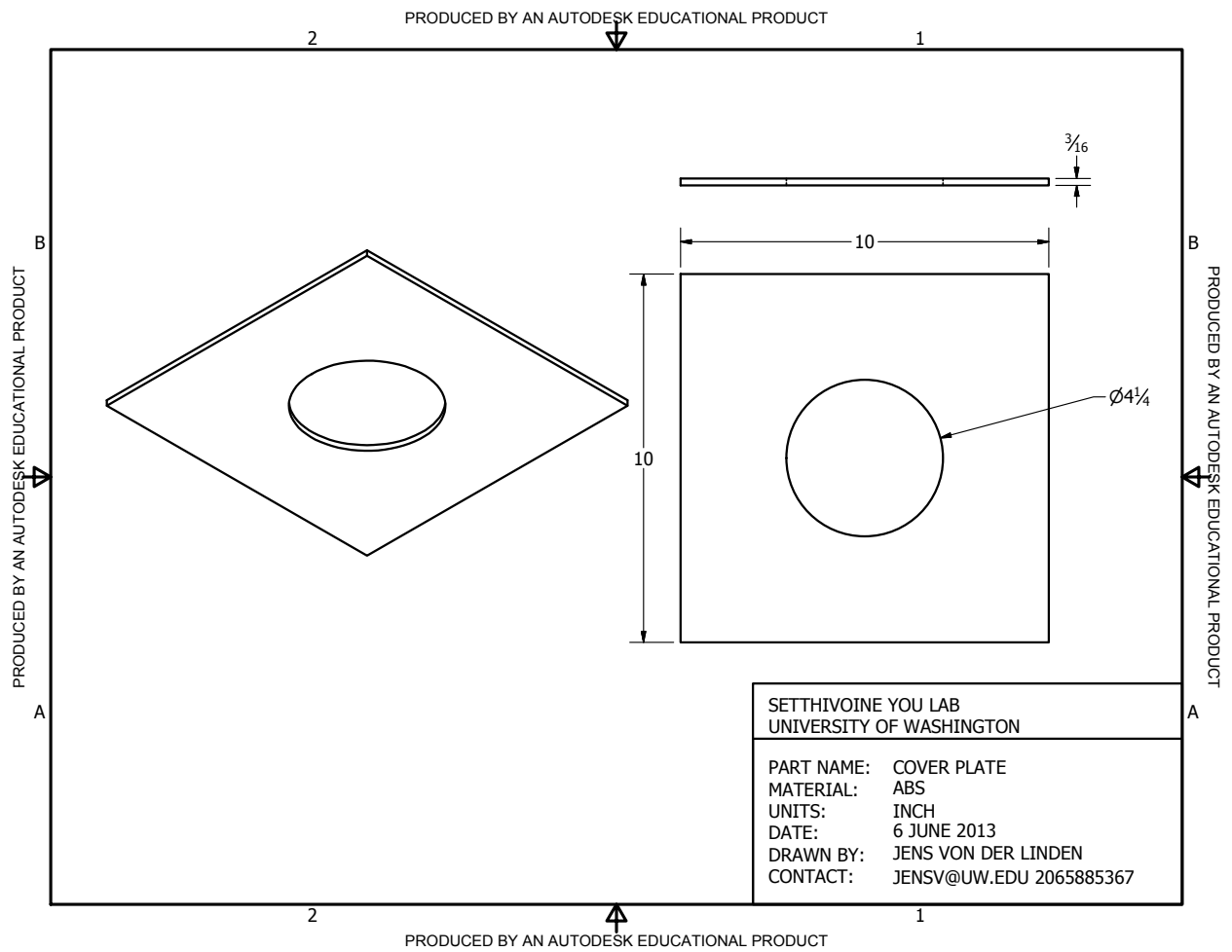


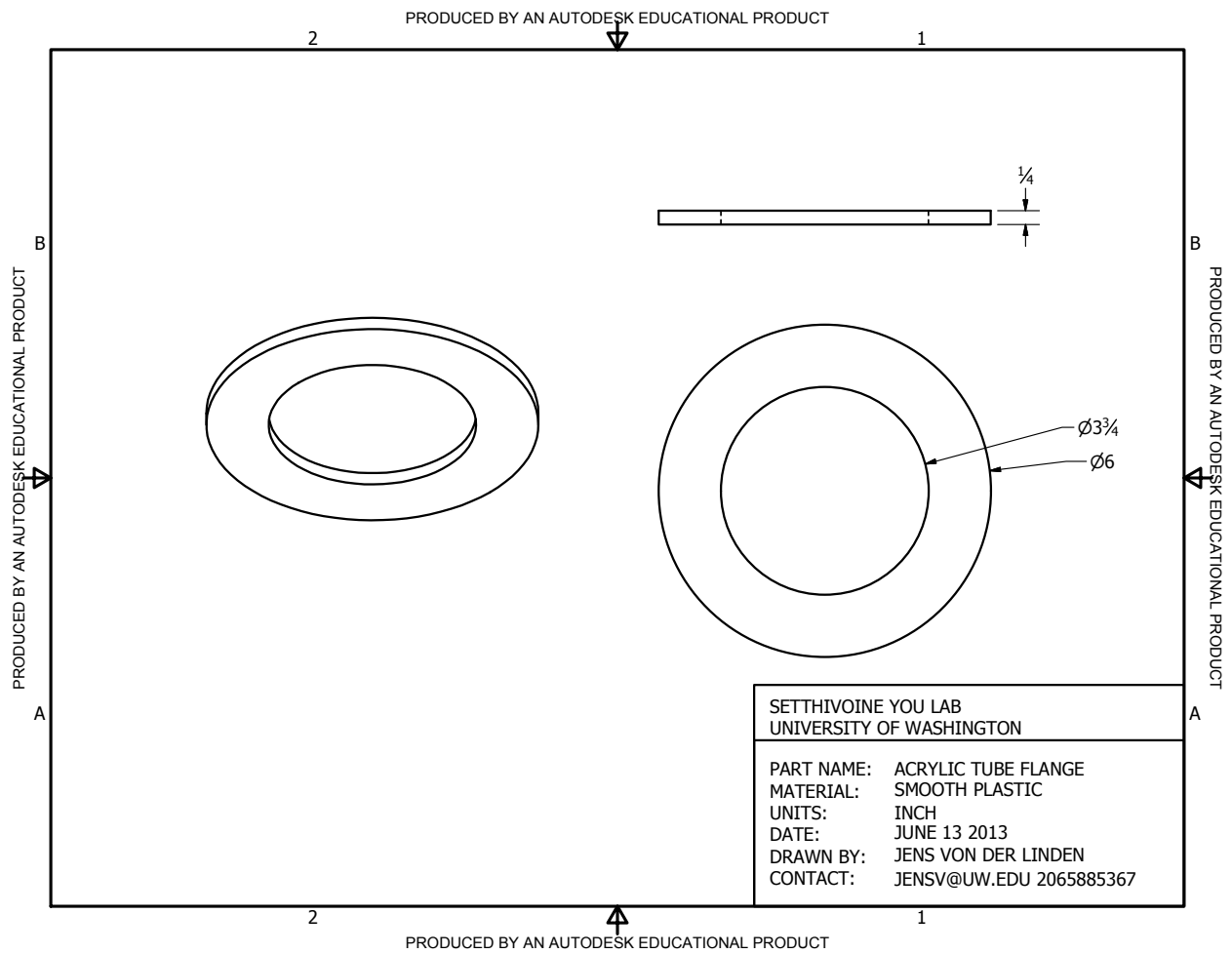


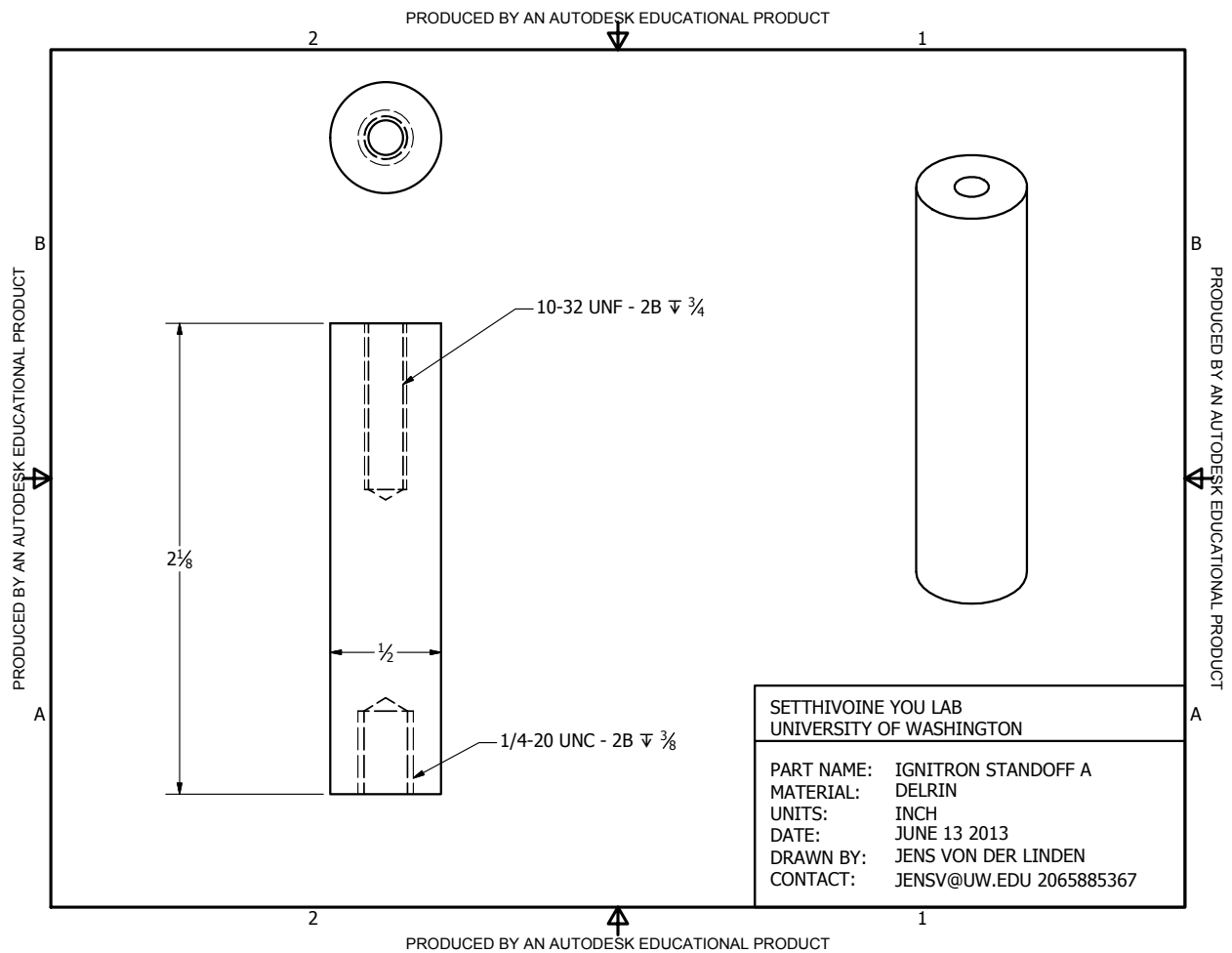
C.2.3 *Ignitron cover parts*

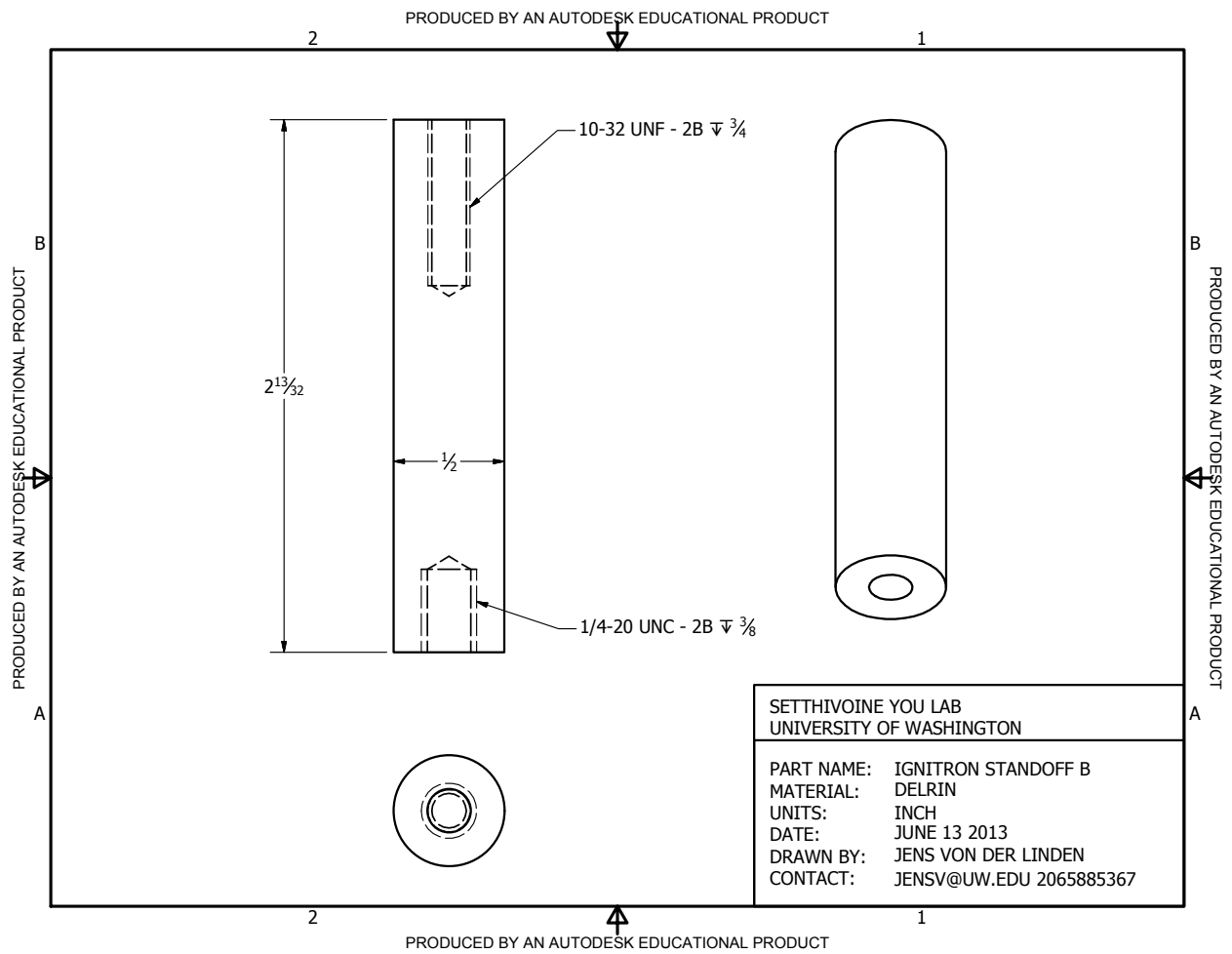




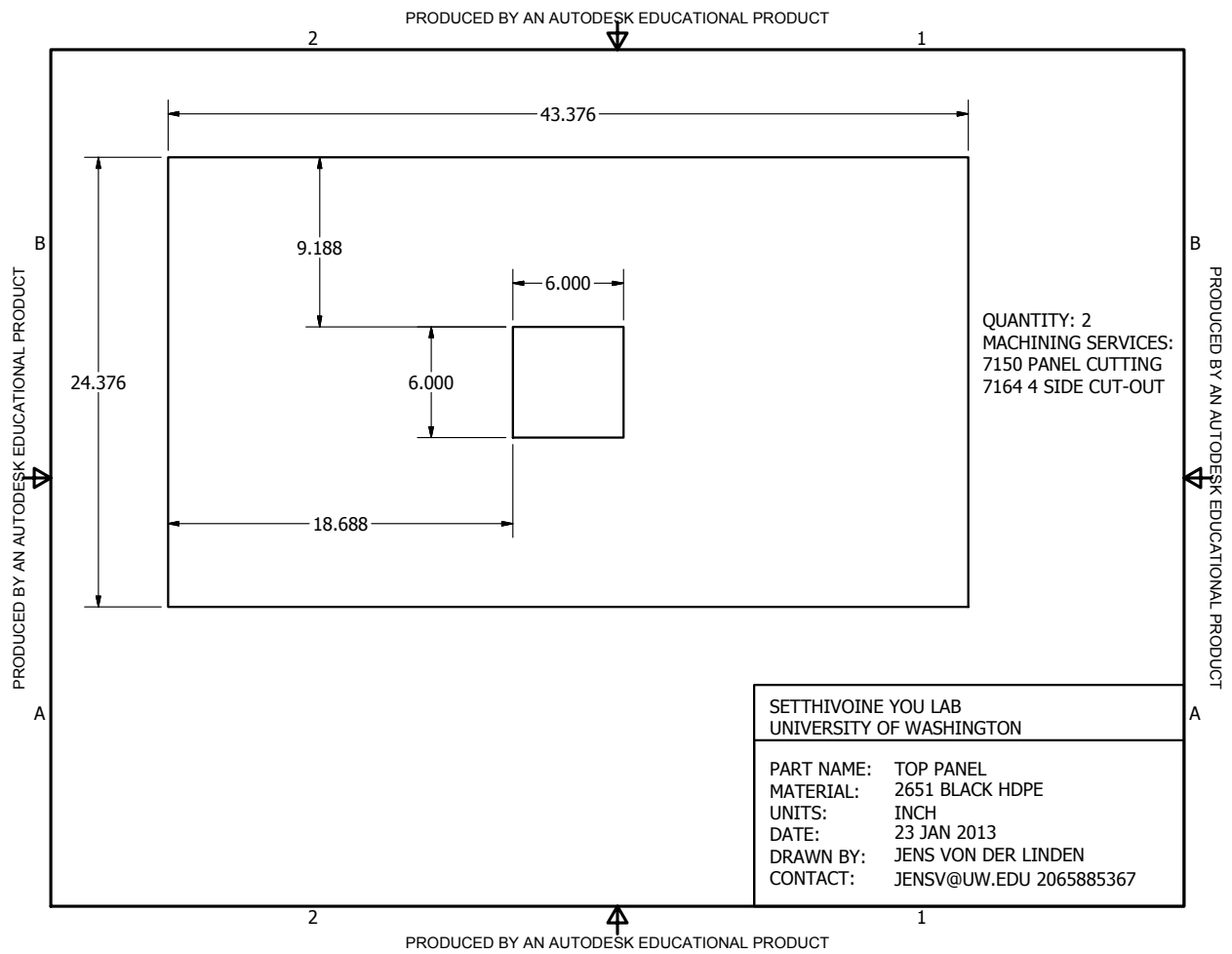


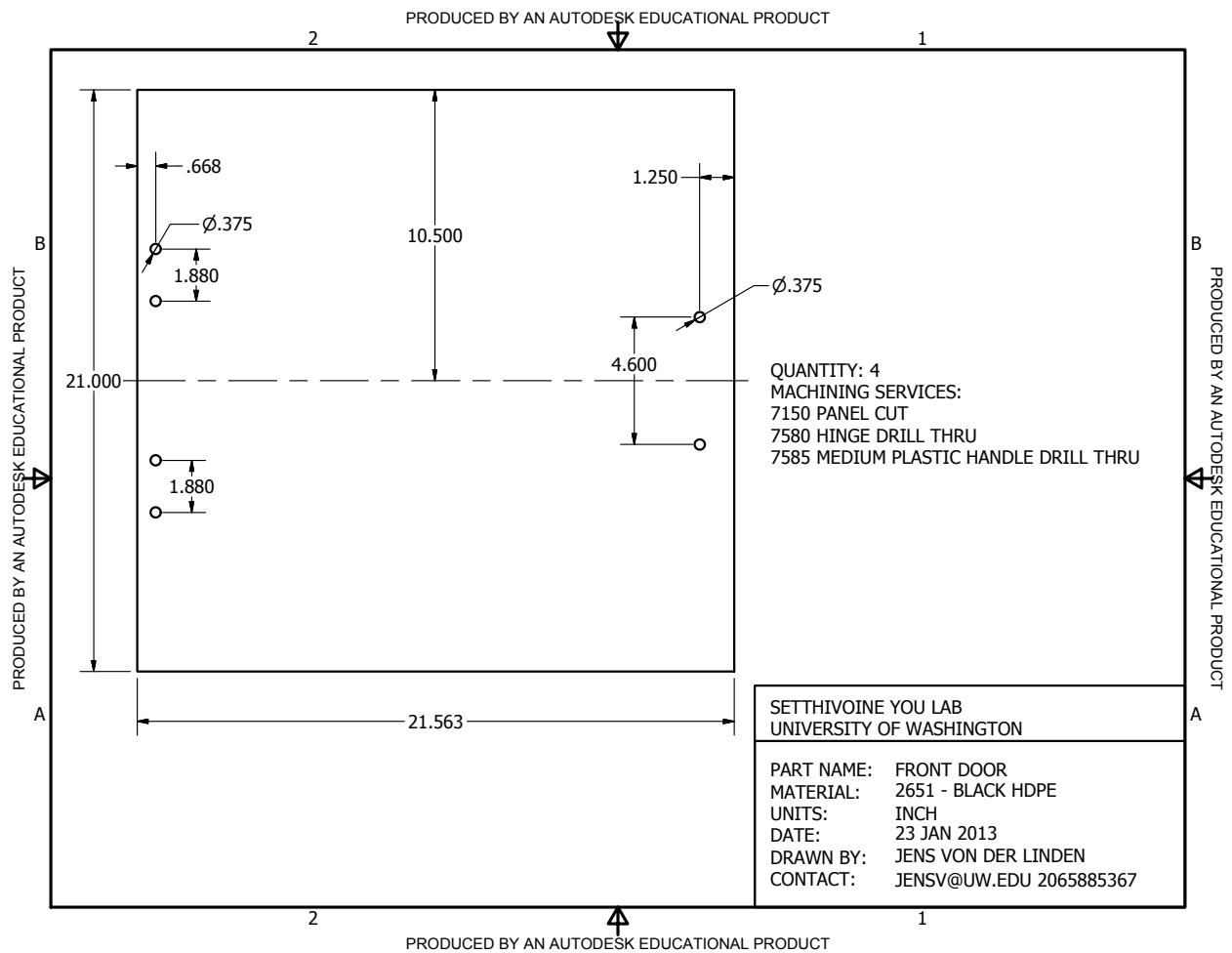


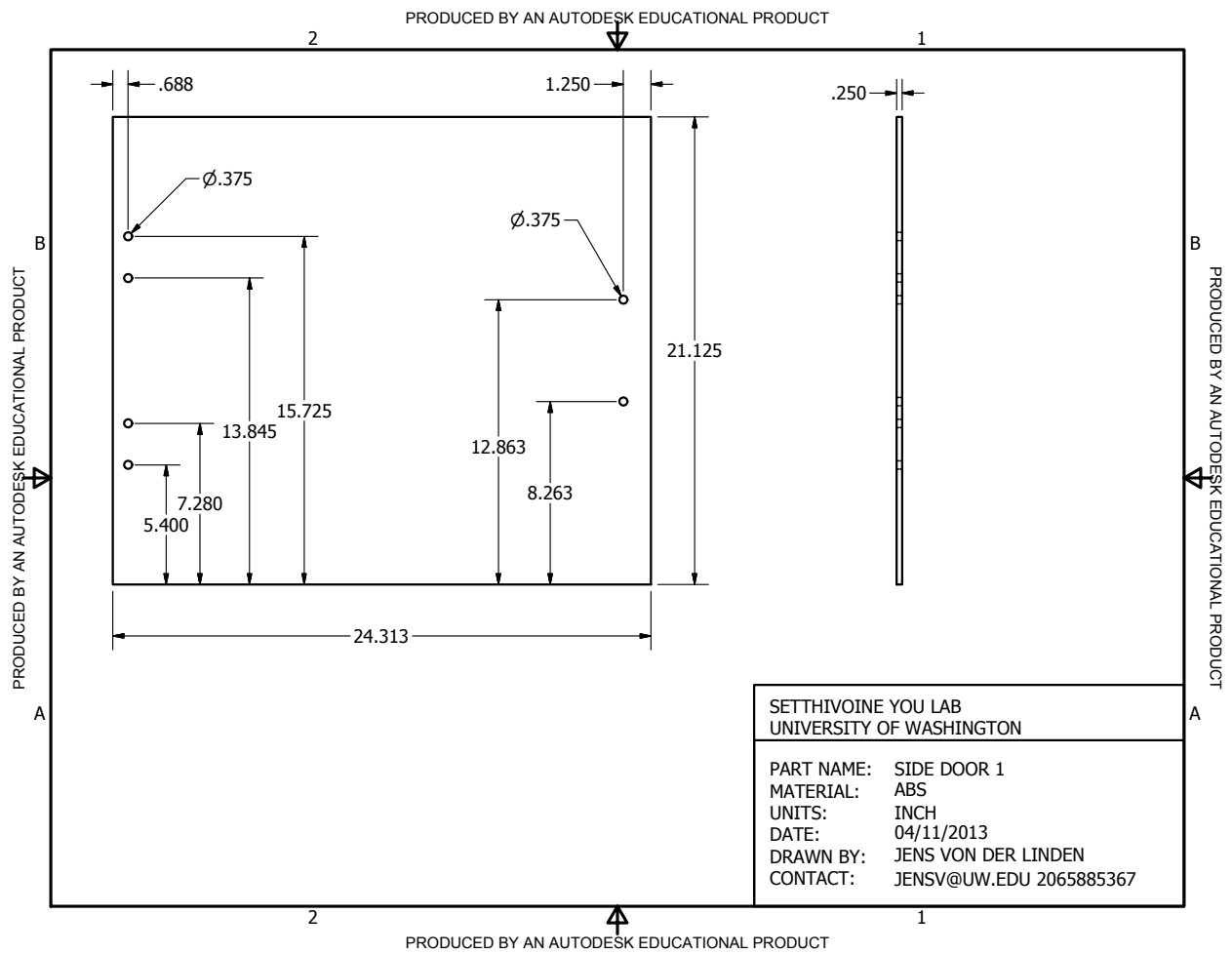


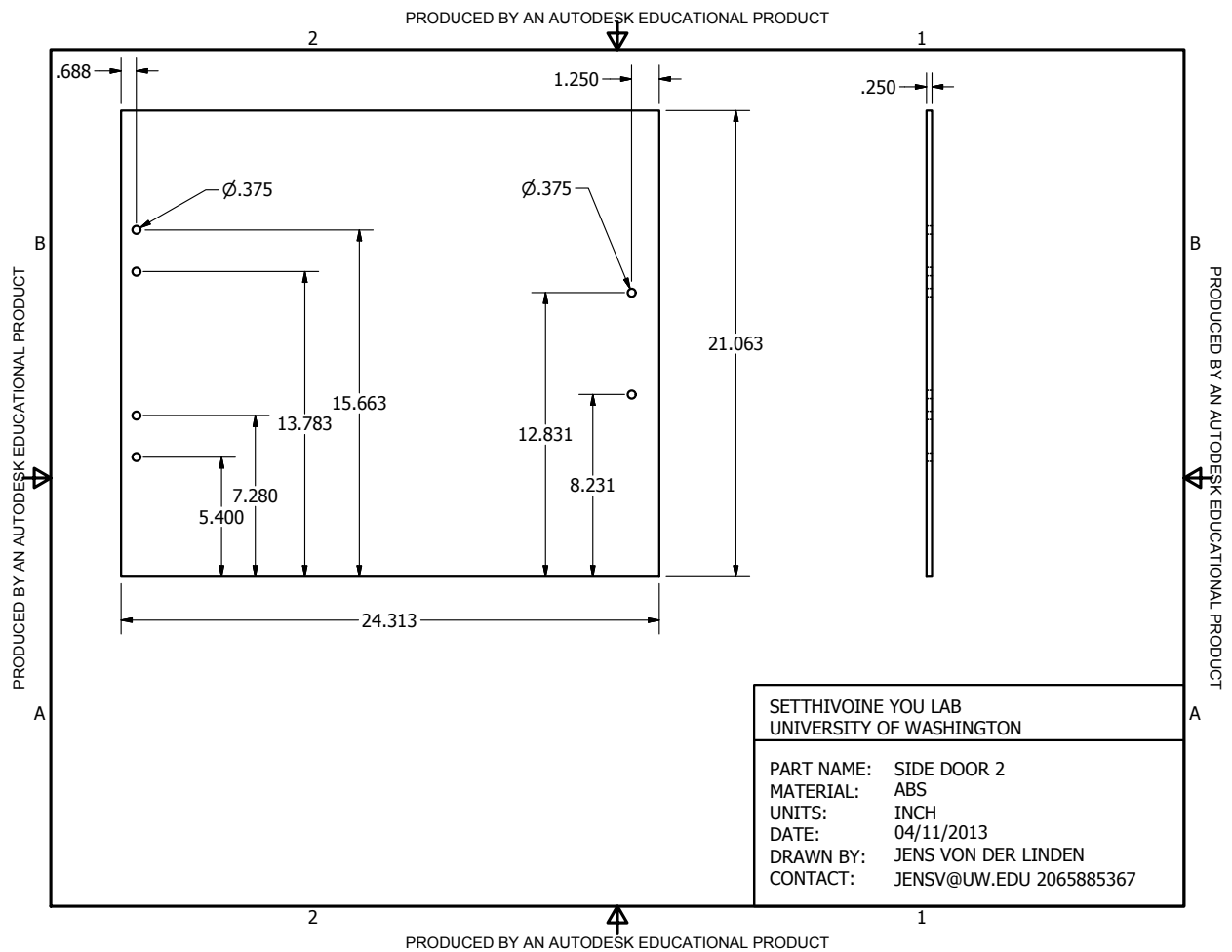


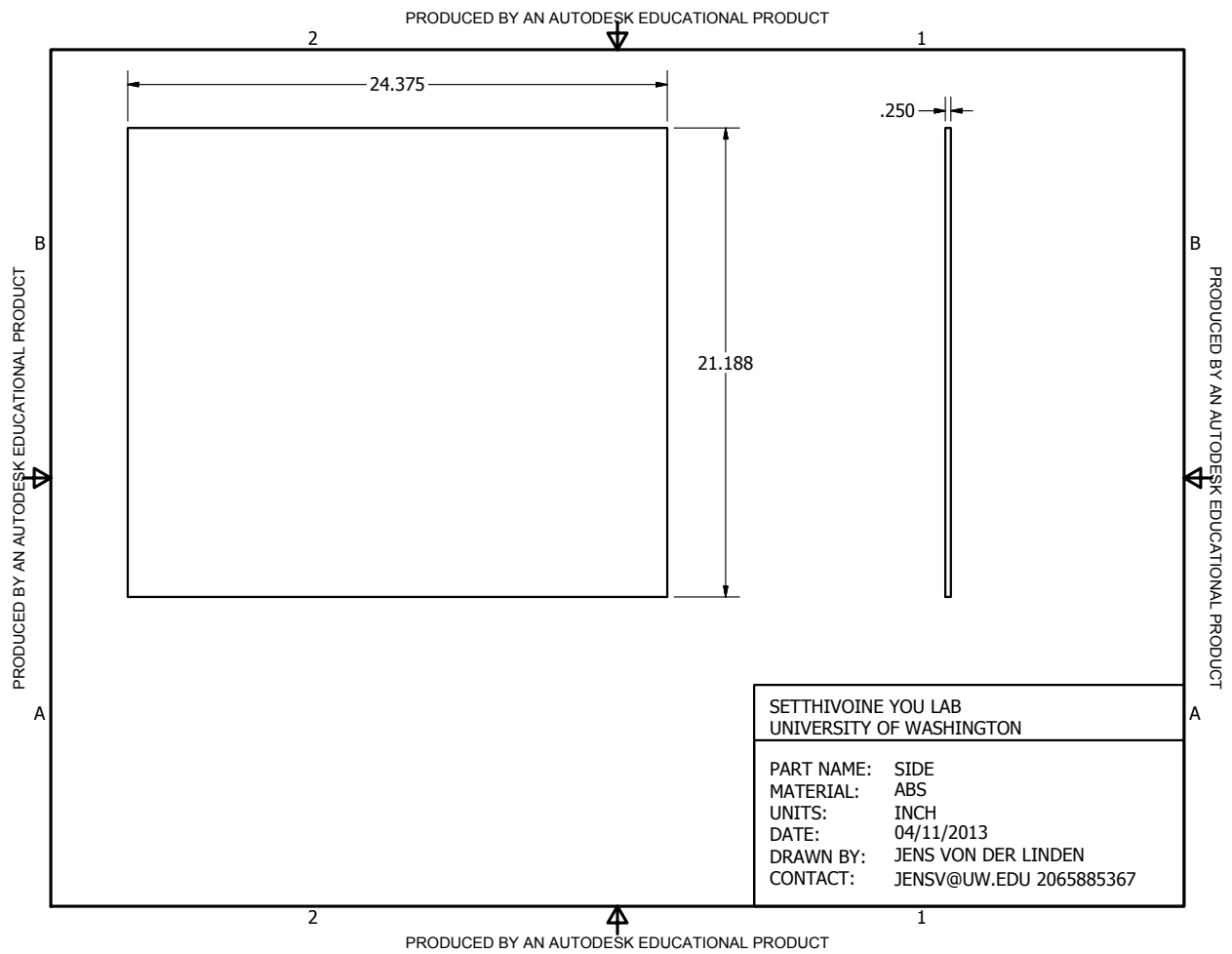
C.2.4 *Panels*

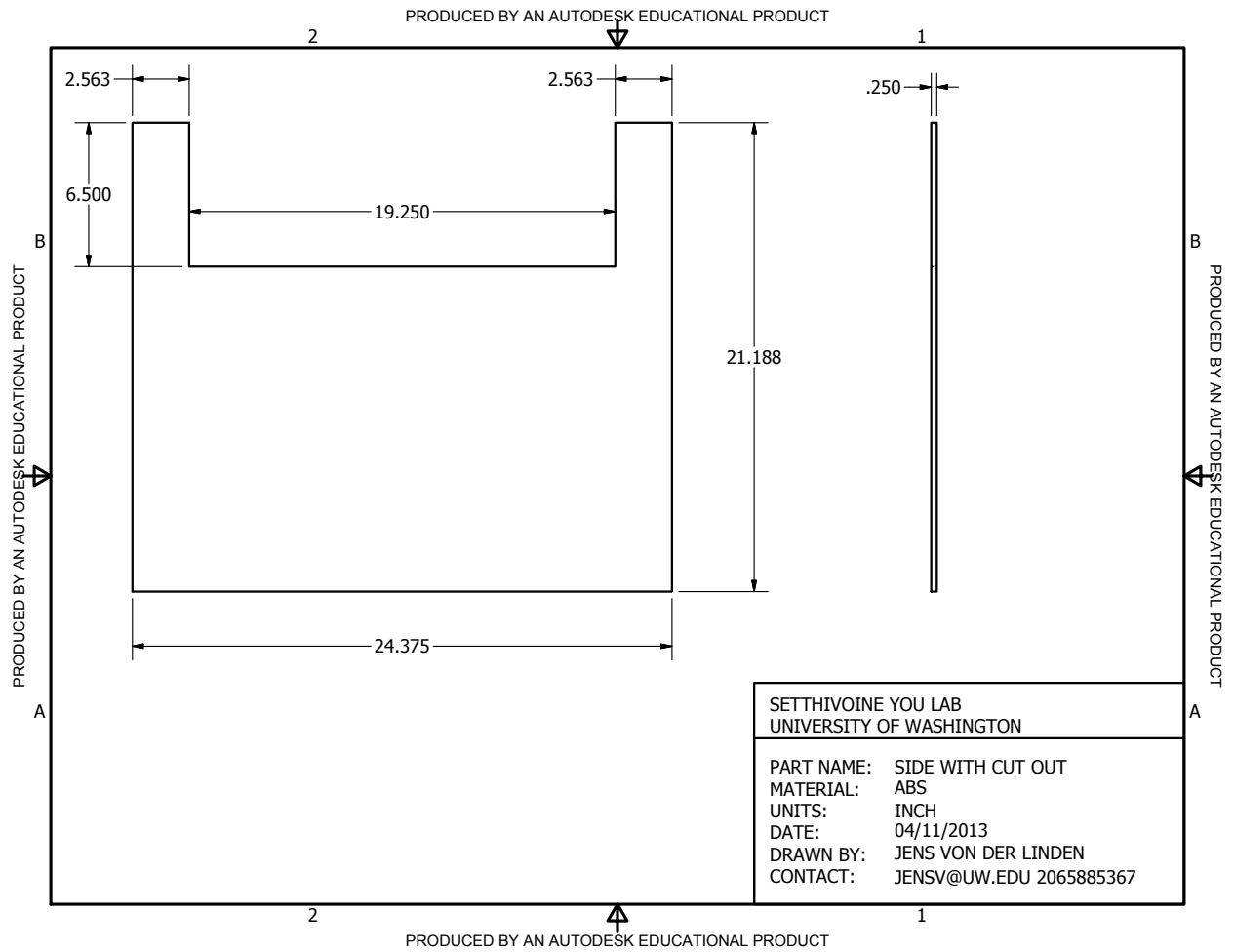


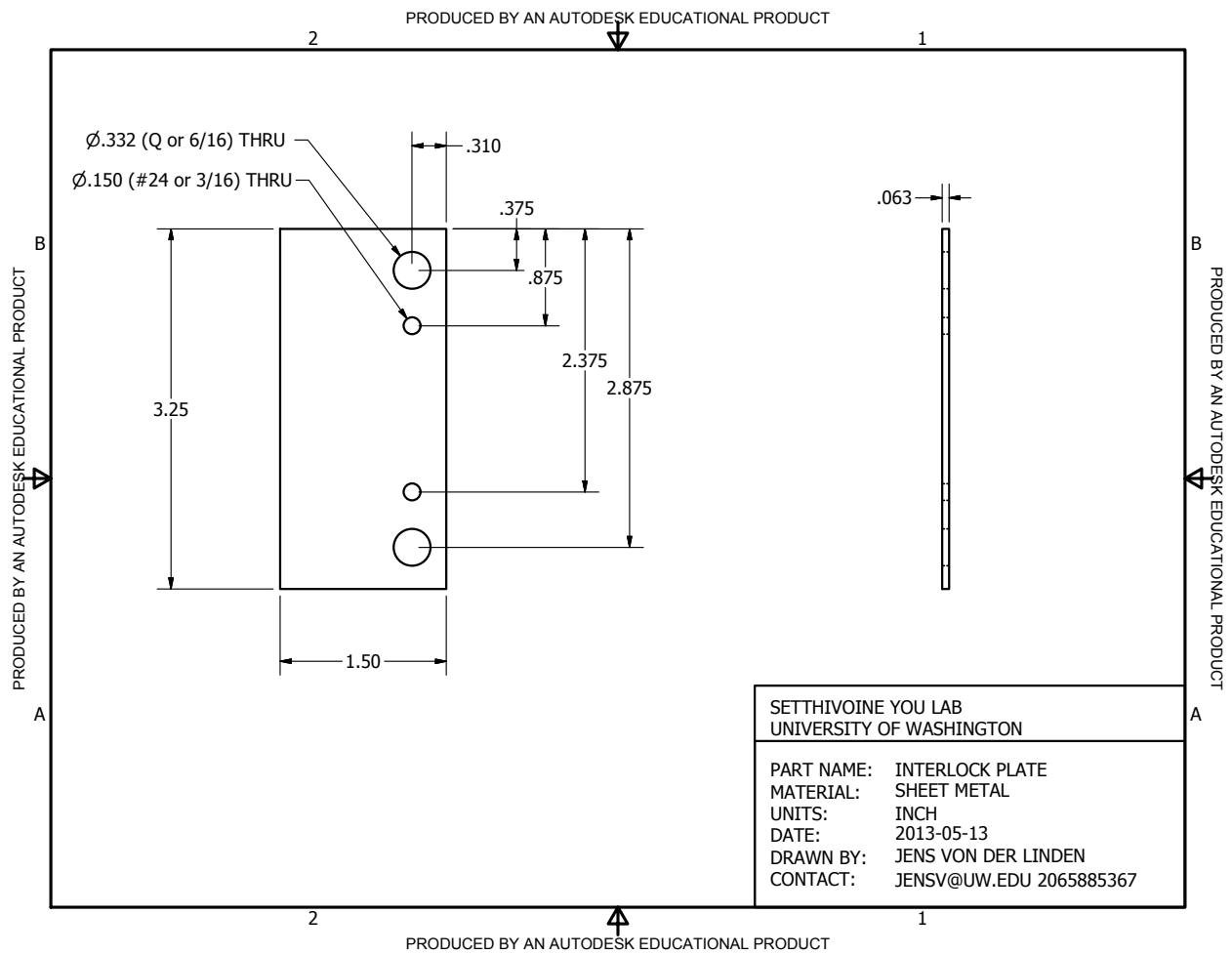


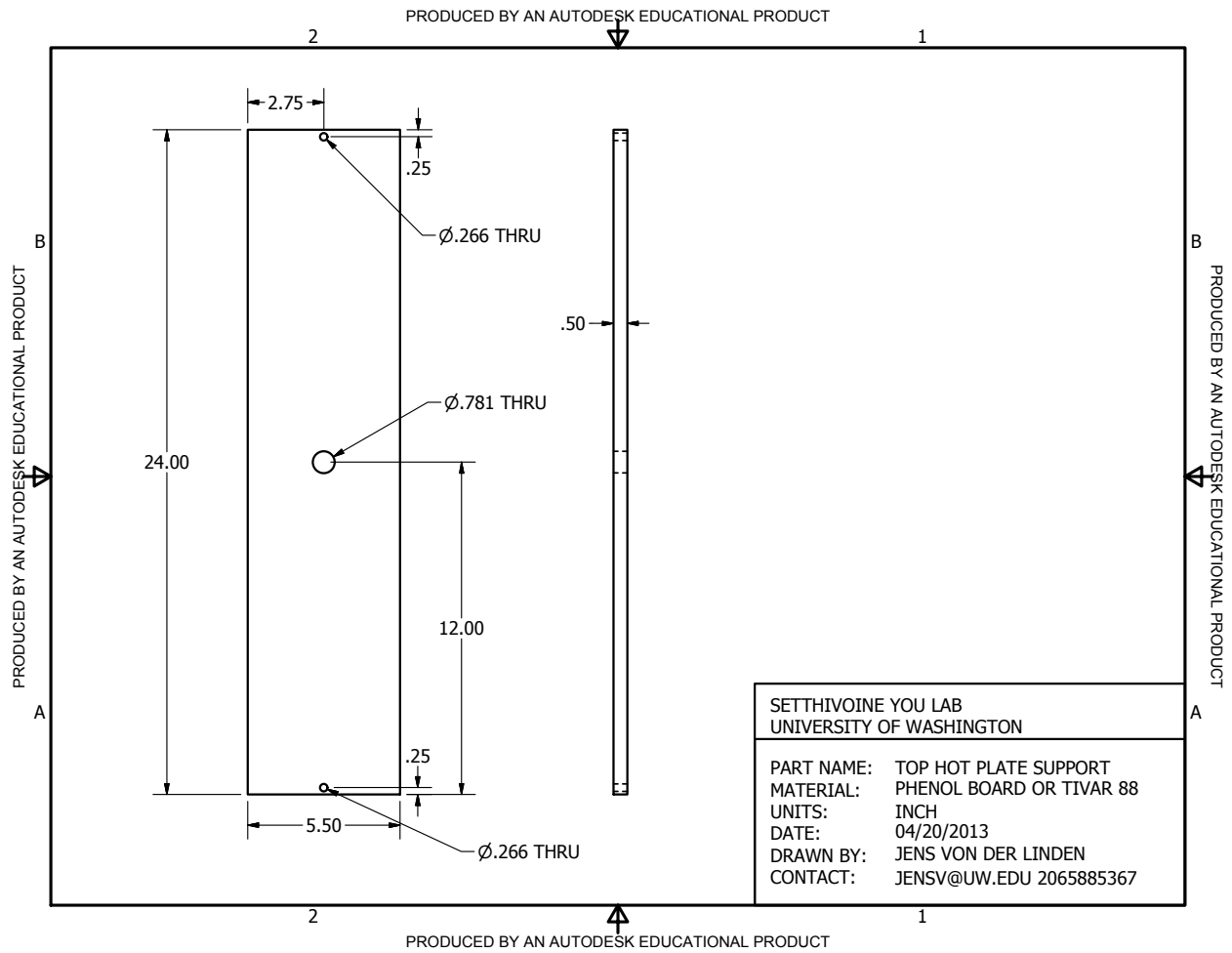


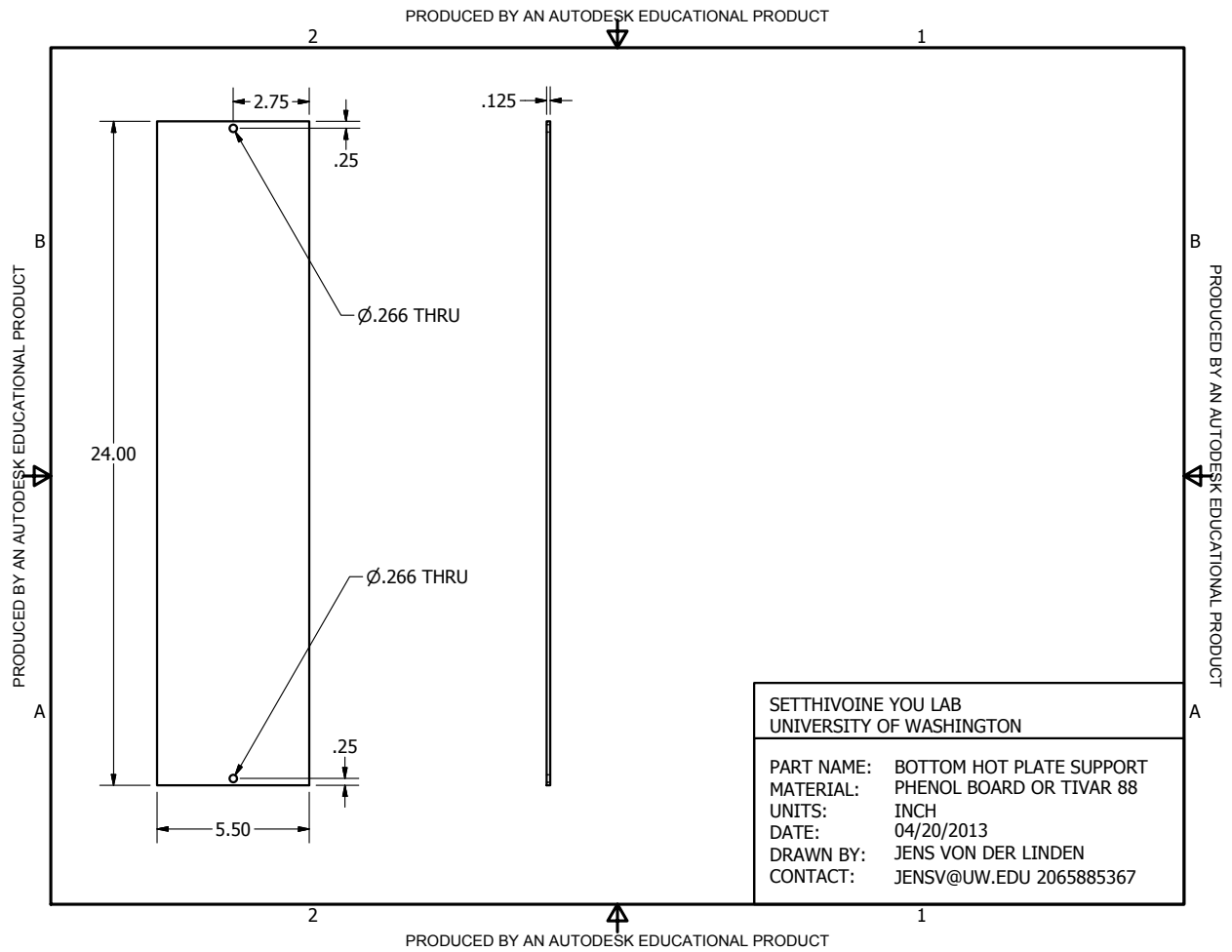


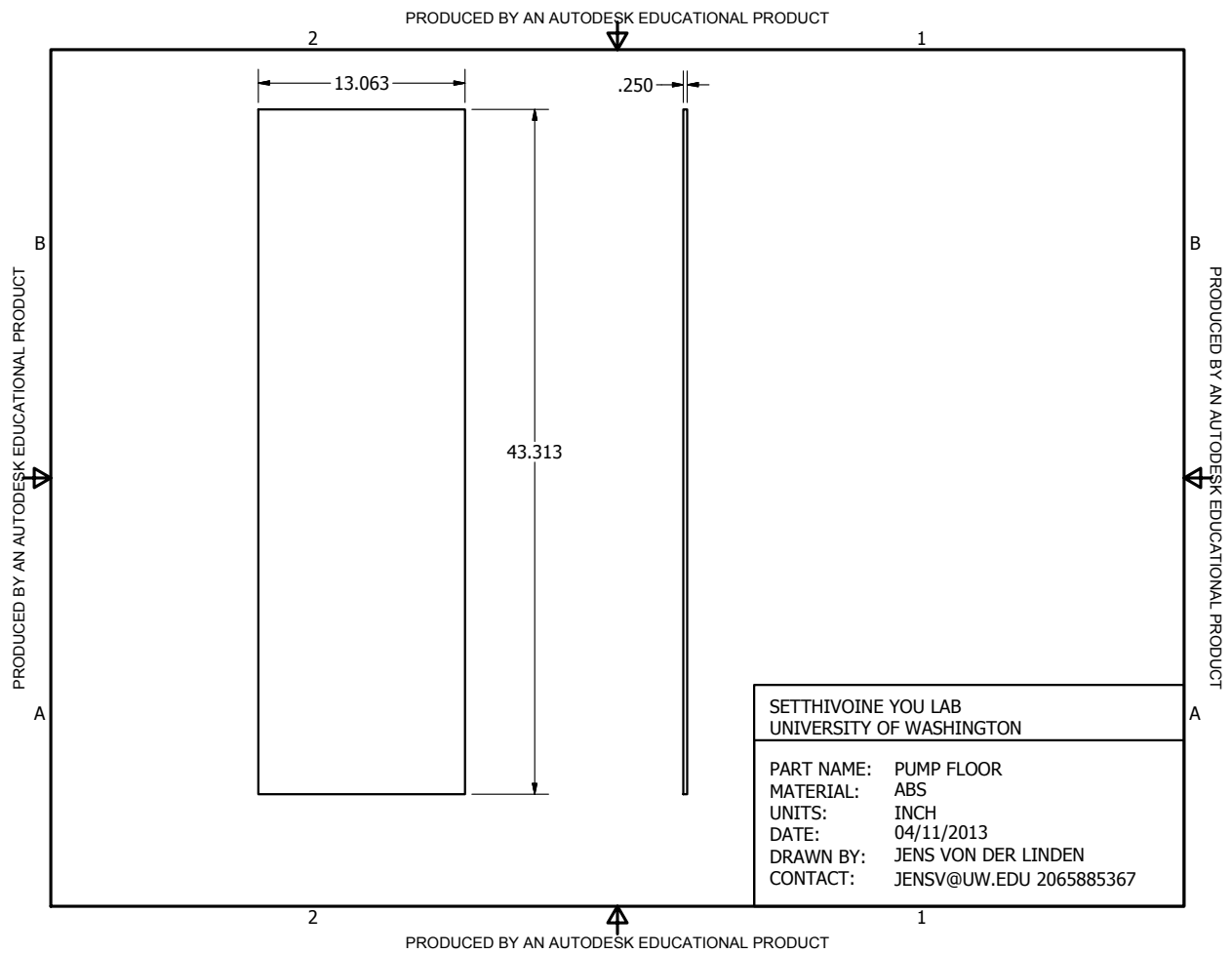


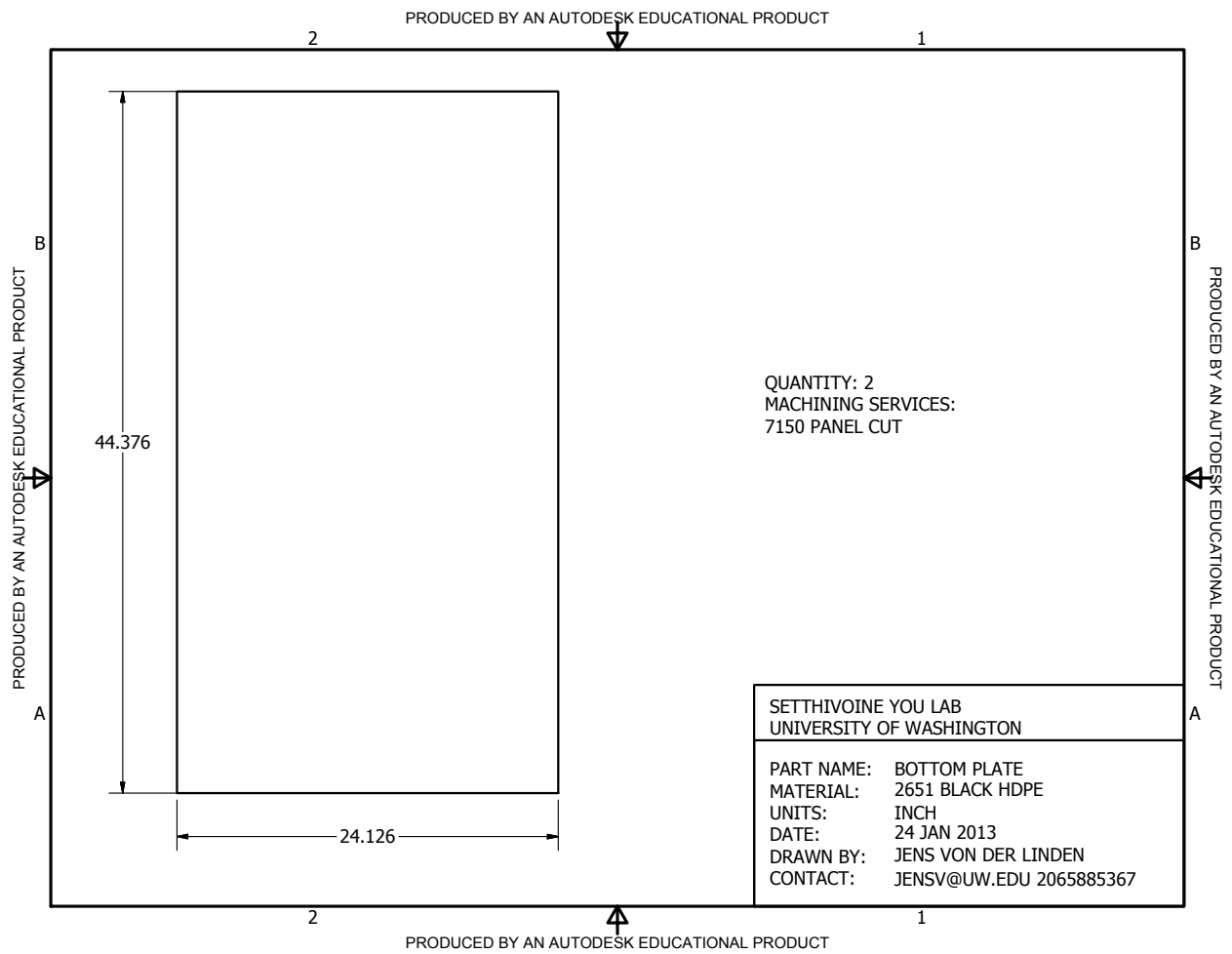












Appendix D

CANONICAL FLUX TUBE AND HELICITY RECONSTRUCTION CODE

This appendix contains scripts used to reconstruct and plot canonical flux tubes in VisIt and calculate their helicity from experimental measurements of magnetic field, density, electron temperature and Mach numbers of a plasma. Only the main scripts are printed the underlying modules can be found at Zenodo

<https://doi.org/10.5281/zenodo.581197> [84].

D.1 Dependencies

- python 2.7.12
- numpy 1.11.2
- scipy 0.18.1
- matplotlib 1.5.3
- seaborn 0.7.1
- sqlite 3.13
- vtk 6.3.0
- MDSplus 7.7.1 and mdsplus python module (alpha7.0.144)
- VisIt 2.10.3 and corresponding visit python module

The dependencies can be installed with the anaconda python distribution. The MD-Plus can be found at <http://www.mdsplus.org/index.php/Introduction>. The mdsplus python module can be found at <https://pypi.python.org/pypi/MDSplus>. VisIt can be found at <https://visit.llnl.gov>. Instructions for installing the VisIt <https://visit.llnl.gov/manuals>.

D.2 RSX data and analysis scripts

This code processes both raw data and processed data from the RSX experiment. The RSX data and RSX data analysis codes have not been released yet. Without these inputs the code can not currently be run, however, it could be adapted to run on other datasets. When they are a note will be added to the Github repository and Zenodo on how to obtain them.

D.3 Directory structure

1. Create two directories output, source. 2. Git clone or copy the repo into source.

D.4 Important files

Each of these files has documentation that can be accessed with `python filename -help`

write_measurements_to_unstructured_grid.py reads processed Bdot and triple probe, and raw Mach probe measurements and writes them to unstructured vtk files files.

fit_field_null.py reads unstructured Bx and By fields and finds the field nulls in a measurement plane.

interpolate_measurements.py interpolates fields from unstructured measurements to rectangular grid.

calculate_dependent_quantities.py calculates the dependent quantities needed to plot flux tubes and calculate helicity from interpolated measurements.

calculate_helicity.py calculates gauge-dependent and relative helicities.

vis_canonical_fluxtubes.py plots frames of canonical flux tube animations. Plot options include ion, electron canonical flux tubes, temperature and density isosurfaces, current contours in an x-y plane.

thesis_figures/thesis_figures.ipynb a jupyter notebook generating the figures for the 5th chapter of my thesis.

D.5 Reference

von der Linden. 2017. Investigating the Dynamics of Canonical Flux Tubes. (PhD thesis) (In preparation.)

D.6 Contact

Jens von der Linden jensv@uw.edu

D.7 Main Scripts

D.7.1 *write_measurements_to_unstructured_grid.py*

```

1  #!/Users/vonderlinden2/anaconda/bin/python
2  # -*- coding: utf-8 -*-
3  """
4  Created on Feb 14 2017
5
6  @author: Jens von der Linden
7
8  Read processed measurements
9  and write to unstructured vtk files files.
10 The processed measurements are magnetic field, density, temperature
11 and Mach number.
12 Mach number is calculated directly from the raw MDSplus Mach probe
13 voltages, all other data is read from IDL output files from the RSX data analysis
14 scripts.
15 Only measurement points slightly larger than the
16 intended interpolation spaces are kept and Delaunay triangulated
17 to define the unstructured grid.
18 """
19 import argparse
20 import numpy as np

```

```

21 from datetime import date
22 from datetime import datetime
23 import os
24
25 from mach_probe_analysis import ion_current_to_mach_number as ic_to_mach
26 from read_from_sql import read_from_sql
27 from write_to_vtk import prepare_measurements as pm
28 from write_to_vtk import unstructured_grid as ug
29
30
31 def main(args):
32     r"""
33     Read processed measurements and write to unstructured vtk files.
34     """
35     now = datetime.now().strftime("%Y-%m-%d-%H-%M")
36     out_dir = '../output/boxed_unstructured_measurements/' + now
37     try:
38         os.makedirs(out_dir)
39     except:
40         pass
41
42     planes = [0.249, 0.302, 0.357, 0.416]
43     bx_measurements = pm.read_idl('bx')
44     by_measurements = pm.read_idl('by')
45     bz_measurements = pm.read_idl('bz')
46     te_measurements = pm.read_idl('te')
47     n_measurements = pm.read_idl('n')
48     mach_y_measurements, mach_z_measurements = pm.read_mach_probe_data(args)
49
50     bx_all_planes = pm.cut_and_average_quantity(bx_measurements,
51                                                args.bx_extent, planes)
52     by_all_planes = pm.cut_and_average_quantity(by_measurements,
53                                                args.by_extent, planes)
54     bz_all_planes = pm.cut_and_average_quantity(bz_measurements,
55                                                args.bz_extent, planes)
56     n_all_planes = pm.cut_and_average_quantity(n_measurements,
57                                                args.n_extent,
58                                                planes,
59                                                bounds=args.n_bounds)
60     te_all_planes = pm.cut_and_average_quantity(te_measurements, args.te_extent,
61                                                planes, bounds=args.te_bounds)
62     mach_y_plane = pm.cut_and_average_quantity(mach_y_measurements, args.mach_y_extent,
63                                                [0.416], bounds=args.mach_bounds)
64     mach_z_plane = pm.cut_and_average_quantity(mach_z_measurements, args.mach_z_extent,
65                                                [0.416], bounds=args.mach_bounds)
66
67
68     n_three_planes = pm.remove_plane(0.302, n_all_planes)
69     te_three_planes = pm.remove_plane(0.302, te_all_planes)
70
71     ug.save_to_unstructured_grid(bx_all_planes, 'bx', out_dir,
72                                prefix=args.output_prefix)
73     ug.save_to_unstructured_grid(by_all_planes, 'by', out_dir,
74                                prefix=args.output_prefix)
75     ug.save_to_unstructured_grid(bz_all_planes, 'bz', out_dir,
76                                prefix=args.output_prefix)
77     ug.save_to_unstructured_grid(te_three_planes, 'te', out_dir,

```

```

78         prefix=args.output_prefix)
79     ug.save_to_unstructured_grid(n_three_planes, 'n', out_dir,
80         prefix=args.output_prefix)
81     ug.save_to_unstructured_grid(mach_y_plane, 'mach_y', out_dir,
82         prefix=args.output_prefix)
83     ug.save_to_unstructured_grid(mach_z_plane, 'mach_z', out_dir,
84         prefix=args.output_prefix)
85
86 def parse_args():
87     r"""
88     Read Arguments.
89     """
90     parser = argparse.ArgumentParser(description='Create unstructured VTK from measurements')
91     parser.add_argument('--bx_extent',
92         help='spatial extent of Bx measurements',
93         nargs=6, type=float,
94         default=[-0.032, 0.028, -0.022, 0.032, 0.249, 0.416])
95     parser.add_argument('--by_extent',
96         help='spatial extent of By measurements',
97         nargs=6, type=float,
98         default=[-0.032, 0.028, -0.022, 0.032, 0.249, 0.416])
99     parser.add_argument('--bz_extent',
100        help='spatial extent of Bz measurements',
101        nargs=6, type=float,
102        default=[-0.032, 0.028, -0.022, 0.032, 0.249, 0.416])
103     parser.add_argument('--te_extent',
104        help='spatial extent of temperature measurements',
105        nargs=6, type=float,
106        default=[-0.026, 0.028, -0.03, 0.029, 0.249, 0.416])
107     parser.add_argument('--te_bounds',
108        help='sensible bounds for temperature measurements',
109        nargs=2, type=float,
110        default=[1e-3, 1e3])
111     parser.add_argument('--n_extent',
112        help='spatial extent of density measurements',
113        nargs=6, type=float,
114        default=[-0.026, 0.028, -0.03, 0.029, 0.249, 0.416])
115     parser.add_argument('--n_bounds',
116        help='sensible bounds for density measurements',
117        nargs=2, type=float,
118        default=[1e3, 1e22])
119     parser.add_argument('--mach_time_steps',
120        help='# of time steps to extract from one gyration', type=int,
121        default=250)
122     parser.add_argument('--shot_database', help='path to shot database',
123        default='/home/jensv/rsx/jens_analysis/helicity_tools/shots_database/shots.db')
124     parser.add_argument('--table_name', help='name of sql table',
125        default='Shots')
126     parser.add_argument('--min_spectral',
127        help=("minimum spectral energy around gyration"
128             "frequency to include shot"),
129        type=float,
130        default=1.6e-8)
131     parser.add_argument('--mach_y_extent',
132        help='spatial extent of mach measurements to include',
133        nargs=6, type=float,
134        default=[-0.052, 0.052, -0.022, 0.032, 0.249, 0.416])

```

```

135     parser.add_argument('--mach_z_extent',
136                         help='spatial extent of mach measurements to include',
137                         nargs=6, type=float,
138                         default=[-0.032, 0.032, -0.022, 0.032, 0.249, 0.416])
139     parser.add_argument('--mach_bounds',
140                         help='bounds on mach measurements', nargs=2, type=float,
141                         default=[-10, 10])
142     parser.add_argument('--output_prefix',
143                         help='prefix of output files',
144                         default='_boxed_unstructured_')
145     args = parser.parse_args()
146     return args
147
148 if __name__ == '__main__':
149     args = parse_args()
150     main(args)

```

D.7.2 *fit_field_null.py*

```

1  r"""
2  Fits field line null.
3
4  Created March 28 2017 by Jens von der Linden.
5
6  Fit field nulls of the Bx and By magnetic field with
7  iterative circle fitting to the field lines.
8
9  Reads unstructured vtk files and generates Bx and By interpolators.
10 """
11
12 import argparse
13 from scipy.interpolate import LinearNDInterpolator
14 import numpy as np
15 from scipy.optimize import leastsq
16 from scipy import odr
17 from scipy import ndimage
18 from scipy.integrate import odeint, dblquad
19 from datetime import datetime
20 import os
21 from scipy.interpolate import LinearNDInterpolator
22
23 from write_to_vtk.read_unstructured_vtk import read_unstructured_vtk
24 from write_to_vtk import structured_3d_vtk as struc_3d
25
26
27 def main(args):
28     r"""
29     Fit field nulls of the Bx and By magnetic field with
30     iterative circle fitting to the field lines.
31     """
32     now = datetime.now().strftime("%Y-%m-%d-%H-%M")
33     out_dir = '../output/' + args.output_prefix + '/' + now + '/'
34     try:
35         os.makedirs(out_dir)

```

```

36     except:
37         pass
38
39     in_dir = args.input_path + args.input_date + '/'
40     in_file = args.input_file_text
41
42     centroids = []
43
44
45     bxby_extents = {0: args.bxby_extent_0,
46                   1: args.bxby_extent_1,
47                   2: args.bxby_extent_2,
48                   3: args.bxby_extent_3}
49     bz_extents = {0: args.bz_extent_0,
50                 1: args.bz_extent_1,
51                 2: args.bz_extent_2,
52                 3: args.bz_extent_3}
53
54     bxby_extent = bxby_extents[args.plane_number]
55     bz_extent = bz_extents[args.plane_number]
56
57     for time_point in xrange(args.time_steps):
58         print time_point
59         time_str = str(time_point).zfill(4)
60         bx_points, bx_values = read_unstructured_vtk(in_dir + 'bx' +
61                                                    in_file + time_str + '.vtk')
62         by_points, by_values = read_unstructured_vtk(in_dir + 'by' +
63                                                    in_file + time_str + '.vtk')
64         #bz_points, bz_values = read_unstructured_vtk(in_dir + 'bz' +
65                                                    in_file + time_str + '.vtk')
66         #
67         z_value = np.unique(bx_points[:, 2])[args.plane_number]
68
69         z_index = np.where(bx_points[:, 2] == z_value)[0]
70         bx_points = bx_points[z_index, :-1]
71         bx_values = bx_values[z_index]
72         z_index = np.where(by_points[:, 2] == z_value)[0]
73         by_points = by_points[z_index, :-1]
74         by_values = by_values[z_index]
75         #z_index = np.where(bz_points[:, 2] == z_value)[0]
76         #bz_points = bz_points[z_index, :-1]
77         #bz_values = bz_values[z_index]
78
79         bx_interpolator = struc_3d.get_interpolator(bx_points, bx_values)
80         by_interpolator = struc_3d.get_interpolator(by_points, by_values)
81         #bz_interpolator = struc_3d.get_interpolator(bz_points, bz_values)
82         grid_extent = [bxby_extent[0], bxby_extent[1],
83                       -0.02, bxby_extent[3]]
84         grid = np.meshgrid(np.linspace(grid_extent[0], grid_extent[1],
85                                     (grid_extent[1] - grid_extent[0])/
86                                     args.spatial_increment),
87                           np.linspace(grid_extent[2], grid_extent[3],
88                                     (grid_extent[3] - grid_extent[2])/
89                                     args.spatial_increment))
90
91         (centroid, center_points,
92          radii, streamlines,
93          max_index) = find_field_null(grid,

```

```

93             bx_interpolator ,
94             by_interpolator ,
95             launch_point_step_factor=0.05,
96             integration_length=20)
97     centroids.append(centroid)
98
99 centroids = np.asarray(centroids)
100 np.savetxt(out_dir + '/field_nulls.txt', centroids ,
101            header=("magnetic field null positions in z plane # %d plane,"
102                  "determined by"
103                  "fitting circles to integrated field lines starting at max"
104                  "magnitude and moving successive towards the center of circles."
105                  % args.plane_number))
106
107
108 def d_l(l, t, interpolator_x, interpolator_y):
109     r"""
110     Returns d_l for the field line integrator.
111     """
112     return np.asarray([interpolator_x([l[0], l[1]])[0],
113                       interpolator_y([l[0], l[1]])[0]])
114
115
116 def to_min(params, points):
117     r"""
118     Returns circle expression to minimize with least squares.
119     """
120     a = 2.*params[0]
121     b = 2.*params[1]
122     c = params[2]**2 - params[1]**2 - params[0]**2
123     return a*points[0] + b*points[1] + c - points[0]**2 - points[1]**2
124
125
126 def find_field_null(grid, bx_interpolator, by_interpolator,
127                   distance_thres=0.001, filter_size=2,
128                   integration_length=10, integration_steps=100,
129                   launch_point_step_factor=0.1, max_count=50,
130                   params_guess=[0, 0, 0.01]):
131     r"""
132     Find Bx-By field null in a x-y plane
133     by integrating field lines and fitting a circle to them.
134     Move towards the center and iterate process.
135     If leaving the measurement plane
136     extrapolate from last fit circle.
137     Start close to the Bx-By field max.
138     """
139     b_fields_x = bx_interpolator(grid[0][:, :], grid[1][:, :])
140     b_fields_y = by_interpolator(grid[0][:, :], grid[1][:, :])
141     b_fields = [b_fields_x, b_fields_y]
142     x_min, x_max = grid[0].min(), grid[0].max()
143     y_min, y_max = grid[1].min(), grid[1].max()
144     magnitude = np.sqrt(b_fields[0][:, :]**2 + b_fields[1][:, :]**2)
145     filtered_magnitude = ndimage.gaussian_filter(magnitude, filter_size)
146     max_index = np.unravel_index( np.nanargmax(filtered_magnitude),
147                                 filtered_magnitude.shape)
148     center_points = []
149     radii = []

```

```

150     center_points = []
151     streamlines = []
152     direction = [0, 0]
153     distance = 100
154     launch_point = (grid[0][:][max_index], grid[1][:][max_index])
155     count = 0
156     while distance >= distance_thres:
157         #print 'launch', launch_point
158         #print distance
159         t2 = np.linspace(0, integration_length, integration_steps)
160         t1 = np.linspace(0, -integration_length, integration_steps)
161         stream2 = odeint(d_1, launch_point, t2, args=(bx_interpolator, by_interpolator))
162         stream1 = odeint(d_1, launch_point, t1, args=(bx_interpolator, by_interpolator))
163         streamline = np.concatenate((stream1, stream2))
164         size0 = np.sum(np.invert(np.isnan(streamline[:, 0])))
165         size1 = np.sum(np.invert(np.isnan(streamline[:, 1])))
166         min_index = np.argmin([size0, size1])
167         min_size = [size0, size1][min_index]
168         streamline = streamline[np.invert(np.isnan(streamline[:, min_index]))].reshape(min_size, 2)
169         try:
170             circle_params, success = leastsq(to_min, params_guess,
171                                             args=np.asarray([streamline[:, 0],
172                                                             streamline[:, 1]]))
173         except:
174             break
175         direction = [circle_params[0] - launch_point[0], circle_params[1] - launch_point[1]]
176         distance = np.sqrt(direction[0]**2. + direction[1]**2.)
177         center_point = (circle_params[0], circle_params[1])
178         launch_point = [launch_point[0] + direction[0] * launch_point_step_factor,
179                       launch_point[1] + direction[1] * launch_point_step_factor]
180         center_points.append(center_point)
181         #print 'center', center_point
182         radii.append(circle_params[0])
183         streamlines.append(streamline)
184         if (launch_point[0] <= x_min or
185             launch_point[0] >= x_max or
186             launch_point[1] <= y_min or
187             launch_point[1] >= y_max or
188             count > max_count):
189             break
190         count += 1
191     field_null = center_point
192     return field_null, center_points, radii, streamlines, max_index
193
194
195 def integrate_flux(centroid, radius, bz_interpolator, limits, bias_field=0.02):
196     r"""
197     Return axial magnetic flux and error estimate integrated
198     in a circle of given radius around a given centroid.
199     """
200     if (centroid[0] - radius < limits[0] or centroid[0] + radius > limits[1] or
201         centroid[1] - radius < limits[2] or centroid[1] + radius > limits[3]):
202         return -1
203     gfun = lambda x: -np.sqrt(radius**2 - (x-centroid[0])**2)
204     hfun = lambda x: np.sqrt(radius**2 - (x-centroid[0])**2)
205     bz_interpolator_bias = lambda x, y: bz_interpolator(x, y) + bias_field
206     return dblquad(bz_interpolator_bias, centroid[0] - radius,

```

```

207         centroid[0] + radius, gfun, hfun)
208
209
210 def parse_args():
211     r"""
212     Read arguments.
213     """
214     parser = argparse.ArgumentParser(description="Create VTK files of"
215                                     "interpolated measurements")
216     parser.add_argument('--input_path',
217                         help='path to input files',
218                         default='../output/boxed_unstructured_measurements/')
219     parser.add_argument('--input_date',
220                         help='time stamp of input files',
221                         default='2017-04-11-21-07')
222     parser.add_argument('--input_file_text',
223                         help='input file name',
224                         default='_boxed_unstructured_')
225     parser.add_argument('--spatial_increment',
226                         help='Spatial increment of grids',
227                         type=float, default=0.001)
228     parser.add_argument('--derivative_increment',
229                         help="spatial increment used to determine"
230                             "tetrahedron derivative of Delaunay"),
231                         type=float, default=0.0001)
232     parser.add_argument('--plane_number',
233                         help="z-Plane number on which to find field nulls.",
234                         type=int, default=0)
235     parser.add_argument('--bxby_extent_0',
236                         help='overlapping spatial extent of bx by',
237                         nargs=6, type=float,
238                         default=[-0.027, 0.025, -0.057, 0.040, 0.249, 0.416])
239     parser.add_argument('--bxby_extent_1',
240                         help='overlapping spatial extent of bx by',
241                         nargs=6, type=float,
242                         default=[-0.027, 0.027, -0.073, 0.041, 0.249, 0.416])
243     parser.add_argument('--bxby_extent_2',
244                         help='overlapping spatial extent of bx by',
245                         nargs=6, type=float,
246                         default=[-0.047, 0.031, -0.021, 0.028, 0.249, 0.416])
247     parser.add_argument('--bxby_extent_3',
248                         help='overlapping spatial extent of bx by',
249                         nargs=6, type=float,
250                         default=[-0.061, 0.031, -0.026, 0.03, 0.249, 0.416])
251     parser.add_argument('--bz_extent_0',
252                         help='spatial extent of bz',
253                         nargs=6, type=float,
254                         default=[-0.027, 0.025, -0.06, 0.041, 0.249, 0.416])
255     parser.add_argument('--bz_extent_1',
256                         help='spatial extent of bz',
257                         nargs=6, type=float,
258                         default=[-0.27, 0.027, -0.076, 0.041, 0.249, 0.416])
259     parser.add_argument('--bz_extent_2',
260                         help='spatial extent of bz',
261                         nargs=6, type=float,
262                         default=[-0.044, 0.031, -0.021, 0.03, 0.249, 0.416])
263     parser.add_argument('--bz_extent_3',

```

```

264         help='spatial extent of bz',
265         nargs=6, type=float,
266         default=[-0.072, 0.031, -0.026, 0.03, 0.249, 0.416])
267     parser.add_argument('--output_prefix',
268         help='prefix of output files',
269         default='field_nulls')
270     parser.add_argument('--bias_field_magnitude',
271         help='magnitude of axial bias magnetic field',
272         type=float,
273         default=0.02)
274     parser.add_argument('--time_steps',
275         help='number of time steps', type=int,
276         default=250)
277     args = parser.parse_args()
278     return args
279
280
281 if __name__ == '__main__':
282     args = parse_args()
283     main(args)

```

D.7.3 *interpolate_measurements.py*

```

1  #!/Users/vonderlinden2/anaconda/bin/python
2  # -*- coding: utf-8 -*-
3  """
4  Created on Mon Aug 1 18:07:14 2016
5
6  @author: Jens von der Linden
7
8  Interpolate unstructured fields to rectilinear grid.
9  Read unstructured fields from unstructured vtk file.
10 Write interpolated fields to rectilinear vtk file.
11 """
12 import argparse
13 import numpy as np
14 from scipy.interpolate import LinearNDInterpolator
15 from datetime import date
16 from datetime import datetime
17 import os
18
19 from write_to_vtk.read_unstructured_vtk import read_unstructured_vtk
20 from write_to_vtk import structured_3d_vtk as struc_3d
21
22 def main(args):
23     r"""
24     Interpolate unstructured fields to rectilinear grid.
25     """
26     just_magnetic = args.just_magnetic
27     now = datetime.now().strftime("%Y-%m-%d-%H-%M")
28     out_dir = '../output/' + args.output_prefix + '/' + now + '/'
29     try:
30         os.makedirs(out_dir)
31     except:

```



```

89     n_grad = struc_3d.triangulate_grad(mesh, n_interpolator,
90                                     increment=args.derivative_increment)
91     plane_mesh = [mesh[0][:, :, 0], mesh[1][:, :, 0]]
92     mach_y_grad_plane = struc_3d.triangulate_grad(plane_mesh, mach_y_interpolator,
93                                                  increment=args.derivative_increment)
94     mach_z_grad_plane = struc_3d.triangulate_grad(plane_mesh, mach_z_interpolator,
95                                                  increment=args.derivative_increment)
96
97
98     bx, by, bz = struc_3d.vector_on_mesh((bx_interpolator,
99                                       by_interpolator,
100                                       bz_interpolator), mesh)
101     bx, by, bz = struc_3d.add_vacuum_field([bx, by, bz],
102                                         vacuum_field=args.bias_field_magnitude)
103
104     if not just_magnetic:
105         te = struc_3d.scalar_on_mesh(te_interpolator, mesh)
106         n = struc_3d.scalar_on_mesh(n_interpolator, mesh)
107         mach_y_plane = struc_3d.scalar_on_mesh(mach_y_interpolator,
108                                             plane_mesh)
109         mach_z_plane = struc_3d.scalar_on_mesh(mach_z_interpolator,
110                                             plane_mesh)
111
112         mach_y = np.repeat(mach_y_plane[:, :, np.newaxis],
113                           mesh[0].shape[2], axis=2)
114         mach_z = np.repeat(mach_z_plane[:, :, np.newaxis],
115                           mesh[0].shape[2], axis=2)
116
117         mach_y_dx = np.repeat(mach_y_grad_plane[0][:, :, np.newaxis],
118                              mesh[0].shape[2], axis=2)
119         mach_y_dy = np.repeat(mach_y_grad_plane[1][:, :, np.newaxis],
120                              mesh[0].shape[2], axis=2)
121         mach_y_dz = np.zeros(mesh[0].shape)
122
123         mach_z_dx = np.repeat(mach_z_grad_plane[0][:, :, np.newaxis],
124                              mesh[0].shape[2], axis=2)
125         mach_z_dy = np.repeat(mach_z_grad_plane[0][:, :, np.newaxis],
126                              mesh[0].shape[2], axis=2)
127         mach_z_dz = np.zeros(mesh[0].shape)
128
129         fields = ([bx] + [by] + [bz] + [n] + [te] +
130                 [mach_y] + [mach_z] +
131                 list(bx_grad) +
132                 list(by_grad) +
133                 list(bz_grad) +
134                 list(n_grad) +
135                 list(te_grad) +
136                 [mach_y_dx] + [mach_y_dy] + [mach_y_dz] +
137                 [mach_z_dx] + [mach_z_dy] + [mach_z_dz])
138
139         quantity_names = ['B_x', 'B_y', 'B_z',
140                          'n', 'Te',
141                          'mach_y', 'mach_z',
142                          'B_x_dx', 'B_x_dy', 'B_x_dz',
143                          'B_y_dx', 'B_y_dy', 'B_y_dz',
144                          'B_z_dx', 'B_z_dy', 'B_z_dz',
145                          'n_dx', 'n_dy', 'n_dz',
146                          'Te_dx', 'Te_dy', 'Te_dz',

```

```

146             'mach_y_dx', 'mach_y_dy', 'mach_y_dz',
147             'mach_z_dx', 'mach_z_dy', 'mach_z_dz']
148     else:
149         fields = ([bx] + [by] + [bz] +
150                 list(bx_grad) +
151                 list(by_grad) +
152                 list(bz_grad))
153
154     quantity_names = ['B_x', 'B_y', 'B_z',
155                     'B_x_dx', 'B_x_dy', 'B_x_dz',
156                     'B_y_dx', 'B_y_dy', 'B_y_dz',
157                     'B_z_dx', 'B_z_dy', 'B_z_dz']
158
159
160     x, y, z, variables = struc_3d.prepare_for_rectilinear_grid(mesh, fields,
161                                                             quantity_names)
162
163     vtk_file_path = out_dir + args.output_prefix
164     struc_3d.write_fields_to_rectilinear_grid(vtk_file_path,
165                                             x, y, z, variables,
166                                             time_point)
167
168 def parse_args():
169     r"""
170     Read arguments.
171     """
172     parser = argparse.ArgumentParser(description="Create VTK files of"
173                                         "interpolated measurements")
174     parser.add_argument('--input_path',
175                       help='path to input files',
176                       default='../output/boxed_unstructured_measurements/')
177     parser.add_argument('--input_date',
178                       help='time stamp of input files',
179                       default='2017-04-04-13-44')
180     parser.add_argument('--input_file_text',
181                       help='input file name',
182                       default='_boxed_unstructured_')
183     parser.add_argument('--spatial_increment',
184                       help='Spatial increment of output file grids',
185                       type=float, default=0.001)
186     parser.add_argument('--derivative_increment',
187                       help="spatial increment used to determine"
188                           "tetrahedron derivative of Delaunay"),
189                       type=float, default=0.0001)
190     parser.add_argument('--joint_extent',
191                       help='overlapping spatial extent of all parameters',
192                       nargs=6, type=float,
193                       default=[-0.022, 0.024, -0.02, 0.029, 0.249, 0.416])
194     parser.add_argument('--output_prefix',
195                       help='prefix of output files',
196                       default='data_interp_to_rect_grid')
197     parser.add_argument('--bias_field_magnitude',
198                       help='magnitude of axial bias magnetic field',
199                       type=float,
200                       default=0.02)
201     parser.add_argument('--time_steps',
202                       help='number of time steps', type=int,

```

```

203             default=250)
204     parser.add_argument('--just_magnetic',
205                        help='only interpolate bdot measurements',
206                        action='store_true', default=False)
207     #parser.add_argument('--just_one_time_step',
208                        # help='only interpolate first time step',
209                        # action='store_true', default=False)
210     args = parser.parse_args()
211     return args
212
213 if __name__ == '__main__':
214     args = parse_args()
215     main(args)

```

D.7.4 calculate_dependent_quantities.py

```

1  #!/Users/vonderlinden2/anaconda/bin/python
2  # -*- coding: utf-8 -*-
3  """
4  Created on Mon Aug 1 18:07:14 2016
5
6  @author: Jens von der Linden
7
8  Calculate the dependent fields from interpolated
9  measurements.
10 Optionally filter the fields with Gaussian kernels of given
11 standard deviation for sensitivity / uncertainty analysis.
12
13 The dependent fields are:
14 ion_vorticity,
15 ion_vorticity_smooth,
16 current,
17 current_smooth,
18 density_plane_normalized,
19 temperature_plane_normalized,
20 vector_potential,
21 b_field_ref,
22 vector_potential_ref,
23 ion_vorticity_ref,
24 ion_vorticity_smooth_ref,
25 ion_velocity_ref,
26 ion_velocity_smooth_ref
27 """
28 import argparse
29 import numpy as np
30 from scipy.constants import mu_0
31 from scipy.constants import elementary_charge as q_e
32 from scipy.constants import proton_mass as m_i
33 from astropy.convolution import convolve, convolve_fft
34 from scipy.ndimage import gaussian_filter
35 from scipy import ndimage
36 from scipy.signal import fftconvolve
37 import scipy
38 from datetime import date

```

```

39 from datetime import datetime
40 import visit_writer
41 import os
42
43 from vector_comparison import read_rectilinear_vtk as rrv
44 from write_to_vtk import structured_3d_vtk as struc_3d
45 from invert_curl.invert_curl import devore_invert_curl
46 from write_to_vtk.reference_field import determine_reference_fields as ref_fields
47 from vector_calculus import vector_calculus as vc
48
49 def main(args):
50     r"""
51     Calculate the dependent fields from interpolated
52     measurements.
53     """
54     just_magnetic = args.just_magnetic
55     interpolate_nan = args.interpolate_nan
56     now = datetime.now().strftime("%Y-%m-%d-%H-%M")
57     out_dir = '../output/' + args.output_prefix + '/' + now + '/'
58     try:
59         os.makedirs(out_dir)
60     except:
61         pass
62     in_dir = args.input_path + args.input_date + '/'
63     in_file = args.input_file_text
64     input_path = in_dir + in_file
65
66     if not just_magnetic:
67         fields_to_read = ('B_x', 'B_y', 'B_z',
68                          'n', 'Te',
69                          'mach_y', 'mach_z',
70                          'B_x_dx', 'B_x_dy', 'B_x_dz',
71                          'B_y_dx', 'B_y_dy', 'B_y_dz',
72                          'B_z_dx', 'B_z_dy', 'B_z_dz',
73                          'n_dx', 'n_dy', 'n_dz',
74                          'Te_dx', 'Te_dy', 'Te_dz',
75                          'mach_y_dx', 'mach_y_dy', 'mach_y_dz',
76                          'mach_z_dx', 'mach_z_dy', 'mach_z_dz')
77         mach_fields_to_read = ('mach_y', 'mach_y_dx', 'mach_y_dy', 'mach_y_dz')
78     else:
79         fields_to_read = ('B_x', 'B_y', 'B_z',
80                          'B_x_dx', 'B_x_dy', 'B_x_dz',
81                          'B_y_dx', 'B_y_dy', 'B_y_dz',
82                          'B_z_dx', 'B_z_dy', 'B_z_dz')
83
84     u_x_time_points_plus = np.roll(np.arange(250), int(np.round(250*0.25)))
85     u_x_time_points_minus = np.roll(np.arange(250), -int(np.round(250*0.25)))
86     xlow, xhigh, ylow, yhigh, zlow, zhigh = args.to_cut
87
88
89     for time_point in xrange(args.time_steps):
90         print time_point
91         input_file = input_path + str(time_point).zfill(4) + '.vtk'
92         fields = {}
93         for field in fields_to_read:
94             read = rrv.read_scalar(input_file, field)
95             fields[field] = read[1][ylow:yhigh, xlow:xhigh, zlow:zhigh]

```

```

96         if args.filter_gaussian:
97             fields[field] = filter_data(fields[field],
98                                       filter_sigma=args.filter_sigma,
99                                       filter_truncate=args.filter_truncate)
100
101     mesh = read[0]
102     mesh[0] = mesh[0][ylow:yhigh, xlow:xhigh, zlow:zhigh]
103     mesh[1] = mesh[1][ylow:yhigh, xlow:xhigh, zlow:zhigh]
104     mesh[2] = mesh[2][ylow:yhigh, xlow:xhigh, zlow:zhigh]
105
106     bx_grad = [fields['B_x_dx'], fields['B_x_dy'], fields['B_x_dz']]
107     by_grad = [fields['B_y_dx'], fields['B_y_dy'], fields['B_y_dz']]
108     bz_grad = [fields['B_z_dx'], fields['B_z_dy'], fields['B_z_dz']]
109
110     ## current
111     ##
112     current = 1/mu_0*np.asarray(vc.curl(None,
113                                     vector_grad=[bx_grad,
114                                                  by_grad,
115                                                  bz_grad]))
116     current_smooth = []
117     for direction in xrange(len(current)):
118         current_dir = np.array(current[direction])
119         for z_step in xrange(len(current[0, 0, :])):
120             current_dir[:, :, z_step] = (gaussian_filter(current_dir[:, :, z_step],
121                                                         args.filter_width,
122                                                         mode='reflect'))
123         current_smooth.append(current_dir)
124
125     ## density and temperature
126     ##
127     if not just_magnetic:
128         density = fields['n']
129         grad_density = (fields['n_dx'], fields['n_dy'], fields['n_dz'])
130         temperature = fields['Te']
131         grad_temperature = (fields['Te_dx'], fields['Te_dy'], fields['Te_dz'])
132
133         density_plane_normalized = normalize_scalar_by_plane(density)
134         temperature_plane_normalized = normalize_scalar_by_plane(temperature)
135         density_smooth = boxcar_filter(density,
136                                       args.filter_width)
137         temperature_smooth = boxcar_filter(temperature,
138                                          args.filter_width)
139         density_smooth_plane_normalized = normalize_scalar_by_plane(density_smooth)
140         temperature_smooth_plane_normalized = normalize_scalar_by_plane(temperature_smooth)
141         density_constant = args.density_constant_factor*np.ones(density.shape)
142         temperature_smooth_norm = temperature_smooth/np.nanmax(temperature_smooth)
143         temperature_norm = (temperature/
144                             np.nanmax(temperature))
145
146     ## velocity and vorticity
147     ##
148     mach_file = (input_path +
149                 str(u_x_time_points_plus[time_point]).zfill(4) +
150                 '.vtk')
151     mach_x_fields = {}
152     for field in mach_fields_to_read:

```



```

210     ion_velocity = ion_velocity_p
211     ion_vorticity = ion_vorticity_p
212     ion_vorticity_smooth = ion_vorticity_p_smooth
213
214     ## Vector Potential
215     ##
216     b_field = [fields['B_x'], fields['B_y'], fields['B_z']]
217     vector_potential = devore_invert_curl(mesh,
218                                     b_field)
219
220     b_field_dynamic = np.array(b_field)
221     b_field_dynamic[2] = b_field[2] - args.bias_field_magnitude
222     vector_potential_dynamic = devore_invert_curl(mesh,
223                                     b_field_dynamic)
224
225     ## Reference fields
226     ##
227     (vector_potential_ref,
228     b_field_ref,
229     b_scalar_potential_ref) = ref_fields(mesh, b_field,
230                                     return_scalar_ref=True)
231
232     (vector_potential_dynamic_ref,
233     b_field_dynamic_ref,
234     b_scalar_potential_dynamic_ref) = ref_fields(mesh, b_field_dynamic,
235                                     return_scalar_ref=True)
236
237     if not just_magnetic:
238         (ion_velocity_smooth_ref,
239         ion_vorticity_smooth_ref,
240         i_scalar_potential_smooth_ref) = ref_fields(mesh, ion_vorticity_smooth,
241                                     return_scalar_ref=True)
242
243         (ion_velocity_ref,
244         ion_vorticity_ref,
245         i_scalar_potential_ref) = ref_fields(mesh, ion_vorticity,
246                                     return_scalar_ref=True)
247
248     fields = ([b_field[0]] + [b_field[1]] + [b_field[2]] +
249              list(current_smooth) + list(current) +
250              [density] + [temperature] +
251              [density_smooth_plane_normalized] +
252              [temperature_smooth_plane_normalized] +
253              [density] + [temperature] +
254              [density_plane_normalized] +
255              [temperature_plane_normalized] +
256              list(ion_velocity) +
257              list(ion_vorticity_smooth) + list(ion_vorticity) +
258              list(vector_potential) + list(b_field_ref) +
259              list(vector_potential_ref) +
260              list(ion_velocity_ref) +
261              list(ion_vorticity_smooth_ref) +
262              list(ion_vorticity_ref))
263
264     quantity_names = ['B_x', 'B_y', 'B_z',
265                      'j_x', 'j_y', 'j_z',
266                      'j_raw_x', 'j_raw_y', 'j_raw_z',
267                      'n', 'Te',
268                      'n_plane_normalized', 'Te_plane_normalized',
269                      'n_raw', 'Te_raw',
270                      'n_raw_plane_normalized',

```

```

267         'Te_raw_plane_normalized',
268         'u_i_x_plus', 'u_i_y', 'u_i_z',
269         'w_i_x_plus', 'w_i_y_plus', 'w_i_z_plus',
270         'w_i_raw_x_plus', 'w_i_raw_y_plus', 'w_i_raw_z_plus',
271         'A_x', 'A_y', 'A_z',
272         'B_ref_x', 'B_ref_y', 'B_ref_z',
273         'A_ref_x', 'A_ref_y', 'A_ref_z',
274         'u_i_ref_x', 'u_i_ref_y', 'u_i_ref_z',
275         'w_i_ref_x', 'w_i_ref_y', 'w_i_ref_z',
276         'w_i_raw_ref_x', 'w_i_raw_ref_y', 'w_i_raw_ref_z']
277
278     else:
279         fields = ([b_field[0]] + [b_field[1]] + [b_field[2]] +
280                  list(current_smooth) + list(current) +
281                  list(b_field_dynamic) +
282                  list(b_field_dynamic_ref) +
283                  list(vector_potential_dynamic) +
284                  list(vector_potential_dynamic_ref) +
285                  [b_scalar_potential_ref] +
286                  [b_scalar_potential_dynamic_ref])
287
288         quantity_names = ['B_x', 'B_y', 'B_z',
289                           'j_x', 'j_y', 'j_z',
290                           'j_raw_x', 'j_raw_y', 'j_raw_z',
291                           'A_x', 'A_y', 'A_z',
292                           'B_ref_x', 'B_ref_y', 'B_ref_z',
293                           'A_ref_x', 'A_ref_y', 'A_ref_z',
294                           'B_dynamic_x', 'B_dynamic_y', 'B_dynamic_z',
295                           'B_dynamic_ref_x', 'B_dynamic_ref_y', 'B_dynamic_ref_z',
296                           'A_dynamic_x', 'A_dynamic_y', 'A_dynamic_z',
297                           'A_dynamic_ref_x', 'A_dynamic_ref_y', 'A_dynamic_ref_z',
298                           'phi_b_ref',
299                           'phi_b_dynamic_ref']
300
301
302     for i, field in enumerate(fields):
303         fields[i] = field.astype('float64')
304
305     x, y, z, variables = struc_3d.prepare_for_rectilinear_grid(mesh, fields,
306                                                                quantity_names)
307
308     vtk_file_path = out_dir + args.output_prefix
309     struc_3d.write_fields_to_rectilinear_grid(vtk_file_path,
310                                             x, y, z, variables,
311                                             time_point)
312
313     def filter_data(data, filter_sigma=None,
314                   filter_truncate=None):
315         r"""
316         Filter (with Gaussian).
317         """
318         if filter_sigma:
319             if filter_truncate:
320                 filtered = ndimage.gaussian_filter(data, filter_sigma,
321                                                    truncate=filter_truncate)
322             else:
323                 filtered = ndimage.gaussian_filter(data, filter_sigma)

```

```

324     else:
325         filtered = data
326     return filtered
327
328
329 def parse_args():
330     r"""
331     Read arguments.
332     """
333     parser = argparse.ArgumentParser(description=("Create VTK files "
334                                               "of canonical quantities"))
335     parser.add_argument('--input_path',
336                        help='path to input files',
337                        default='../output/data_interp_to_rect_grid/')
338     parser.add_argument('--input_date',
339                        help='time stamp of input files',
340                        default='2017-05-10-11-53')
341     parser.add_argument('--input_file_text',
342                        help='input file name',
343                        default='data_interp_to_rect_grid')
344     parser.add_argument('--output_prefix',
345                        help='prefix of output files',
346                        default='canonical_quantities')
347     parser.add_argument('--to_cut',
348                        help=("number of indicies to cut on"
349                              "each side to remove NaNs e.g."
350                              "xlow xhigh ylow yhigh zlow zhigh"),
351                        nargs=6, type=int,
352                        default=[2, -1, 3, -3, 0, -1])
353     parser.add_argument('--filter_width',
354                        help='width of boxcar filter for derivatives',
355                        type=float, default=5)
356     parser.add_argument('--interpolate_nan',
357                        help='use astropy option to interpolate nans before filtering' +
358                              ' may not work well because nans are usually located at edge.',
359                        type=bool, default=False)
360     parser.add_argument('--density_constant_factor',
361                        help='value used for constant density parameters ',
362                        type=float,
363                        default=1e18)
364     parser.add_argument('--bias_field_magnitude',
365                        help='magnitude of axial bias magnetic field,' +
366                              'used to calculate dynamic field.',
367                        type=float,
368                        default=0.02)
369     parser.add_argument('--time_steps',
370                        help='# of time steps', type=int,
371                        default=250)
372     parser.add_argument('--just_magnetic',
373                        help='only calculate magnetic quantities',
374                        action='store_true',
375                        default=False)
376     parser.add_argument('--filter_gaussian',
377                        help="run with averaging on all measured quantities,"
378                              "used to average measurements for uncertainty analysis",
379                        default=False, action='store_true')
380     parser.add_argument('--filter_sigma',

```

```

381             help='standard deviation of gaussian filter ',
382             type=float ,
383             default=3)
384     parser.add_argument('--filter_truncate',
385                       help='truncate Gaussian filter at this multiple of sigma',
386                       type=float ,
387                       default=3)
388     args = parser.parse_args()
389     return args
390
391
392 def normalize_scalar_by_plane(scalar):
393     r"""
394     Return scalar normalized by the maximum in each z plane.
395
396     Notes
397     -----
398     To find the max in each plane take nanmax in x and y direction.
399     Each nanmax reduces the number of dimensions by 1.
400     """
401     scalar = np.array(scalar)
402     maxes = np.nanmax(np.nanmax(scalar, axis=0), axis=0)
403     return scalar / maxes[None, None, :]
404
405
406 def remove_edges_vector(quantity,
407                         x_start=2, x_end=None,
408                         y_start=0, y_end=-2,
409                         z_start=0, z_end=-1):
410     r"""
411     Returns vector field with edges removed.
412
413     Notes
414     -----
415     Usually used to remove nans from interpolation, if parts of the grid were outside
416     of the convex hull of the measurement points.
417     """
418     for index in xrange(len(quantity)):
419         quantity[index] = quantity[index][y_start:y_end, x_start:x_end, z_start:z_end]
420     return quantity
421
422
423 def remove_edges_scalar(quantity,
424                        x_start=2, x_end=None,
425                        y_start=0, y_end=-2,
426                        z_start=0, z_end=-1):
427     r"""
428     Returns vector field with edges removed.
429
430     Notes
431     -----
432     Usually used to remove nans from interpolation, if parts of the grid were outside
433     of the convex hull of the measurement points
434     """
435     quantity = quantity[y_start:y_end, x_start:x_end, z_start:z_end]
436     return quantity
437

```

```

438
439 def boxcar_filter(quantity, width, interpolate_nan=False):
440     r"""
441     Filter scalar field with boxcar of given width.
442     """
443     quantity = np.array(quantity)
444     nan_indexes = np.where(np.isnan(quantity))
445     quantity[nan_indexes] = 0
446     boxcar = np.ones((width, width, width))
447     boxcar /= boxcar.sum()
448     if interpolate_nan:
449         return convolve_fft(quantity, boxcar,
450                             boundary='wrap',
451                             interpolate_nan=True,
452                             fftn=scipy.fftpack.fft,
453                             ifftn=scipy.fftpack.ifft)
454     else:
455         return fftconvolve(quantity, boxcar, mode='same')
456
457
458 def grad_ion_velocity(mach, grad_mach, te, grad_te):
459     r"""
460     Return grad of ion velocity.
461
462     Notes
463     -----
464     The grad of ion velocity depends on the grad of mach number and temperature.
465     """
466     factor = q_e/m_i
467     term1 = np.sqrt(te*factor)*(grad_mach)
468     term2 = mach*factor*grad_te/(2.*np.sqrt(factor*te))
469     return term1 + term2
470
471
472
473
474 if __name__ == '__main__':
475     args = parse_args()
476     main(args)

```

D.7.5 calculate_helicity.py

```

1  #! /Users/vonderlinden2/anaconda/bin/python
2  # -*- coding: utf-8 -*-
3  """
4  Created on Mon Aug 1 18:07:14 2016
5
6  @author: Jens von der Linden
7
8  Calculate gauge dependent and relative helicities.
9  Read field quantities from rectilinear vtk files.
10 Write out helicity to ASCII files.
11 """
12 import argparse

```

```

13 import numpy as np
14 from scipy.constants import mu_0
15 from scipy.constants import elementary_charge as q_e
16 from scipy.constants import proton_mass as m_i
17 from scipy.integrate import trapz
18 from datetime import date
19 from datetime import datetime
20 import visit_writer
21 import os
22 from vector_comparison import read_rectilinear_vtk as rrv
23 from write_to_vtk import structured_3d_vtk as struc_3d
24 import write_to_vtk.helicities as hel
25
26
27 def main(args):
28     r"""
29     Calculate gauge dependent and relative helicities.
30     """
31     just_magnetic = args.just_magnetic
32     now = datetime.now().strftime("%Y-%m-%d-%H-%M")
33     out_dir = '../output/' + args.output_prefix + '/' + now
34     try:
35         os.makedirs(out_dir)
36     except:
37         pass
38     in_dir = args.input_path + args.input_date + '/'
39     in_file = args.input_file_text
40     input_path = in_dir + in_file
41     xlow, xhigh = args.to_cut[:2]
42     ylow, yhigh = args.to_cut[2:4]
43     zlow, zhigh = args.to_cut[4:6]
44
45     if not just_magnetic:
46         fields_to_read = ('B_x', 'B_y', 'B_z',
47                          'B_ref_x', 'B_ref_y', 'B_ref_z',
48                          'A_x', 'A_y', 'A_z',
49                          'A_ref_x', 'A_ref_y', 'A_ref_z',
50                          'u_i_x_plus', 'u_i_y', 'u_i_z',
51                          'u_i_ref_x', 'u_i_ref_y', 'u_i_ref_z',
52                          'w_i_raw_x_plus', 'w_i_raw_y_plus', 'w_i_raw_z_plus',
53                          'w_i_raw_ref_x', 'w_i_raw_ref_y', 'w_i_raw_ref_z',
54                          'w_i_x_plus', 'w_i_y_plus', 'w_i_z_plus',
55                          'w_i_ref_x', 'w_i_ref_y', 'w_i_ref_z', 'n')
56     else:
57         fields_to_read = ('B_x', 'B_y', 'B_z',
58                          'B_ref_x', 'B_ref_y', 'B_ref_z',
59                          'A_x', 'A_y', 'A_z',
60                          'A_ref_x', 'A_ref_y', 'A_ref_z')
61
62
63     for time_point in xrange(args.time_steps):
64         print time_point
65         input_file = (input_path +
66                      str(time_point).zfill(4) +
67                      '.vtk')
68         fields = {}
69         for field in fields_to_read:

```



```

127             ion_vorticity_ref ,
128             dx, dy, dz)
129 rel_cross_helicity = hel.rel_cross_helicity(ion_velocity ,
130             ion_velocity_ref ,
131             b_field ,
132             b_field_ref ,
133             dx, dy, dz)
134 rel_kin_helicity_raw_vorticity = hel.rel_kin_helicity(ion_velocity ,
135             ion_velocity_ref ,
136             ion_vorticity_raw ,
137             ion_vorticity_raw_ref ,
138             dx, dy, dz)
139 rel_cross_helicity_raw_vorticity = hel.rel_cross_helicity(ion_velocity ,
140             ion_velocity_ref ,
141             b_field ,
142             b_field_ref ,
143             dx, dy, dz)
144
145 ## helicities with density dependence
146 ##
147 kin_helicity_n = hel.kinetic_helicity(ion_velocity ,
148             ion_vorticity ,
149             dx, dy, dz, density=n)
150 kin_helicity_raw_vorticity_n = hel.kinetic_helicity(ion_velocity ,
151             ion_vorticity_raw ,
152             dx, dy, dz,
153             density=n)
154 cross_helicity_n = hel.cross_helicity(ion_velocity ,
155             b_field ,
156             dx, dy, dz,
157             density=n)
158 rel_kin_helicity_n = hel.rel_kin_helicity(ion_velocity ,
159             ion_velocity_ref ,
160             ion_vorticity ,
161             ion_vorticity_ref ,
162             dx, dy, dz, density=n)
163 rel_cross_helicity_n = hel.rel_cross_helicity(ion_velocity ,
164             ion_velocity_ref ,
165             b_field ,
166             b_field_ref ,
167             dx, dy, dz, density=n)
168 rel_kin_helicity_raw_vorticity_n = hel.rel_kin_helicity(ion_velocity ,
169             ion_velocity_ref ,
170             ion_vorticity_raw ,
171             ion_vorticity_raw_ref ,
172             dx, dy, dz, density=n)
173 rel_cross_helicity_raw_vorticity_n = hel.rel_cross_helicity(ion_velocity ,
174             ion_velocity_ref ,
175             b_field ,
176             b_field_ref ,
177             dx, dy, dz,
178             density=n)
179 mag_helicity_n = hel.magnetic_helicity(vector_potential ,
180             b_field ,
181             dx, dy, dz,
182             density=n)
183

```

```

184         rel_mag_helicity_n = hel.rel_mag_helicity(vector_potential ,
185                                                     vector_potential_ref ,
186                                                     b_field ,
187                                                     b_field_ref ,
188                                                     dx, dy, dz,
189                                                     density=n)
190
191
192
193     mag_helicity = hel.magnetic_helicity(vector_potential ,
194                                         b_field ,
195                                         dx, dy, dz)
196
197     rel_mag_helicity = hel.rel_mag_helicity(vector_potential ,
198                                             vector_potential_ref ,
199                                             b_field ,
200                                             b_field_ref ,
201                                             dx, dy, dz)
202
203     if not just_magnetic:
204         with open(out_dir +
205                 "/kinetic_helicity.txt", "a") as myfile:
206             myfile.write(str(kin_helicity) + '\n')
207         with open(out_dir +
208                 "/kinetic_helicity_raw_vorticity.txt",
209                 "a") as myfile:
210             myfile.write(str(kin_helicity_raw_vorticity) + '\n')
211         with open(out_dir +
212                 "/cross_helicity.txt", "a") as myfile:
213             myfile.write(str(cross_helicity) + '\n')
214         with open(out_dir +
215                 "/relative_kinetic_helicity.txt", "a") as myfile:
216             myfile.write(str(rel_kin_helicity) + '\n')
217         with open(out_dir +
218                 "/relative_cross_helicity.txt", "a") as myfile:
219             myfile.write(str(rel_cross_helicity) + '\n')
220         with open(out_dir +
221                 "/relative_kinetic_helicity_raw_vorticity.txt",
222                 "a") as myfile:
223             myfile.write(str(rel_kin_helicity_raw_vorticity) + '\n')
224         with open(out_dir +
225                 "/relative_cross_helicity_raw_vorticity.txt",
226                 "a") as myfile:
227             myfile.write(str(rel_cross_helicity_raw_vorticity) + '\n')
228
229     ## with density dependence
230     ##
231     with open(out_dir +
232             "/kinetic_helicity_n_dependence.txt", "a") as myfile:
233         myfile.write(str(kin_helicity_n) + '\n')
234     with open(out_dir +
235             "/kinetic_helicity_raw_vorticity_n_dependence.txt",
236             "a") as myfile:
237         myfile.write(str(kin_helicity_raw_vorticity_n) + '\n')
238     with open(out_dir +
239             "/cross_helicity_n_dependence.txt", "a") as myfile:
240         myfile.write(str(cross_helicity_n) + '\n')
241     with open(out_dir +

```

```

241         "/relative_kinetic_helicity_n_dependence.txt", "a") as myfile:
242     myfile.write(str(rel_kin_helicity_n) + '\n')
243     with open(out_dir +
244             "/relative_cross_helicity_n_dependence.txt", "a") as myfile:
245         myfile.write(str(rel_cross_helicity_n) + '\n')
246     with open(out_dir +
247             "/relative_kinetic_helicity_raw_vorticity_n_dependence.txt",
248             "a") as myfile:
249         myfile.write(str(rel_kin_helicity_raw_vorticity_n) + '\n')
250     with open(out_dir +
251             "/relative_cross_helicity_raw_vorticity_n_dependence.txt",
252             "a") as myfile:
253         myfile.write(str(rel_cross_helicity_raw_vorticity_n) + '\n')
254     with open(out_dir +
255             "/magnetic_helicity_n_dependence.txt", "a") as myfile:
256         myfile.write(str(mag_helicity_n) + '\n')
257     with open(out_dir +
258             "/relative_magnetic_helicity_n_dependence.txt", "a") as myfile:
259         myfile.write(str(rel_mag_helicity_n) + '\n')
260
261
262     with open(out_dir +
263             "/magnetic_helicity.txt", "a") as myfile:
264         myfile.write(str(mag_helicity) + '\n')
265     with open(out_dir +
266             "/relative_magnetic_helicity.txt", "a") as myfile:
267         myfile.write(str(rel_mag_helicity) + '\n')
268
269 def parse_args():
270     r"""
271     """
272     parser = argparse.ArgumentParser(description='Calculate helicity')
273     parser.add_argument('--input_path',
274                         help='path to input files',
275                         default='../output/canonical_quantities/')
276     parser.add_argument('--input_date',
277                         help='time stamp of input files',
278                         default='2017-04-04-16-33')
279     parser.add_argument('--input_file_text',
280                         help='input file name',
281                         default='canonical_quantities')
282     parser.add_argument('--output_prefix',
283                         help='prefix of output files',
284                         default='helicity')
285     parser.add_argument('--time_steps',
286                         help='number of time steps',
287                         type=int,
288                         default=250)
289     parser.add_argument('--to_cut',
290                         help=("number of indicies to cut on"
291                                "each side to remove NaNs e.g."
292                                "xlow xhigh ylow yhigh zlow zhigh"),
293                         nargs=6,
294                         default=['0', 'None', '0', 'None', '0', 'None'])
295     parser.add_argument('--just_magnetic',
296                         help='only calculate magnetic quantities',
297                         action='store_true',

```

```

298             default=False)
299     args = parser.parse_args()
300     to_cut_list = []
301     for to_cut in args.to_cut:
302         if to_cut == 'None':
303             to_cut_list.append(None)
304         else:
305             to_cut_list.append(int(to_cut))
306     args.to_cut = to_cut_list
307     return args
308
309
310 if __name__ == '__main__':
311     args = parse_args()
312     main(args)

```

D.7.6 *vis_canonical_fluxtubes.py*

```

1  #!/home/jensv/anaconda/bin/python
2  # -*- coding: utf-8 -*-
3  """
4  Created on Fri Aug 19 14:38:10 2016
5
6  @author: Jens von der Linden
7
8  Plot frames of canonical flux tube animations.
9  Plot options include ion, electron canonical flux tubes,
10 temperature and density isosurfaces, current contours
11 in an x-y plane.
12 """
13
14 from datetime import datetime as date
15 import numpy as np
16 import os
17 from scipy.constants import elementary_charge, proton_mass
18 from glob import glob
19 import sys
20 visit_path1 = "/home/jensv/visit/visit2_10_3.linux-x86_64/2.10.3/linux-x86_64/lib/site-packages"
21 visit_path2 = "/home/jensv/visit/visit2_10_3.linux-x86_64/bin/"
22 sys.path.append(visit_path1)
23 sys.path.append(visit_path2)
24 os.environ["PATH"] += os.pathsep + visit_path1
25 os.environ["PATH"] += os.pathsep + visit_path2
26 import visit
27 import argparse
28
29 tan = (209, 178, 111, 255)
30 olive = (110, 117, 14, 255)
31 dim_grey = (105, 105, 105, 255)
32 black = (0, 0, 0, 255)
33 dark_grey = (169, 169, 169, 255)
34 red = (255, 0, 0, 255)
35 dark_red = (84, 0, 0, 255)
36 green = (0, 154, 0, 255)

```

```

37 navy = (0, 0, 128, 255)
38 aqua = (0, 255, 255, 255)
39
40 def define_expressions(visit):
41     r"""
42     Define Visit expressions.
43     """
44     visit.DefineVectorExpression("B", "{B_x, B_y, B_z}")
45     visit.DefineVectorExpression("B_norm", "{B_norm_x, B_norm_y, "
46         "B_norm_z}")
47     visit.DefineVectorExpression("B_perp", "{B_x, B_y, 0}")
48     visit.DefineVectorExpression("B_para", "{0, 0, B_z}")
49     visit.DefineScalarExpression("B_para_scalar", "B_z")
50
51     visit.DefineVectorExpression("Omega_e_times_density", "B*n")
52
53     visit.DefineVectorExpression("A_vacuum", "{A_vacuum_x, A_vacuum_y, 0}")
54     visit.DefineVectorExpression("A", "{A_x, A_y, A_z}")
55
56     visit.DefineVectorExpression("J_smooth", "{j_x, j_y, j_z}")
57     visit.DefineScalarExpression("J_smooth_mag", "sqrt(j_x^2 + j_y^2 + j_z^2)")
58     visit.DefineVectorExpression("J_smooth_perp", "{j_x, j_y, 0}")
59     visit.DefineVectorExpression("J_smooth_para", "{0, 0, j_z}")
60     visit.DefineVectorExpression("J_smooth_para_mag", "j_z")
61
62     visit.DefineVectorExpression("J_raw", "{j_raw_x, j_raw_y, j_raw_z}")
63     visit.DefineScalarExpression("J_raw_mag", "sqrt(j_raw_x^2 + "
64         "j_raw_y^2 + "
65         "j_raw_z^2)")
66     visit.DefineVectorExpression("J_raw_perp", "{j_raw_x, j_raw_y, 0}")
67     visit.DefineVectorExpression("J_raw_para", "{0, 0, j_raw_z}")
68
69     visit.DefineScalarExpression("divergence_B", "divergence(B)")
70     visit.DefineScalarExpression("divergence_Omega_i_raw_plus",
71         "divergence(Omega_i_raw_plus)")
72     visit.DefineScalarExpression("divergence_Omega_i_plus",
73         "divergence(Omega_i_plus)")
74
75     visit.DefineVectorExpression("J_raw_filtered_by_Te",
76         "J_raw * Te_raw_normalized")
77     visit.DefineVectorExpression("J_raw_filtered_by_Te^2",
78         "J_raw * Te_raw_normalized^2")
79     visit.DefineVectorExpression("J_raw_filtered_by_Te^3",
80         "J_raw * Te_raw_normalized^3")
81     visit.DefineVectorExpression("J_raw_filtered_by_Te^4",
82         "J_raw * Te_raw_normalized^4")
83     visit.DefineVectorExpression("J_raw_filtered_by_Te_smooth",
84         "J_raw * Te_smooth_normalized")
85     visit.DefineVectorExpression("J_raw_filtered_by_Te_smooth^2",
86         "J_raw * Te_smooth_normalized^2")
87     visit.DefineVectorExpression("J_raw_filtered_by_Te_smooth^3",
88         "J_raw * Te_smooth_normalized^3")
89     visit.DefineVectorExpression("J_raw_filtered_by_Te_smooth^4",
90         "J_raw * Te_smooth_normalized^4")
91
92     visit.DefineVectorExpression("u_i_plus", "{u_i_x_plus, u_i_y, u_i_z}")
93     visit.DefineVectorExpression("u_i_plus_perp", "{dot(u_i_plus, {1, 0, 0}), dot(u_i_plus, "

```

```

94         "{0, 1, 0}), 0}")
95 visit.DefineVectorExpression("u_i_plus_para", "{0, 0, dot(u_i_plus, {0, 0, 1})}")
96
97 visit.DefineVectorExpression("omega_i_plus", "{w_i_x_plus, w_i_y_plus, w_i_z_plus}")
98 visit.DefineVectorExpression("omega_i_plus_perp", "{dot(omega_i_plus, {1, 0, 0}),"
99         "dot(omega_i_plus, {0, 1, 0}), 0}")
100 visit.DefineVectorExpression("omega_i_plus_para", "{0, 0, dot(omega_i_plus, "
101         "{0, 0, 1})}")
102
103 visit.DefineVectorExpression("omega_i_raw_plus",
104         "{w_i_raw_x_plus, w_i_raw_y_plus, w_i_raw_z_plus}")
105 visit.DefineVectorExpression("omega_i_raw_plus_perp", "{dot(omega_i_raw_plus, {1, 0, 0}),"
106         "dot(omega_i_raw_plus, {0, 1, 0}), 0}")
107 visit.DefineVectorExpression("omega_i_raw_plus_para", "{0, 0, dot(omega_i_raw_plus, "
108         "{0, 0, 1})}")
109
110 visit.DefineVectorExpression("Omega_i_plus",
111         str(elementary_charge) + "*B + " + str(proton_mass) +
112         "*omega_i_plus")
113 visit.DefineVectorExpression("Omega_i_plus_perp", "{dot(Omega_i_plus, {1, 0, 0}), "
114         "dot(Omega_i_plus, {0, 1, 0}), 0}")
115 visit.DefineVectorExpression("Omega_i_plus_para", "{0, 0, dot(Omega_i_plus, "
116         "{0, 0, 1})}")
117 visit.DefineScalarExpression("Omega_i_plus_para_scalar",
118         "dot(Omega_i_plus, {0, 0, 1})")
119
120 visit.DefineVectorExpression("Omega_i_raw_plus",
121         str(elementary_charge) + "*B + " + str(proton_mass) +
122         "*omega_i_raw_plus")
123 visit.DefineVectorExpression("Omega_i_raw_plus_perp", "{dot(Omega_i_raw_plus, {1, 0, 0}), "
124         "dot(Omega_i_raw_plus, {0, 1, 0}), 0}")
125 visit.DefineVectorExpression("Omega_i_raw_plus_para", "{0, 0, dot(Omega_i_raw_plus, "
126         "{0, 0, 1})}")
127 visit.DefineScalarExpression("Omega_i_raw_plus_para_scalar",
128         "dot(Omega_i_raw_plus, {0, 0, 1})")
129
130 visit.DefineVectorExpression("Omega_i_plus_density_dependence",
131         "n*(%e *B + %e *omega_i_plus) +"
132         "cross(gradient(n), %e *A + %e * u_i_plus)"
133         "% (elementary_charge , proton_mass ,
134         elementary_charge , proton_mass))")
135 visit.DefineVectorExpression("Omega_i_plus_density_dependence_perp",
136         "{dot(Omega_i_plus_density_dependence, {1, 0, 0}), "
137         "dot(Omega_i_plus_density_dependence, {0, 1, 0}), 0}")
138 visit.DefineVectorExpression("Omega_i_plus_density_dependence_para",
139         "{0, 0, dot(Omega_i_plus_density_dependence, "
140         "{0, 0, 1})}")
141 visit.DefineScalarExpression("Omega_i_plus_density_dependence_para_scalar",
142         "dot(Omega_i_plus_density_dependence, {0, 0, 1})")
143
144 visit.DefineVectorExpression("Omega_i_raw_plus_density_dependence",
145         "n*(%e *B + %e *omega_i_raw_plus) +"
146         " cross(gradient(n), %e *A + %e * u_i_plus)"
147         "% (elementary_charge , proton_mass ,
148         elementary_charge , proton_mass))")
149 visit.DefineVectorExpression("Omega_i_raw_plus_density_dependence_perp",
150         "{dot(Omega_i_raw_plus_density_dependence, {1, 0, 0}), "

```

```

151         "dot(Omega_i_raw_plus_density_dependence, {0, 1, 0}), 0}")
152 visit.DefineVectorExpression("Omega_i_raw_plus_density_dependence_para",
153     "{0, 0, dot(Omega_i_raw_plus_density_dependence, "
154     "{0, 0, 1})}")
155 visit.DefineScalarExpression("Omega_i_raw_plus_density_dependence_para_scalar",
156     "dot(Omega_i_raw_plus_density_dependence, {0, 0, 1})")
157
158 visit.DefineVectorExpression("Omega_i_plus_times_density",
159     "n*(%e *B + %e *omega_i_plus)" %
160     (elementary_charge, proton_mass))
161 visit.DefineVectorExpression("Omega_i_plus_times_density_perp",
162     "{dot(Omega_i_plus_times_density, {1, 0, 0}), "
163     "dot(Omega_i_plus_times_density, {0, 1, 0}), 0}")
164 visit.DefineVectorExpression("Omega_i_plus_times_density_para",
165     "{0, 0, dot(Omega_i_plus_density_dependence, "
166     "{0, 0, 1})}")
167 visit.DefineScalarExpression("Omega_i_plus_times_density_para_scalar",
168     "dot(Omega_i_plus_times_density, {0, 0, 1})")
169
170 visit.DefineVectorExpression("Omega_i_raw_plus_times_density",
171     "n*(%e *B + %e *omega_i_raw_plus)" %
172     (elementary_charge, proton_mass))
173 visit.DefineVectorExpression("Omega_i_raw_plus_times_density_perp",
174     "{dot(Omega_i_raw_plus_density_dependence, {1, 0, 0}), "
175     "dot(Omega_i_raw_plus_times_density, {0, 1, 0}), 0}")
176 visit.DefineVectorExpression("Omega_i_raw_plus_times_density_para",
177     "{0, 0, dot(Omega_i_raw_plus_times_density, "
178     "{0, 0, 1})}")
179 visit.DefineScalarExpression("Omega_i_raw_plus_times_density_para_scalar",
180     "dot(Omega_i_raw_plus_times_density, {0, 0, 1})")
181
182
183 ## Omega_e density dependence
184 ##
185 visit.DefineVectorExpression("Omega_e_density_dependence",
186     "n*B + cross(gradient(n), A)")
187 visit.DefineVectorExpression("Omega_e_density_dependence_perp",
188     "{dot(Omega_e_density_dependence, {1, 0, 0}), "
189     "dot(Omega_e_density_dependence, {0, 1, 0}), 0}")
190 visit.DefineVectorExpression("Omega_e_density_dependence_para",
191     "{0, 0, dot(Omega_e_plus_density_dependence, "
192     "{0, 0, 1})}")
193 visit.DefineScalarExpression("Omega_e_density_dependence_para_scalar",
194     "dot(Omega_e_density_dependence, {0, 0, 1})")
195
196
197
198 ## u_i_x(t) = u_i_y(t MINUS tau*0.25)
199 ##
200 visit.DefineVectorExpression("u_i_minus",
201     "{u_i_x_minus, u_i_y, u_i_z}")
202 visit.DefineVectorExpression("u_i_minus_perp",
203     "{dot(u_i_minus, {1, 0, 0}), dot(u_i_minus, "
204     "{0, 1, 0}), 0}")
205 visit.DefineVectorExpression("u_i_minus_para", "{0, 0, dot(u_i_minus, {0, 0, 1})}")
206 visit.DefineScalarExpression("u_i_minus_para_scalar", "dot(u_i_minus, {0, 0, 1})")
207

```

```

208 visit.DefineVectorExpression("omega_i_minus", "{w_i_minus_x, w_i_minus_y, w_i_minus_z}")
209 visit.DefineVectorExpression("omega_i_minus_perp", "{dot(omega_i_minus, {1, 0, 0}),"
210     "dot(omega_i_minus, {0, 1, 0}), 0}")
211 visit.DefineVectorExpression("omega_i_minus_para", "{0, 0, dot(omega_i_minus, "
212     "{0, 0, 1})}")
213 visit.DefineScalarExpression("omega_i_minus_para_scalar", "dot(omega_i_minus, "
214     "{0, 0, 1}")")
215
216 visit.DefineVectorExpression("omega_i_raw_minus",
217     "{w_i_raw_x_minus, w_i_raw_y_minus, w_i_raw_z_minus}")
218 visit.DefineVectorExpression("omega_i_minus_raw_perp",
219     "{dot(omega_i_raw_minus, {1, 0, 0}),"
220     "dot(omega_i_raw_minus, {0, 1, 0}), 0}")
221 visit.DefineVectorExpression("omega_i_minus_raw_para",
222     "{0, 0, dot(omega_i_raw_minus, "
223     "{0, 0, 1})}")
224 visit.DefineScalarExpression("omega_i_raw_minus_para_scalar",
225     "dot(omega_i_raw_minus, "
226     "{0, 0, 1}")")
227
228 visit.DefineVectorExpression("Omega_i_minus", str(elementary_charge) +
229     "*B +" + str(proton_mass) +
230     "*omega_i_minus")
231 visit.DefineVectorExpression("Omega_i_minus_perp", "{dot(Omega_i_minus, {1, 0, 0}), "
232     "dot(Omega_i_minus, {0, 1, 0}), 0}")
233 visit.DefineVectorExpression("Omega_i_minus_para", "{0, 0, dot(Omega_i_minus, "
234     "{0, 0, 1})}")
235 visit.DefineScalarExpression("Omega_i_minus_para_scalar",
236     "dot(Omega_i_minus, {0, 0, 1})")
237
238 visit.DefineVectorExpression("Omega_i_raw_minus",
239     str(elementary_charge) + "*B +" + str(proton_mass) +
240     "*omega_i_raw_minus")
241 visit.DefineVectorExpression("Omega_i_raw_minus_perp", "{dot(Omega_i_raw_minus, {1, 0, 0}), "
242     "dot(Omega_i_raw_minus, {0, 1, 0}), 0}")
243 visit.DefineVectorExpression("Omega_i_raw_minus_para", "{0, 0, dot(Omega_i_raw_minus, "
244     "{0, 0, 1})}")
245 visit.DefineScalarExpression("Omega_i_raw_minus_para_scalar",
246     "dot(Omega_i_raw_minus, {0, 0, 1})")
247
248 visit.DefineVectorExpression("Omega_i_minus_density_dependence",
249     "n*(%e *B + %e *omega_i_minus) +"
250     " cross(gradient(n), %e *A + %e * u_i_minus)" %
251     (elementary_charge, proton_mass,
252     elementary_charge, proton_mass))
253 visit.DefineVectorExpression("Omega_i_minus_density_dependence_perp",
254     "{dot(Omega_i_minus_density_dependence, {1, 0, 0}), "
255     "dot(Omega_i_minus_density_dependence, {0, 1, 0}), 0}")
256 visit.DefineVectorExpression("Omega_i_minus_density_dependence_para",
257     "{0, 0, dot(Omega_i_minus_density_dependence, "
258     "{0, 0, 1})}")
259 visit.DefineScalarExpression("Omega_i_minus_density_dependence_para_scalar",
260     "dot(Omega_i_minus_density_dependence, {0, 0, 1})")
261
262 visit.DefineVectorExpression("Omega_i_raw_minus_density_dependence",
263     "n*(%e *B + %e *omega_i_raw_minus) +"
264     " cross(gradient(n), %e *A + %e * u_i_minus)" %

```

```

265         (elementary_charge , proton_mass ,
266         elementary_charge , proton_mass))
267 visit .DefineVectorExpression ("Omega_i_raw_minus_density_dependence_perp",
268         "{dot(Omega_i_raw_minus_density_dependence, {1, 0, 0}), "
269         "dot(Omega_i_raw_minus_density_dependence, {0, 1, 0}), 0}")
270 visit .DefineVectorExpression ("Omega_i_raw_minus_density_dependence_para",
271         "{0, 0, dot(Omega_i_raw_minus_density_dependence, "
272         "{0, 0, 1})}")
273 visit .DefineScalarExpression ("Omega_i_raw_minus_density_dependence_para_scalar",
274         "dot(Omega_i_raw_minus_density_dependence, {0, 0, 1})")
275
276 visit .DefineVectorExpression ("Omega_i_minus_times_density",
277         "n*(%e *B + %e *omega_i_minus)" %
278         (elementary_charge , proton_mass))
279 visit .DefineVectorExpression ("Omega_i_minus_times_density_perp",
280         "{dot(Omega_i_plus_times_density, {1, 0, 0}), "
281         "dot(Omega_i_minus_times_density, {0, 1, 0}), 0}")
282 visit .DefineVectorExpression ("Omega_i_minus_times_density_para",
283         "{0, 0, dot(Omega_i_plus_density_dependence, "
284         "{0, 0, 1})}")
285 visit .DefineScalarExpression ("Omega_i_minus_times_density_para_scalar",
286         "dot(Omega_i_minus_times_density, {0, 0, 1})")
287
288 visit .DefineVectorExpression ("Omega_i_raw_minus_times_density",
289         "n*(%e *B + %e *omega_i_raw_minus)" %
290         (elementary_charge , proton_mass))
291 visit .DefineVectorExpression ("Omega_i_raw_minus_times_density_perp",
292         "{dot(Omega_i_raw_minus_density_dependence, {1, 0, 0}), "
293         "dot(Omega_i_raw_minus_times_density, {0, 1, 0}), 0}")
294 visit .DefineVectorExpression ("Omega_i_raw_minus_times_density_para",
295         "{0, 0, dot(Omega_i_raw_minus_times_density, "
296         "{0, 0, 1})}")
297 visit .DefineScalarExpression ("Omega_i_raw_minus_times_density_para_scalar",
298         "dot(Omega_i_raw_minus_times_density, {0, 0, 1})")
299
300 ## Canonical momentum fields
301 visit .DefineVectorExpression ("P_i", "%e*A + %e*u_i_plus" %
302         (elementary_charge , proton_mass))
303 visit .DefineVectorExpression ("P_i_times_density", "n*P_i")
304
305 ## Reference fields
306 visit .DefineVectorExpression ("B_ref", "{B_ref_x, B_ref_y, B_ref_z}")
307 visit .DefineVectorExpression ("A_ref", "{A_ref_x, A_ref_y, A_ref_z}")
308 visit .DefineVectorExpression ("u_i_ref",
309         "{u_i_ref_x, u_i_ref_y, u_i_ref_z}")
310 visit .DefineVectorExpression ("omega_i_ref",
311         "{omega_i_ref_x, omega_i_ref_y, omega_i_ref_z}")
312 # visit .DefineVectorExpression ("u_i_ref_raw_vort",
313 #         "{u_i_raw_ref_x, u_i_raw_ref_y, u_i_raw_ref_z}")
314 visit .DefineVectorExpression ("omega_i_ref_raw",
315         "{w_i_raw_ref_x, w_i_raw_ref_y, w_i_raw_ref_z}")
316 visit .DefineVectorExpression ("P_i_ref", "%e*A_ref + %e*u_i_ref" %
317         (elementary_charge , proton_mass))
318 visit .DefineVectorExpression ("P_i_ref_times_density", "n*P_i_ref")
319 visit .DefineVectorExpression ("P_i_ref_raw_vort", "%e*A_ref + %e*u_i_ref_raw_vort" %
320         (elementary_charge , proton_mass))
321 visit .DefineVectorExpression ("P_i_ref_raw_vort_times_density", "n*P_i_ref_raw_vort")

```

```

322 visit.DefineVectorExpression("Omega_i_ref", "%e*B_ref + %e*omega_i_ref_raw" %
323     (elementary_charge, proton_mass))
324 visit.DefineVectorExpression("Omega_i_ref_times_density", "n*Omega_i_ref")
325 visit.DefineVectorExpression("Omega_i_ref_density_dependence",
326     "n*(%e *B_ref + %e *omega_i_ref) +"
327     "cross(gradient(n), %e *A_ref + %e * u_i_ref)"
328     % (elementary_charge, proton_mass,
329     elementary_charge, proton_mass))
330 visit.DefineVectorExpression("Omega_i_ref_raw_vort",
331     "%e*B_ref + %e*omega_i_ref_raw" %
332     (elementary_charge, proton_mass))
333 visit.DefineVectorExpression("Omega_i_ref_raw_vort_time_density",
334     "n*Omega_i_ref_raw_vort")
335 visit.DefineVectorExpression("Omega_i_ref_raw_vort_density_dependence",
336     "n*(%e *B_ref + %e *omega_i_ref_raw) +"
337     "cross(gradient(n), %e *A_ref + %e * u_i_ref_raw_vort)"
338     % (elementary_charge, proton_mass,
339     elementary_charge, proton_mass))
340
341
342 ## Relative fields
343 visit.DefineVectorExpression("B_rel", "B + B_ref")
344 visit.DefineVectorExpression("B_rel_minus", "B - B_ref")
345 visit.DefineVectorExpression("A_rel", "A - A_ref")
346 visit.DefineVectorExpression("u_i_rel", "u_i_plus - u_i_ref")
347 visit.DefineVectorExpression("u_i_rel_plus", "u_i_plus + u_i_ref")
348 #visit.DefineVectorExpression("u_i_rel_raw_vort", "u_i_plus - u_i_ref_raw_vort")
349 #visit.DefineVectorExpression("u_i_rel_plus_raw_vort", "u_i_plus + u_i_ref_raw_vort")
350 visit.DefineVectorExpression("omega_i_rel", "omega_i_plus + omega_i_ref")
351 visit.DefineVectorExpression("omega_i_rel_raw", "omega_i_raw_plus + omega_i_ref_raw")
352 visit.DefineVectorExpression("P_i_rel", "P_i - P_i_ref")
353 visit.DefineVectorExpression("P_i_rel_times_density",
354     "P_i_times_density - P_i_ref_times_density")
355 visit.DefineVectorExpression("P_i_rel_raw_vort", "P_i - P_i_ref_raw_vort")
356 visit.DefineVectorExpression("P_i_rel_raw_vort_times_density",
357     "P_i_rel_raw_vort_times_density - P_i_ref_raw_vort_times_density")
358 visit.DefineVectorExpression("Omega_i_rel", "Omega_i_plus + Omega_i_ref")
359 visit.DefineVectorExpression("Omega_i_rel_times_density",
360     "Omega_i_plus_times_density + Omega_i_ref_times_density")
361 visit.DefineVectorExpression("Omega_i_rel_density_dependence",
362     "Omega_i_plus_density_dependence + Omega_i_ref_density_dependence")
363 visit.DefineVectorExpression("Omega_i_raw_rel",
364     "Omega_i_raw_plus + Omega_i_ref_raw_vort")
365 visit.DefineVectorExpression("Omega_i_raw_rel_times_density",
366     "Omega_i_raw_plus_times_density +"
367     "Omega_i_ref_raw_vort_times_density")
368 visit.DefineVectorExpression("Omega_i_ref_raw_density_dependence",
369     "Omega_i_raw_plus_density_dependence +"
370     "Omega_i_ref_raw_vort_density_dependence")
371
372 ## Dynamic fields
373 visit.DefineVectorExpression("B_dynamic", "{B_dynamic_x, B_dynamic_y, B_dynamic_z}")
374 visit.DefineVectorExpression("A_dynamic", "{A_dynamic_x, A_dynamic_y, A_dynamic_z}")
375 visit.DefineVectorExpression("B_dynamic_ref", "{B_dynamic_ref_x, "
376     "B_dynamic_ref_y, B_dynamic_ref_z}")
377 visit.DefineVectorExpression("A_dynamic_ref", "{A_dynamic_ref_x, "
378     "A_dynamic_ref_y, A_dynamic_ref_z}")

```

```

379
380 ## Helicity density
381 visit.DefineScalarExpression("mag_helicity_density", "dot(A, B)")
382 visit.DefineScalarExpression("mag_ref_helicity_density", "dot(A_ref, B_ref)")
383 visit.DefineScalarExpression("mag_rel_helicity_density", "dot(A-A_ref, B+B_ref)")
384 visit.DefineScalarExpression("mag_dynamic_helicity_density", "dot(A_dynamic, B_dynamic)")
385 visit.DefineScalarExpression("mag_dynamic_ref_helicity_density",
386     "dot(A_dynamic_ref, B_dynamic_ref)")
387 visit.DefineScalarExpression("mag_dynamic_rel_helicity_density",
388     "dot(A_dynamic - A_dynamic_ref, B_dynamic + B_dynamic_ref)")
389 visit.DefineScalarExpression("kin_helicity_density",
390     "dot(u_i_plus, omega_i_raw_plus)")
391 visit.DefineScalarExpression("kin_ref_helicity_density",
392     "dot(u_i_ref_raw, omega_i_ref_raw)")
393 visit.DefineScalarExpression("kin_rel_helicity_density",
394     "dot(u_i_plus - u_i_ref_raw, omega_i_raw_plus + omega_i_ref_raw)")
395 visit.DefineScalarExpression("cross_helicity_density",
396     "2.*dot(B, u_i_plus)")
397 visit.DefineScalarExpression("cross_ref_helicity_density",
398     "2.*dot(B_ref, u_i_ref)")
399 visit.DefineScalarExpression("cross_rel_helicity_density",
400     "(dot(u_i_plus - u_i_ref, B + B_ref)"
401     "+ dot(u_i_plus + u_i_ref, B - B_ref))")
402
403
404 def normalize_scalar(visit, scalar_name,
405     normalized_scalar_name):
406     r"""
407     Determine max of scalar.
408     """
409     visit.AddPlot("Pseudocolor", scalar_name)
410     visit.DrawPlots()
411     visit.Query("Max")
412     max = visit.GetQueryOutputValue()
413     visit.DefineScalarExpression(normalized_scalar_name,
414     "%s - %g" % (scalar_name, max))
415     visit.DeleteActivePlots()
416
417
418 def launch_points_inner_outer(center, plane=0.249,
419     radius_inner=0.001, radius_outer=0.005,
420     num_inner=80, num_outer=60,
421     return_cut_point=False):
422     r"""
423     Calculate points on a circle outline for a given center point.
424     """
425     thetas = circle_with_cut_thetas(num_outer)
426     points_outer = launch_points(center, thetas, radius=radius_outer,
427     plane=plane)
428
429     thetas = full_circle_thetas(num_inner)
430     points_inner = launch_points(center, thetas, radius=radius_inner,
431     plane=plane)
432
433     cut_point_x = points_outer[(num_outer-1)*3]
434     cut_point_y = points_outer[(num_outer-1)*3+1]
435     cut_point = [cut_point_x, cut_point_y]

```

```

436     if return_cut_point:
437         return points_outer, points_inner, cut_point
438     else:
439         return points_outer, points_inner
440
441
442 def full_circle_thetas(num_points):
443     r"""
444     Return a linear space of angles.
445     """
446     thetas = np.linspace(0, 2.*np.pi, num_points)
447     return thetas
448
449
450 def circle_with_cut_thetas(num_points):
451     r"""
452     Return a linear space of angles with a cut from 3/4pi to 5/4pi.
453     """
454     thetas = np.linspace(0, 3./4.*np.pi, num_points)
455     thetas = np.concatenate((thetas, np.linspace(5./4.*np.pi, 2.*np.pi,
456                                               num_points)))
457     return thetas
458
459
460 def launch_points(center, thetas, radius=0.003,
461                 plane=0.249):
462     r"""
463     Return launch points for field lines.
464     """
465     x_points = radius * np.cos(thetas) + center[0]
466     y_points = radius * np.sin(thetas) + center[1]
467     z_points = plane * np.ones(x_points.size)
468     points = np.empty((x_points.size + y_points.size + z_points.size))
469     points[0::3] = x_points
470     points[1::3] = y_points
471     points[2::3] = z_points
472     points = tuple(points)
473     return points
474
475
476 def setup_scalar_isosurface(visit, quantity,
477                             colortable="PuRd", max_val=1., min_val=0.9):
478     r"""
479     Setup iso_surface. Works best if quantity is plane normalized.
480     """
481     visit.AddPlot("Pseudocolor", quantity, 1, 0)
482     PseudocolorAtts = visit.PseudocolorAttributes()
483     PseudocolorAtts.colorTableName = colortable
484     PseudocolorAtts.opacityType = PseudocolorAtts.Constant
485     PseudocolorAtts.opacity = 0.25
486     PseudocolorAtts.smoothingLevel = 0
487     PseudocolorAtts.legendFlag = 0
488     visit.SetPlotOptions(PseudocolorAtts)
489
490     visit.AddOperator("Isosurface", 0)
491     IsosurfaceAtts = visit.IsosurfaceAttributes()
492

```

```

493     IsosurfaceAtts.contourNLevels = 5
494     IsosurfaceAtts.contourValue = ()
495     IsosurfaceAtts.contourPercent = ()
496     IsosurfaceAtts.contourMethod = IsosurfaceAtts.Level
497     IsosurfaceAtts.minFlag = 1
498     IsosurfaceAtts.min = min_val
499     IsosurfaceAtts.maxFlag = 1
500     IsosurfaceAtts.max = max_val
501     visit.SetOperatorOptions(IsosurfaceAtts, 0)
502     return PseudocolorAtts, IsosurfaceAtts
503
504 def setup_current_pseudocolor(visit, current_to_use,
505                               colortable="PRGn_Stepped", max_val=1e6,
506                               min_val=-1e6, invert=True, horizontal=True):
507     r"""
508     Setup pseudocolor current plot.
509     """
510     visit.AddPlot("Pseudocolor", current_to_use, 1, 0)
511     PseudocolorAtts = visit.PseudocolorAttributes()
512     PseudocolorAtts.scaling = PseudocolorAtts.Linear
513     PseudocolorAtts.limitsMode = PseudocolorAtts.OriginalData
514     PseudocolorAtts.colorTableName = colortable
515     PseudocolorAtts.invertColorTable = invert
516
517     if max_val:
518         PseudocolorAtts.maxFlag = 1
519         PseudocolorAtts.max = max_val
520     if min_val:
521         PseudocolorAtts.minFlag = 1
522         PseudocolorAtts.min = min_val
523
524     visit.SetPlotOptions(PseudocolorAtts)
525     visit.AddOperator("Slice", 0)
526     SliceAtts = visit.SliceAttributes()
527     SliceAtts.originType = SliceAtts.Intercept
528     SliceAtts.originIntercept = 0.249
529     SliceAtts.axisType = SliceAtts.ZAxis
530     SliceAtts.project2d = 0
531     visit.SetOperatorOptions(SliceAtts, 0)
532
533     colorbar = visit.GetAnnotationObject('Plot0000')
534     colorbar.SetDrawMinMax(0)
535
536     if horizontal:
537         colorbar.SetOrientation("HorizontalBottom")
538         colorbar.SetFontHeight(0.017)
539         colorbar.SetNumberFormat('%#3.1g')
540         colorbar.SetManagePosition(0)
541         colorbar.SetPosition((0.05, 0.99))
542     return PseudocolorAtts, SliceAtts
543
544
545 def setup_massless_electron_canonical_flux_tubes(visit, points_outer,
546                                                  points_inner):
547     r"""
548     Setup two massless electron canonical flux tubes i.e. magnetic flux tubes.
549     Intended to be inner and outer flux tubes.

```



```

607                                     forward_color=tan,
608                                     backward_color=olive):
609     r"""
610     Setup two ion canonical flux tubes, one integrating in the forward
611     direction, one integrating in the backward direction.
612     """
613     visit.AddPlot("Streamline", "Omega_i", 1, 0)
614     StreamlineAtts_forward = visit.StreamlineAttributes()
615     StreamlineAtts_forward.sourceType = StreamlineAtts_forward.SpecifiedPointList
616     StreamlineAtts_forward.SetPointList(points_foward)
617     StreamlineAtts_forward.coloringMethod = StreamlineAtts_forward.Solid
618     StreamlineAtts_forward.colorTableName = "Default"
619     StreamlineAtts_forward.singleColor = forward_color
620     StreamlineAtts_forward.integrationDirection = StreamlineAtts_forward.Forward
621     StreamlineAtts_forward.legendFlag = 0
622     visit.SetPlotOptions(StreamlineAtts_forward)
623
624     visit.AddPlot("Streamline", "Omega_i", 1, 0)
625     StreamlineAtts_backward = visit.StreamlineAttributes()
626     StreamlineAtts_backward.sourceType = StreamlineAtts_backward.SpecifiedPointList
627     StreamlineAtts_backward.SetPointList(points_backward)
628     StreamlineAtts_backward.coloringMethod = StreamlineAtts_backward.Solid
629     StreamlineAtts_backward.colorTableName = "Default"
630     StreamlineAtts_backward.singleColor = backward_color
631     StreamlineAtts_backward.integrationDirection = StreamlineAtts_backward.Backward
632     StreamlineAtts_backward.legendFlag = 0
633     visit.SetPlotOptions(StreamlineAtts_backward)
634
635     return StreamlineAtts_forward, StreamlineAtts_backward
636
637
638 def setup_backward_and_B_stream(visit, name, launch_points,
639                                B_launch_points, color=green, B_color=red):
640     r"""
641     Setup fiedlines for a magnetic flux tube and for a backward integrated quantity.
642     """
643     visit.AddPlot("Streamline", 'B', 1, 0)
644     StreamlineAtts_B = visit.StreamlineAttributes()
645     StreamlineAtts_B.sourceType = StreamlineAtts_B.SpecifiedPointList
646     StreamlineAtts_B.SetPointList(B_launch_points)
647     StreamlineAtts_B.coloringMethod = StreamlineAtts_B.Solid
648     StreamlineAtts_B.colorTableName = "Default"
649     StreamlineAtts_B.singleColor = B_color
650     StreamlineAtts_B.integrationDirection = StreamlineAtts_B.Forward
651     StreamlineAtts_B.legendFlag = 0
652     visit.SetPlotOptions(StreamlineAtts_B)
653
654
655     visit.AddPlot("Streamline", name, 1, 0)
656     StreamlineAtts_backward = visit.StreamlineAttributes()
657     StreamlineAtts_backward.sourceType = StreamlineAtts_backward.SpecifiedPointList
658     StreamlineAtts_backward.SetPointList(launch_points)
659     StreamlineAtts_backward.coloringMethod = StreamlineAtts_backward.Solid
660     StreamlineAtts_backward.colorTableName = "Default"
661     StreamlineAtts_backward.singleColor = color
662     StreamlineAtts_backward.integrationDirection = StreamlineAtts_backward.Backward
663     StreamlineAtts_backward.legendFlag = 0

```

```

664     visit.SetPlotOptions(StreamlineAtts_backward)
665
666     return StreamlineAtts_B, StreamlineAtts_backward
667
668
669 def setup_field_line(visit, quantity,
670                     launch_point=(0.01, 0.01), launch_z=0.249,
671                     color=dark_red):
672     r"""
673     Setup single field line plot to better see twistedness.
674     """
675     visit.AddPlot("Streamline", quantity, 1, 0)
676     StreamlineAtts_line = visit.StreamlineAttributes()
677     StreamlineAtts_line.sourceType = StreamlineAtts_line.SpecifiedPoint
678     StreamlineAtts_line.pointSource = (launch_point[0], launch_point[1], launch_z)
679     StreamlineAtts_line.coloringMethod = StreamlineAtts_line.Solid
680     StreamlineAtts_line.singleColor = color
681     StreamlineAtts_line.legendFlag = 0
682     StreamlineAtts_line.showSeeds = 0
683     StreamlineAtts_line.lineWidth = 8
684     visit.SetPlotOptions(StreamlineAtts_line)
685     return StreamlineAtts_line
686
687
688 def setup_annotations(visit, time_scale=1, time_offset=0):
689     r"""
690     Setup Annotations: scale tick font size, label font size,
691     hide unnecessary text.
692     """
693     AnnotationAtts = visit.AnnotationAttributes()
694     AnnotationAtts.axes3D.autoSetScaling = 0
695     AnnotationAtts.axes3D.xAxis.title.visible = 0
696     AnnotationAtts.axes3D.yAxis.title.visible = 0
697     AnnotationAtts.axes3D.zAxis.title.visible = 0
698     AnnotationAtts.axes3D.xAxis.label.font.scale = 3
699     AnnotationAtts.axes3D.xAxis.label.scaling = -2
700     AnnotationAtts.axes3D.yAxis.label.font.scale = 3
701     AnnotationAtts.axes3D.yAxis.label.scaling = -2
702     AnnotationAtts.axes3D.zAxis.label.font.scale = 3
703     AnnotationAtts.axes3D.zAxis.label.scaling = -2
704     AnnotationAtts.userInfoFlag = 0
705     AnnotationAtts.databaseInfoFlag = 0
706     AnnotationAtts.databaseInfoTimeScale = time_scale
707     AnnotationAtts.databaseInfoTimeOffset = time_offset
708     visit.SetAnnotationAttributes(AnnotationAtts)
709     return AnnotationAtts
710
711
712 def set_default_view(visit):
713     r"""
714     Set default view for viewing fluxtubes.
715     If view needs to be modified it is best to align visit with gui and save
716     parameters from visit.GetView3D().
717     """
718     view = visit.GetView3D()
719     view.SetViewNormal((-0.731293, 0.40847, 0.546227))
720     view.SetFocus((0.00202222, 0.000976744, 0.331997))

```

```

721     view.SetViewUp((0.322268, 0.91274, -0.251095))
722     view.SetViewAngle(30)
723     view.SetParallelScale(0.088383)
724     view.SetNearPlane(-0.176766)
725     view.SetImagePan((0, 0))
726     view.SetImageZoom(1.5)
727     view.SetPerspective(1)
728     view.SetEyeAngle(2)
729     view.SetCenterOfRotationSet(0)
730     view.SetCenterOfRotation((0.00202222, 0.000976744, 0.331997))
731     view.SetAxis3DScaleFlag(0)
732     view.SetAxis3DScales((1, 1, 1))
733     view.SetShear((0, 0, 1))
734     view.SetWindowValid(0)
735     visit.SetView3D(view)
736
737
738 def set_default_lighting(visit):
739     r"""
740     Set lightening to light up contour plot in z=0.249 plane
741     when default view is used.
742     """
743     light0 = visit.LightAttributes()
744     light0.enabledFlag = 1
745     light0.type = light0.Camera
746     light0.direction = (-0.5, 0, -0.5)
747     light0.color = (255, 255, 255, 255)
748     light0.brightness = 1
749     visit.SetLight(0, light0)
750
751
752 def set_default_view_thesis(visit):
753     r"""
754     Set default view for viewing fluxtubes.
755     If view needs to be modified it is best to align visit with gui and save
756     parameters from visit.GetView3D().
757     """
758     View3DAtts = visit.View3DAttributes()
759     View3DAtts.viewNormal = (-0.652048, 0.487146, 0.580966)
760     View3DAtts.focus = (0.00151111, 0.0045, 0.331997)
761     View3DAtts.viewUp = (0.365672, 0.873317, -0.321872)
762     View3DAtts.viewAngle = 30
763     View3DAtts.parallelScale = 0.0883679
764     View3DAtts.nearPlane = -0.176736
765     View3DAtts.farPlane = 0.176736
766     View3DAtts.imagePan = (-0.0429026, -0.00832011)
767     View3DAtts.imageZoom = 0.95
768     View3DAtts.perspective = 1
769     View3DAtts.eyeAngle = 2
770     View3DAtts.centerOfRotationSet = 0
771     View3DAtts.centerOfRotation = (0.00151111, 0.0045, 0.331997)
772     View3DAtts.axis3DScaleFlag = 0
773     View3DAtts.axis3DScales = (1, 1, 1)
774     View3DAtts.shear = (0, 0, 1)
775     View3DAtts.windowValid = 0
776     visit.SetView3D(View3DAtts)
777

```

```

778
779 def set_default_view_lower_angle(visit):
780     r"""
781     Set view with lower angle for viewing fluxtubes.
782     If view needs to be modified it is best to align visit with gui and save
783     parameters from visit.GetView3D().
784     """
785     view = visit.GetView3D()
786     view.setViewNormal((-0.776189, 0.193398, 0.600106))
787     view.setFocus((0.00202222, 0.000976744, 0.331997))
788     view.setViewUp((0.138771, 0.980856, -0.136615))
789     view.setViewAngle(30)
790     view.setParallelScale(0.088383)
791     view.setNearPlane(-0.176766)
792     view.setFarPlane(0.175437)
793     view.setImagePan((0, 0))
794     view.setImageZoom(1)
795     view.setPerspective(1)
796     view.setEyeAngle(2)
797     view.setCenterOfRotationSet(0)
798     view.setCenterOfRotation((0.00202222, 0.000976744, 0.331997))
799     view.setAxis3DScaleFlag(0)
800     view.setAxis3DScales((1, 1, 1))
801     view.setShear((0, 0, 1))
802     view.setWindowValid(0)
803     visit.SetView3D(view)
804
805
806 def set_positive_x_view(visit):
807     r"""
808     Set view along positive x for viewing fluxtubes.
809     If view needs to be modified it is best to align visit with gui and save
810     parameters from visit.GetView3D().
811     """
812     view = visit.GetView3D()
813     view.SetViewNormal((-0.00997631, 0.0600385, 0.0335938))
814     view.SetFocus((0.00202222, -0.00202703, 0.331997))
815     view.SetViewUp((0.0598395, 0.998184, 0.00689852))
816     view.SetViewAngle(30)
817     view.SetParallelScale(0.0877186)
818     view.SetNearPlane(-0.175437)
819     view.SetImagePan((0, 0))
820     view.SetImageZoom(1)
821     view.SetPerspective(1)
822     view.SetEyeAngle(2)
823     view.SetCenterOfRotationSet(0)
824     view.SetCenterOfRotation((0.00202222, -0.00202703, 0.331997))
825     view.SetAxis3DScaleFlag(0)
826     view.SetAxis3DScales((1, 1, 1))
827     view.SetShear((0, 0, 1))
828     view.SetWindowValid(1)
829     visit.SetView3D(view)
830
831
832 def set_postive_z_view(visit):
833     r"""
834     Set view along positive z for viewing fluxtubes.

```

```

835     If view needs to be modified it is best to align visit with gui and save
836     parameters from visit.GetView3D().
837     """
838     view = visit.GetView3D()
839     view.SetViewNormal((0.00944856, 0.0379894, 0.999233))
840     view.SetFocus((0.00202222, -0.00202703, 0.331997))
841     view.SetViewUp((-0.00367716, 0.9999274, 0.0037961))
842     view.SetViewAngle(30)
843     view.SetParallelScale(0.0877186)
844     view.SetNearPlane(-0.175437)
845     view.SetImagePan((0, 0))
846     view.SetImageZoom(2.14359)
847     view.SetPerspective(1)
848     view.SetEyeAngle(2)
849     view.SetCenterOfRotationSet(0)
850     view.SetCenterOfRotation((0.00202222, -0.00202703, 0.331997))
851     view.SetAxis3DScaleFlag(0)
852     view.SetAxis3DScales((1, 1, 1))
853     view.SetShear((0, 0, 1))
854     view.SetWindowValid(1)
855     visit.SetView3D(view)
856
857
858 def set_negative_z_view(visit):
859     r"""
860     Set view along negative z for viewing fluxtubes.
861     If view needs to be modified it is best to align visit with gui and save
862     parameters from visit.GetView3D().
863     """
864     view = visit.GetView3D()
865     view.SetViewNormal((-0.00894299, -0.00985814, 0.999911))
866     view.SetFocus((0.00202222, 0.000976744, 0.331997))
867     view.SetViewUp((0.00367716, 0.999944, 0.00989136))
868     view.SetViewAngle(30)
869     view.SetParallelScale(0.0877186)
870     view.SetNearPlane(-0.175437)
871     view.SetImagePan((0, 0))
872     view.SetImageZoom(2.14359)
873     view.SetPerspective(1)
874     view.SetEyeAngle(2)
875     view.SetCenterOfRotationSet(0)
876     view.SetCenterOfRotation((0.00202222, -0.00202703, 0.331997))
877     view.SetAxis3DScaleFlag(0)
878     view.SetAxis3DScales((1, 1, 1))
879     view.SetShear((0, 0, 1))
880     view.SetWindowValid(1)
881     visit.SetView3D(view)
882
883
884 def determine_j_mag_extrema(database_path, plane_num=0):
885     r"""
886     Determine extrema over time of current across all shots.
887     Can be sued to set min and max values for colormaps.
888     """
889     numpy_archives = glob(database_path + '*.npz')
890     data = np.load(numpy_archives[0])
891     j_x = data['j_x'][:, :, plane_num]

```

```

892     j_y = data['j_y'][:, :, plane_num]
893     j_z = data['j_z'][:, :, plane_num]
894     j_mag = np.sqrt(j_x**2. + j_y**2. + j_z**2.)
895     j_mag_max = np.nanmax(j_mag)
896     j_mag_min = np.nanmin(j_mag)
897     for archive in numpy_archives[1:]:
898         data = np.load(archive)
899         j_x = data['j_x'][:, :, plane_num]
900         j_y = data['j_y'][:, :, plane_num]
901         j_z = data['j_z'][:, :, plane_num]
902         j_mag = np.sqrt(j_x**2. + j_y**2. + j_z**2.)
903         j_mag_max = np.nanmax(j_mag) if np.nanmax(j_mag) > j_mag_max else j_mag_max
904         j_mag_min = np.nanmin(j_mag) if np.nanmin(j_mag) < j_mag_min else j_mag_min
905     return j_mag_max, j_mag_min
906
907
908 def set_save_settings(visit):
909     r"""
910     Set and return save_atts.
911     """
912     save_atts = visit.SaveWindowAttributes()
913     save_atts.format = save_atts.PNG
914     save_atts.height = 1080
915     save_atts.width = 1920
916     save_atts.family = 0
917     visit.SetSaveWindowAttributes(save_atts)
918     return save_atts
919
920
921 def setup_slider(visit):
922     r"""
923     Add a time slider with us text label.
924     """
925     slider = visit.CreateAnnotationObject("TimeSlider")
926     slider.SetText("$time us")
927     slider.SetRounded(0)
928     slider.SetVisible(1)
929
930
931 def main():
932     r"""
933     Plot frames of canonical flux tube animations.
934     """
935     args = parse_args()
936     database_prefix = args.database_prefix + args.database_date
937     visit.Launch()
938     today = date.now().strftime('%Y-%m-%d-%H-%M')
939     out_dir = '../output/canonical_flux_tubes/' + today
940     try:
941         os.makedirs(out_dir)
942     except:
943         pass
944
945
946 if args.interactive_session:
947     visit.OpenDatabase(database_prefix + args.database_postfix + ".*.vtk database")
948     define_expressions(visit)

```



```

1006         plot_count += 1
1007
1008     if args.velocity:
1009         (velocity_stream_1,
1010          velocity_stream_2) = setup_outer_inner_ion_canonical_flux_tubes(visit,
1011                                                                           'u_i_plus',
1012                                                                           points_inner,
1013                                                                           points_outer,
1014                                                                           outer_color=aqua,
1015                                                                           inner_color=navy)
1016
1017         plot_count += 2
1018
1019     if args.view == 'default':
1020         if not args.for_wide_screen:
1021             set_default_view_thesis(visit)
1022         else:
1023             set_default_view(visit)
1024     elif args.view == 'default_lower_angle':
1025         set_default_view_lower_angle(visit)
1026     elif args.view == 'positive_z':
1027         set_postive_z_view(visit)
1028     elif args.view == 'negative_z':
1029         set_negative_z_view(visit)
1030     elif args.view == 'positive_x':
1031         set_positive_x_view(visit)
1032     set_default_lighting(visit)
1033     setup_slider(visit)
1034
1035     if args.double_stream:
1036         stream_launch_point = (field_nulls[args.start_time_point][0] + args.x_offset,
1037                                field_nulls[args.start_time_point][1] + args.y_offset)
1038         setup_field_line(visit, args.double_stream,
1039                          launch_point=(stream_launch_point[0] + 0.001,
1040                                         stream_launch_point[1] + 0.))
1041         setup_field_line(visit, args.double_stream,
1042                          launch_point=(stream_launch_point[0] + 0.,
1043                                         stream_launch_point[1] + 0.001))
1044         setup_field_line(visit, args.double_stream,
1045                          launch_point=(stream_launch_point[0] - 0.001,
1046                                         stream_launch_point[1] + 0.))
1047         setup_field_line(visit, args.double_stream,
1048                          launch_point=(stream_launch_point[0] + 0.,
1049                                         stream_launch_point[1] - 0.001))
1050         setup_field_line(visit, args.double_stream,
1051                          launch_point=(stream_launch_point[0] + 0.005,
1052                                         stream_launch_point[1] + 0.))
1053         setup_field_line(visit, args.double_stream,
1054                          launch_point=(stream_launch_point[0] + 0.,
1055                                         stream_launch_point[1] + 0.005))
1056         setup_field_line(visit, args.double_stream,
1057                          launch_point=(stream_launch_point[0] - 0.005,
1058                                         stream_launch_point[1] + 0.))
1059         setup_field_line(visit, args.double_stream,
1060                          launch_point=(stream_launch_point[0] + 0.,
1061                                         stream_launch_point[1] - 0.005))
1062

```

```

1063         setup_field_line(visit , args.double_stream ,
1064                         launch_point=stream_launch_point)
1065
1066         setup_field_line(visit , 'B',
1067                         launch_point=stream_launch_point , color=red)
1068
1069
1070     visit.DrawPlots()
1071     save_atts = set_save_settings(visit)
1072     ending = '.png'
1073     visit.SetTimeSliderState(time_points[0])
1074     if not args.for_wide_screen:
1075         visit.ResizeWindow(1, 960, 1000)
1076     else:
1077         visit.ResizeWindow(1, 1920, 1080)
1078
1079     if args.wait_for_manual_settings:
1080         visit.OpenGUI()
1081         comment = raw_input()
1082
1083
1084     for index, time_point in enumerate(time_points):
1085         print time_point
1086         plot_number = 0
1087         save_atts.fileName = output_path + str(index + args.file_number_offset).zfill(4) + ending
1088         visit.SetSaveWindowAttributes(save_atts)
1089
1090         if args.current_plane:
1091             plot_number += 1
1092         if args.temperature_tubes:
1093             plot_number += 1
1094         if args.density_tubes:
1095             plot_number += 1
1096
1097         (points_outer ,
1098         points_inner ,
1099         cut_point) = launch_points_inner_outer(field_nulls[index],
1100                                             return_cut_point=True)
1101
1102         if args.stationary_tube:
1103             (points_outer ,
1104             points_inner ,
1105             cut_point) = launch_points_inner_outer(args.stationary_center ,
1106                                                 return_cut_point=True)
1107
1108
1109         if args.ion:
1110             visit.SetActivePlots(plot_number)
1111             StreamlineAtts_ion_outer.SetPointList(points_outer)
1112             visit.SetPlotOptions(StreamlineAtts_ion_outer)
1113             plot_number += 1
1114
1115             visit.SetActivePlots(plot_number)
1116             StreamlineAtts_ion_inner.SetPointList(points_inner)
1117             visit.SetPlotOptions(StreamlineAtts_ion_inner)
1118             plot_number += 1
1119
1120         if args.electron:

```



```

1177 parser.add_argument('--electron', help='plot canonical electron flux tubes',
1178                     action='store_true', default=False)
1179 parser.add_argument('--ion', help='plot canonical ion flux tubes', action='store_true', default=False)
1180 parser.add_argument('--current',
1181                     help='plot thin current flux tube surrounded by electron / magnetic flux tube',
1182                     action='store_true', default=False)
1183 parser.add_argument('--interactive_session', action='store_true', default=False)
1184 parser.add_argument('--current_to_use', default='j_z')
1185 parser.add_argument('--omega_to_use', default='Omega_i_raw_plus_times_density')
1186 parser.add_argument('--view', help='pre-configured_views: default, default_lower_angle, positive_z, negative_z, positive_x', default
    = 'default')
1187 parser.add_argument('--wait_for_manual_settings',
1188                     help='flag makes program wait for input before rendering time series.',
1189                     default=False, action='store_true')
1190 parser.add_argument('--double_stream', help='plot canonical streamline and magnetic of given variable', default=None)
1191 parser.add_argument('--x_offset', help='x offset of single streamline', default=0, type=int)
1192 parser.add_argument('--y_offset', help='y offset of single streamline', default=0, type=int)
1193 parser.add_argument('--file_number_offset', help='offset in file numbering', default=0, type=int)
1194 parser.add_argument('--turn_off_density_start', help='time step at which to start turning off density cloud.', type=int, default=
    None)
1195 parser.add_argument('--turn_off_density_end', help='time step at which to end turning off density cloud', type=int, default=None)
1196 parser.add_argument('--velocity', action='store_true', default=False)
1197 parser.add_argument('--stationary_tube', help="flag to hold flux tube launch point"
1198                    "stationary",
1199                    action='store_true', default=False)
1200 parser.add_argument('--stationary_center',
1201                     help='launch_point of stationary tube',
1202                     nargs=2,
1203                     type=float,
1204                     default = [0, 0])
1205 parser.add_argument('--time_shift',
1206                     help='shift gyration phase',
1207                     type=int, default=125)
1208 parser.add_argument('--for_wide_screen',
1209                     help='set resolution and view settings for wide screen animations',
1210                     action='store_true', default=False)
1211 args = parser.parse_args()
1212 return args
1213
1214 if __name__ == '__main__':
1215     main()

```

VITA

Jens von der Linden was born in Mt. Lebanon, PA. At age 6 he moved with his family to Germany. In 2005, he earned his Abitur at Gymnasium Gerresheim in Düsseldorf, Germany. He returned to the USA for his undergraduate studies. As an undergraduate he worked in the Devlin experimental cosmology group, the accelerator physics group at Oak Ridge National Laboratory, and the DIII-D experiment at General Atomics. He earned a Bachelor of Arts with a major in Physics and a minor in Mathematics from the University of Pennsylvania in 2009. During his graduate studies, he volunteered as a science communication fellow at the Pacific Science Center and as an instructor at Software Carpentry. He spent a year conducting part of his dissertation research at Lawrence Livermore National Laboratory where he was supported by the Department of Energy Office of Science Graduate Student Research Program. He earned a Doctor of Philosophy from the William E. Boeing Department of Aeronautics & Astronautics at the University of Washington in 2017.